

Research Project Number 2015-17-TE

DEVELOPMENT OF THE MANITOBA CONSTRAINED-WIDTH, TALL WALL BARRIER



Submitted by

Scott K. Rosenbaugh, M.S.C.E., E.I.T.
Research Associate Engineer

Jennifer D. Schmidt, Ph.D., P.E.
Research Assistant Professor

Elizabeth M. Regier
Undergraduate Research Assistant

Ronald K. Faller, Ph.D., P.E.,
Research Associate Professor
MwRSF Director

MIDWEST ROADSIDE SAFETY FACILITY

Nebraska Transportation Center
University of Nebraska-Lincoln
130 Whittier Research Center
2200 Vine Street
Lincoln, Nebraska 68583-0853
(402) 472-0965

Submitted to

MANITOBA INFRASTRUCTURE

Traffic Engineering
420 – 215 Garry Street
Winnipeg, Manitoba R3C 3P3

TECHNICAL REPORT DOCUMENTATION PAGE

1. Report No. TRP-03-356-16	2.	3. Recipient's Accession No.	
4. Title and Subtitle Development of the Manitoba Constrained-Width, Tall Wall Barrier		5. Report Date September 26, 2016	
7. Author(s) Rosenbaugh, S.K., Schmidt, J.D., Regier, E.M., and Faller, R.K.		8. Performing Organization Report No. TRP-03-356-16	
9. Performing Organization Name and Address Midwest Roadside Safety Facility (MwRSF) Nebraska Transportation Center University of Nebraska-Lincoln 130 Whittier Research Center 2200 Vine Street Lincoln, Nebraska 68583-0853		10. Project/Task/Work Unit No.	
12. Sponsoring Organization Name and Address Manitoba Infrastructure Traffic Engineering 420 – 215 Garry Street Winnipeg, Manitoba R3C 3P3		11. Contract (C) or Grant (G) No. 2015-17-TE	
13. Type of Report and Period Covered Final Report: 2015 – 2016		14. Sponsoring Agency Code 2015-17-TE	
15. Supplementary Notes			
16. Abstract <p>Manitoba Infrastructure (MI) desired a new, tall concrete median barrier capable of satisfying the Test Level 5 (TL-5) safety requirements of the <i>Manual for Assessing Safety Hardware</i> (MASH). The barrier was designed with a 1,250-mm (49¼-in.) height, a maximum width of 600 mm (23¾ in.), and to resist a 845-kN (190-kip) load applied at the top of the barrier. The Manitoba Constrained-Width, Tall Wall was optimized to withstand the design load while minimizing the amount of steel reinforcement. Variations of the barrier were developed, including a bridge rail, and roadside barrier.</p> <p>The bridge rail was considered to be the critical design due to its narrow width and anchorage to a thin, cantilevered bridge deck. Thus, one full-scale vehicle crash test was conducted on the bridge rail system to verify the entire family of barriers. The 45.7-m (150-ft) long single-slope bridge rail had a height of 1,250 mm (49¼ in.) and widths of 450 mm (17¾ in.) and 250 mm (10 in.) at the base and top, respectively. The upstream 22.86 m (75 ft) of the barrier was installed on a 280-mm (11-in.) thick simulated bridge deck. A 168-mm (6⅝-in.) gap in the bridge rail and a 20-mm (¾-in.) gap in the bridge deck were placed at the deck mid-span to simulate an expansion joint. A steel cover plate was placed over the barrier joint to prevent vehicle snag. During the test, the tractor trailer impacted just upstream from the joint and was safely redirected. The barrier sustained minor damage in the form of cracks and spalling. Data from on board accelerometers located near the front tandem axles was analyzed to estimate the impact load, which ranged between 1,027 kN and 1,183 kN (231 kips and 266 kips). However, the actual maximum loading applied by the rear tandem axles was thought to be significantly higher.</p> <p>Anchorage options were developed for use with the TL-5 barrier system, including a foundation slab, an independent footing, and an asphalt keyway. Additionally, transitions systems were detailed for the connection of the TL-5 median barrier to various other new and existing barrier shapes. Finally, implementation guidance was provided.</p>			
17. Document Analysis/Descriptors Roadside Safety, Crash Test, MASH, TL-5, Single Slope Barrier, Concrete Barrier, Bridge Rail		18. Availability Statement No restrictions	
19. Security Class (this report) Unclassified	20. Security Class (this page) Unclassified	21. No. of Pages 179	22. Price

DISCLAIMER STATEMENT

This report was completed with funding from Manitoba Infrastructure. The contents of this report reflect the views and opinions of the authors who are responsible for the facts and the accuracy of the data presented herein. The contents do not necessarily reflect the official views or policies of Manitoba Infrastructure. This report does not constitute a standard, specification, regulation, product endorsement, or an endorsement of manufacturers.

UNCERTAINTY OF MEASUREMENT STATEMENT

The Midwest Roadside Safety Facility (MwRSF) has determined the uncertainty of measurements for several parameters involved in standard full-scale crash testing and non-standard testing of roadside safety features. Information regarding the uncertainty of measurements for critical parameters is available upon request by the sponsor.

INDEPENDENT APPROVING AUTHORITY

The Independent Approving Authority (IAA) for the data contained herein was Mr. Bob Bielenberg, Research Associate Engineer.

ACKNOWLEDGEMENTS

The authors wish to acknowledge several sources that made a contribution to this project: (1) Manitoba Infrastructure for sponsoring this project; and (2) MwRSF personnel for constructing the barrier and conducting the crash test.

Acknowledgement is also given to the following individuals who made a contribution to the completion of this research project.

Midwest Roadside Safety Facility

J.D. Reid, Ph.D., Professor
J.C. Holloway, M.S.C.E., E.I.T., Test Site Manager
K.A. Lechtenberg, M.S.M.E., E.I.T., Research Associate Engineer
R.W. Bielenberg, M.S.M.E., E.I.T., Research Associate Engineer
C.S. Stolle, Ph.D., Research Assistant Professor
A.T. Russell, B.S.B.A., Shop Manager
S.M. Tighe, Laboratory Mechanic
D.S. Charroin, Laboratory Mechanic
M.A. Rasmussen, Laboratory Mechanic
E.W. Krier, Laboratory Mechanic
Undergraduate and Graduate Research Assistants

Manitoba Infrastructure and Transportation

Harald Larsen, P.Eng., Roadside Safety Engineer
Andrew Pankratz, P.Eng., Senior Bridge Design Engineer
Glenn Cuthbertson, P.Eng., Director, Traffic Engineering
Diana Emerson, P.Eng., Traffic Services Engineer

TABLE OF CONTENTS

TECHNICAL REPORT DOCUMENTATION PAGE i

DISCLAIMER STATEMENT ii

UNCERTAINTY OF MEASUREMENT STATEMENT ii

INDEPENDENT APPROVING AUTHORITY..... ii

ACKNOWLEDGEMENTS iii

TABLE OF CONTENTS..... iv

LIST OF FIGURES vi

LIST OF TABLES ix

1 INTRODUCTION 1

 1.1 Background 1

 1.2 Objective 2

 1.3 Scope..... 2

2 LITERATURE REVIEW 3

3 DESIGN CRITERIA 6

 3.1 Geometric Requirements and Material Specifications 6

 3.2 Barrier Design Strength 7

 3.3 Deck Design Strength 8

4 BARRIER ANALYSIS AND DESIGN 10

 4.1 Bridge Rail Design..... 10

 4.2 Deck Design..... 14

 4.3 End Section Design for Testing 14

5 DESIGN DETAILS 16

6 TEST REQUIREMENTS AND EVALUATION CRITERIA 44

 6.1 Test Requirements 44

 6.2 Evaluation Criteria 45

7 TEST CONDITIONS..... 47

 7.1 Test Facility 47

 7.2 Vehicle Tow and Guidance System..... 47

 7.3 Impact Point 47

 7.4 Test Vehicle 48

 7.5 Data Acquisition Systems 54

 7.5.1 Accelerometers 54

 7.5.2 Rate Transducers..... 54

7.5.3 Retroreflective Optic Speed Trap	55
7.5.4 Digital Photography	55
8 FULL-SCALE CRASH TEST NO. MAN-1	58
8.1 Weather Conditions	58
8.2 Test Description	58
8.3 Barrier Damage	66
8.4 Vehicle Damage	72
8.5 Occupant Risk	76
8.6 Discussion	77
9 Data Analysis of Test No. MAN-1	79
9.1 Vehicle Roll	79
9.2 Impact Load Estimation	79
10 MEDIAN AND ROADSIDE CONFIGURATIONS	84
10.1 TL-5 Median Barrier Configuration	84
10.2 Alternative Anchorage Options for Median Barrier	89
10.3 TL-4 Median Barrier Configuration	94
10.4 TL-5 Roadside Barrier Anchorage Options	97
11 TL-5 Barrier Transitions	102
11.1 TL-5 Median Barrier to TL-4 Median Barrier	102
11.2 TL-5 Median Barrier to 815-mm (32-in.) Tall F-Shape Barrier	106
11.3 TL-5 Median Barrier to Dual TL-5 Roadside Barriers	110
11.4 TL-5 Median Barrier to Dual 815-mm (32-in.) F-Shape Roadside Barriers	114
11.5 TL-4 Median Barrier to Vertical Barrier	118
11.6 Treatment for Gaps in TL-5 Median Barrier Spanning Sign Supports	121
12 SUMMARY, CONCLUSIONS, AND RECOMMENDATIONS	127
12.1 Summary and Conclusions	127
12.2 Installation Recommendations	130
13 REFERENCES	134
14 APPENDICES	139
Appendix A. Material Specifications	140
Appendix B. Vehicle Center of Gravity Determination	155
Appendix C. Vehicle Deformation Records	157
Appendix D. Accelerometer and Rate Transducer Data Plots, Test No. MAN-1	162

LIST OF FIGURES

Figure 1. General Configuration of Manitoba Bridge Rail.....	10
Figure 2 Test Installation Layout, Test No. MAN-1	18
Figure 3. Layout Detail, Test No. MAN-1.....	19
Figure 4. Rail Joint with Cover Plate, Test No. MAN-1	20
Figure 5. Bridge Deck A and Rail A, Test No. MAN-1	21
Figure 6. Bridge Deck A and Rail A Reinforcement Layout, Test No. MAN-1	22
Figure 7. Bridge Rail A Detail, Test No. MAN-1	23
Figure 8. Bridge Deck A Detail, Test No. MAN-1.....	24
Figure 9. Bridge Deck A Section, Test No. MAN-1	25
Figure 10. Bridge Deck A Section, Test No. MAN-1	26
Figure 11. Bridge Deck B and Rail B, Test No. MAN-1.....	27
Figure 12. Bridge Deck B and Rail B Sections, Test No. MAN-1	28
Figure 13. Bridge Rail B Detail, Test No. MAN-1.....	29
Figure 14. Bridge Deck B Detail, Test No. MAN-1	30
Figure 15. Bridge Deck B Section, Test No. MAN-1.....	31
Figure 16. Bridge Deck B Section, Test No. MAN-1.....	32
Figure 17. Grade Beam Detail, Test No. MAN-1.....	33
Figure 18. Rail Joint Cap, Test No. MAN-1.....	34
Figure 19. Rail Joint Cap Component Detail, Test No. MAN-1	35
Figure 20. Upstream Barrier End Cap, Test No. MAN-1	36
Figure 21. Downstream Barrier End Cap. Test No. MAN-1	37
Figure 22. Barrier End Cap Components, Test No. MAN-1	38
Figure 23. Rebar Bill of Bars, Test No. MAN-1	39
Figure 24. Bent Rebar Details, Test No. MAN-1	40
Figure 25. Bill of Materials, Test No. MAN-1	41
Figure 26. Test Installation Photographs, Test No. MAN-1.....	42
Figure 27. Barrier Joint Photographs, Test No. MAN-1.....	43
Figure 28. Test Vehicle, Test No. MAN-1	49
Figure 29. Test Vehicle with Colored Tires, Test No. MAN-1	50
Figure 30. Test Vehicle Ballast, Test No. MAN-1	51
Figure 31. Vehicle Dimensions, Test No. MAN-1	52
Figure 32. Target Geometry, Test No. MAN-1	53
Figure 33. Camera Location Diagram, Test No. MAN-1	57
Figure 34. Impact Location, Test No. MAN-1	59
Figure 35. Summary of Test Results and Sequential Photographs, Test No. MAN-1	61
Figure 36. Additional Sequential Photographs, Test No. MAN-1.....	62
Figure 37. Additional Sequential Photographs, Test No. MAN-1.....	63
Figure 38. Documentary Photographs, Test No. MAN-1	64
Figure 39. Vehicle Final Position and Trajectory Marks, Test No. MAN-1	65
Figure 40. System Damage, Test No. MAN-1.....	68
Figure 41. System Damage, Test No. MAN-1.....	69
Figure 42. System Damage, Cover Plate Removed, Test No. MAN-1	70
Figure 43. Deck Damage, Test No. MAN-1.....	71
Figure 44. Vehicle Damage, Test No. MAN-1	73
Figure 45. Vehicle Damage, Test No. MAN-1	74

Figure 46. Fifth Wheel Plate Damage, Test No. MAN-1	75
Figure 47. Estimated Impact Load, Test No. MAN-1	81
Figure 48. Barrier Deflection vs. Time, Test No. MAN-1	83
Figure 49. Manitoba Constrained-Width, Tall Wall, Median Barrier Details	87
Figure 50. Median Barrier Reinforcement Details	88
Figure 51. Footing Anchorage Details for Median Barrier.....	91
Figure 52. Footing Reinforcement Details for Median Barrier	92
Figure 53. Asphalt Keyway Anchorage Details for Median Barrier Interior Sections.....	93
Figure 54. TL-4 Median Barrier Details	96
Figure 55. TL-5 Roadside Barrier Details	98
Figure 56. TL-5 Roadside Barrier Anchorage Bar Details	99
Figure 57. TL-5 Roadside Configuration Footing Details.....	100
Figure 58. TL-5 Roadside Configuration Footing Reinforcement Details	101
Figure 59. Transition Details, TL-5 Median Barrier to TL-4 Single Slope Barrier.....	104
Figure 60. Transition Details, TL-5 Median Barrier to TL-4 Single Slope Barrier.....	105
Figure 61. TL-5 Median Barrier and F-Shape Median Barrier Comparison	106
Figure 62. Transition Details, TL-5 Median Barrier to F-Shape Barrier.....	108
Figure 63. Transition Details, TL-5 Median Barrier to F-Shape Barrier.....	109
Figure 64. Transition Details, TL-5 Median Barrier to Dual TL-5 Roadside Barriers.....	112
Figure 65. Transition Details, TL-5 Median Barrier to Dual TL-5 Roadside Barriers.....	113
Figure 66. Flared Dual Roadside Barriers for Increased Gap Widths	114
Figure 67. Transition Details, TL-5 Median Barrier to Dual F-Shape Roadside Barriers.....	116
Figure 68. Transition Details, TL-5 Median Barrier to Dual F-Shape Roadside Barriers.....	117
Figure 69. Transition Details, TL-4 Median Barrier to Vertical Parapet.....	119
Figure 70. Transition Details, TL-4 Median Barrier to Vertical Parapet.....	120
Figure 71. MI Treatment Concept for Barrier Gaps Spanning Sign Support Structures	124
Figure 72. Treatment Details for TL-5 Barrier Gaps Spanning Large Sign Supports	125
Figure 73. Treatment Details for TL-5 Barrier Gaps Spanning Large Sign Supports	126
Figure 74. Recommended Reinforcement Configurations for the TL-5 Bridge Rail	131
Figure 75. Longitudinal Recess for Roadway Delineators	132
Figure 76. Cantilevered Barrier Extensions over Large Expansion Joints	133
Figure A-1. Countersunk Bolts, Item d1	143
Figure A-2. 3/8-in. Diameter, 4-in. Long Stud, Item d3	144
Figure A-3. Description of component 20M Rebar, Item b1, b10.....	145
Figure A-4. Steel Cover Plate, Items c2 and c3.....	146
Figure A-5. Steel End Caps, Items c5, c6, c7, c8, c9.....	147
Figure A-6. Steel Cover Plate, Item c1	148
Figure A-7. Steel Cover Plate, Item c4.....	149
Figure A-8. 15M Rebar, Items b3, b7, b9.....	150
Figure A-9. 15M Rebar, Items b2, b4, b5	151
Figure A-10. Grade Beam #4 Rebar, Item b6.....	152
Figure A-11. Grade Beam #5 Rebar, Items b8, b12, b13	153
Figure A-12. Grade Beam #6 Rebar, Item b11	154
Figure B-1. Vehicle Mass Distribution, Test No. MAN-1	155
Figure B-2. Vehicle Mass Distribution, Test No. MAN-1	156
Figure C-1. Floor Pan Deformation Data – Set 1, Test No. MAN-1	158
Figure C-2. Floor Pan Deformation Data – Set 2, Test No. MAN-1	159

Figure C-3. Occupant Compartment Deformation Data – Set 1, Test No. MAN-1160
Figure C-4. Occupant Compartment Deformation Data – Set 2, Test No. MAN-1161
Figure D-1. 10-ms Average Longitudinal Deceleration (DTS - Cab), Test No. MAN-1163
Figure D-2. Longitudinal Change in Velocity (DTS - Cab), Test No. MAN-1164
Figure D-3. Longitudinal Occupant Displacement (DTS - Cab), Test No. MAN-1165
Figure D-4. 10-ms Average Lateral Deceleration (DTS - Cab), Test No. MAN-1166
Figure D-5. Lateral Change in Velocity (DTS - Cab), Test No. MAN-1167
Figure D-6. Lateral Occupant Displacement (DTS - Cab), Test No. MAN-1168
Figure D-7. Vehicle Angular Displacements (DTS - Cab), Test No. MAN-1169
Figure D-8. Acceleration Severity Index (DTS - Cab), Test No. MAN-1170
Figure D-9. CFC 60 Longitudinal Deceleration (SLICE-2 - Trailer), Test No. MAN-1171
Figure D-10. CFC 60 50-ms Average Longitudinal Deceleration (SLICE-2 - Trailer), Test
No. MAN-1172
Figure D-11. Longitudinal Change in Velocity (SLICE-2 - Trailer), Test No. MAN-1173
Figure D-12. CFC60 Lateral Deceleration (SLICE-2 - Trailer), Test No. MAN-1174
Figure D-13. CFC60 50-ms Average Lateral Deceleration (SLICE-2 - Trailer), Test No.
MAN-1175
Figure D-14. Lateral Change in Velocity (SLICE-2 - Trailer), Test No. MAN-1176
Figure D-15. Vehicle Angular Displacements (SLICE-2 - Trailer), Test No. MAN-1177
Figure D-16. Acceleration Severity Index (SLICE-2), Test No. MAN-1178

LIST OF TABLES

Table 1. Summary of Tractor-Trailer Crash Tests, Barrier Descriptions and Impact Conditions4
Table 2. Summary of Tractor-Trailer Crash Tests, Resulting Barrier and Deck Damage.....5
Table 3. TL-5 Concrete Barrier Strengths8
Table 4. Crash Tested TL-5 Bridge Rails, Parapet and Deck Strengths.....9
Table 5. Optimization Analysis Results for Bridge Rail Configurations13
Table 6. MASH TL-5 Crash Test Conditions for Longitudinal Barriers.....44
Table 7. MASH Evaluation Criteria for Longitudinal Barriers and Bridge Rails46
Table 8. Impact Locations for Rear Tandem Axles in TL-5 Crash Tests.....48
Table 9. Camera Speeds and Lens Settings, Test No. MAN-156
Table 10. Weather Conditions, Test No. MAN-158
Table 11. Sequential Description of Impact Events, Test No. MAN-160
Table 12. Maximum Occupant Compartment Deformations by Location76
Table 13. Summary of OIV, ORA, THIV, PHD, and ASI Values, Test No. MAN-177
Table 14. Maximum Roll Angle for Trailer during TL-5 Crash Tests79
Table 15. TL-5 Design Loads from Ongoing Study NCHRP 20-22(2) [32]83
Table 16. Optimization Analysis Results for Median Barrier Configurations86
Table 17. Summary of Safety Performance Evaluation Results.....129
Table A-1. Test No. MAN-1, Bill of Materials141
Table A-2. Concrete Compressive Strength Data.....142

1 INTRODUCTION

1.1 Background

Manitoba Infrastructure (MI) currently utilizes 825-mm (32-in.) tall, F-shape concrete barriers along high-speed roadways. However, an increased barrier height is often desired in medians to eliminate headlight glare from opposing traffic. Additionally, an increase to the volume of truck traffic has increased the need to utilize a barrier system capable of containing heavy trucks. Thus, MI desired a tall concrete barrier that satisfied the Test Level 5 (TL-5) safety requirements found in the American Association of State Highway and Transportation Officials (AASHTO) *Manual for Assessing Safety Hardware (MASH)* [1].

MI conducted a review of previously designed TL-5 barriers and elected to alter the cross-section shape of its barrier from the previous F-shape to a single-slope shape. The State Departments of Transportation for both California and Texas have developed high containment, concrete median barriers utilizing a constant slope on the front face of the barrier [2-4]. Both barriers have a height of 1,070 mm (42 in.), but they differ slightly in face geometry as the slopes measure 9.1 and 10.8 degrees from vertical, respectively. However, MI required a taller barrier to eliminate headlight glare. Utilizing the guidelines provided in National Cooperative Highway Research Program's (NCHRP) *Synthesis of Highway Practice 66* [5], MI desired a barrier height of 1,250 mm (49¼ in.). Additionally, MI desired a footprint width of 600 mm (23¾ in.) to match current roadway median geometries. Thus, MI desired to modify the California Single-Slope barrier to match these geometric requirements.

Variations of both single-slope barriers have previously been developed by other transportation agencies desiring high-capacity concrete barriers. However, the barrier height has not typically been altered. Increasing the barrier height above the standard 1,070 mm (42 in.) would likely restrict the amount of roll experienced by the tractor trailer during redirection, thus reducing the time duration of the impulse wave and increasing the load imparted to the barrier. Additionally, taller barriers may potentially result in an increased applied load height. Impacts with 1,070 mm (42 in.) tall barriers have resulted in the box extending over and leaning on the top of the barrier during redirection. With a taller barrier, the trailer box could impact the barrier laterally and apply loads near the top of the barrier. An increased applied load height would require more anchorage strength to prevent barrier overturning. Subsequently, in order to increase the height of a TL-5 barrier, additional reinforcement and barrier anchorage may be required to maintain the structural integrity of the system.

Finally, MI desired to utilize the new barrier system in a variety of different installation applications, including as a median barrier, roadside barrier, and bridge rail. Therefore, a need existed to develop a new family of MASH TL-5 concrete barriers to satisfy MI's geometric desires and encompass multiple installation configurations. Additionally, transitions would be needed to attach the new barrier system to existing barriers and/or new lower-height (lower-containment level) barriers.

1.2 Objective

The objective of this research effort was to develop a tall, single slope, concrete barrier system to satisfy MASH TL-5 safety performance criteria. The barrier was to be modeled after the California Single-Slope barrier, have a height of 1,250 mm (49¼ in.), and have a maximum base width of 600 mm (23¾ in.). Multiple configurations of the new barrier system were desired including median, roadside, and bridge rail applications. Both interior and end sections (adjacent to discontinuities) were to be developed. The new barrier was to be optimized to minimize installation costs while satisfying MASH TL-5 standards. Additionally, a bridge deck with minimal thickness and maximum cantilever overhang distance was desired to support the new bridge rail. Finally, transitions from the new TL-5 barrier to various existing barrier structures were to be developed.

1.3 Scope

The research objective was achieved by performing several tasks. First, a literature review was conducted on previous crash tests involving tractor-trailer vehicles impacting bridge rails, roadside barriers, and median barriers. The structural capacities of these systems were calculated, and the level of damage sustained to the system was noted. Next, the barrier width and reinforcement configuration was optimized to minimize installation costs while satisfying MASH TL-5 structural requirements. Design efforts focused on a single-sided bridge rail configuration since narrower barriers are more likely to sustain damage during impact events than wider, symmetric barriers. A full-scale crash test was then conducted with a 36,000-kg (80,000-lb) van-type tractor trailer impacting a 46 m (150 ft) long bridge rail installation according to MASH test no. 5-12. The successfully-tested TL-5 bridge rail was modified into multiple other configurations, including median and roadside applications. Finally, multiple transitions were developed to attach the new TL-5 barriers to various new and existing concrete barrier systems.

2 LITERATURE REVIEW

At the onset of the project, a literature review was conducted on previously crash-tested, TL-5 barrier systems. The review focused on testing of van-style tractor-trailers impacting bridge rails and concrete roadside and median barriers. In all, nine tests on bridge rails and four tests on concrete median barriers were reviewed. Eleven of the tests were conducted according to the impact criteria of National Cooperative Highway Research Program (NCHRP) Report No. 350 [6], which are the same for test no. 5-12 in the current MASH standard. The remaining two tests were conducted in accordance with the 1989 edition of AASHTO's *Guide Specifications for Bridge Railings* [7]. The main difference between the crash testing standards was the required weight of the tractor trailer from the AASHTO guide was 22,680 kg (50,000 lb), while NCHRP Report No. 350 and MASH required a vehicle weight of 36,287 kg (80,000 lb). All 13 of these crash tests resulted in vehicle redirection and satisfactory barrier performance.

The literature review focused on the geometry and strength of each of these high-containment barrier systems. The geometric shape, height, and width of each barrier were documented along with the mass, speed, and angle of the impacting vehicle. Deck thicknesses and cantilever overhang distances were also recorded for the nine bridge rails. Additionally, the material strengths and reinforcement configurations were documented in order to calculate barrier and deck strengths. System strengths were utilized in establishing the design strength for the new Manitoba barrier and are discussed in Chapter 3. Finally, the damage sustained by each system was documented in order to compare performances between the barrier systems. The crash tests are summarized in Tables 1 and 2.

Table 1. Summary of Tractor-Trailer Crash Tests, Barrier Descriptions and Impact Conditions

Test No.	Ref. No.	Configuration	Barrier Shape	Barrier Height mm (in.)	Deck Thickness mm (in.)	Deck Overhang mm (in.)	Impact Speed km/h (mph)	Impact Angle	Vehicle Mass kg (lb)
Test 6	[8]	Bridge Rail	Open Concrete Rail with Steel Rail	914/1,372 (36/54)	191 (7.5)	762 (30)	79.0 (49.1)	15°	36,183 (79,770)
2416-1	[9]	Bridge Rail	F-Shape with Steel Rail	1,270 (50)	203 (8)	457 (18)	77.9 (48.4)	14.5°	36,324 (80,080)
7069-10	[10]	Bridge Rail	F-Shape	1,067 (42)	254 (10)	991 (39)	84.0 (52.2)	14°	22,680 (50,000)
7069-13	[10]	Bridge Rail	Vertical	1,067 (42)	254 (10)	991 (39)	82.7 (51.4)	16.2°	22,702 (50,050)
405511-2	[11]	Bridge Rail	Vertical	1,067 (42)	254 (10)	991 (39)	80.1 (49.8)	14.5°	36,000 (79,366)
ACBR-1	[12]	Bridge Rail	Open Concrete Rail	1,067 (42)	254 (10)	1,321 (52)	79.5 (49.4)	16.3°	35,822 (78,975)
7D 04/HK	[13-14]	Bridge Rail	Steel New Jersey with Steel Rail	980/1,595 (38.5/62.8)	Unknown	Unknown	67.6 (42.0)	20°	38,000 (83,776)
SBG-1	[15]	Bridge Rail	Modified New Jersey Shape	1,050 (41.3)	340 (13.5)	1,000 (39.4)	81.3 (50.5)	15.6°	35,934 (79,220)
RYU-1	[16]	Bridge Rail	Modified New Jersey Shape	1,050 (41.3)	450 (17.7)	1,000 (39.4)	79.0 (49.1)	14.6°	36,129 (79,650)
TL5CMB-2	[17]	Median Barrier	Modified Single Slope	1,067 (42)	NA	NA	84.9 (52.8)	15.4°	36,154 (79,705)
4798-13	[18]	Median Barrier	New Jersey Shape	1,067 (42)	NA	NA	83.8 (52.1)	16.5°	36,369 (80,180)
7162-1	[19]	Median Barrier	New Jersey Shape	1,067 (42)	NA	NA	79.8 (49.6)	15.1°	36,287 (80,000)
7046-3	[21]	Instrumented Wall	Vertical Wall	2,286 (90)	NA	NA	88.5 (55)	15.3°	36,324 (80,080)

NA = Not Applicable

Table 2. Summary of Tractor-Trailer Crash Tests, Resulting Barrier and Deck Damage

Test No.	Barrier Damage	Deck Damage
Test 6	40 mm (1.5 in.) concrete rail displacement, 300 mm (12 in.) steel rail displacement, cracking in rail;	Cracking in bridge deck extending 9 m (30 ft) upstream and 15 m (50 ft) downstream of impact
2416-1	13 mm (0.5 in.) concrete rail displacement, 150 mm (6 in.) steel rail displacement, Anchor failure on post 5 & 6	Unavailable
7069-10	Spalling along top of barrier Contact marks and gouging	Unavailable
7069-13	Spalling along top of barrier Contact marks and gouging	Unavailable
405511-2	Spalling along top of barrier Contact marks and gouging	Unavailable
ACBR-1	100 mm (4 in.) displacement in rail Cracking gouging and spalling on face of rail Small pieces fractured off from top of barrier	Cracking in deck Significant spalling/fracture behind posts
7D 04/HK	Contact marks and gouging Bent and dented panels Barriers displaced (slid) backward	None documented in report
SBG-1	Contact marks and gouging	None documented in report
RYU-1	Contact marks and gouging	None documented in report
TL5CMB-2	Contact marks and gouging Spalling along top of barrier Minor cracking	NA
4798-13	Unavailable	NA
7162-1	Contact marks and gouging Spalling along the top of the barrier Cracking – up to 6 mm (¼ in.) wide	NA
7046-3	NA	NA

NA = Not Applicable

5

3 DESIGN CRITERIA

3.1 Geometric Requirements and Material Specifications

Although median barrier, roadside barrier, and bridge rail configurations were all desired for the new MASH TL-5 concrete barrier, the bridge rail was considered the most critical design as it was single-sided with the narrowest cross section, thus requiring the most anchorage strength. Additionally, the bridge rail required attachment to a thin, cantilever bridge deck, which was more susceptible to damage than a foundation slab or footing utilized for the median or roadside applications. Thus, design and testing was to focus on the bridge rail configuration. Then, pending a successful crash test, the other configurations would be designed to have equivalent strength as the bridge rail. Both interior and end sections (adjacent to discontinuities) of the barrier were designed.

The new median barrier and bridge rail systems were required to have a height of 1,250 mm (49¼ in.) and a maximum base width of 600 mm (23¾ in.). The barrier was to have a constant slope face geometry with a 9 degree slope from vertical, creating a 200-mm (8-in.) lateral offset from its base to its top. The bridge deck was to have a minimum thickness of 250 mm (10 in.), and the backside of the barrier was to be offset from the edge of the deck by 50 mm (2 in.). Barrier reinforcement was to consist of both longitudinal and transverse steel with additional reinforcing bars required to anchor the barrier to the deck.

System discontinuities can create higher stresses and a higher risk of component failure. Thus, the full-scale test was to be conducted on a test installation incorporating an expansion and contraction joint in both the bridge rail and the deck. Typical joints in MI bridge decks were an average of 215 mm (8.5 in.) wide and consisted of steel components utilized to transfer shear across the joint. Concrete barriers cannot be cast directly on these adjustable steel joints, so gaps the size of the steel joint hardware were often left in the barrier system. Therefore, a similar width gap was to be placed within the test installation. Development of a steel cover plate was desired to span across the open joint in the barrier and protect a vehicle from snagging on exposed ends of the barrier. The cap would be anchored only to the upstream side of the joint to allow the joint to expand and contract. A steel cover plate design currently utilized by MI served as the basis for the barrier joint design herein.

The new TL-5 barrier was to be designed, constructed, and evaluated with materials in compliance with MI's standard specifications. MI specifies that 35 MPa (5,000 psi) concrete design strength be used for its bridge decks and concrete bridge barriers in the design process. For construction, MI specifies the minimum concrete design strength be increased to 45 MPa (6,500 psi) for enhanced durability. Since the as-constructed concrete design strength is 45 MPa (6,500 psi) or greater for current bridge barriers, it was thought more prudent to crash test a barrier using the higher concrete design strength as this would be more representative of the as-constructed barriers. Thus, the concrete was required to have a minimum compressive strength of 45 MPa (6,500 psi). Reinforcement was to consist of Steel Grade 400W Canadian Metric Rebar with sizes between 10M and 20M. Transverse steel bars were to be spaced at intervals divisible by 50 mm (2 in.) with a 100-mm (4-in.) minimum spacing. Steel reinforcement required 75 mm

(3 in.) of concrete cover with the exception of a 50-mm (2-in.) cover allowance for the bottom layer of deck reinforcement.

3.2 Barrier Design Strength

According to the *AASHTO LRFD Bridge Design Specifications* [20], a TL-5 barrier should be designed to support a 552-kN (124-kips) lateral load applied at the top of the barrier. However, a review of prior research and current barrier designs indicated that this design load may be too low. Thus, the recommended load application height at the top of the barrier was utilized during the development of MI's new TL-5 barrier, but the magnitude of the load was refined based on previous research.

An extensive study of vehicle impact loads was previously conducted at the Texas A&M Transportation Institute (TTI) in which an instrumented vertical wall was subjected to impacts from multiple vehicles. Load cells within the wall were used to measure the magnitude of each impact event [21]. Of specific interest to this study, a 36,000-kg (79,400-lb) tractor trailer impacted the wall at 86 km/h (55 mph) and 15 degrees, matching the MASH TL-5 impact criteria. The peak lateral load of the tractor trailer was measured to be 980 kN (220 kips) during the impact of the trailer's rear tandem axles against the wall.

Barrier strengths were also calculated for previously designed and successfully crash tested TL-5 barriers. Barrier capacities were calculated utilizing Yield Line Theory, a common analysis method for concrete barriers and recommended by the *AASHTO LRFD Bridge Design Specifications* [20]. The list of barriers shown previously in Tables 1 and 2 was pared down to include only barriers tested to the current MASH TL-5 impact criteria and avoid barriers that may not satisfy current strength requirements. Additionally, barrier systems containing either steel rail components or Fiber Reinforced Polymer (FRP) reinforcement were also disregarded as these systems would require different analysis techniques. Although the California Single-Slope barrier was never crash tested with heavy vehicles, it has been widely considered to be a TL-5 barrier and has been listed in the *AASHTO Roadside Design Guide* [22] as a TL-5 barrier. Thus, the California Single-Slope barrier was included in the barrier strength analysis. The five barriers that were analyzed are listed along with their calculated strengths in Table 3.

Four of the five barriers listed in Table 3 had design strengths below the 980-kN (220-kip) load measured from testing with the instrumented wall, although all barriers were within 10 percent of this measured value. Only one of the tested TL-5 barriers listed in Table 3 sustained heavy damage during the impact, as the open concrete rail evaluated in test no. ACBR-1 showed rail, post, and deck damage. Damage to the other four barriers consisted of only contact marks, gouging, and minor cracking. Therefore, Yield Line Theory was thought to underestimate the actual capacity of a concrete barrier, especially for closed shaped barriers, and the design strength required of a concrete barrier to satisfy MASH TL-5 is likely lower than the strength of existing TL-5 barrier systems. In recognition of Yield Line Theory's conservative nature and through discussions with the project sponsor, a minimum design load of 845 kN (190 kips) was selected for the new MI TL-5 barrier.

Table 3. TL-5 Concrete Barrier Strengths

System Shape	Height mm (in.)	Configuration	Ref. No.	Crash Test No.	Barrier Strength ¹ kN (kips)
New Jersey Barrier	1,067 (42)	Median	[18]	4798-13	1,913 (430)
Vertical	1,067 (42)	Bridge Rail	[11]	405511-2	890 (200)
Open Concrete Rail	1,067 (42)	Bridge Rail	[12]	ACBR-1	939 (211)
Single Slope – Modified for Head Ejection	1,067 (42)	Median	[17]	TL5CMB-2	956 (215)
California Single Slope	1,067 (42)	Median	[22]	NA	916 (206)

¹ Barrier Strengths Calculated with Load Applied at Top of Barrier, 1,067 mm (42 in.)

3.3 Deck Design Strength

The strength of a bridge deck supporting a TL-5 concrete bridge rail must satisfy three design cases in order to comply with the *AASHTO LRFD Bridge Guide Specifications* [20]:

1. A 552-kN (124-kip) lateral load applied to the face of the bridge rail and transferred down to the deck as both a shear force and moment.
2. A 356-kN (80-kip) vertical load applied to the cantilever portion of the bridge deck
3. The bending strength of the deck must be equal to or greater than the overturning moment strength of the barrier (M_c term in Yield Line analysis of the barrier).

In practice, the first two design cases rarely control the design strength of the bridge deck. Design Case 2 only controls for decks with large cantilever distances (i.e., greater than 2 m (6.5 ft) between the edge of the outer most girder and the edge of the deck). The prescribed lateral load in Design Case 1 is much lower in magnitude than the targeted design strength of the barrier, 845 kN (190 kips), so it would not control the deck design strength either. Therefore, Design Case 3 typically controls the required strength of the bridge deck.

Previous crash testing has demonstrated the ability of bridge decks with bending strengths lower than the barrier M_c to support TL-5 impacts without damage. Table 4 contains a summary of four TL-5 crash tests on concrete bridge rails supported by simulated bridge decks. The overturning strength of each barrier, M_c , and the bending strength of each simulated bridge deck was calculated and is shown as strength per unit length. The ratio of the deck strength to the barrier overturning strength was also calculated. Three of the reviewed crash tests featured bridge decks with strengths significantly lower than that provided by the barrier (strength ratios less than 1.0). Two of these reduced-capacity decks, which had strength ratios of 0.71 and 0.85, sustained no structural damage during the full-scale crash test. Thus, previous testing has demonstrated the ability of decks with only 71 percent of the barrier M_c to adequately support

the barrier during impact events. After consulting with the project sponsors, a deck strength of 85 percent of the barrier M_c was selected as the design strength for the new TL-5 bridge rail.

Table 4. Crash Tested TL-5 Bridge Rails, Parapet and Deck Strengths

Test No.	Ref. No.	Barrier		Deck			
		Shape	M_c kN-m/m (k-in./ft)	Thickness mm (in.)	Strength kN-m/m (k-in/ft)	$\frac{\text{Strength}}{\text{Barrier } M_c}$	Damage
7069-10	[10]	F-shape	147 (397)	254 (10)	125 (336)	0.85	None
405511-2	[11]	Vertical	105 (284)	254 (10)	75 (203)	0.71	None
ACBR-1	[12]	Open Concrete Rail	219 (590)	254 (10)	102 (276)	0.47	Cracking in deck, fractures behind posts
SBG-1	[15]	New Jersey	169 (456)	340 (13.5)	249 (673)	1.47	None

4 BARRIER ANALYSIS AND DESIGN

4.1 Bridge Rail Design

Through discussions with the project sponsor, MI, a general barrier configuration was established for the new TL-5 bridge rail. The rail would be a 1,250-mm (49¹/₄-in.) tall, single-slope barrier with a vertical back side. Steel reinforcement would consist of both longitudinal bars and transverse stirrups. The stirrups would be U-shaped with the open ends extending into the narrow top of the rail. Minimum bend radii for larger bars prohibited a continuous loop stirrup from fitting inside the narrow top of the barrier. A sketch of the general configuration is shown in Figure 1.

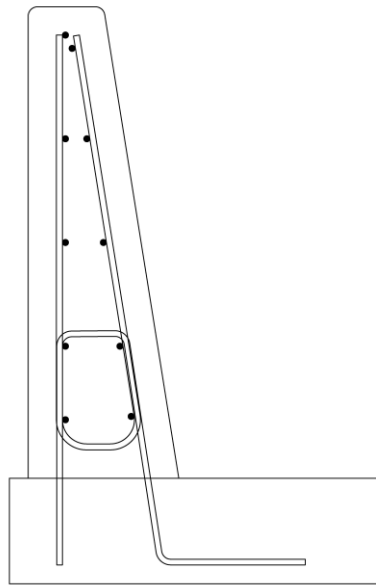


Figure 1. General Configuration of Manitoba Bridge Rail

Variables within the general design configuration included barrier width, size and number of longitudinal bars, and size and spacing of the transverse steel U-bars. For a median (double-sided) configuration, a 200-mm (8-in.) top width resulted in the maximum targeted base width of 600 mm (23³/₄ in.). However, a narrower, single-sided configuration occupied less space and could be widened without unacceptably encroaching towards traffic. Thus, barrier top widths of both 200 mm (8 in.) and 250 mm (10 in.) were considered. Top widths greater than 250 mm (10 in.) were undesirable.

All steel reinforcement was to consist of bar sizes ranging between 10M and 20M. The barrier longitudinal steel was to consist of either 10 or 12 bars, divided evenly between the front and back sides of the barrier. These quantities created desirable bar spacings between 200 mm and 300 mm (8 in. and 12 in.) along the height of the barrier. The transverse steel U-bars were to be spaced at intervals divisible by 50 mm (2 in.) with a minimum spacing of 100 mm (4 in.), (e.g., 100 mm, 150 mm, 200 mm, etc.).

The bridge rail design was optimized to satisfy the minimum design strength, 845 kN (190 kips), and to minimize the cost of the barrier system. The strength of the various configuration possibilities was calculated utilizing Yield Line Theory, as recommended by the *AASHTO LRFD Bridge Design Specifications* [20], assuming the lateral impact load was applied to the top of the barrier at a height of 1,250 mm (49¼ in.) and distributed over 2.4 m (8 ft). Construction costs for the various configurations were thought to be closely related with the amount of steel reinforcement within the barrier. Thus, the amount of steel in each configuration was calculated per unit length, kg/m, and these values were utilized to compare the relative costs of each design configuration.

Design configurations were analyzed utilizing an iterative approach, changing only one variable at a time. For a specific width, longitudinal rebar configuration, and stirrup bar size, the largest stirrup spacing to satisfy the 845-MPa (190-kip) strength requirement was determined. The resulting barrier configuration was documented, and the amount of steel per unit length was calculated. This process was repeated for each possible combination of width, longitudinal bar size, longitudinal bar quantity, and stirrup size. Additionally, since design configurations for both interior and end sections were required for the new bridge rail, the entire procedure was conducted twice, once with the Yield Line equation for interior sections and the second time with the equation for end sections.

Early in the analysis procedure, it was noted that 10M bars, when used as longitudinal steel or stirrups, did not provide enough strength to satisfy the 845-kN (190-kip) design load. As such, 10M bars were removed from the list of possible bar sizes, and only 15M and 20M bars were considered. The results of the optimization analysis are shown in Table 5.

As expected, the design configurations with a 250-mm (10-in.) top width tended to contain less steel than the 200-mm (8-in.) top width designs. The increased width resulted in increased strength and decreased the required steel by an average of 4 kg/m (3 lb/ft) for interior sections and 10 kg/m (7 lb/ft) for end sections. This reduction in steel was more than enough to offset the cost of the additional concrete required for a wider barrier. Thus, the 250-mm (10-in.) top width designs were favored over the narrower widths.

The barrier configuration that resulted in the lowest amount of steel utilized a 250-mm (10-in.) top width, ten 15M longitudinal bars, and 20M stirrups spaced at 400 mm (15¾ in.). This interior configuration required only 29.7 kg/m (20.0 lb/ft) of steel, about 1 kg/m (0.7 lb/ft) less than any other design. This configuration also allowed for a stirrup spacing 150 mm (6 in.) larger than the configuration with the second lowest amount of steel, thus requiring less steel ties. Therefore, this configuration was identified as the optimal design for interior barrier sections.

For construction purposes, it was desired to keep the longitudinal steel the same for both the interior and end section configurations. Ideally, only the stirrup spacing would be reduced for end sections adjacent to rail discontinuities. Conveniently, the end section configuration that resulted in the second lowest amount of steel matched perfectly with the optimal interior configuration. This end section was identical to the interior section, except the stirrup spacing was reduced from 400 mm (15¾ in.) to 200 mm (8 in.), or half of the interior section configuration. Therefore, combination of these two configurations, highlighted in Table 5, were

selected as the optimal designs for MI's new TL-5 bridge rail and were recommended for further evaluation through full-scale crash testing.

During the Yield Line analysis of the barrier end section, a critical length, L_{CR} , of 2.7 m (8.8 ft) was calculated. Thus, it was recommended that the end section configuration with reduced stirrup spacing extend at least 2.7 m (8.8 ft) from any rail discontinuity.

Although the strength analysis herein was conducted assuming a load height of 1,250 mm (49¼ in.), it was recognized that other designers may utilize different load heights and different design loads. For comparison purposes, the strength of the selected interior design configuration was also calculated assuming load heights of 860 mm (34 in.) and 1,090 mm (43 in.). These applied load heights resulted in strength capacities of 1,143 kN (257 kips) and 970 kN (218 kips), respectively.

Table 5. Optimization Analysis Results for Bridge Rail Configurations

Top Barrier Width (mm)	Longitudinal Steel		Transverse Steel	Interior Section			End Section		
	No. of Bars	Size	Size	Transverse Steel Spacing (mm)	Barrier Strength (kN)	Total Steel (kg/m)	Transverse Steel Spacing (mm)	Barrier Strength (kN)	Total Steel (kg/m)
200	10	15M	15M	200	927	34.4	100	1,136	53.1
200	12	15M	15M	200	978	37.5	100	1,150	56.2
200	10	20M	15M	250	897	38.5	100	1,168	60.9
200	12	20M	15M	250	847	43.2	100	1,184	65.6
200	10	15M	20M	300	906	34.4	150	1,077	53.1
200	12	15M	20M	300	883	37.5	150	1,090	56.2
200	10	20M	20M	400	862	37.6	200	892	51.6
200	12	20M	20M	400	909	42.3	200	908	56.3
250	10	15M	15M	250	916	30.6	150	889	40.6
250	12	15M	15M	300	860	31.3	150	904	43.8
250	10	20M	15M	300	920	36.0	150	922	48.5
250	12	20M	15M	350	888	38.9	150	942	53.2
250	10	15M	20M	400	874	29.7	200	983	43.7
250	12	15M	20M	450	858	31.3	200	998	46.9
250	10	20M	20M	500	860	34.8	250	847	46.0
250	12	20M	20M	500	915	39.5	250	866	50.7

4.2 Deck Design

An optimized bridge deck was designed to support the new TL-5 bridge rail. The deck was required to be a minimum of 250 mm (10 in.) thick and contain an upper and lower mat of steel reinforcement. The upper and lower mats were to have concrete covers of 75 mm. (3 in.) and 50 mm (2 in.), respectively. A 15M bar spaced at 350 mm (13¾ in.) was prescribed as the longitudinal steel in both reinforcement mats, which was typical of large bridges in Manitoba. The lateral steel bar configurations needed to be designed to support the new bridge rail.

As discussed previously in Section 3.3, the design strength for the bridge deck was established as 85 percent of the overturning strength of the bridge rail, M_c . The bridge rail designs selected for further evaluation in Section 4.1 had M_c strengths of 135 kN-m/m (30.3 kip-ft/ft) and 259 kN-m/m (58.3 kip-ft/ft) for the interior and end section configurations, respectively. By multiplying these M_c values by 0.85, the deck design strengths were established as 114 kN-m/m (25.7 kip-ft/ft) for regions supporting interior bridge rail sections and 220 kN-m/m (49.5 kip-ft/ft) for regions supporting end sections near discontinuities.

For constructability purposes, it was desired for the lateral steel bars in the deck to be spaced to match the barrier stirrups so that transverse steel from both structures could be tied together. Thus, the lateral bars in the deck were targeted for placement at intervals of 400 mm and 200 mm (15¾ in. and 8 in.) for interior and end sections, respectively. However, in order to satisfy the design strength requirements for the deck, the lateral steel in the top mat was doubled, which still allowed every other bar to be tied to the barrier stirrups.

The selected deck configuration was 280 mm (11 in.) thick and consisted of 20M bars spaced at 200 mm (8 in.) along the top mat of steel and 15M bars spaced at 400 mm (15¾ in.) along the bottom mat. This configuration gave the interior deck section a strength of 121 kN-m/m (27.3 kip-ft/ft). Similar to the bridge rail reinforcement, the lateral steel bars in the deck end section were doubled, resulting in a spacing of 100 mm (4 in.) for the 20M bars and 200 mm (8 in.) for the 15M bars. The deck end section had a calculated strength matching the targeted design strength of 220 kN-m/m (49.5 kip-ft/ft).

The length of the deck overhang, the cantilever portion of the barrier adjacent to the edge of the deck, was desired to be 1,300 mm (51¼ in.). This distance represented the largest of the overhang lengths typically utilized by MI. Utilizing a distance of 1,300 mm (51¼ in.), the dead weight of the barrier, and the 356-kN (80-kip) vertical load recommended by loading Case 2 of the *AASHTO LRFD Bridge Guide Specifications*, resulted in a design load of 58 kN-m/m (13 kip-ft/ft). This design load was only 50 percent of the strength of the deck, so the 1,300 mm (51¼ in.) overhang distance was acceptable for use with the new TL-5 bridge rail and deck designs.

4.3 End Section Design for Testing

Expansion and contraction joints in concrete barriers create discontinuities and weak points within a barrier system. Thus, full-scale crash testing was intended to be conducted with the tractor trailer vehicle impacting just upstream from a simulated joint in the bridge rail and

deck. However, the calculated strength of the barrier end section was higher than that of the interior sections, 983 kN (221 kips) as compared to 874 kN (196 kips). An argument could have been made that the interior section was weaker than the end section. To ensure the interior section could withstand a TL-5 impact, the design of the barrier end section was altered only for the full-scale crash test. By extending the spacing of the barrier stirrups from 200 mm (8 in.) to 230 mm (9 in.), the design strength of the end section was reduced to 874 kN (196 kips), matching the capacity of the interior section. This configuration was utilized for full-scale crash testing, but the recommended configuration for real-world installations would still utilize the original 200-mm (8-in.) spacing. Spacing of the lateral steel bars in the deck was also increased to match the transverse steel in the barrier end sections.

During the Yield Line analysis of the barrier end section, a critical length, L_{CR} , of 2.7 m (8.8 ft) was calculated. Thus, it was recommended that the end section configuration with a reduced stirrup spacing extend at least 2.7 m (8.8 ft) from any rail discontinuity. For the test installation shown in Chapter 5, end section reinforcement pattern covered a distance of 2.86 m (9.4 ft) on each side of the open joint.

5 DESIGN DETAILS

The test installation was comprised of a reinforced concrete bridge rail installed on a simulated concrete bridge deck. The total length of the barrier was 45.72 m (150 ft). The upstream half of the barrier was installed on a simulated reinforced concrete bridge deck, while the downstream half was installed on the test site's concrete tarmac. Design details for the test installation are shown in Figures 2 through 25. Photographs of the test installation are shown in Figures 26 and 27. Material specifications, mill certifications, and certificates of conformity for the system materials are shown in Appendix A.

The bridge rail was a 1,250-mm (49¼-in.) tall, single slope barrier, with a slope measuring 9 degrees from vertical. The bridge rail was 250 mm (10 in.) wide at the top and 450 mm (17¾ in.) wide at the bottom, which matched MI's current TL-4 vertical-back F-shape barrier used on bridge decks. Barrier reinforcement consisted of both longitudinal bars and U-shaped stirrups, as shown in Figures 7 and 12. All barrier reinforcement had a concrete cover of 75 mm (3 in.). The edges of the bridge rail contained 20 mm (¾ in.) chamfers, and the back of the barrier was 50 mm (2 in.) from the edge of the bridge deck.

The bridge rail contained a simulated expansion/contraction joint consisting of a 168-mm (6⅝-in.) open gap in the barrier. This distance was selected to represent typical gaps widths in real-world installations and to match up with the transverse steel reinforcement in the deck without requiring abnormal rebar spacing. A cover plate, fabricated from 13-mm (½-in.) thick steel, was placed over the joint and bolted to the upstream side of the barrier, as shown in Figures 18 and 19. The bolts were 19-mm (¾-in.) diameter, flat head, countersunk bolts that laid flush with the cover plate when installed. Steel end caps, containing the corresponding nuts, as shown in Figures 20 through 22, were cast into the ends of the bridge rail adjacent to the open gap. The barrier was recessed 19 mm (¾ in.) adjacent to the joint so that the cover plate was flush with the face of the barrier. Additionally, the leading edge of the cover plate cap was chamfered to prevent vehicle snagging. Photographs of the joint with and without the cover plate are shown in Figure 27. End section reinforcement, characterized by reduced stirrup spacing, was utilized for a distance of 2.86 m (9.4 ft) both upstream and downstream from the open joint.

The simulated bridge deck was 2.9 m (9.5 ft) wide, 280 mm (11 in.) thick, and 22.86 m (75 ft) long. The inner section of the bridge deck was anchored to the adjacent concrete tarmac utilizing epoxied dowel bars. The middle of the bridge deck was supported by a 600-mm (23⅝-in.) tall by 600-mm (23⅝-in.) wide grade beam, as shown in Figures 6 and 17. The cantilevered portion of the simulated bridge deck extended 1.3 m (51¼ in.) past the grade beam. An open joint gap, measuring 19-mm (¾-in.) wide, ran through the middle of the bridge deck and aligned with the center of the open joint in the rail. No connection hardware was utilized to connect the upstream and downstream halves of the bridge deck. The deck was reinforced with upper and lower steel rebar mats. End section reinforcement, characterized by an increase in transverse steel bars, was placed underneath the barrier end sections on both sides of the joint.

The bridge rail, deck, and grade beam were all cast with a concrete mix with a targeted 28-day compressive design strength of 45 MPa (6,500 psi). Concrete cylinders were tested for

strength at 14 days after casting, 28 days after casting, and two days after the test was conducted for all of the concrete pours, as shown in Appendix A. Two days after the full-scale test, the average concrete strengths of the barrier and deck were 47.6 MPa (6,900 psi) and 55.6 MPa (8,065 psi), respectively. Steel reinforcement in the bridge rail and deck consisted of Steel Grade 400W Canadian Metric Rebar, while the grade beam was reinforced with ASTM A615 Grade 60 rebar.

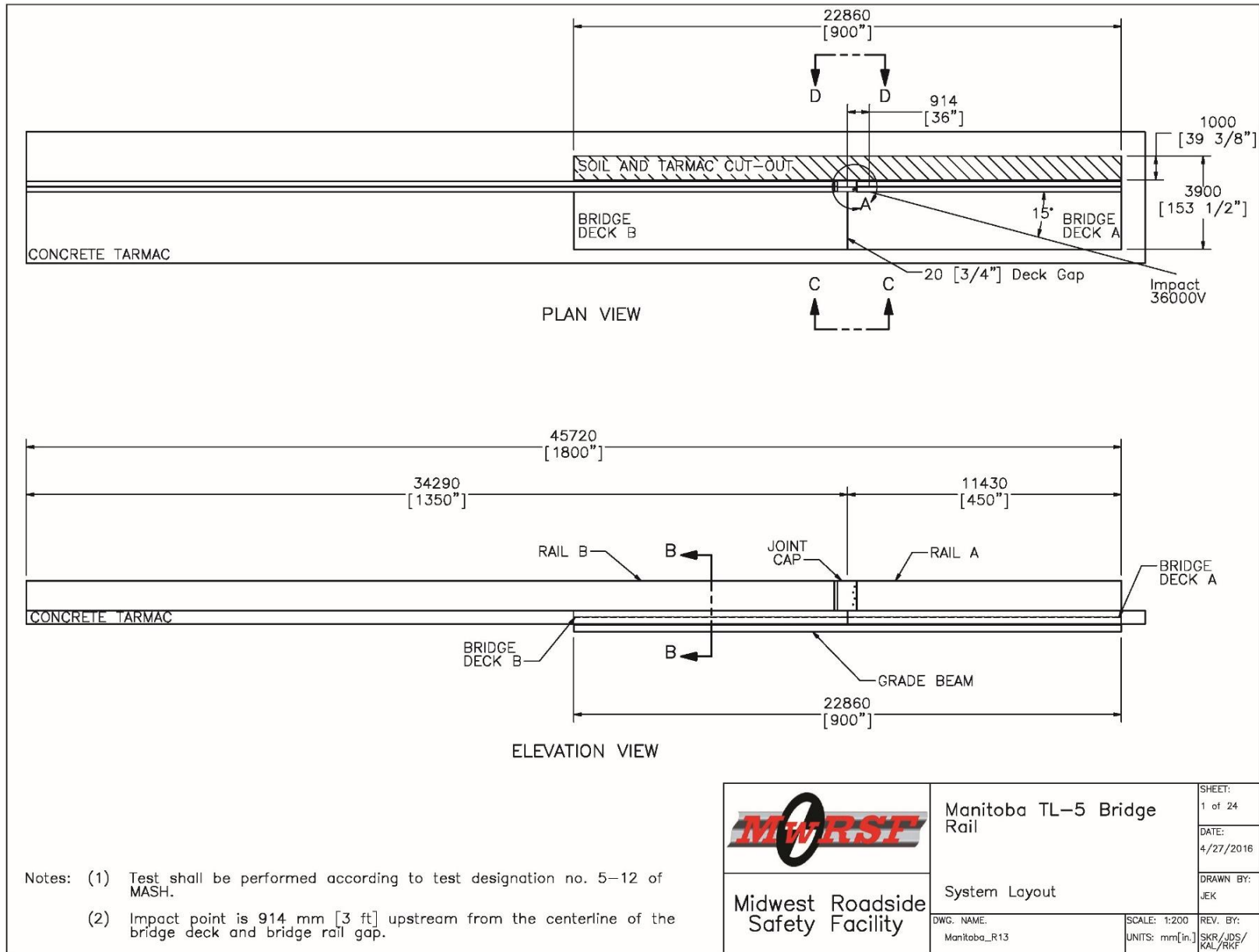


Figure 2 Test Installation Layout, Test No. MAN-1

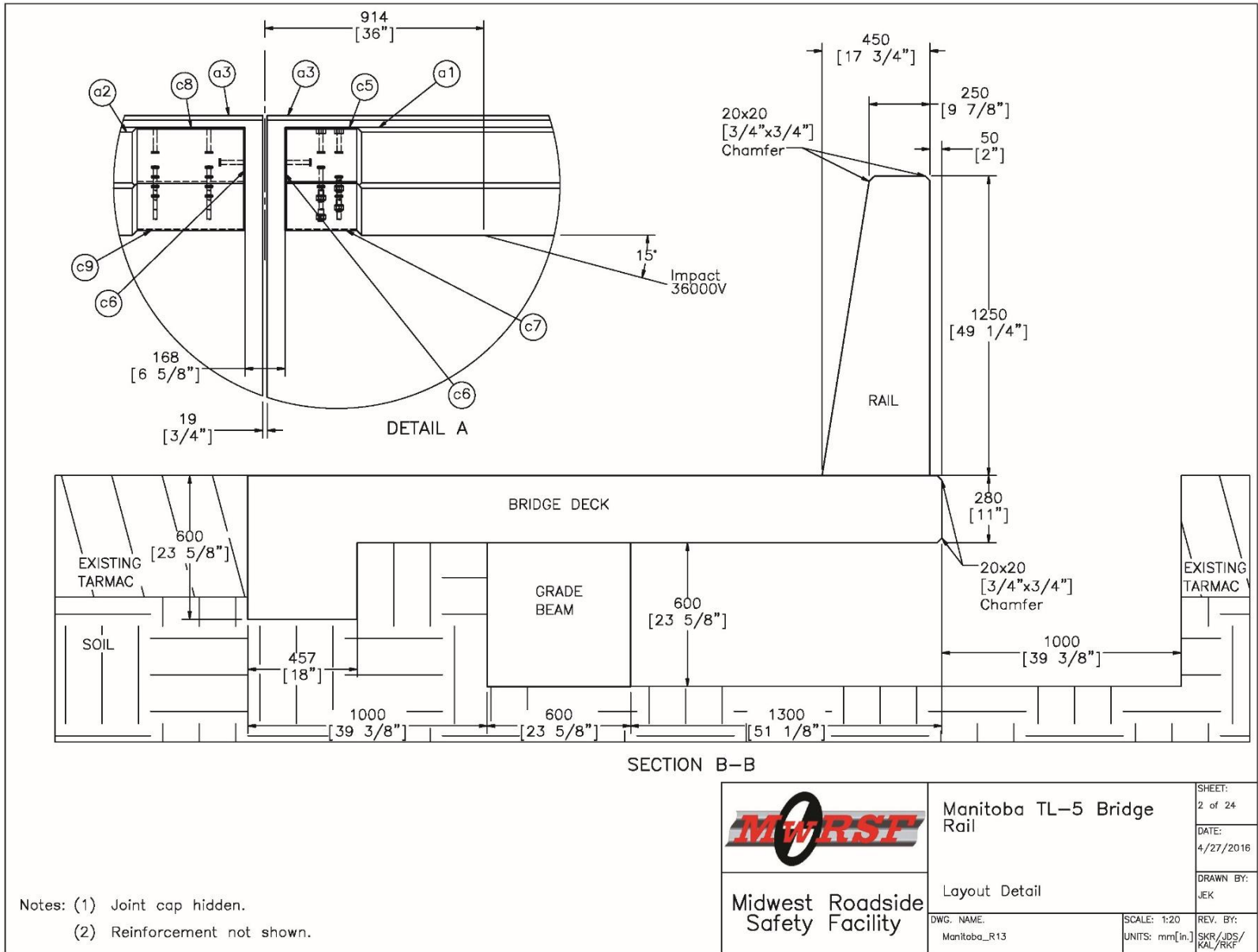


Figure 3. Layout Detail, Test No. MAN-1

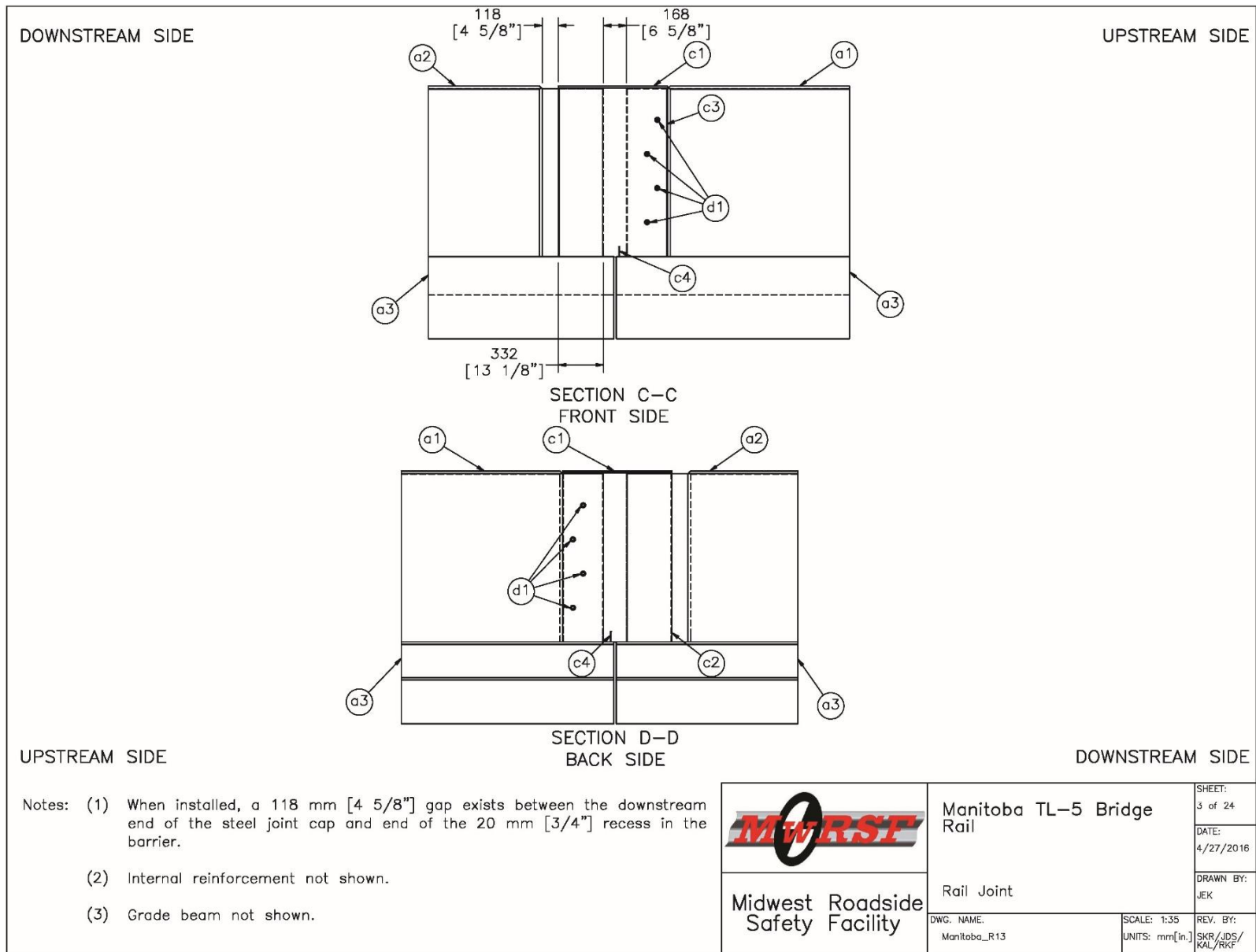


Figure 4. Rail Joint with Cover Plate, Test No. MAN-1

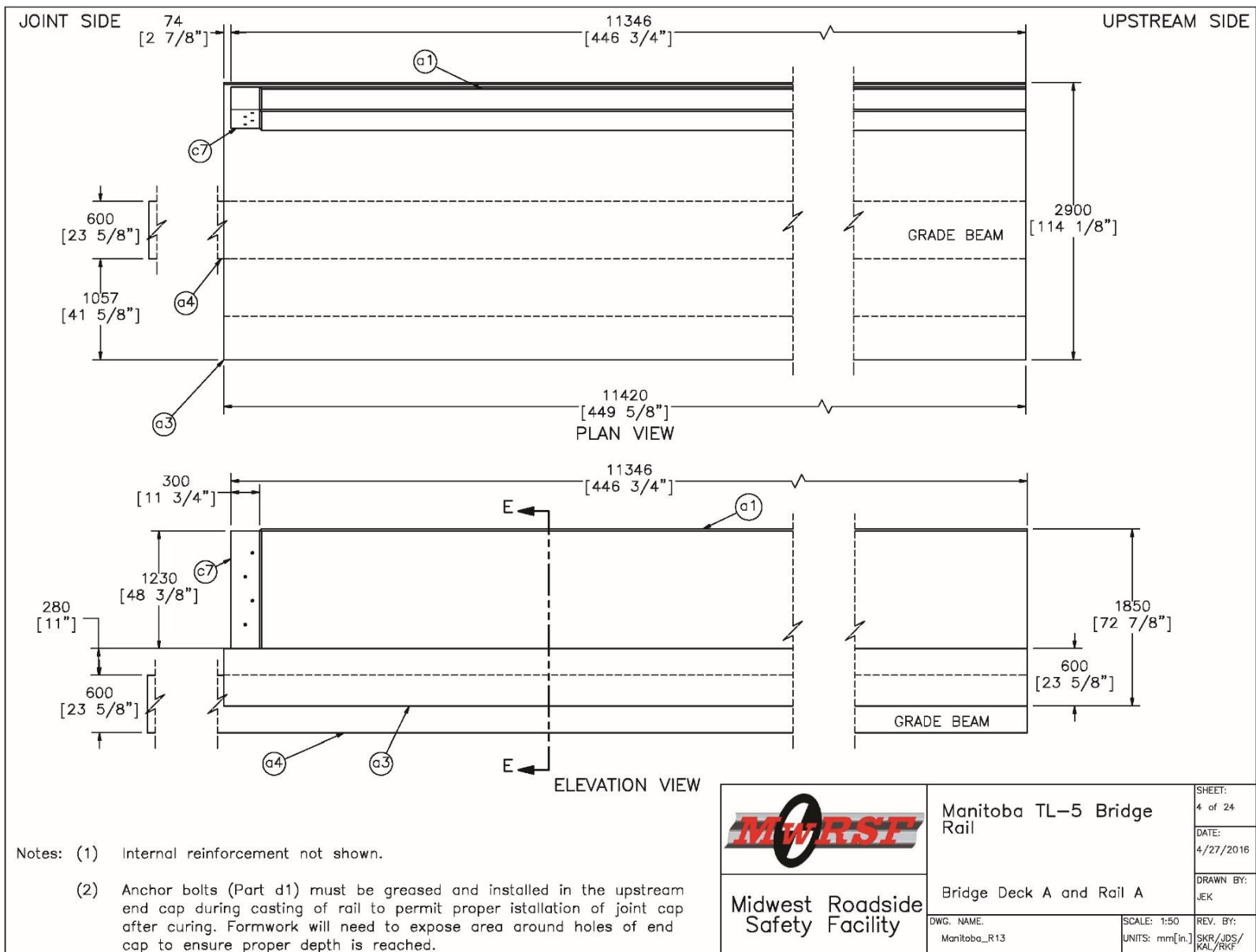


Figure 5. Bridge Deck A and Rail A, Test No. MAN-1

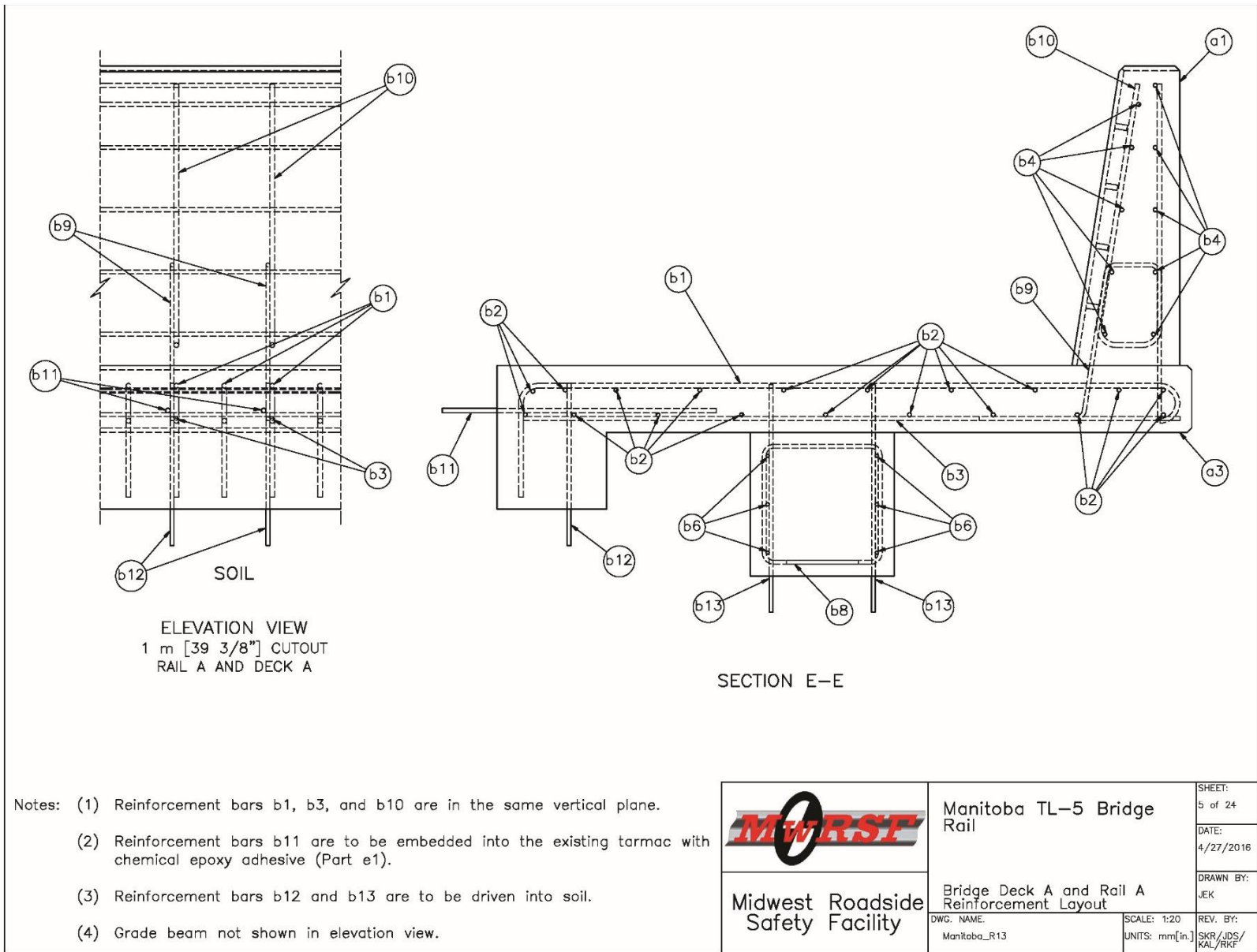


Figure 6. Bridge Deck A and Rail A Reinforcement Layout, Test No. MAN-1

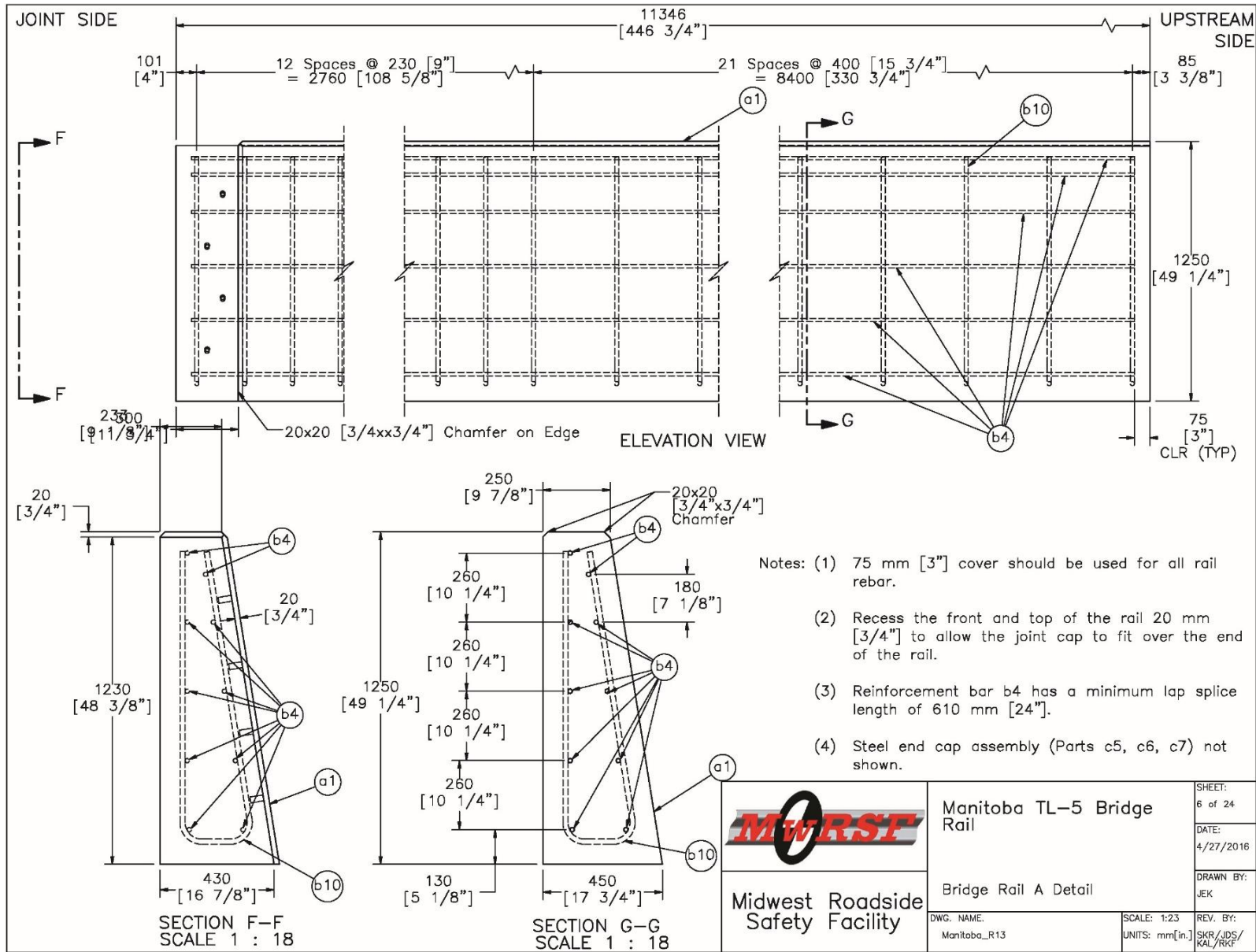


Figure 7. Bridge Rail A Detail, Test No. MAN-1

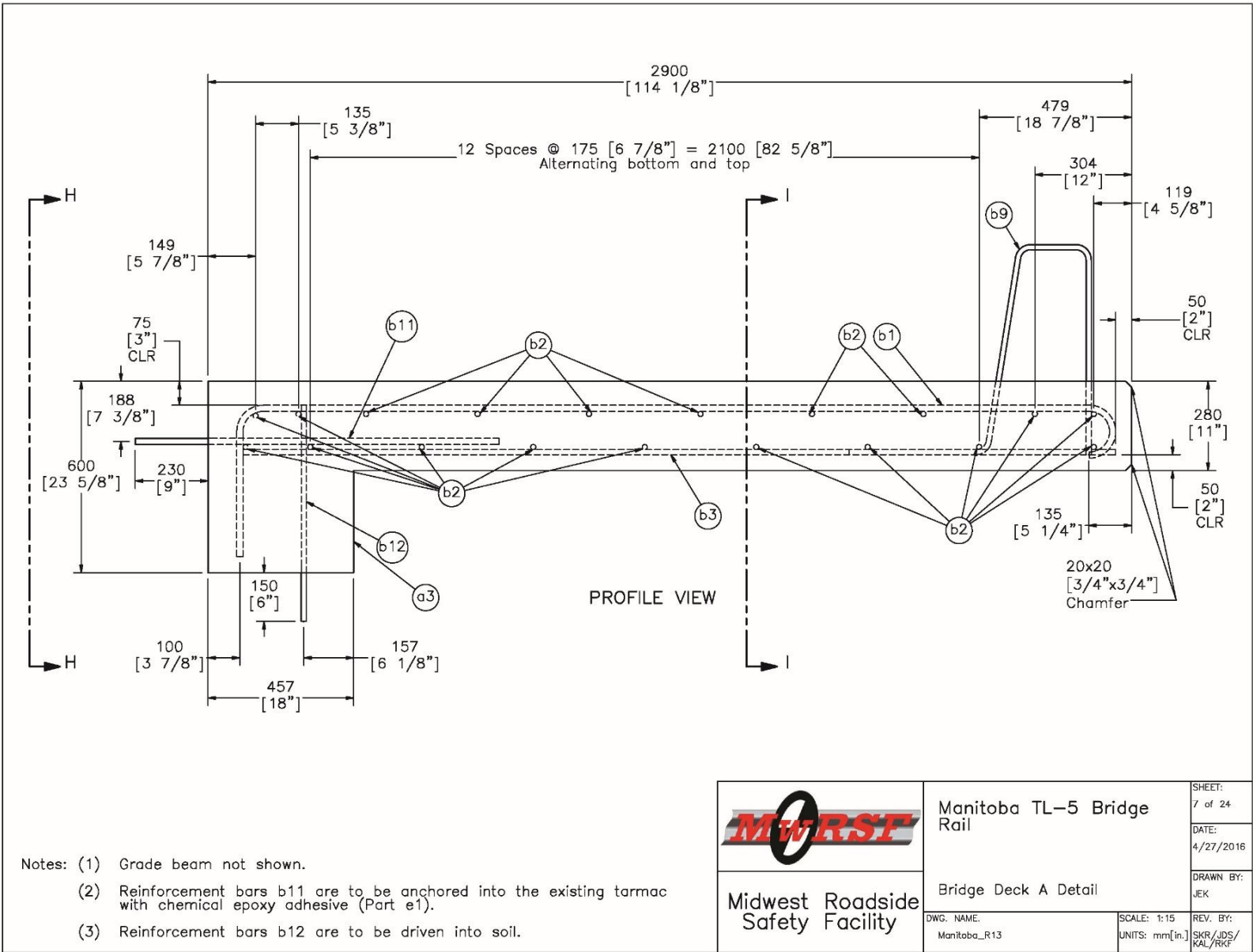


Figure 8. Bridge Deck A Detail, Test No. MAN-1

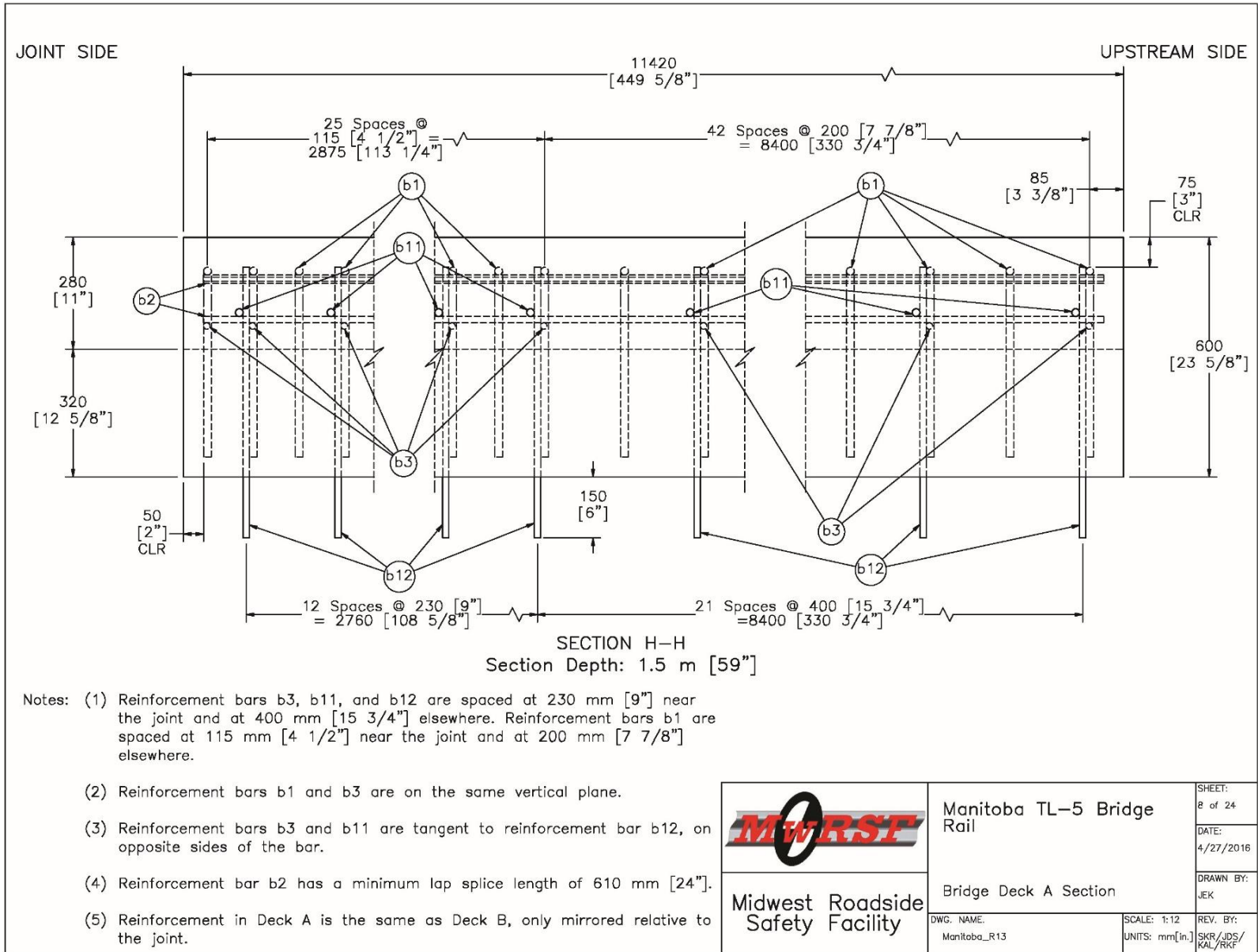


Figure 9. Bridge Deck A Section, Test No. MAN-1

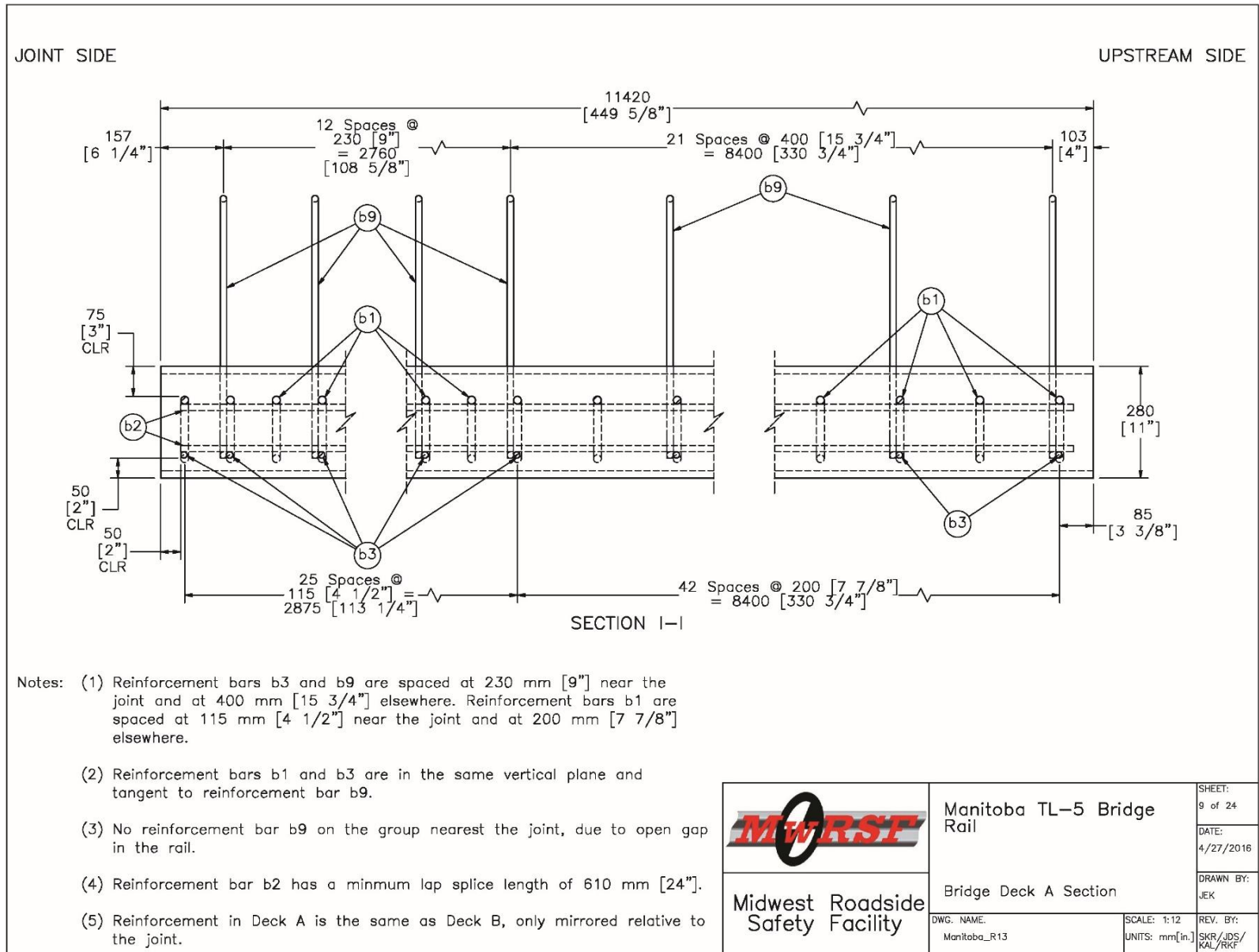


Figure 10. Bridge Deck A Section, Test No. MAN-1

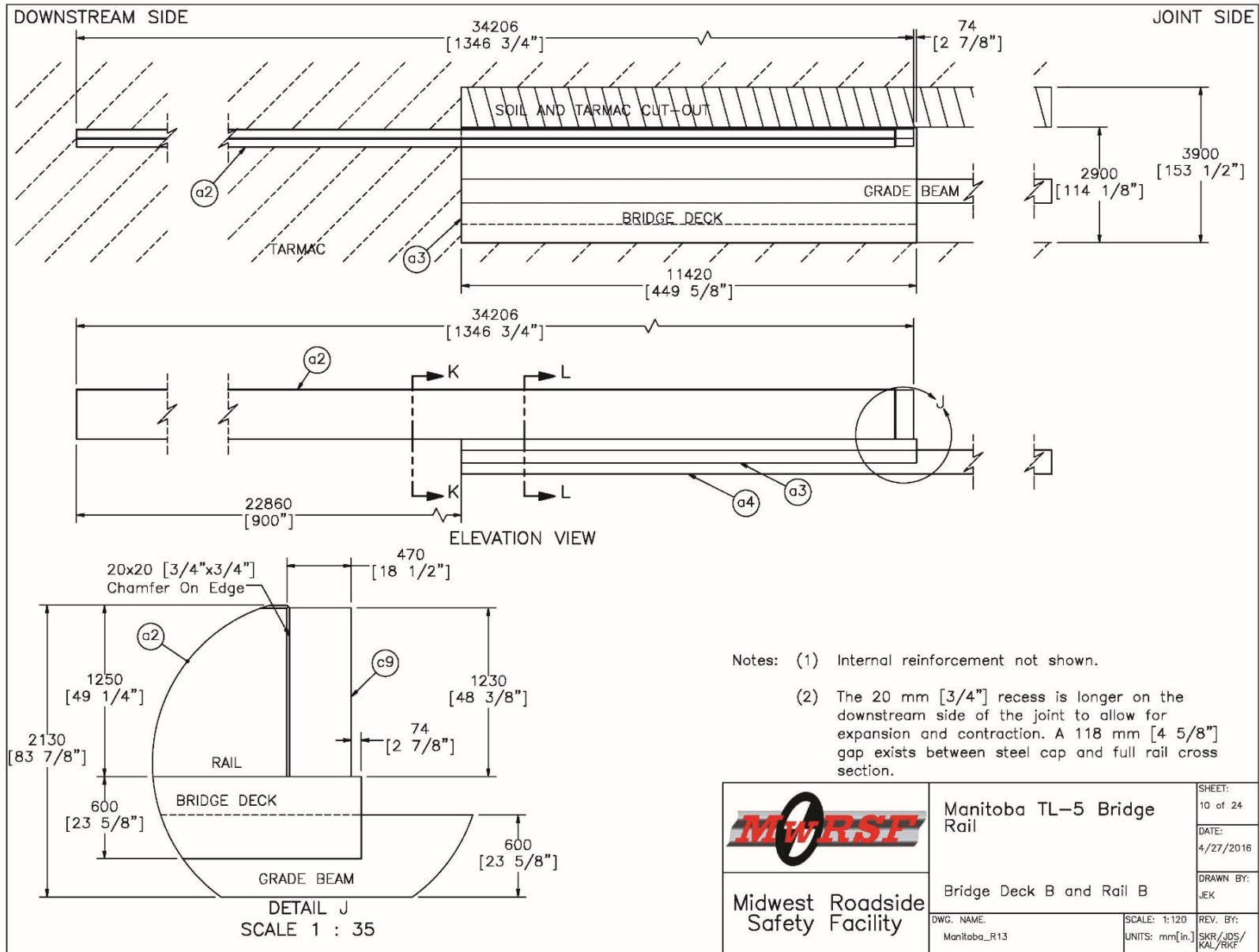


Figure 11. Bridge Deck B and Rail B, Test No. MAN-1

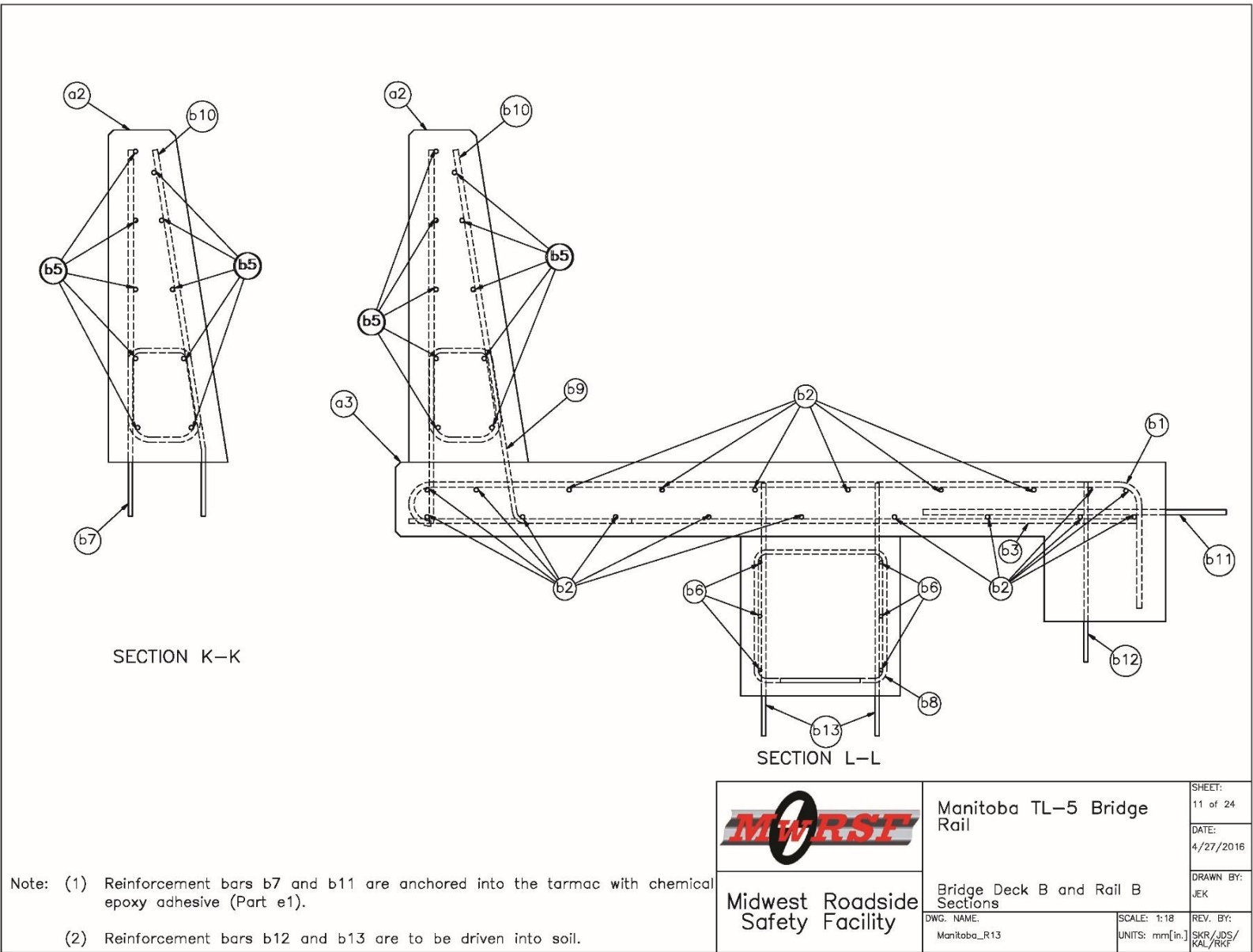


Figure 12. Bridge Deck B and Rail B Sections, Test No. MAN-1

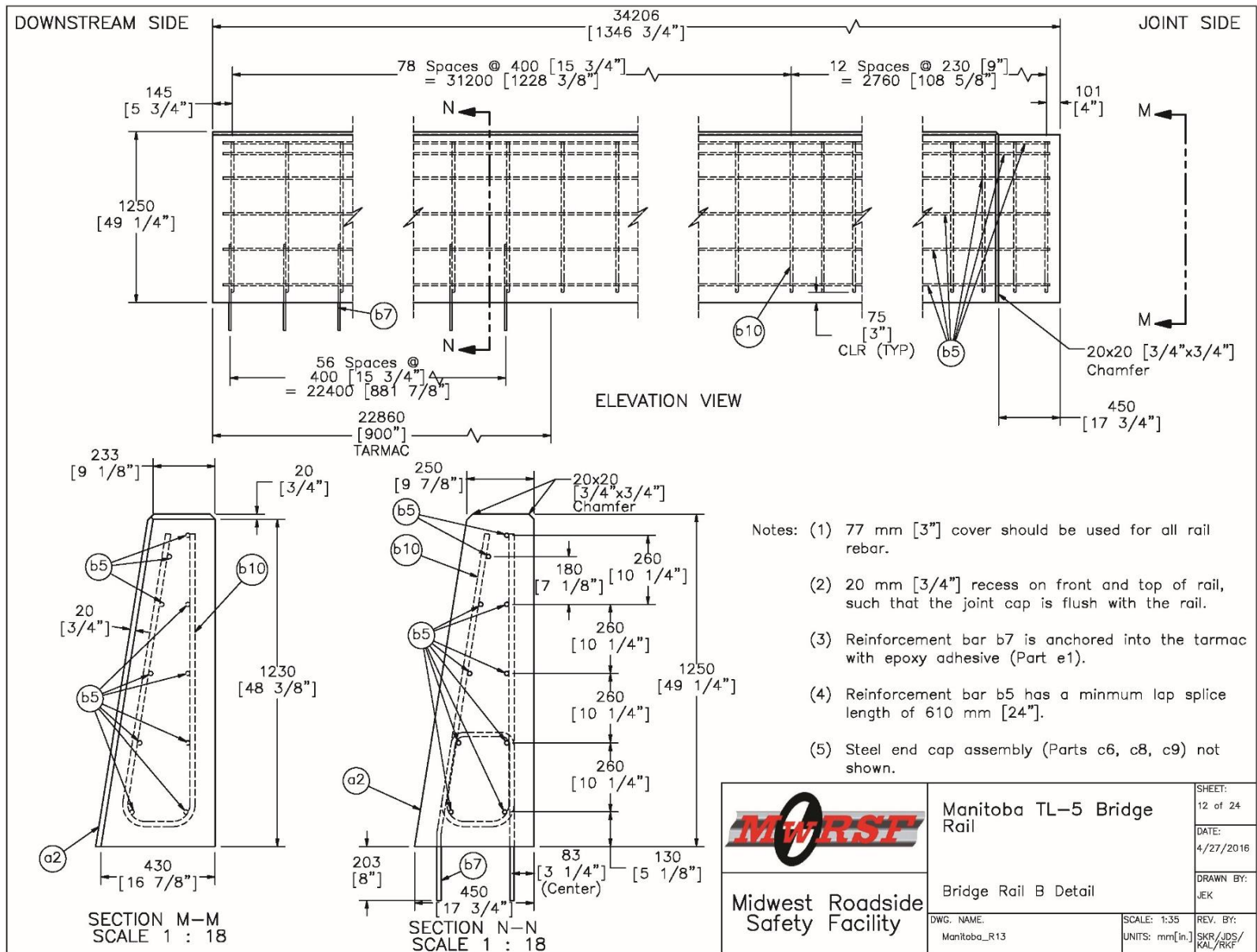


Figure 13. Bridge Rail B Detail, Test No. MAN-1

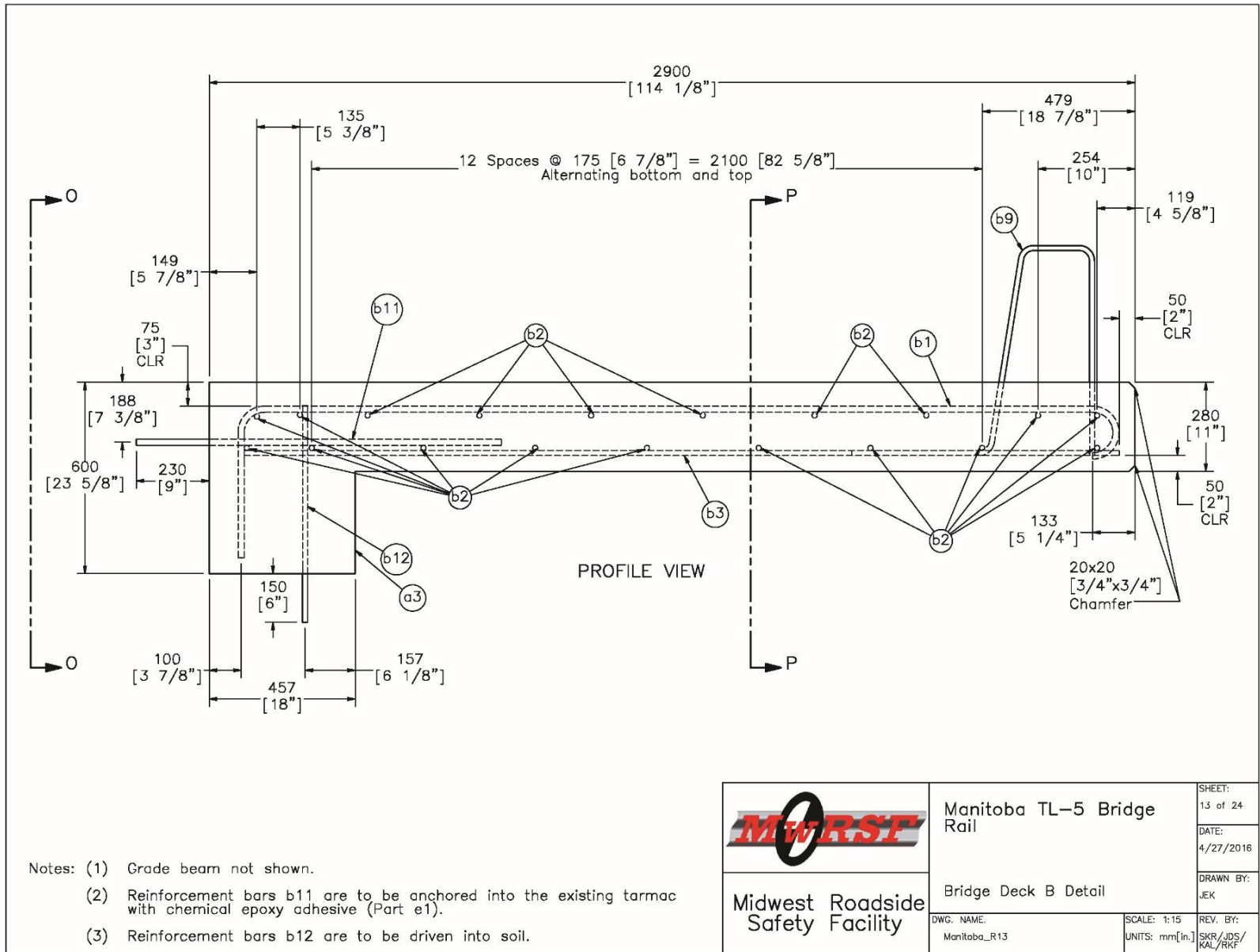


Figure 14. Bridge Deck B Detail, Test No. MAN-1

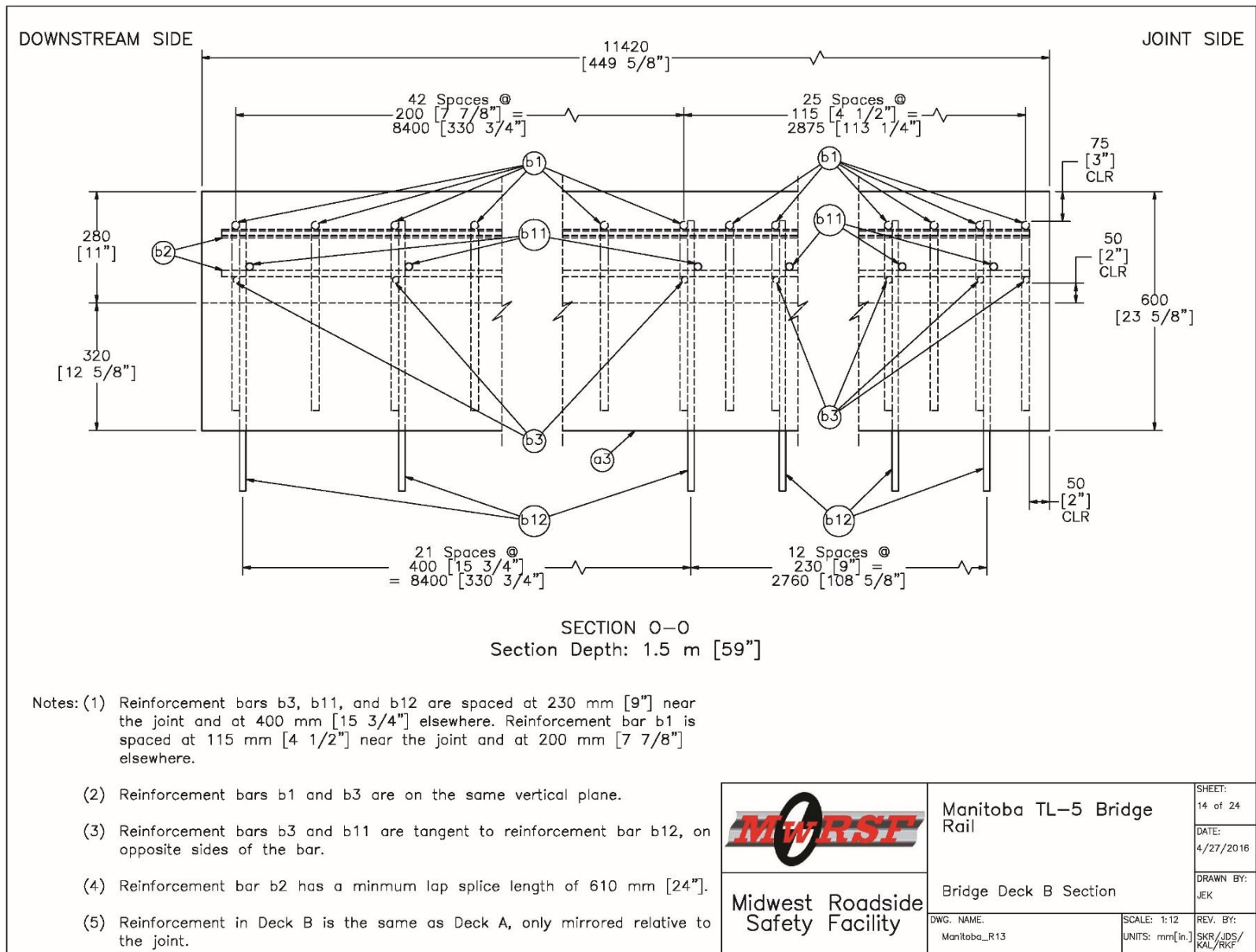


Figure 15. Bridge Deck B Section, Test No. MAN-1

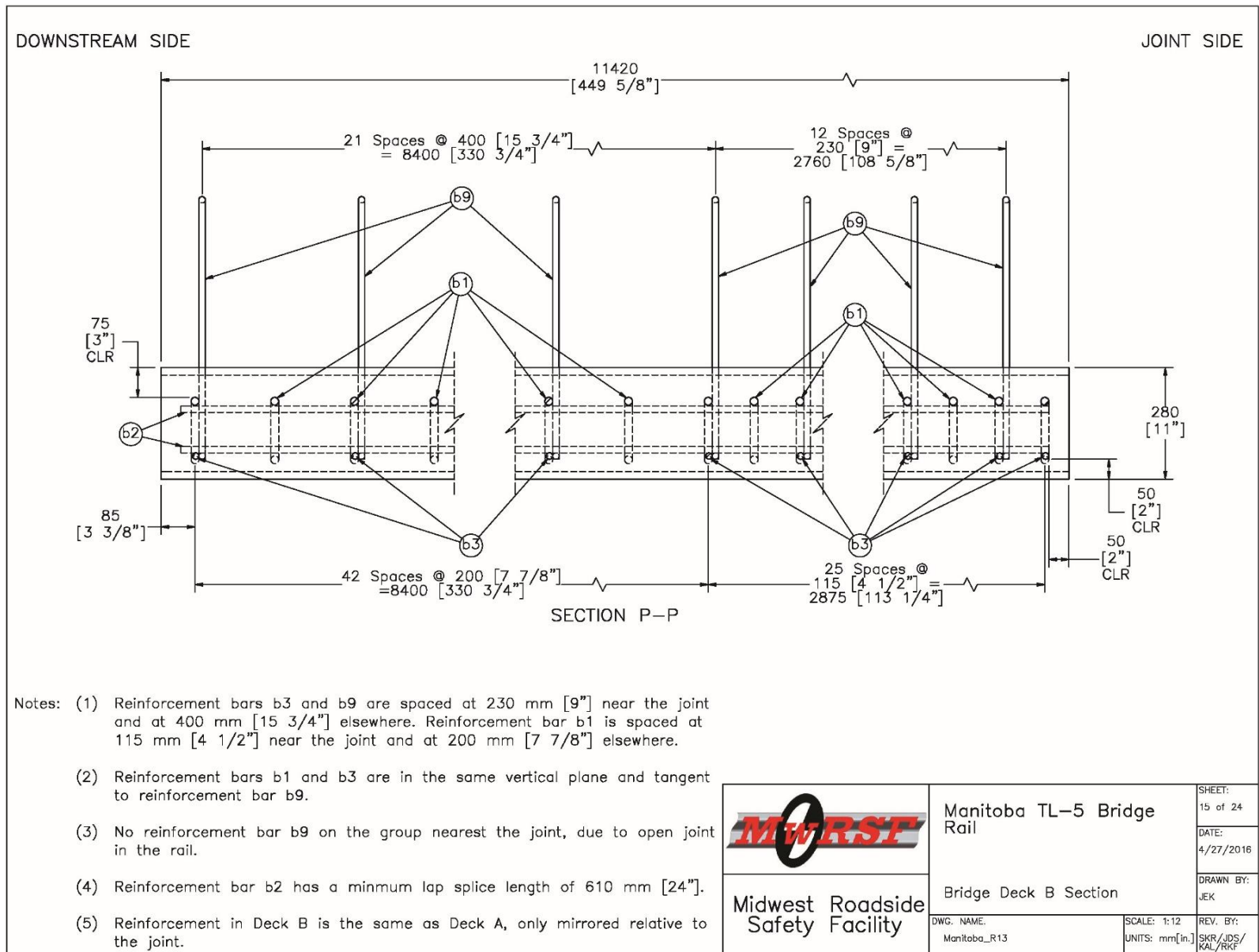


Figure 16. Bridge Deck B Section, Test No. MAN-1

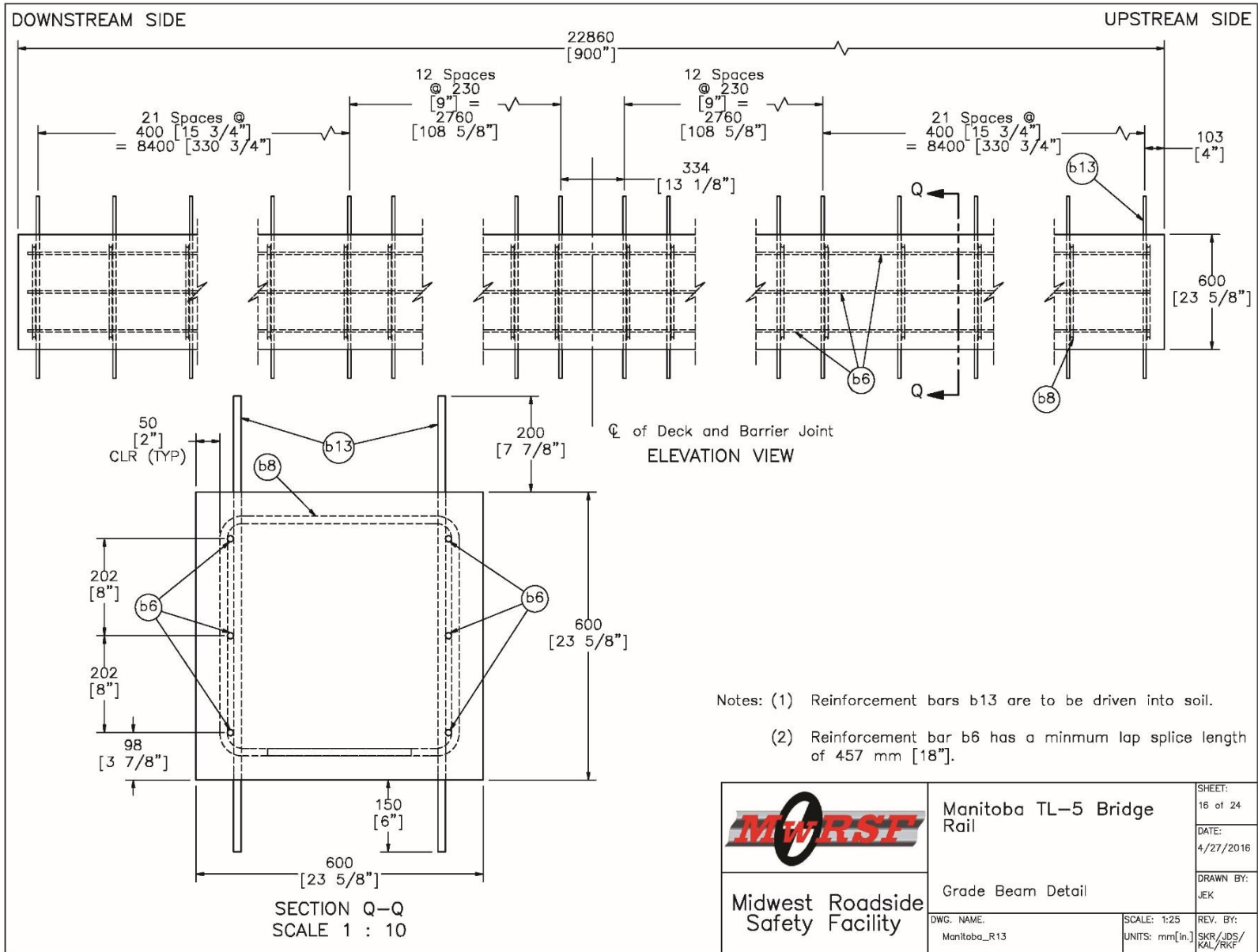


Figure 17. Grade Beam Detail, Test No. MAN-1

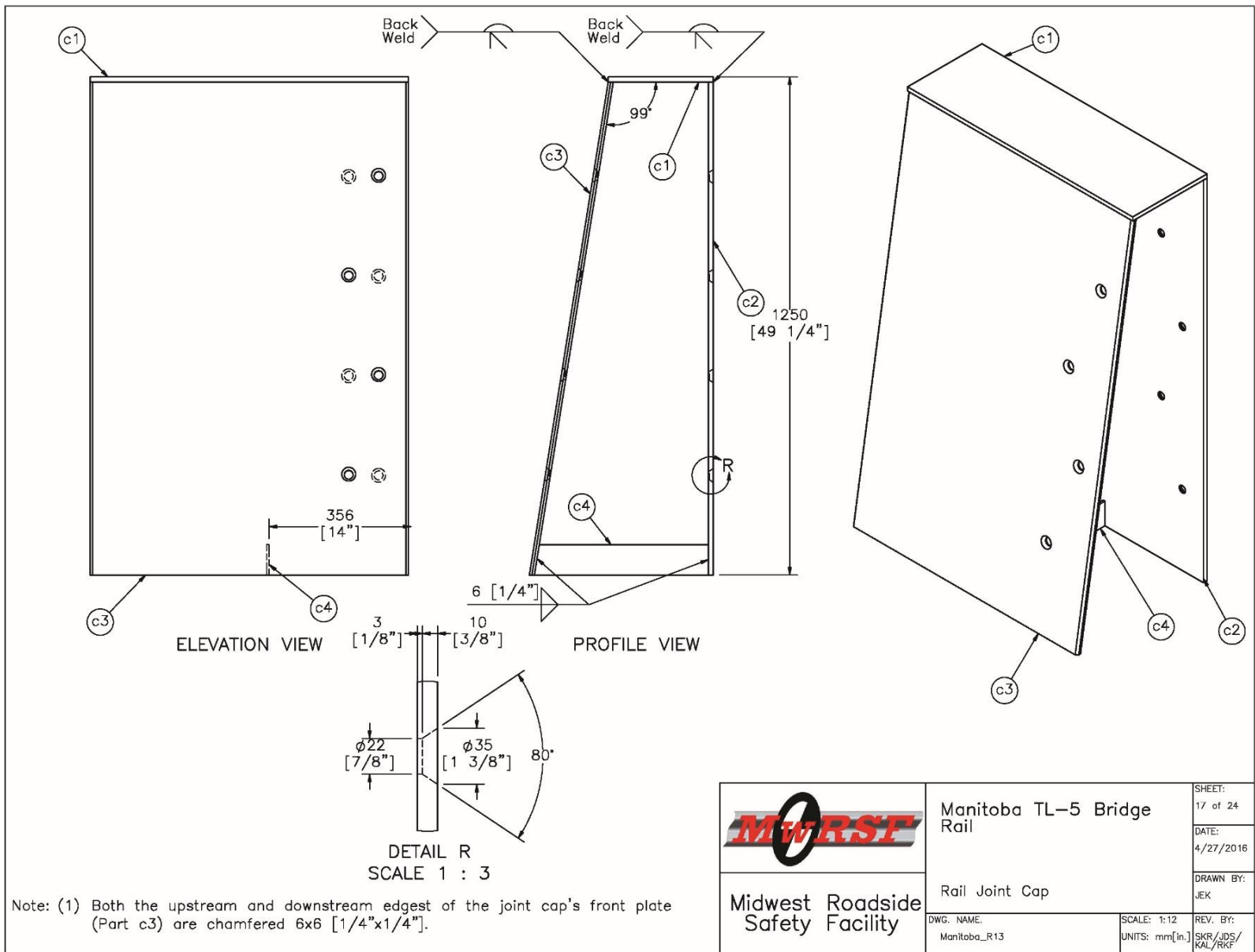


Figure 18. Rail Joint Cap, Test No. MAN-1

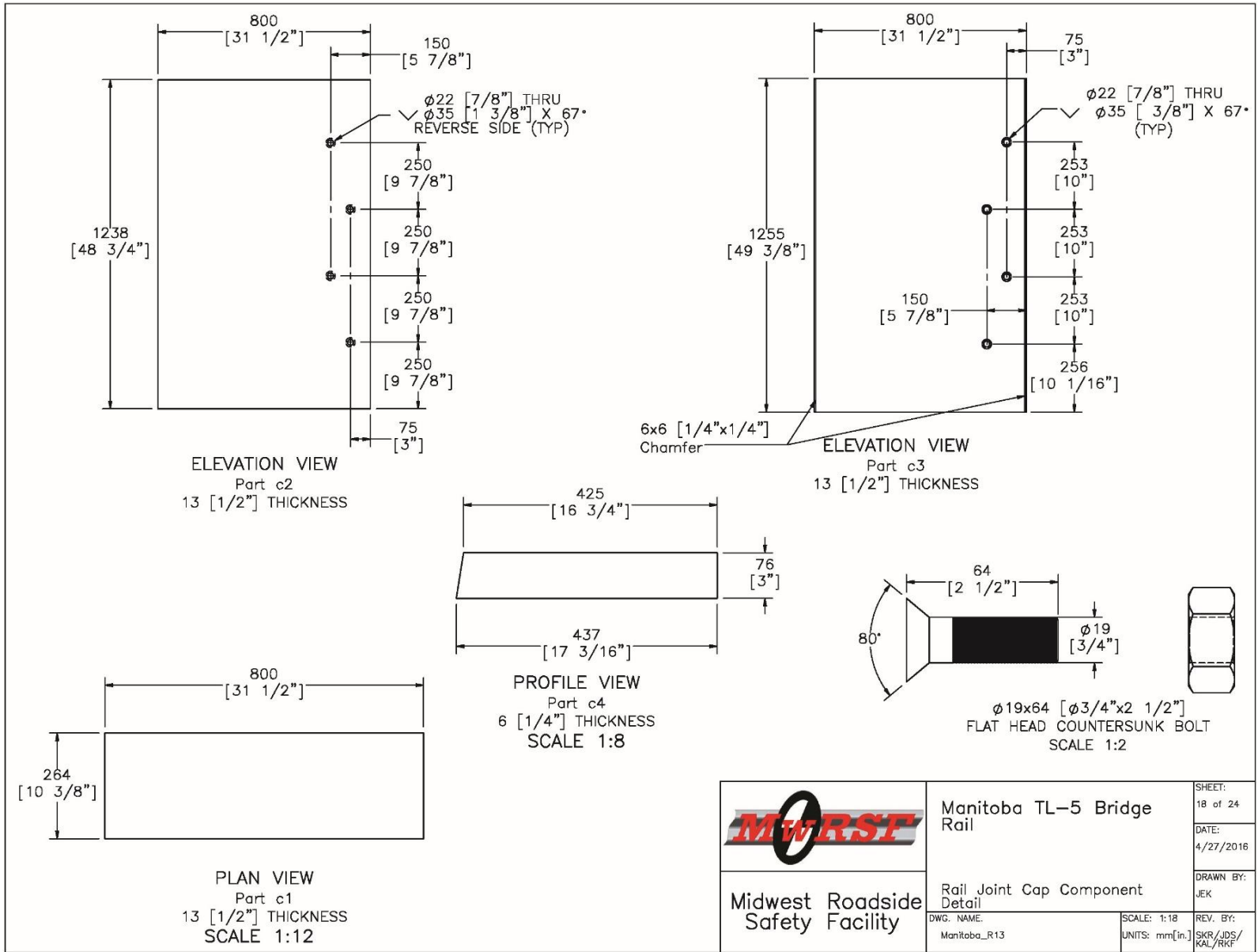



Figure 19. Rail Joint Cap Component Detail, Test No. MAN-1

 Midwest Roadside Safety Facility	Manitoba TL-5 Bridge Rail	SHEET: 18 of 24
	Rail Joint Cap Component Detail	DATE: 4/27/2016
DWG. NAME: Manitoba_R13	SCALE: 1:18 UNITS: mm[in.]	DRAWN BY: JEK
		REV. BY: SKR/JDS/ KAL/RKF

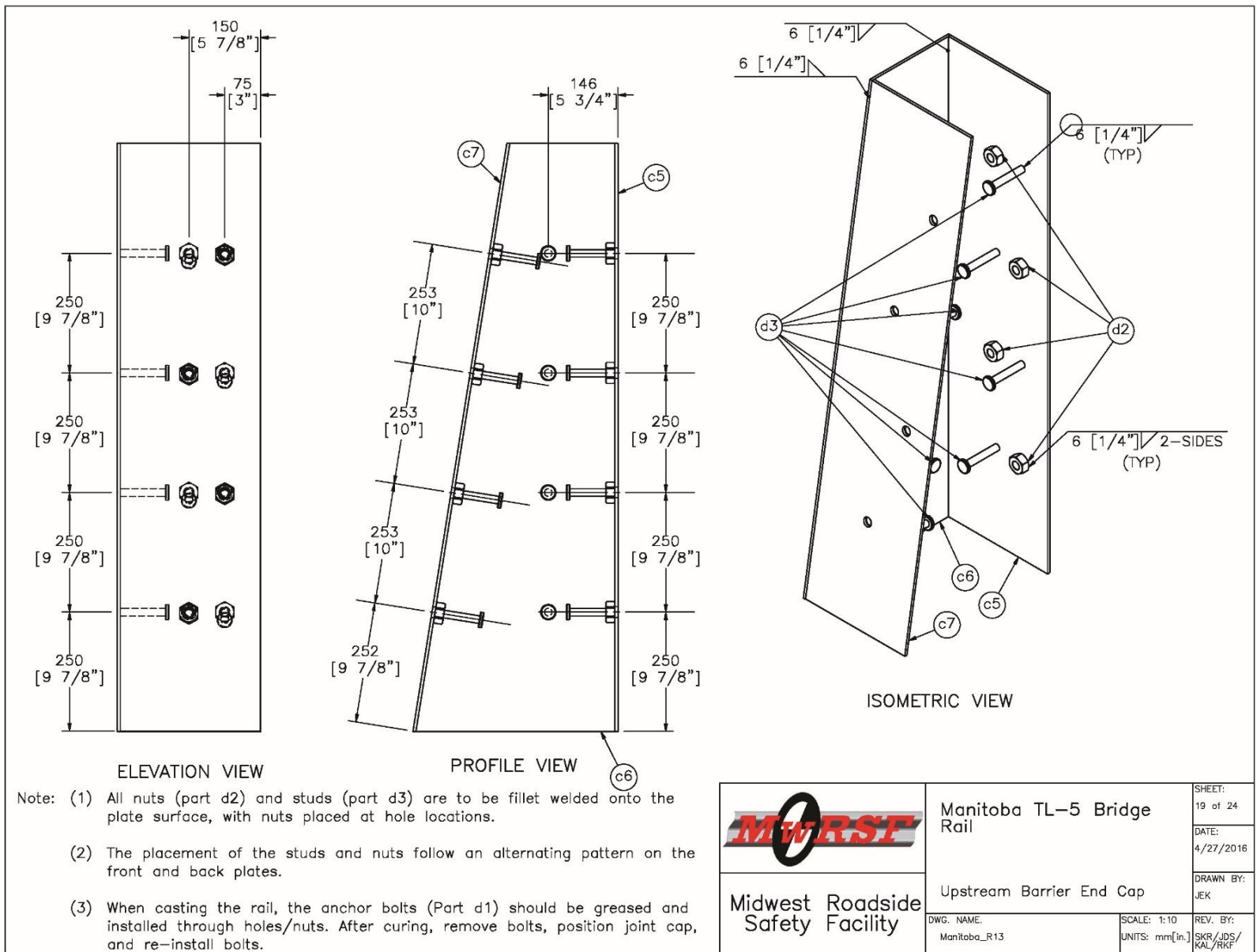


Figure 20. Upstream Barrier End Cap, Test No. MAN-1

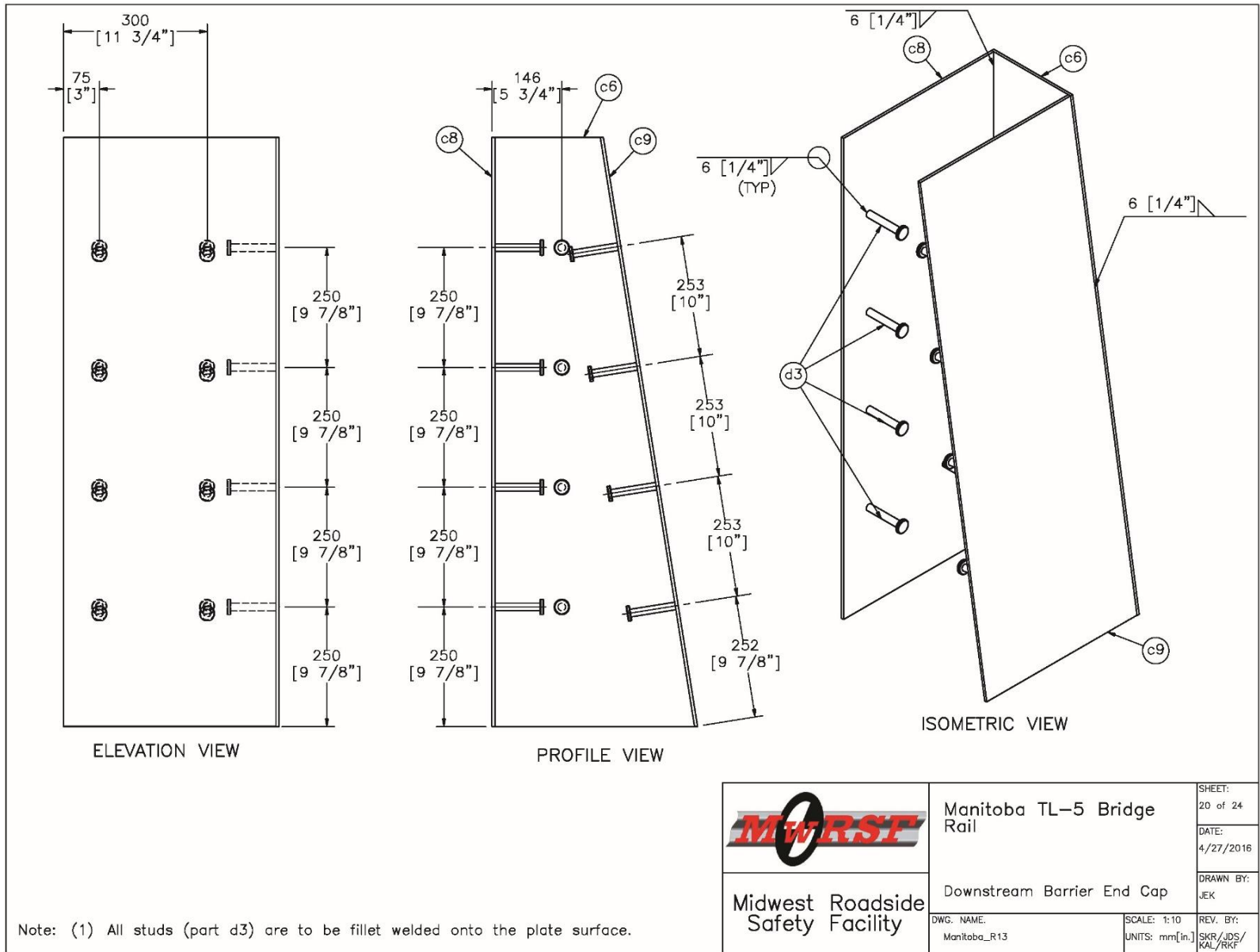


Figure 21. Downstream Barrier End Cap. Test No. MAN-1

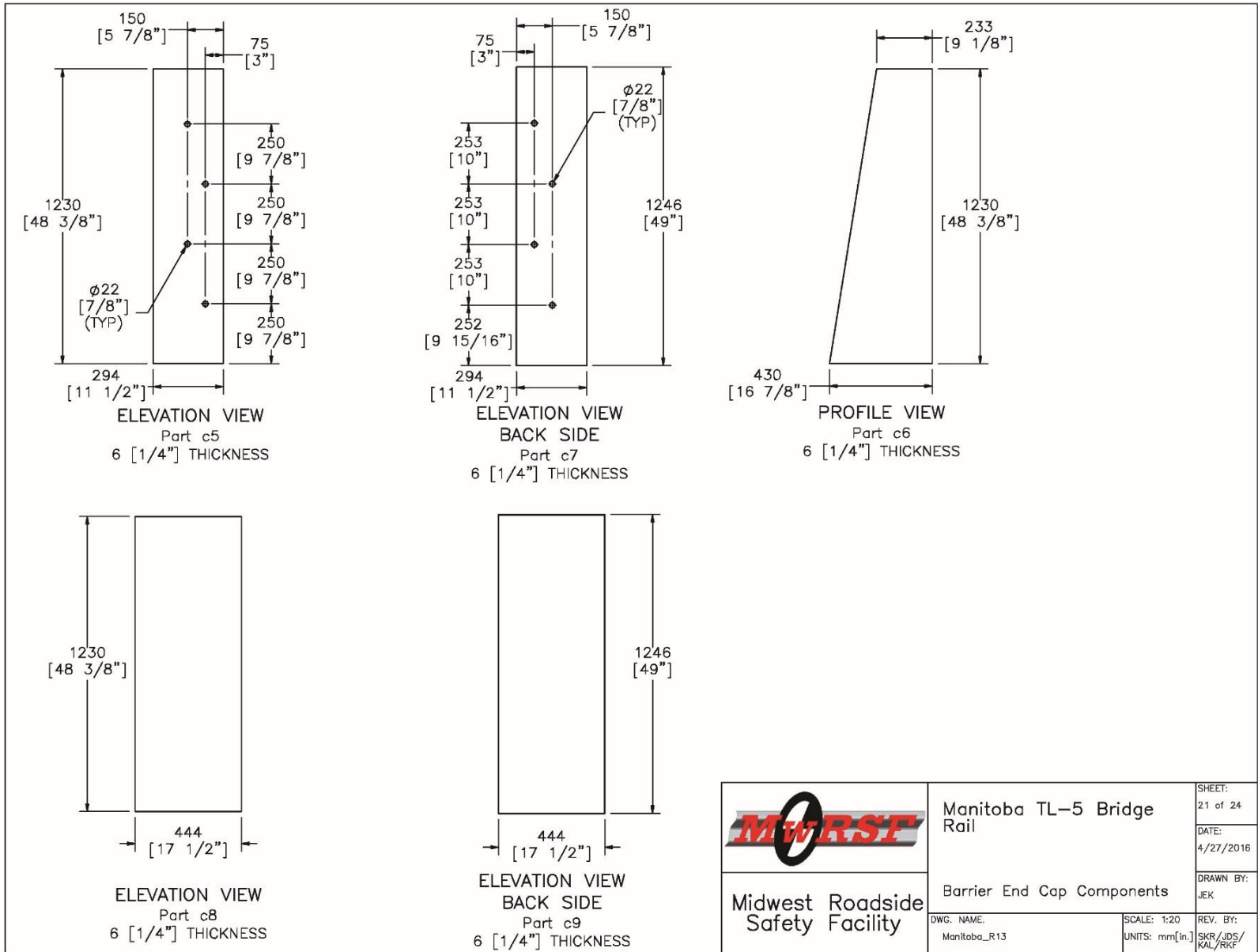
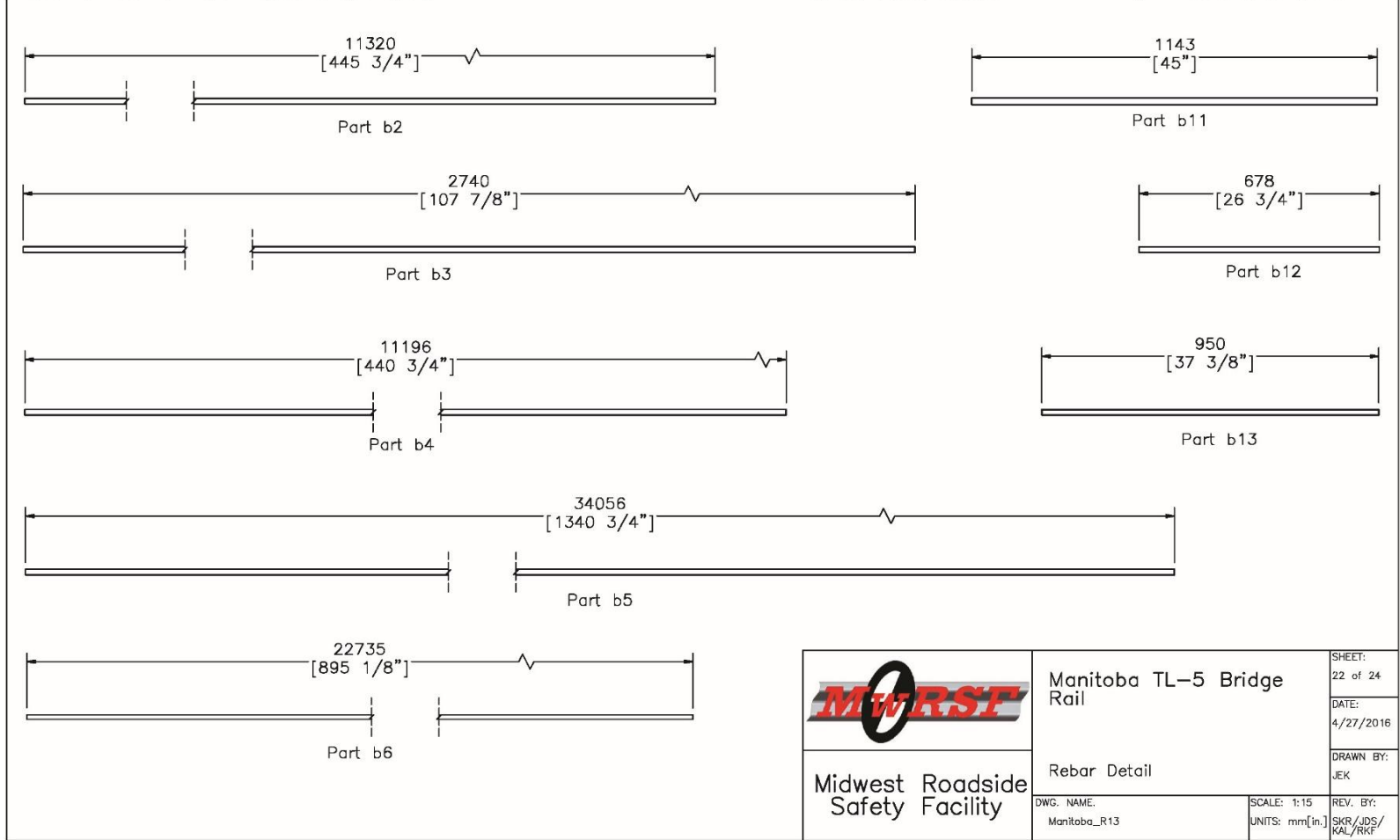



Figure 22. Barrier End Cap Components, Test No. MAN-1

Bill of Bars						
Bar	QTY	Size	Total Length	Location	Material	
b2	38	M15	11.32 m [445 3/4"], Minimum Lap Length 610 [24"]	Bridge Deck A & B, Longitudinal	Steel Grade 400W	
b3	70	M15	2.74 m [107 7/8"]	Bridge Deck A & B, Lateral	Steel Grade 400W	
b4	10	M15	11.196 m [440 3/4"], Minimum Lap Length 610 [24"]	Rail A, Longitudinal	Steel Grade 400W	
b5	10	M15	34.056 m [1340 3/4"], Minimum Lap Length 610 [24"]	Rail B, Longitudinal	Steel Grade 400W	
b6	6	#4	22.735 m [895 1/8"], Minimum Lap Length 457 [18"]	Grade Beam, Longitudinal	ASTM A615 Gr. 60	
b11	68	#6	1.143 m [45"]	Deck A & B, to Tarmac	ASTM A615 Gr. 60	
b12	68	#5	0.678 m [26 3/4"]	Deck A & B, to Soil	ASTM A615 Gr. 60	
b13	136	#5	0.95 m [37 3/8"]	Grade Beam, Vertical	ASTM A615 Gr. 60	



 Midwest Roadside Safety Facility	Manitoba TL-5 Bridge Rail	SHEET: 22 of 24
	Rebar Detail	DATE: 4/27/2016
DWG. NAME: Manitoba_R13	SCALE: 1:15 UNITS: mm[in.]	DRAWN BY: JEK
		REV. BY: SKR/JDS/ KAL/RKF

39

Figure 23. Rebar Bill of Bars, Test No. MAN-1

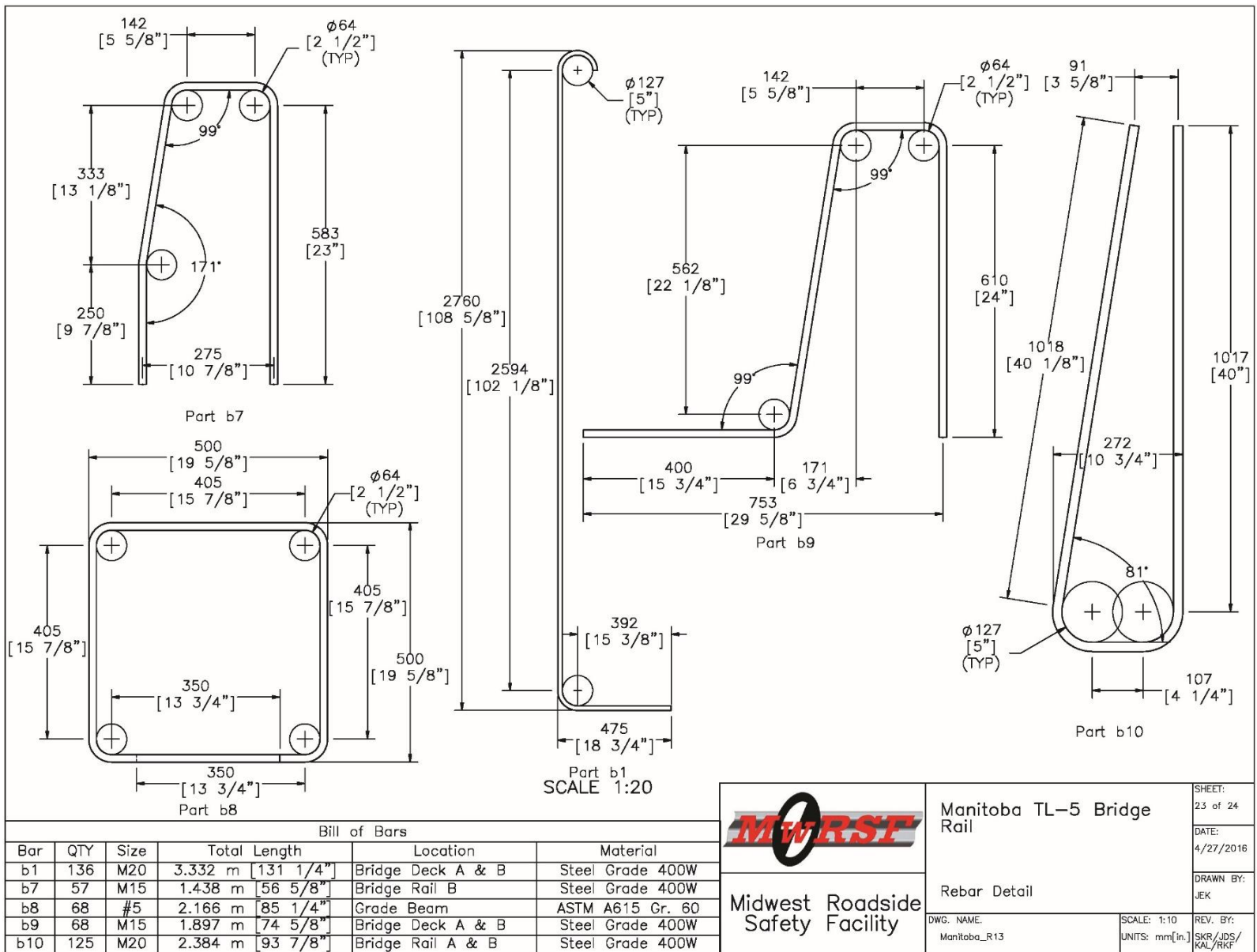


Figure 24. Bent Rebar Details, Test No. MAN-1




Item No.	QTY.	Description	Material Spec	Hardware Guide						
a1	1	Bridge Rail Concrete 1 – 4.96 cubic meters [175.16 cubic ft]	Min. f'c = 45 MPa [6,527 psi]	–						
a2	1	Bridge Rail Concrete 2 – 17.97 cubic meters [634.60 cubic ft]	Min. f'c = 45 MPa [6,527 psi]	–						
a3	2	Bridge Deck Concrete Fill – 10.73 cubic meters [387.40 cubic ft]	Min. f'c = 45 MPa [6,527 psi]	–						
a4	1	Grade Beam Concrete Fill – 8.23 cubic meters [290.64 cubic ft]	Min. f'c = 45 MPa [6,527 psi]	–						
b1	136	M20 Bar – 3.332 m [131 1/4"] Long, Bent, Bridge Deck A & B	Steel Grade 400W	–						
b2	38	M15 Bar – 11.320 m [445 3/4"] Long, Bridge Deck A & B	Steel Grade 400W	–						
b3	70	M15 Bar – 2.740 m [107 7/8"] Long, Bridge Deck A & B	Steel Grade 400W	–						
b4	10	M15 Bar – 11.196 m [440 3/4"] Long, Bridge Rail A	Steel Grade 400W	–						
b5	10	M15 Bar – 34.056 m [1340 3/4"] Long, Bridge Rail B	Steel Grade 400W	–						
b6	6	#4 Bar – 22.735 m [895 1/8"] Long, Grade Beam	ASTM A615 Gr. 60	–						
b7	57	M15 Bar – 1.438 m [56 5/8"] Long, Bent, Bridge Rail B	Steel Grade 400W	–						
b8	68	#5 Bar – 2.166 m [85 1/4"] Long, Bent, Grade Beam	ASTM A615 Gr. 60	–						
b9	68	M15 Bar – 1.897 m [74 5/8"] Long, Bent, Bridge Deck A & B	Steel Grade 400W	–						
b10	125	M20 Bar – 2.384 m [93 7/8"] Long, Bent, Bridge Rail A & B	Steel Grade 400W	–						
b11	68	#6 Bar – 1.143 m [45"] Long, Bridge Deck A & B	ASTM A615 Gr. 60	–						
b12	68	#5 Bar – 0.678 m [26 3/4"] Long, Bridge Deck A & B	ASTM A615 Gr. 60	–						
b13	136	#5 Bar – 0.950 m [37 3/8"] Long, Grade Beam	ASTM A615 Gr. 60	–						
c1	1	800x264x13 [31 1/2"x10 3/8"x1/2"] Plate	ASTM A572	–						
c2	1	1238x800x13 [48 3/4"x31 1/2"x1/2"] Plate	ASTM A572	–						
c3	1	1255x800x13 [49 7/16"x31 1/2"x1/2"] Plate	ASTM A572	–						
c4	1	386x76x6 [15 3/16"x3"x1/4"] Plate	ASTM A572	–						
c5	1	1230x294x6 [48 3/8"x11 5/8"x1/4"] Plate	ASTM A572	–						
c6	2	1230x430x6 [48 3/8"x16 7/8"x1/4"] Plate	ASTM A572	–						
c7	1	1246x294x6 [49"x11 5/8"x1/4"] Plate	ASTM A572	–						
c8	1	1230x444x6 [48 3/8"x17 1/2"x1/4"] Plate	ASTM A572	–						
c9	1	1246x444x6 [49"x17 1/2"x1/4"] Plate	ASTM A572	–						
d1	8	3/4" [19] Dia. 2–1/2" [64] Long Flat Head Countersunk Bolt	F835	–						
d2	8	3/4" [19] Dia. Hex Nut	A563	–						
d3	32	5/8" [16] Dia. x 4" [102] Long Stud	Steel Any Grade	–						
e1	1	Chemical Epoxy Adhesive	Min. Bond Strength = 10 MPa [1,450 psi]	–						
<table border="1" style="width: 100%; border-collapse: collapse;"> <tr> <td rowspan="2" style="text-align: center; vertical-align: middle;">  Midwest Roadside Safety Facility </td> <td style="text-align: center; vertical-align: middle;"> Manitoba TL–5 Bridge Rail </td> <td style="font-size: small;"> SHEET: 24 of 24 DATE: 4/27/2016 DRAWN BY: JEK </td> </tr> <tr> <td style="text-align: center; vertical-align: middle;"> Bill of Materials </td> <td style="font-size: small;"> DWG. NAME: Manitoba_R13 SCALE: 1:500 UNITS: mm[in.] </td> <td style="font-size: small;"> REV. BY: SKR/JDS/ KAL/RKF </td> </tr> </table>					 Midwest Roadside Safety Facility	Manitoba TL–5 Bridge Rail	SHEET: 24 of 24 DATE: 4/27/2016 DRAWN BY: JEK	Bill of Materials	DWG. NAME: Manitoba_R13 SCALE: 1:500 UNITS: mm[in.]	REV. BY: SKR/JDS/ KAL/RKF
 Midwest Roadside Safety Facility	Manitoba TL–5 Bridge Rail	SHEET: 24 of 24 DATE: 4/27/2016 DRAWN BY: JEK								
	Bill of Materials	DWG. NAME: Manitoba_R13 SCALE: 1:500 UNITS: mm[in.]	REV. BY: SKR/JDS/ KAL/RKF							

Figure 25. Bill of Materials, Test No. MAN-1



Figure 26. Test Installation Photographs, Test No. MAN-1

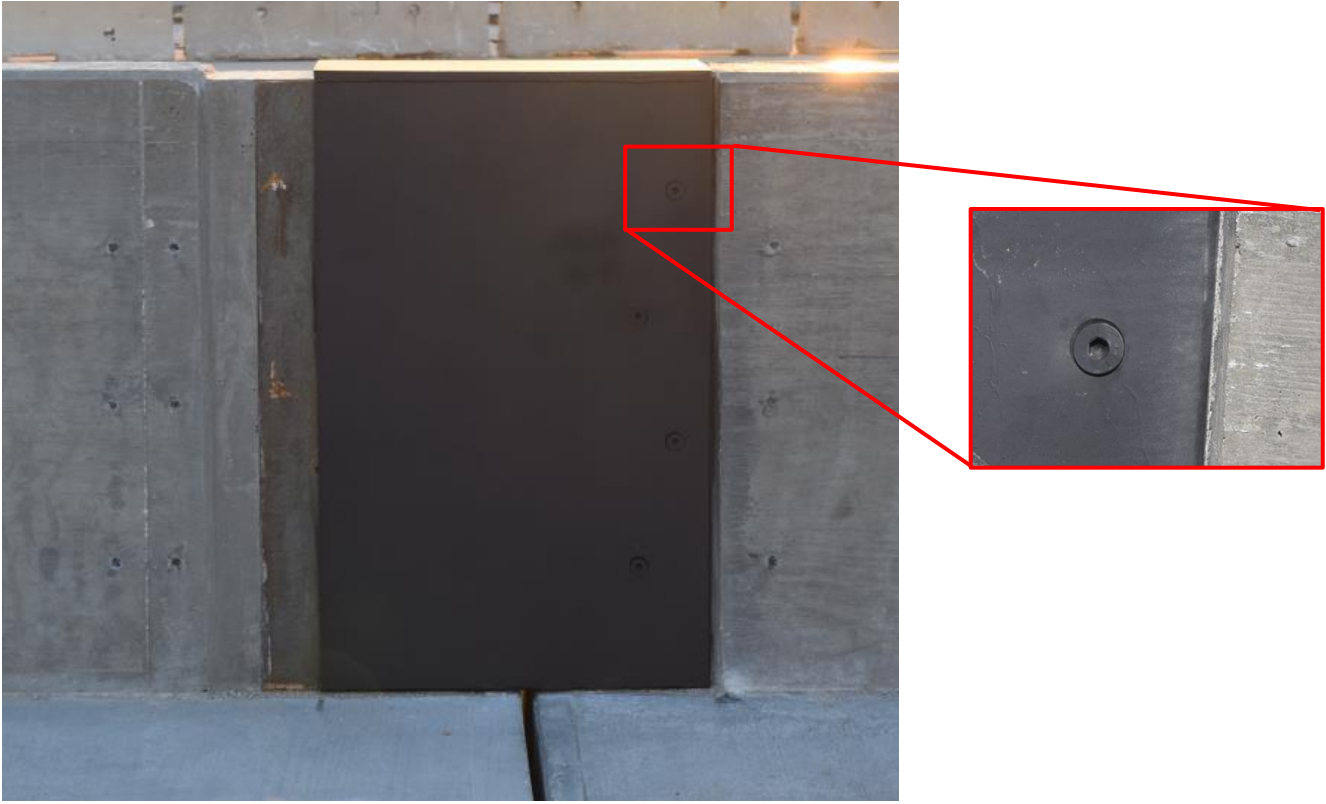


Figure 27. Barrier Joint Photographs, Test No. MAN-1

6 TEST REQUIREMENTS AND EVALUATION CRITERIA

6.1 Test Requirements

New barrier systems must satisfy the current roadside safety standards in order to be deemed crashworthy. According to the TL-5 evaluation criteria of MASH, longitudinal barrier systems, including concrete bridge rails, must be subjected to three full-scale vehicle crash tests, as summarized in Table 6.

Table 6. MASH TL-5 Crash Test Conditions for Longitudinal Barriers

Test Article	Test Designation No.	Test Vehicle	Vehicle Weight, kg (lb)	Impact Conditions		Evaluation Criteria ¹
				Speed, km/h (mph)	Angle, deg.	
Longitudinal Barrier	5-10	1100C	1100 (2420)	100 (62)	25	A,D,F,H,I
	5-11	2270P	2270 (5000)	100 (62)	25	A,D,F,H,I
	5-12	36000V	36000 (79,300)	80 (50)	15	A,D,G

¹ Evaluation criteria explained in Table 7.

Following a review of previous crash testing into concrete barrier systems, only the 36000V tractor trailer test was determined to be critical for the evaluation of the Manitoba TL-5 bridge rail. Even though test 5-12 is conducted at a lower speed and angle than the other tests, the large increase in mass of the 36000V vehicle results in an impact severity almost four times higher than the pickup truck test and about eight times higher than the small car test. Thus, test 5-12 would impart the highest impact loads to the barrier and be the critical test for evaluating the strength of the bridge rail and deck.

Vehicle stability was not considered to be critical for either of the passenger vehicles. Previous crash testing of the 2270P pickup into an 11-degree single-sloped concrete bridge rail and a vertical-faced concrete bridge rail both resulted in successful MASH tests with minimal vehicle roll and pitch displacements [23-24]. The 9-degree slope of the Manitoba bridge rail is between these two tested systems, so the vehicle performance in terms of stability has been effectively bracketed by the previous crash tests. Similarly, previous 1100C crash tests have been successfully conducted on a New Jersey-shaped concrete barrier and a vertical steel gate [25-26]. New Jersey-shaped barriers have long been considered to cause more vehicle instabilities as they induce vehicle climb and roll during impact. With the small car remaining stable through impacts with a New Jersey barrier and a vertical-faced barrier, there was little concern for 1100C stability during impact with the Manitoba bridge rail. Additionally, National Cooperative Highway Research Program (NCHRP) *Web-Only Document 157* determined single-slope barriers with a 9-degree slope to be crashworthy to MASH performance standards as long as they have adequate

structural capacity [27]. Therefore, test nos. 5-10 and 5-11 were not deemed to be critical tests and were not conducted as part of this study.

6.2 Evaluation Criteria

Evaluation criteria for full-scale vehicle crash testing are based on three appraisal areas: (1) structural adequacy; (2) occupant risk; and (3) vehicle trajectory after collision. Criteria for structural adequacy are intended to evaluate the ability of the bridge railing to contain and redirect impacting vehicles. In addition, controlled lateral deflection of the test article is acceptable. Occupant risk evaluates the degree of hazard to occupants in the impacting vehicle. Post-impact vehicle trajectory is a measure of the potential of the vehicle to result in a secondary collision with other vehicles and/or fixed objects, thereby increasing the risk of injury to the occupants of the impacting vehicle and/or other vehicles. These evaluation criteria are summarized in Table 7 and defined in greater detail in MASH. The full-scale vehicle crash test was conducted and reported in accordance with the procedures provided in MASH.

In addition to the standard occupant risk measures, the Post-Impact Head Deceleration (PHD), the Theoretical Head Impact Velocity (THIV), and the Acceleration Severity Index (ASI) were determined and reported on the test summary sheet. Additional discussion on PHD, THIV and ASI is provided in MASH.

Table 7. MASH Evaluation Criteria for Longitudinal Barriers and Bridge Rails

Structural Adequacy	A. Test article should contain and redirect the vehicle or bring the vehicle to a controlled stop; the vehicle should not penetrate, underide, or override the installation although controlled lateral deflection of the test article is acceptable.							
Occupant Risk	D. Detached elements, fragments or other debris from the test article should not penetrate or show potential for penetrating the occupant compartment, or present an undue hazard to other traffic, pedestrians, or personnel in a work zone. Deformations of, or intrusions into, the occupant compartment should not exceed limits set forth in Section 5.3 and Appendix E of MASH.							
	F. The vehicle should remain upright during and after collision. The maximum roll and pitch angles are not to exceed 75 degrees.							
	G. It is preferable, although not essential, that the vehicle remain upright during and after collision.							
	H. Occupant Impact Velocity (OIV) (see Appendix A, Section A5.3 of MASH for calculation procedure) should satisfy the following limits:							
	Occupant Impact Velocity Limits							
	<table border="1" style="width: 100%; border-collapse: collapse;"> <thead> <tr> <th style="width: 50%;">Component</th> <th style="width: 25%;">Preferred</th> <th style="width: 25%;">Maximum</th> </tr> </thead> <tbody> <tr> <td>Longitudinal and Lateral</td> <td style="text-align: center;">9.1 m/s (30 ft/s)</td> <td style="text-align: center;">12.2 m/s (40 ft/s)</td> </tr> </tbody> </table>			Component	Preferred	Maximum	Longitudinal and Lateral	9.1 m/s (30 ft/s)
Component	Preferred	Maximum						
Longitudinal and Lateral	9.1 m/s (30 ft/s)	12.2 m/s (40 ft/s)						
I. The Occupant Ridedown Acceleration (ORA) (see Appendix A, Section A5.3 of MASH for calculation procedure) should satisfy the following limits:	Occupant Ridedown Acceleration Limits							
<table border="1" style="width: 100%; border-collapse: collapse;"> <thead> <tr> <th style="width: 50%;">Component</th> <th style="width: 25%;">Preferred</th> <th style="width: 25%;">Maximum</th> </tr> </thead> <tbody> <tr> <td>Longitudinal and Lateral</td> <td style="text-align: center;">15.0 g's</td> <td style="text-align: center;">20.49 g's</td> </tr> </tbody> </table>			Component	Preferred	Maximum	Longitudinal and Lateral	15.0 g's	20.49 g's
Component	Preferred	Maximum						
Longitudinal and Lateral	15.0 g's	20.49 g's						

7 TEST CONDITIONS

7.1 Test Facility

The testing facility is located at the Lincoln Air Park on the northwest side of the Lincoln Municipal Airport and is approximately 8 km (5 miles) northwest of the University of Nebraska-Lincoln.

7.2 Vehicle Tow and Guidance System

A reverse-cable tow system with a 1:2 mechanical advantage was used to propel the test vehicle. The distance traveled and the speeds of the tow vehicles were one-half that of the test vehicle. The test vehicle was released from the tow cable before impact with the barrier system. A digital speedometer on the tow vehicle increased the accuracy of the test vehicle impact speed.

A vehicle guidance system developed by Hinch [28] was used to steer the test vehicle. A guide flag, attached to the left-front wheel and the guide cable, was sheared off before impact with the barrier system. The 9.5-mm ($\frac{3}{8}$ -in.) diameter guide cable was tensioned to approximately 15.6 kN (3,500 lb) and supported both laterally and vertically every 30.5 m (100 ft) by hinged stanchions. The hinged stanchions stood upright while holding up the guide cable, but as the vehicle was towed down the line, the guide flag struck and knocked each stanchion to the ground.

7.3 Impact Point

MASH specifies that the critical impact point for a 36000V vehicle be selected to induce maximum loading to a critical portion of the barrier system. The maximum load from the vehicle impact was expected to occur when the rear tandem axles would strike the barrier, while the critical portion of the barrier was adjacent to the open joint in the rail and deck. Thus, the impact point was selected such that the rear tandem axles of the tractor trailer would impact the bridge rail upstream from the joint. Table 2.7 in MASH suggests that the rear tandem axles will impact approximately 0.3 m (1 ft) upstream from the vehicle's initial impact point. To further analyze this offset, a review was conducted on previous TL-5 crash tests conducted to NCHRP Report 350 and MASH safety standards, since they have the same impact conditions. As shown in Table 8, the center of the rear tandem axles of 36000V vehicles typically impact the barrier 0.3 m to 1.2m (1 ft to 4 ft) upstream from the initial impact point. To ensure both axles of the rear tandem axles apply load to the upstream side of the joint, the center of the rear tandem axles needed to impact the system approximately 1.2 m (4 ft) upstream from the joint. Thus, the initial impact point was selected to be 0.9 m (3 ft) upstream from the center of the joint. This impact location also allowed for the evaluation of snag on the joint cover plate since the front wheels of the tractor would impact approximately 508 mm (20 in.) upstream from the front edge of the steel cover plate.

Table 8. Impact Locations for Rear Tandem Axles in TL-5 Crash Tests

Test No.	Reference	Tandem Axle Impact Location Relative to Initial Vehicle Impact ¹
Test 6	[8]	0.9 m (3 ft)
2416-1	[9]	1.2 m (4 ft)
405511-2	[11]	0.3 m (1 ft)
ACBR-1	[12]	1.1 m (3.5 ft)
SBG-1	[15]	1.1 m (3.5 ft)
RYU-1	[16]	2.3 (7.5 ft)
TL5CMB-2	[16]	0.9 m (3 ft)

¹ Positive values measured upstream from initial vehicle impact

7.4 Test Vehicle

For test no. MAN-1, a 2004 International 9200 tractor with a 2001 Wabash National 16-m (53-ft) trailer was used as the test vehicle. The curb, test inertial, and gross static vehicle weights were 13,481 kg (29,720 lb), 36,322 kg (80,076 lb), and 36,322 kg (80,076 lb), respectively. The impact-side tires were sprayed with different colored chalk in order to determine where each wheel impacted the bridge rail during the test. From front to rear, the five tires were colored blue, orange, green, yellow, and red. Portable concrete barriers utilized to ballast the vehicle trailer were bolted to the floor, anchored to the walls with nylon straps, and supported laterally by foam. The test vehicle is shown Figures 28 through 30, and vehicle dimensions are shown in Figure 31.

The longitudinal component of the center of gravity (c.g.) was determined using the measured axle weights. The concrete barriers were mounted in the trailer such that the ballast c.g. satisfied MASH requirements. The location of the ballast c.g. is shown in Figures 31 and 32. Data used to calculate the location of the c.g. and ballast information are shown in Appendix B.

Square, black- and white-checked targets were placed on the vehicle for reference to be viewed from the high-speed digital video cameras and aid in the video analysis, as shown in Figure 32. Round, checkered targets were placed on the center of gravity on both sides of the trailer.

The front wheels of the test vehicle were aligned to vehicle standards, except the toe-in value was adjusted to zero so that the vehicle would track properly along the guide cable. A remote-controlled brake system was installed in the test vehicle so the vehicle could be brought safely to a stop after the test.



Figure 28. Test Vehicle, Test No. MAN-1



Figure 29. Test Vehicle with Colored Tires, Test No. MAN-1



Figure 30. Test Vehicle Ballast, Test No. MAN-1

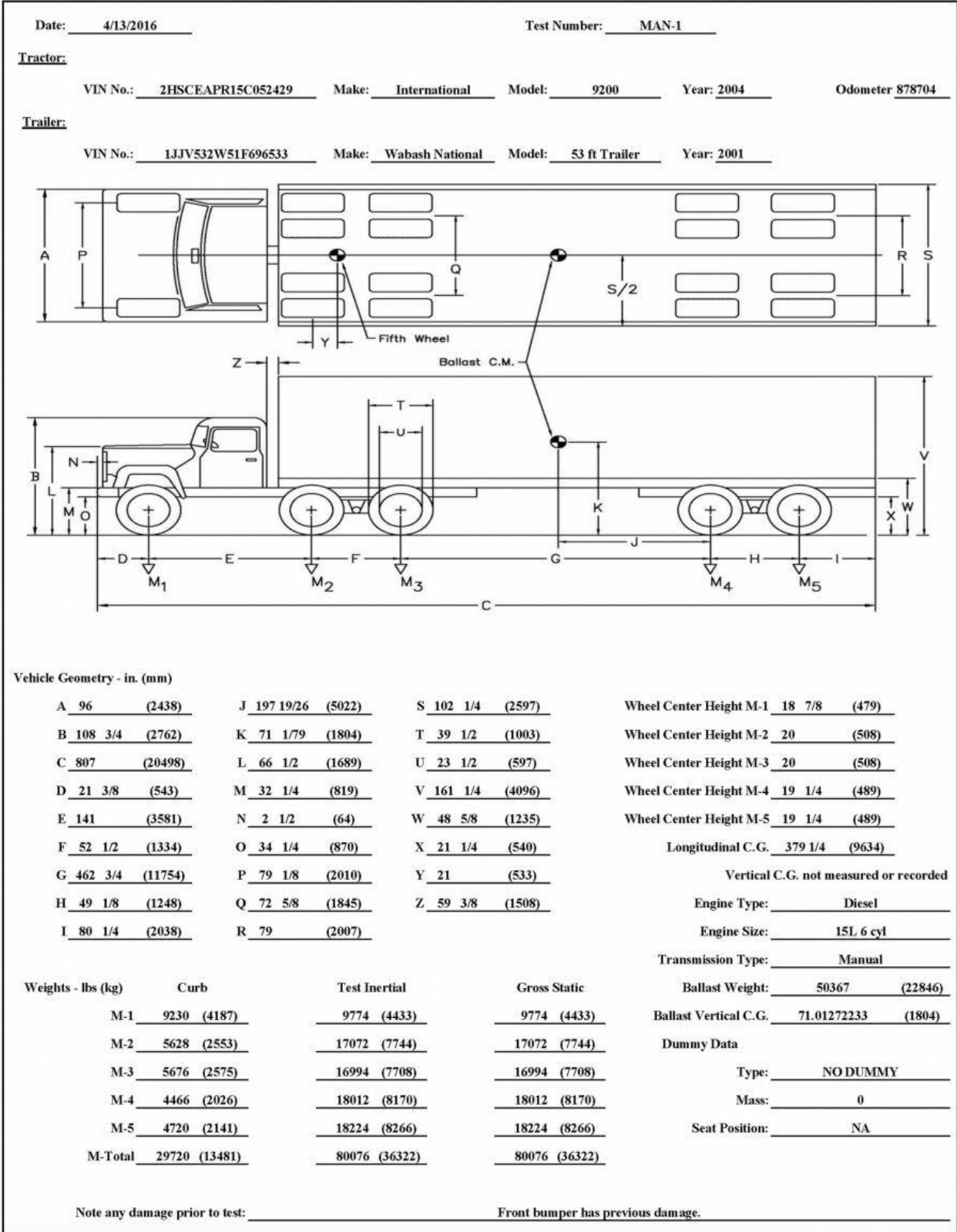


Figure 31. Vehicle Dimensions, Test No. MAN-1

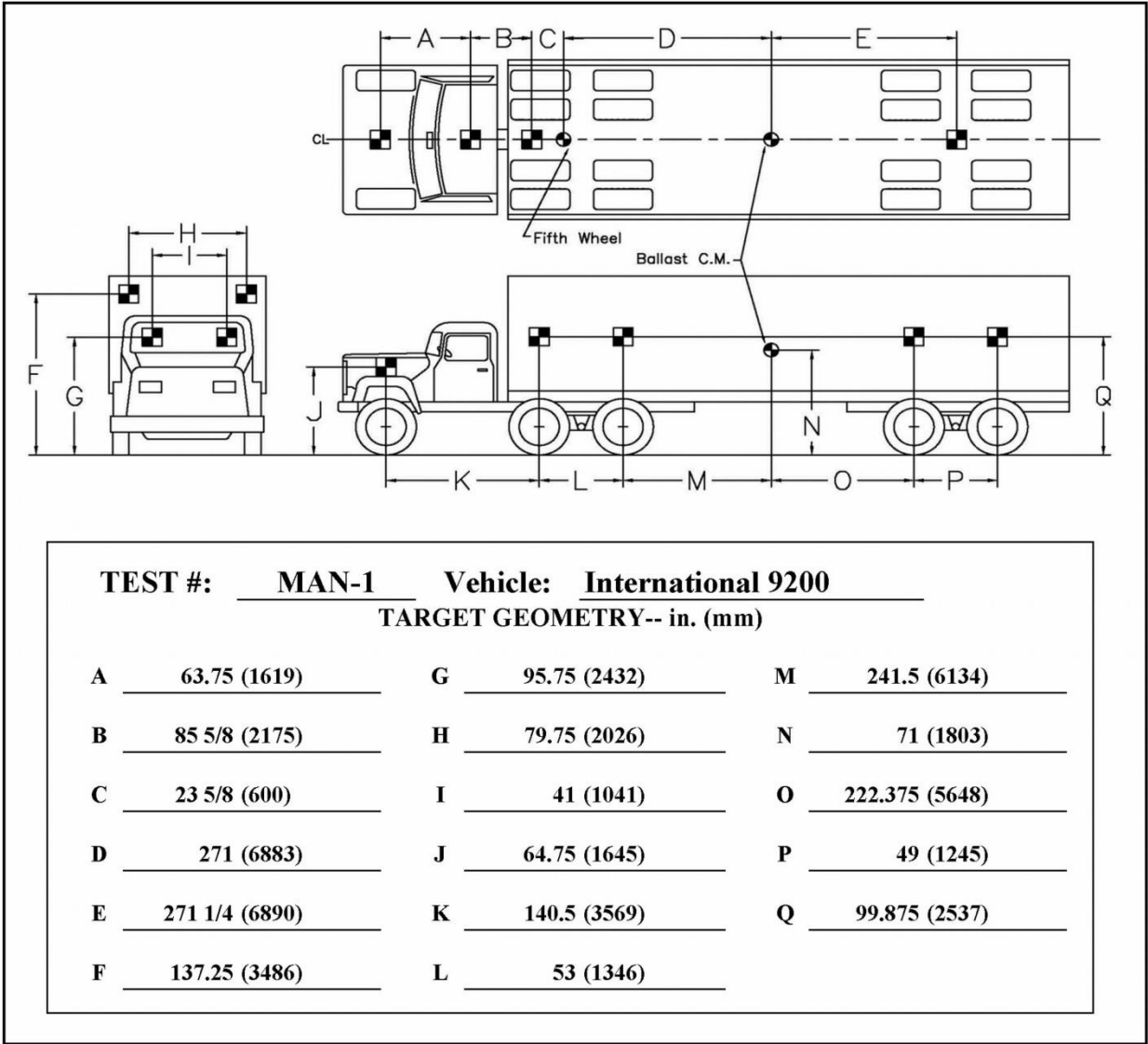


Figure 32. Target Geometry, Test No. MAN-1

7.5 Data Acquisition Systems

7.5.1 Accelerometers

Three environmental shock and vibration sensor/recorder systems were used to measure the accelerations in the longitudinal, lateral, and vertical directions. The first two systems, the SLICE-1 and SLICE-2 units, were modular data acquisition systems manufactured by Diversified Technical Systems, Inc. (DTS) of Seal Beach, California. The acceleration sensors were mounted inside the bodies of custom built SLICE 6DX event data recorders and recorded data at 10,000 Hz to the onboard microprocessor. Each SLICE 6DX was configured with 7 GB of non-volatile flash memory, a range of ± 500 g's, a sample rate of 10,000 Hz, and a 1,650 Hz (CFC 1000) anti-aliasing filter. The "SLICEWare" computer software programs and a customized Microsoft Excel worksheet were used to analyze and plot the accelerometer data.

The third accelerometer system, DTS, was a two-arm piezoresistive accelerometer system manufactured by Endevco of San Juan Capistrano, California. Five independent accelerometers were used to measure the longitudinal (2), lateral (2), and vertical accelerations at a sample rate of 10,000 Hz. The accelerometers were configured and controlled using a system developed and manufactured by DTS. More specifically, data was collected using a DTS Sensor Input Module (SIM), Model TDAS3-SIM-16M. The SIM was configured with 16 MB SRAM and 8 sensor input channels with 250 kB SRAM/channel. The SIM was mounted on a TDAS3-R4 module rack. The module rack was configured with isolated power/event/communications, 10BaseT Ethernet and RS232 communication, and an internal backup battery. Both the SIM and module rack were crashworthy. The "DTS TDAS Control" computer software program and a customized Microsoft Excel worksheet were used to analyze and plot the accelerometer data. The electronic accelerometer data obtained from all accelerometers was filtered using the SAE Class 60 and the SAE Class 180 Butterworth filter conforming to the SAE J211/1 specifications [29].

Each of the accelerometer systems was placed at a different location along the center axis of the vehicle. The DTS unit and three of its accelerometers, measuring in the longitudinal, lateral, and vertical directions, were placed inside the cab of the tractor to measure the accelerations imparted to a passenger. The secondary longitudinal and lateral accelerometers were mounted to the tractor frame cross member located directly in front of the tractor tandems. The SLICE-1 unit was mounted to the trailer frame directly behind the rear tandems, while the SLICE-2 unit was mounted inside the trailer directly above the front tandems. The secondary DTS accelerometers and both SLICE units were placed in an effort to measure the loads imparted to the bridge rail through both sets of tandem wheels. Unfortunately, the SLICE-1 unit experienced technical difficulties, did not trigger properly, and did not record the impact event.

7.5.2 Rate Transducers

Two identical angular rate sensor systems mounted inside the bodies of the SLICE-1 and SLICE-2 event data recorders were used to measure the rates of rotation of the test vehicle. Each SLICE MICRO Triax ARS had a range of 1,500 degrees/sec in each of the three directions (roll, pitch, and yaw) and recorded data at 10,000 Hz to the onboard microprocessors. The raw data

measurements were then downloaded, converted to the proper Euler angles for analysis, and plotted. The “SLICEWare” computer software program and a customized Microsoft Excel worksheet were used to analyze and plot the angular rate sensor data. Due to their placement on the vehicle, both SLICE units would be measuring angular displacements of the trailer.

A third angular rate sensor, the ARS-1500, with a range of 1,500 degrees/sec in each of the three directions (roll, pitch, and yaw) was used to measure the rates of rotation of the tractor/cab. The angular rate sensor was mounted on an aluminum block inside the test vehicle near the center of gravity and recorded data at 10,000 Hz to the DTS SIM. The raw data measurements were then downloaded, converted to the proper Euler angles for analysis, and plotted. The “DTS TDAS Control” computer software program and a customized Microsoft Excel worksheet were used to analyze and plot the angular rate sensor data.

7.5.3 Retroreflective Optic Speed Trap

Two retroreflective optic speed traps were used to determine the speed of the tractor-trailer before impact. Five retroreflective targets, spaced at approximately 457-mm (18-in.) intervals, were applied to the side of the vehicle. When the emitted beam of light was reflected by the targets and returned to an Emitter/Receiver, a signal was sent to the data acquisition computer, recording at 10,000 Hz, as well as the external LED box activating the LED flashes. The speed was then calculated using the spacing between the retroreflective targets and the time between the signals. The optic sensors were placed such that they would record all five targets just prior to the vehicle impacting the barrier. LED lights and high-speed digital video analysis were only used as a backup in the event that vehicle speeds cannot be determined from the electronic data.

7.5.4 Digital Photography

Five AOS high-speed digital video cameras, twelve GoPro digital video cameras, and four JVC digital video cameras were utilized to film test no. MAN-1. Camera details, camera operating speeds, lens information, and a schematic of the camera locations relative to the system are shown in Table 9 and Figure 33. GoPro nos. 13 and 14 were placed underneath the system. GoPro no. 14 had a dead battery at test time, so it is not pictured in the schematic below.

The high-speed videos were analyzed using ImageExpress MotionPlus, TEMA Motion, and RedLake MotionScope software programs. Actual camera speed and camera divergence factors were considered in the analysis of the high-speed videos. A Nikon D50 digital still camera was also used to document pre- and post-test conditions for all tests.

Table 9. Camera Speeds and Lens Settings, Test No. MAN-1

No.	Type	Operating Speed (frames/sec)	Lens	Lens Setting
AOS-5	AOS X-PRI Gigabit	500	Canon TVZoom 17-102	17
AOS-6	AOS X-PRI Gigabit	500	Sigma 28-70	70
AOS-7	AOS X-PRI Gigabit	500	Vivitar 135 mm Fixed	-
AOS-8	AOS S-VIT 1531	500	Sigma 28-70 DG	70
AOS-9	AOS TRI-VIT	500	Kowa Fixed	-
GP-3	GoPro Hero 3+	120		
GP-4	GoPro Hero 3+	120		
GP-5	GoPro Hero 3+	120		
GP-6	GoPro Hero 3+	120		
GP-7	GoPro Hero 4	240		
GP-8	GoPro Hero 4	240		
GP-9	GoPro Hero 4	120		
GP-10	GoPro Hero 4	240		
GP-11	GoPro Hero 4	120		
GP-12	GoPro Hero 4	120		
GP-13	GoPro Hero 4	120		
GP-14	GoPro Hero 4	120		
JVC-1	JVC – GZ-MC500 (Everio)	29.97		
JVC-2	JVC – GZ-MG27u (Everio)	29.97		
JVC-3	JVC – GZ-MG27u (Everio)	29.97		
JVC-4	JVC – GZ-MG27u (Everio)	29.97		

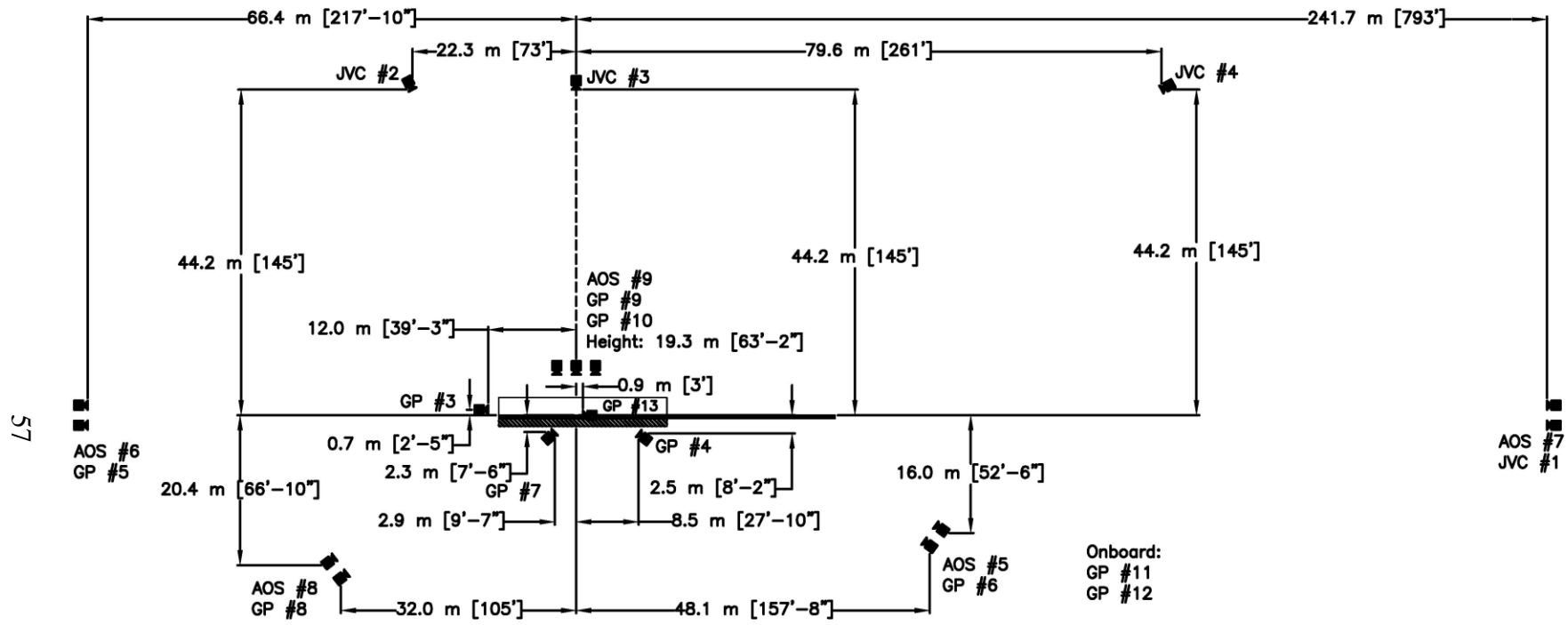


Figure 33. Camera Location Diagram, Test No. MAN-1

8 FULL-SCALE CRASH TEST NO. MAN-1

8.1 Weather Conditions

Test no. MAN-1 was conducted on April 13, 2016 at approximately 2:00 pm. The weather conditions as per the National Oceanic and Atmospheric Administration (station 14939/LNK) were reported and are shown in Table 10.

Table 10. Weather Conditions, Test No. MAN-1

Temperature	77° F (25° C)
Humidity	24%
Wind Speed	16 mph (25.7 km/h)
Wind Direction	200° from True North
Sky Conditions	Sunny
Visibility	10 Statute Miles
Pavement Surface	Dry
Previous 3-Day Precipitation	0 in. (0 mm)
Previous 7-Day Precipitation	0 in. (0 mm)

8.2 Test Description

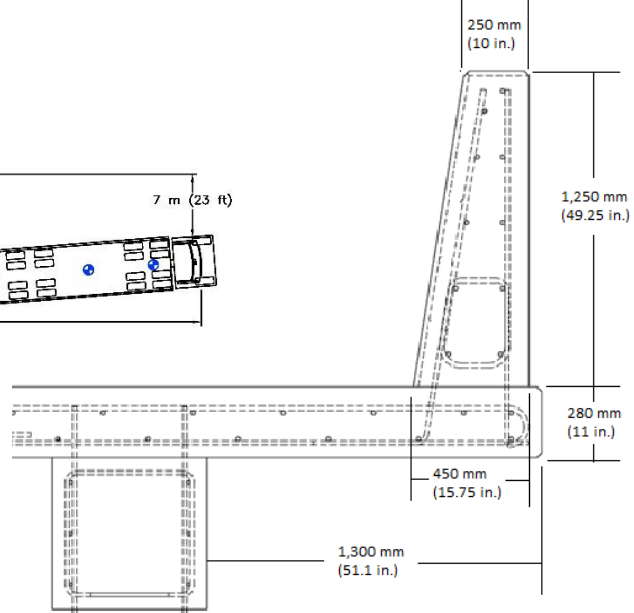
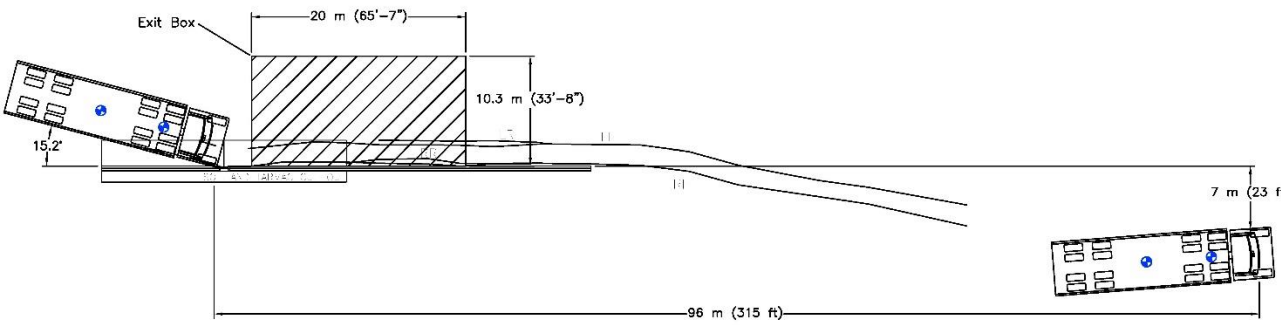
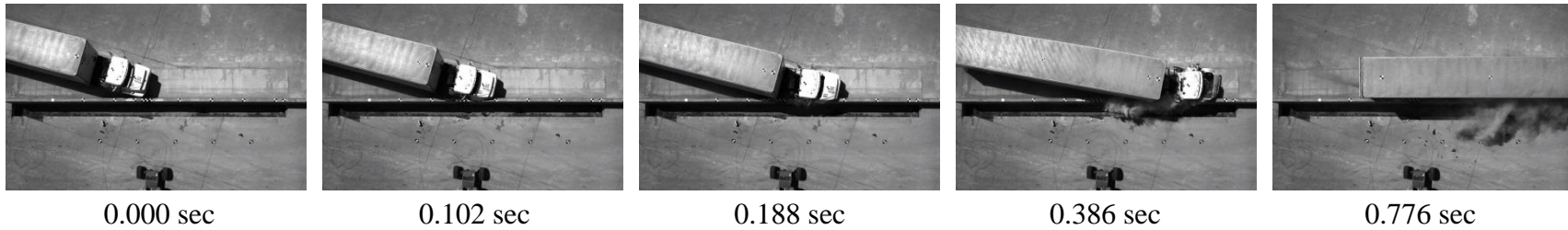
The 36,322-kg (80,076-lb) van-type, tractor-trailer impacted the bridge rail at a speed of 83.2 km/h (51.7 mph) and at an angle of 15.2 degrees. Initial vehicle impact was to occur 914 mm (3 ft) upstream from the midpoint of the barrier gap, as shown in Figure 34, which was selected to cause the rear tandems to impact and load the bridge rail just upstream from the open joint. The actual point of impact was 462 mm (18.2 in.) upstream from the joint. A sequential description of the impact events is contained in Table 11. A summary of the test results and sequential photographs are shown in Figure 35. Additional sequential photographs are shown in Figures 36 through 37. Documentary photographs of the crash test are shown in Figure 38. The vehicle came to rest against a separate concrete barrier approximately 96 m (315 ft) downstream from the impact point. The vehicle trajectory and final position are shown in Figures 35 and 39.



Figure 34. Impact Location, Test No. MAN-1

Table 11. Sequential Description of Impact Events, Test No. MAN-1

TIME (sec)	EVENT
0.000	Vehicle front bumper impacted the system
0.004	Vehicle front bumper began to deform
0.010	Vehicle hood contacted the system
0.014	Vehicle hood began to deform
0.016	Vehicle right-front tire contacted the system
0.044	The upstream deck slab began to flex and deflected downward
0.048	Vehicle cab began to roll toward the system
0.102	Vehicle cab began to yaw away from the system
0.166	Vehicle right-front door contacted the system
0.188	Trailer right-front corner contacted the barrier just upstream from the cover plate
0.190	System began to deflect backward
0.196	Vehicle trailer began to roll toward the system
0.200	Vehicle left-front tire became airborne
0.204	Vehicle trailer began to yaw away from the system
0.210	Downstream deck slab flexed and deflect downward
0.220	Longitudinal crack formed on bottom of downstream deck slab adjacent to joint
0.222	Barrier deflected 36 mm (1.4 in.) and began restoring to its original position
0.256	Concrete on top of barrier spalled off from contact with trailer right-front corner.
0.314	Vehicle cab began to roll away from the system
0.386	Vehicle cab was parallel to system with a maximum roll angle of 16.4 degrees
0.396	Vehicle trailer left rear most tire became airborne
0.436	Vehicle left front tire regained contact with the ground
0.776	Vehicle trailer was parallel to the system
0.778	Rear of trailer and vehicle rear tandems impacted the system, and barrier began to deflect backward
0.802	Barrier reached its maximum deflection of 52 mm (2 in.) and began to rebound
0.824	Vehicle cab began to yaw toward the system
0.972	Vehicle trailer reached maximum roll of 13.3 degrees and began to roll away from the system
1.176	Vehicle trailer left-rear most tire regained contact with the ground
1.768	Vehicle exited the system
5.200	Vehicle impacted a separate concrete barrier downstream from the bridge rail
7.600	Vehicle came to rest 96 m (315 ft) downstream from impact



19

- Test AgencyMwRSF
- Test Number.....MAN-1
- Date4/13/16
- MASH Test Designation No.....5-12
- Test Article.....Manitoba Constrained Width, Tall Wall, Bridge Rail
- Total Length45.72 m (150 ft)
- Key Component – Bridge Rail
 - Height.....1,250 mm (49¼ in.)
 - Top Width250 mm (10 in.)
 - Base Width450 mm (17¾ in.)
 - Open Joint Width168 mm (6⅝ in.)
 - Steel Cover Plate Thickness.....13 mm (½ in.)
- Key Component –Bridge Deck
 - Thickness.....280 mm (11 in.)
 - Overhang Distance1,300 mm (51¼ in.)
 - Open Joint Width19 mm (¾ in.)
- Vehicle Make /Model2004 International 9200 Tractor, 2001 Wabash National Trailer
 - Curb.....13,481 kg (29,720 lb)
 - Test Inertial36,322 kg (80,076 lb)
 - Gross Static36,322 kg (80,076 lb)
- Impact Conditions
 - Speed83.2 km/h (51.7 mph)
 - Angle15.2 deg.
 - Impact Location0.46 m (1.5 ft) upstream from open joint
- Impact Severity (IS).....664 kJ (490 kip-ft) > 548 kJ (404 kip-ft) limit from MASH
- Vehicle Stability.....Satisfactory

- Exit Conditions
 - Speed.....61.6 km/h (38.3 mph)
 - Angle0 deg.
- Exit Box CriterionPass
- Vehicle Stopping Distance96 m (315 ft)
- Vehicle DamageModerate
 - Vehicle Damage Scale [30]1FR-6 and 1-RP-1
 - Collision Deformation Classification [31]1-FREW3 and 1-RDES1
- Maximum Vehicle Roll
 - Cab16.4 deg.
 - Trailer13.3 deg.
- Test Article Damage.....Minimal Cracking and Spalling
- Maximum Test Article Deflections
 - Permanent Set0 mm (0 in.)
 - Dynamic52 mm (2 in.)
 - Working Width949 mm (37.4 in.)

Figure 35. Summary of Test Results and Sequential Photographs, Test No. MAN-1



0.000 sec



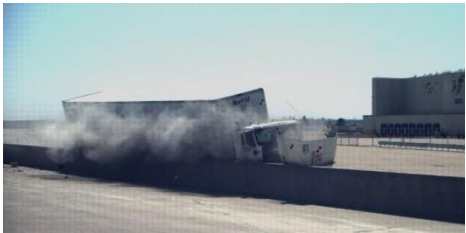
0.250 sec



0.500 sec



0.750 sec



1.000 sec



1.250 sec



0.000 sec



0.250 sec



0.500 sec



0.750 sec



1.000 sec



1.250 sec

Figure 36. Additional Sequential Photographs, Test No. MAN-1



0.000 sec



0.250 sec



0.500 sec



0.750 sec



1.000 sec



1.250 sec



0.000 sec



0.250 sec



0.500 sec



0.750 sec



1.000 sec



1.250 sec

Figure 37. Additional Sequential Photographs, Test No. MAN-1

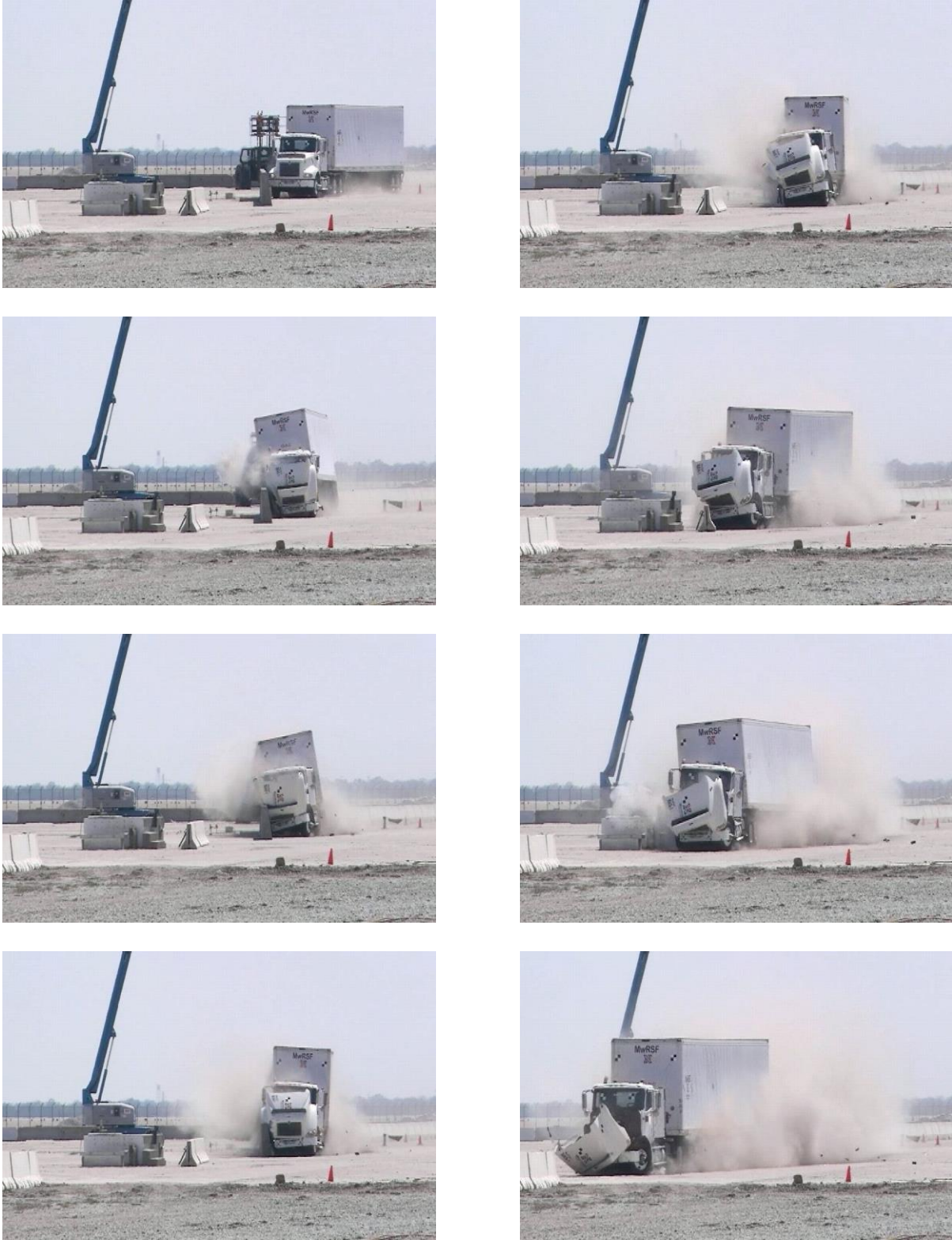


Figure 38. Documentary Photographs, Test No. MAN-1



Figure 39. Vehicle Final Position and Trajectory Marks, Test No. MAN-1

8.3 Barrier Damage

Damage to the test installation was minimal, as shown in Figures 40 through 43. Damage consisted of contact marks, gouging of the concrete, concrete spalling, and minor concrete cracking. The length of vehicle contact along the barrier was 36.1 m (118.6 ft), which spanned from 1,778 mm (70 in.) upstream from the open joint to the downstream end of the barrier.

Tire marks were visible along the front face of the barrier, while scrapes were found on the front and top faces of the barrier. Concrete spalling occurred on the top of the barrier beginning at the downstream end of the steel joint cap and ending approximately 1 m (37 in.) downstream. The amount of the spalling in this area varied, but it had a maximum depth of 52 mm (2 in.). None of the internal steel reinforcement was exposed.

Multiple hairline cracks were found on the barrier system, extending from 4 m (13 ft) upstream from the joint to 3.5 m (11.5 ft) downstream from the joint, as shown in Figures 40 and 41. Barrier cracks were more prevalent near the barrier joint. Cracks on the front side of the barrier ran diagonally from the base of the barrier up and away from the joint. Cracks on the back of the barrier typically aligned with cracks on the front, though a few vertical cracks were also present. All of the cracks in the barrier were less than 1.5 mm ($1/16$ in.) wide.

There were numerous gouges along the front side of the barrier left by contact with the vehicle rims and lug nuts. One set of gouges, measuring up to 13 mm ($1/2$ in.) deep, was located directly adjacent to the upstream edge of the steel cover plate, as shown in Figures 40 and 41. Only a small indentation was found on the chamfered edge of the cover plate at this location. The steel cover plate sustained no further gouging or deformations. Gouging resumed in the concrete bridge rail downstream from the steel end cap and continued for approximately 2 m (6.5 ft). Minor gouges and scrapes were found sporadically on the face of the barrier throughout the rest of the contact region.

Damage to the steel cover plate was largely cosmetic, consisting of contact marks and scrapes. All of the attachment bolts remained in place and in good condition. The cap was removed for further inspection, but no further damage was observed. However, with the cover plate removed, concrete cracks and minor spalling were found on top surface of the barrier on both sides of the open joint, as shown in Figure 42.

The bridge deck sustained only minor cracking as a result of the impact. A series of longitudinal hairline cracks were found on the surface of the downstream half of the bridge deck located directly over the outside edge of the grade beam. Each individual crack was no longer than 450 mm (18 in.), but all together these cracks spanned a total length of approximately 3 m (10 ft). Two cracks with a maximum opening width of 3 mm ($1/8$ in.) extended between the steel end cap and the open joint in the deck on the downstream side of the joint, as shown in Figure 43. These cracks continued through the thickness of the deck and merged into a single crack on the bottom surface of the deck. This crack extended 0.6 m (2 ft) downstream from the joint within the outer 50 mm (2 in.) of the bridge deck behind the barrier. The crack continued up the outside face of the bridge deck and diagonally back toward the joint until it reached the base of the barrier. The bridge deck upstream of the open joint experienced no visible cracking.

The permanent set of the barrier system was 0 mm (0 in.), as measured in the field. The maximum lateral dynamic barrier deflection was 52 mm (2 in.), as measured at the top of the barrier adjacent to the joint and determined from high-speed digital video analysis. The working width of the system, defined as the furthest lateral extent of the vehicle beyond the front of the barrier, was found to be 949 mm (37.4 in.), also determined from high-speed digital video analysis.



Figure 40. System Damage, Test No. MAN-1



Figure 41. System Damage, Test No. MAN-1



Figure 42. System Damage, Cover Plate Removed, Test No. MAN-1



Behind barrier



Behind barrier



Bottom of deck, downstream of joint



Bottom of deck, downstream of joint

Figure 43. Deck Damage, Test No. MAN-1

8.4 Vehicle Damage

The damage to the vehicle was moderate, as shown in Figures 44 through 46. After exiting the test installation, the vehicle impacted a secondary concrete protection barrier. Damage caused by the two impacts independent of each other could not be determined, so the total damage was recorded and discussed herein. Damage sustained from only the impact with the test article is likely less than documented at the vehicle's final resting position.

The majority of the damage was concentrated on the right-front corner and right side of the vehicle cab, where the impact occurred. The vehicle's hood was partially disengaged, but it was still attached by the left hood spring. The middle hood mount was detached, the right hood brace was partially torn and bent inward, and the hood brace on the bumper was crushed backward. There was a 559-mm (22-in.) tear in the right side of the hood and a 330-mm (13-in.) tear in the left side of the hood. The radiator and radiator mount were bent and kinked in multiple locations. Fluid was leaking from a break in the right intake hose coupler and a disengagement of the power steering line. The left side of the front bumper was bent 254 mm (10 in.) backward. Portions of both front fenders and the wheel well interiors disengaged. The right- and left-front shocks both disengaged from their wheel assemblies. The right-front tire assembly was crushed 914 mm (36 in.) backward into the right fuel tank, and the tire separated from the rim. The tire was torn and the rim dented. Multiple dents and scrapes were found on the right diesel fuel tank. The right-side stairs deformed, with the bottom bending upward 102 mm (4 in.) and the top bending 25 mm (1 in.) downward. There was scraping and denting on the bottom of the right-rear side of the cab. The right wind extension on the back of the cab was bent inward 25 mm (1 in.). The top of the right-side door had pulled away from the cab, leaving a 25-mm (1-in.) gap. The interior of the cab experienced deformations to the right-side floor pan.

Although the trailer was still resting on the truck tandem axles, the fifth-wheel plate had torn away from the truck. There was deformation of left-side vehicle support beams under the trailer. The trailer had scraping and dents along the length of its bottom-right edge, with 50 mm (2 in.) of inward crushing extending 432 mm (17 in.) from the front-right corner of the trailer. A 432-mm (17-in.) long tear occurred in the bottom lip of the trailer adjacent to the front-right corner, and a 559-mm (22-in.) long tear occurred in the right-side bottom lip located 1,575 mm (62 in.) behind the front of the trailer. There were 127-mm and 89-mm (5-in. and 3½-in.) long vertical tears in the right side of the trailer located 559 mm and 1,194 mm (22 in. and 47 in.) from the front of the trailer, respectively. The right side of the rear bumper was bent downward, and the right side of the trailer was bulging outward slightly. The left side of the trailer had a 610-mm (24-in.) long tear located 737 mm (29 in.) from the front of the trailer.

The ballast moved very little during the crash test. One precast concrete barrier segment located at the rear of the trailer shifted approximately 100 mm (4 in.) laterally. The nylon strap attaching the rear of this concrete barrier segment to the side wall of the trailer snapped, and the threaded rods attaching the base of this barrier to the trailer floor bent. A few more of the nylon straps tore through the metal anchorage brackets located on the inside of the trailer wall, but the other concrete segments did not show significant permanent displacement.



Figure 44. Vehicle Damage, Test No. MAN-1



Figure 45. Vehicle Damage, Test No. MAN-1



75

Figure 46. Fifth Wheel Plate Damage, Test No. MAN-1

The maximum occupant compartment deformations are listed in Table 12 along with the deformation limits established in MASH for various areas of the occupant compartment. Note that none of the MASH established deformation limits were violated. Complete occupant compartment and vehicle deformations and the corresponding locations are provided in Appendix C.

Table 12. Maximum Occupant Compartment Deformations by Location

LOCATION	MAXIMUM DEFORMATION mm (in.)	MASH ALLOWABLE DEFORMATION mm (in.)
Wheel Well & Toe Pan	58 (2.3)	≤ 229 (9)
Floor Pan & Transmission Tunnel	41 (1.6)	≤ 305 (12)
Side Front Panel (in Front of A-Pillar)	20 (0.8)	≤ 305 (12)
Side Door (Above Seat)	20 (0.8)	≤ 229 (9)
Side Door (Below Seat)	20 (0.8)	≤ 305 (12)
Roof	0 (0)	≤ 102 (4)
Windshield	NA	≤ 76 (3)

8.5 Occupant Risk

Although not required for evaluation in MASH test designation no. 5-12 with a 36000V vehicle, the occupant impact velocities (OIVs) and maximum 0.010 second occupant ridedown accelerations (ORAs) in both the longitudinal and lateral directions were calculated. Three accelerometer units were utilized on the test vehicle, but only one, the DTS, was placed in the occupant compartment. Thus, OIV and ORA values were only calculated from the DTS unit. As a means to compare the results with various other crash tests, THIV, PHD, and ASI values were also calculated from the DTS. Maximum angular displacements were calculated for all units. Unfortunately, the SLICE-1 unit improperly triggered and did not record the impact event. Subsequently, it was not analyzed. The results of the occupant risk data analysis are shown in Table 13. The recorded data from the accelerometers and the rate transducers are shown graphically in Appendix D.

Table 13. Summary of OIV, ORA, THIV, PHD, and ASI Values, Test No. MAN-1

Evaluation Criteria		Transducer		
		DTS (Cab)	SLICE-1 (Trailer – Rear)	SLICE-2 (Trailer - Front)
OIV m/s (ft/s)	Longitudinal	-0.71 (-2.33)	-	NA
	Lateral	-4.92 (-16.15)	-	NA
ORA g's	Longitudinal	-4.04	-	NA
	Lateral	-6.30	-	NA
MAX. ANGULAR DISPL. deg.	Roll	16.4°	-	13.3°
	Pitch	6.7°	-	9.9°
	Yaw	-15.4°	-	-16.2°
THIV m/s (ft/s)		4.41 (14.47)	-	NA
PHD g's		6.52	-	NA
ASI		0.67	-	0.89

8.6 Discussion

The analysis of the test results for test no. MAN-1 showed that the Manitoba Constrained-Width, Tall Wall Bridge Rail adequately contained and redirected the 36,000V vehicle without any permanent displacement of the barrier. There were no detached elements nor fragments which showed potential for penetrating the occupant compartment nor presented undue hazard to other traffic. Deformations of, or intrusions into, the occupant compartment that could have caused serious injury did not occur. The test vehicle did not penetrate nor ride over the barrier and remained upright during and after the collision. Vehicle roll, pitch, and yaw angular displacements, as shown in Appendix D, were deemed acceptable because they did not adversely influence occupant risk safety criteria nor cause rollover. After impact, the vehicle exited the barrier at an angle of 0 degrees and its trajectory did not violate the bounds of the exit box.

The initial impact point was 452 mm (17.8 in.) downstream from the targeted impact point, which falls outside of the +/-305 mm (+/-12 in.) window allowed by MASH. However, the rear tandem axles impacted the bridge rail just upstream from the joint. Chalk marks on the face of the bridge rail left by each tire indicated that the impact of the rear tandem axles was centered about 1.5 m (5 ft) upstream from the joint, and the front of the two wheels impacted at the upstream end of the steel cover plate. The targeted impact point was selected to cause maximum loading (result of rear tandem axles impacting the barrier) adjacent to and upstream from the joint. Although the targeted impact point was outside of MASH tolerances, the intended impact point for the rear tandem axles and location of maximum loading was satisfied. Additionally, the impact speed and angle satisfied MASH criteria. Therefore, test no. MAN-1, conducted on the

Manitoba Constrained-Width, Tall Wall Bridge Rail, was determined to be acceptable according to the MASH safety performance criteria for test designation no. 5-12.

9 Data Analysis of Test No. MAN-1

9.1 Vehicle Roll

The angular rate transducer data was analyzed to estimate vehicle roll. The transducers recorded maximum roll angles of 16 degrees and 13 degrees for the cab and trailer, respectively. Previous TL-5 crash testing has typically resulted in significantly more vehicle roll. However, the vast majority of previously-designed and crash-tested TL-5 barriers utilized a shorter height of 1,067 mm (42 in.). The previous TL-5 crash tests in which roll data was available are summarized in Table 14. The average maximum roll angle for trailers impacting a 1,070 mm (42 in.) tall barrier was calculated to be 36 degrees. All listed crash tests also had a maximum roll angle which was at least two times that observed in test no. MAN-1 for the Manitoba bridge rail. Thus, it is believed that the increased height of the Manitoba bridge rail contributed to a more stable redirection by reducing vehicle roll. The test vehicle was equipped with air ride suspension systems, typical for more recent vehicle models versus the traditional leaf-spring suspension systems, which may have also contributed to the reduction in vehicle roll. However, the reduction in vehicle roll caused solely by the air ride suspension system could not be quantified due to a lack of TL-5 tests conducted with air ride suspension vehicles.

Table 14. Maximum Roll Angle for Trailer during TL-5 Crash Tests

Test No.	Reference	Barrier Description	Barrier Height mm (in.)	Maximum Trailer Roll
ACBR-1	[12]	Open Concrete Bridge Rail	1,067 (42)	38°
RYU-1	[16]	Modified New Jersey Barrier	1,067 (42)	41°
TL5CMB-2	[17]	Modified Single Slope Barrier	1,067 (42)	43°
4798-13	[18]	New Jersey Median Barrier	1,067 (42)	26°
478130-1	[32]	New Jersey Barrier	1,067 (42)	32°
Average			1,067 (42)	36°
MAN-1		Single Slope Bridge Rail	1,250 (49¼)	13°

9.2 Impact Load Estimation

The increased height of the Manitoba bridge rail likely affected the impact loads in two very distinct ways. First, since the trailer impacted the bridge rail laterally, the effective height of the impact load was increased. Impacts into 1,067-mm (42-in.) tall barriers typically result in the vehicle wheels providing the lateral load to the face of the barrier while the trailer extends over and leans on top of the barrier. With both the wheels and the trailer impacting the face of the Manitoba Constrained-Width Tall Wall, the effective height of the impact load was likely increased. Second, the reduced vehicle roll likely increased the magnitude of the impact load. By reducing the vehicle roll, the lateral displacement of the ballasted trailer was reduced and the time in which the lateral momentum of the ballasted trailer was stopped (with respect to the

barrier) was also reduced. According to the impulse-momentum equation, $\int F\delta t = \Delta mv$, in order for the force-impulse to result in the same change in momentum, a reduced impact time requires an increase in force. Therefore, the impact loads into the Manitoba bridge rail were likely greater in magnitude and applied at an increased effective height as compared to previous TL-5 impacts into typical 1,067 mm (42 in.) tall barriers.

As discussed previously in Section 7.5, the test vehicle was equipped with three independent accelerometer units in an effort to quantify the impact load imparted to the barrier during the crash test. The SLICE-1 unit was placed on the trailer frame adjacent to the rear tandem axles. Previous research has shown that the maximum impact load typically results from the impact event involving the rear tandem axles and rear of the trailer with the barrier. Unfortunately, the SLICE-1 unit triggered prematurely and did not record the impact event. The DTS unit was placed in the cab, and extra longitudinal and lateral accelerometers were placed on the truck frame near the front tandem axles and wired into the DTS unit. The SLICE-2 unit was mounted inside the trailer above the front tandem axles. Thus, the DTS extra accelerometers and the SLICE-2 unit were expected to record similar impact load estimates. Unfortunately, during the test, the fifth wheel plate was torn from the truck frame, so the accelerations measured at the truck frame and the trailer were significantly different. Since the majority of the vehicle mass that was carried by the front tandem axles was located in the trailer, data from the extra DTS accelerometers did not provide an accurate estimation for impact load and was discarded. Thus, data from the SLICE-2 unit, which did remain rigidly attached to the trailer throughout the impact event, was utilized to estimate the impact load imparted into the bridge rail.

The impact load was estimated utilizing both the acceleration and angular displacement data from the SLICE-2 unit. The angular rate yaw data was combined with the trailer's initial impact angle to provide the vehicle orientation angle throughout the crash event. Next, the accelerometer data in the longitudinal and lateral directions were processed with a CFC 60 filter and then a 50-ms average to eliminate high-frequency noise and vibrations. The filtered and averaged accelerometer data was then transformed into orthogonal components with orientations normal and tangential to the barrier system using the following equations:

$$\begin{aligned}A_N &= A_x * \text{Sin}(\theta) + A_y * \text{Cos}(\theta) \\A_T &= A_x * \text{Cos}(\theta) - A_y * \text{Sin}(\theta)\end{aligned}$$

where A_N and A_T are the accelerations normal and tangential to the barrier, respectively, θ is the orientation angle of the trailer relative the barrier, and A_x and A_y are the vehicle's local accelerations in the longitudinal and lateral directions, respectively. Finally, these accelerations were then multiplied by the appropriate portion of the vehicle mass to obtain the estimated impact forces.

Because the test vehicle is articulated, different parts of the tractor trailer impacted the wall and transmitted load at different times. Utilizing the entire mass of the 36000V vehicle within this procedure would not be appropriate. Thus, only a component of the vehicle mass should be associated with the accelerations observed by the SLICE-2 unit. The accelerometers were mounted adjacent to the front tandem axles with the intent of utilizing the axle weights as

the mass associated with the recorded accelerations. Unfortunately, the fifth-wheel plate was torn from the truck during the crash test. The plate and trailer kingpin remained within the truck framework, but it is unknown if the rear of the truck acted in unison with the front of the trailer. Thus, two different masses were utilized to bracket the estimated impact load; (1) the actual measured axle weights including both the truck and the trailer, which represents the upper bound for the force magnitude, and (2) the weight of only the front end of the trailer (i.e., measured axle weight minus the stand-alone truck axle weight), which represents a lower bound. The vehicle's test inertial weight for the front tandem axles was 15,452 kg (34,066 lb), while the weight of only the trailer at this location was 13,411 kg (29,566 lb). The results from this analysis are shown in Figure 47.

After coupling the trailer's orientation with the SLICE-2 accelerations, the lateral peak load imparted into the barrier from the front tandem axles was estimated to range between 1,027 kN and 1,183 kN (231 kips and 266 kips), depending on the mass utilized in the calculation. The peak load occurred approximately 0.190 s into the impact event, which corresponded to the time in which the right-front corner of the trailer impacted the top of the barrier. Two additional force spikes of approximately 400 kN (90 kips) followed the initial peak and were likely the result of continued contact between the barrier face and the vehicle front tandem axle wheels and trailer.

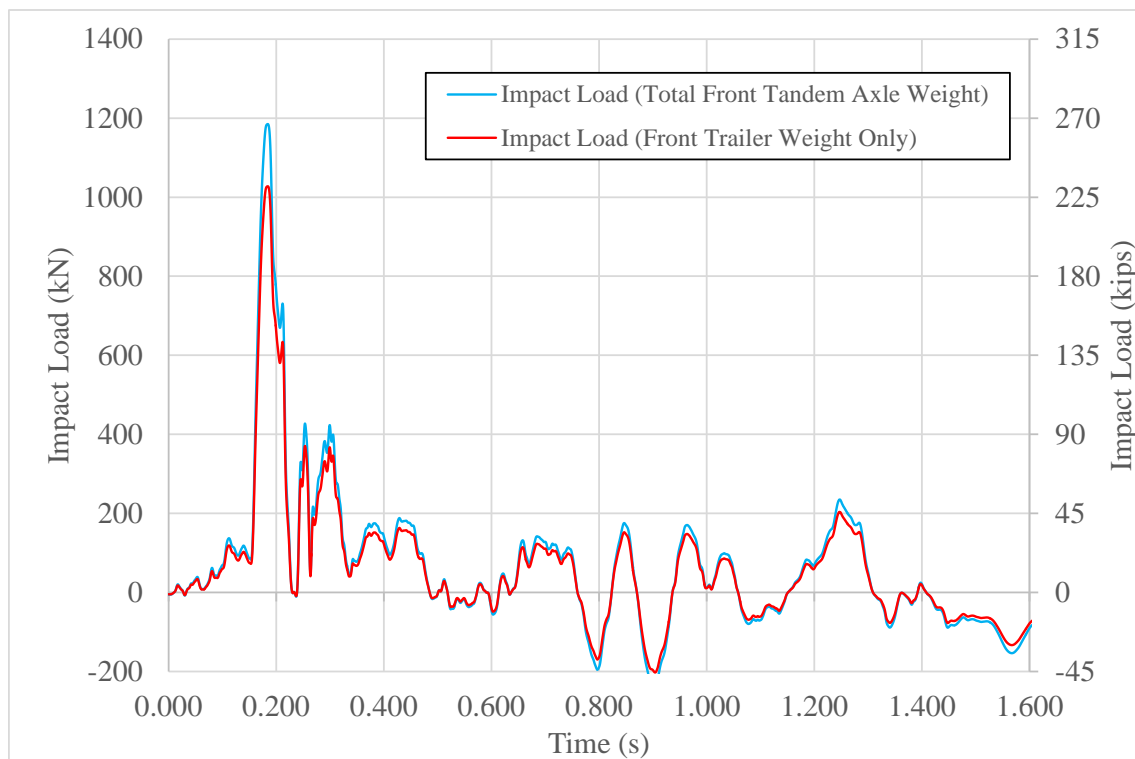


Figure 47. Estimated Impact Load, Test No. MAN-1

The calculated impact loads shown in Figure 47 represented the loads imparted to the barrier by the front tandem axles and front of the trailer. Previous TL-5 crash testing has demonstrated that the maximum impact load typically occurs during the vehicle tail slap (i.e., when the rear tandem axles and rear of the trailer impacts the barrier) [21]. Based on the observed bridge rail deflections, the rear of the trailer likely applied a greater impact load during

test no. MAN-1. As shown in Figure 48, the barrier deflected 36 mm (1.4 in.) as a result of the impact at the front of the trailer. The barrier restored nearly back to its original position before the rear of the trailer impacted the barrier and caused a deflection of 52 mm (2.0 in.). Greater deflections indicate that a higher impact load was likely imparted to the system by the rear of the trailer. Thus, the impact load resulting from the tail slap of the trailer was likely higher than the peak load estimated using the SLICE-2 unit at the front of the trailer. Unfortunately, the SLICE-1 unit that was mounted adjacent to the rear tandem axles experienced technical difficulties and did not record the crash event. Between 0.80 s and 0.95 s after impact, the trailer roll blocked the view of the overhead camera utilized to measure barrier deflections. Thus, the rail displacements measured between 0.80 s and 0.95 s were taken from points outside of the immediate impact region, which resulted in the lower deflections recorded at these times.

The estimated impact load from contact with the front of the trailer ranged between 1,027 kN and 1,183 kN (231 kips and 266 kips), which represented an 18 to 35 percent increase over the calculated Yield Line design strength of the bridge rail, 874 kN (196 kips). The impact load was based on an assumed vehicle mass subjected to the measured accelerations, and the uncertainty of this calculation is unknown. However, the impact load resulting from the rear of the trailer likely produced an even higher impact load, which was much higher than the barrier's design strength. With the bridge rail sustaining only minor damage, the results further demonstrate that Yield Line analysis produces a conservative (low) design strength for solid concrete parapets.

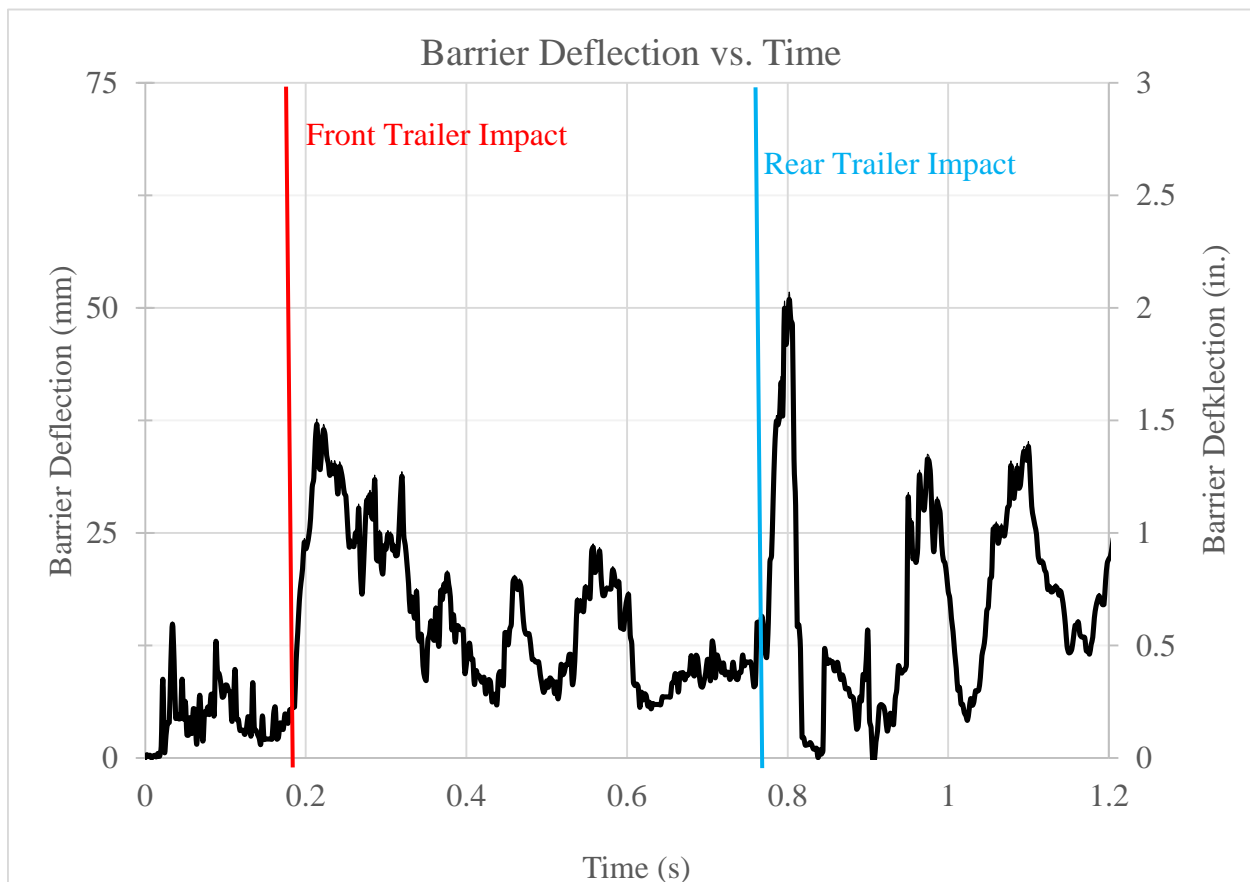


Figure 48. Barrier Deflection vs. Time, Test No. MAN-1

One possible reason for the conservative nature of Yield Line analysis may be the simplification of the impact load to a linearly distributed load applied at a constant height. As witnessed during test no. MAN-1, the vehicle wheels and the bottom of the trailer box were in contact with the barrier and applied load simultaneously. Thus, the impact load is actually applied over multiple areas and at multiple heights. Simplifying the vertical distribution of the impact load into a singular load height is difficult to quantify, and conservative (higher) load heights are typically used.

An ongoing TTI study is utilizing computer simulation to analyze the magnitude and effective load height for TL-5 impacts into barriers with various heights [32]. The current recommendations for TL-5 design loads and effective load heights as a function of barrier height are shown in Table 15. The recommended design load for barriers taller than 1,067 mm (42 in.) of 1,156 kN (260 kips) was similar to the maximum impact load measured during test no. MAN-1. When considering that the vehicle tail slap likely produced a higher impact load, a recommended design load of 1,156 kN (260 kips) may be reasonable for tall, rigid barriers. However, this design load combined with the recommended effective load height of 1,092 mm (43 in.) may result in overly-conservative barrier designs. Recall, the Manitoba bridge rail had a design strength of 874 kN (196 kips) with the load applied at the top of the barrier, 1,250 mm (49¼ in.). Utilizing the recommended effective load height of 1,092 mm (43 in.), the Manitoba bridge rail design strength was calculated to be 970 kN (218 kips), or only 84 percent of the recommended design strength. Test no. MAN-1 resulted in no major structural damage. Thus, these calculations further demonstrate that Yield Line analysis produces conservative design strengths for solid parapets. Therefore, further investigation into the impact load, effective load height, and barrier analysis techniques are warranted to optimize barrier design strengths with TL-5 impact loads.

Table 15. TL-5 Design Loads from Ongoing Study NCHRP 20-22(2) [32]

Barrier Height	Design Loads		
	Dynamic Impact Load	Effective Load Height	Applied Moment
1,067 mm (42 in.)	712 kN (160 kips)	864 mm (34 in.)	615 kN-m (453 kip-ft)
1,067 mm – 1,372 mm (42 in. – 54 in.)	1,156 kN (260 kips)	1,092 mm (43 in.)	1,262 kN-m (932 kip-ft)
>1,372 mm (>54 in.)	1,156 kN (260 kips)	1,321 (52 in.)	1,527 kN-m (1127 kip-ft)

10 MEDIAN AND ROADSIDE CONFIGURATIONS

10.1 TL-5 Median Barrier Configuration

As part of the barrier development effort, median barrier, roadside barrier, and bridge rail configurations of the Manitoba Constrained-Width, Tall Wall barrier system were desired. The bridge rail was developed first and selected for crash testing because it was considered to be the most critical of the configurations. After the successful crash test on the bridge rail, the other two configurations were developed with the same face geometry and equivalent or greater strength.

Design and analysis of the median barrier configuration followed a methodology similar to the development of the bridge rail, as detailed in Section 4.1. However, there were a few differences in the configuration options and the design strength. For a median (double-sided) barrier, a 200-mm (8-in.) top width resulted in the maximum targeted base width of 600 mm (23¾ in.). Thus, the top width of the median barrier was held constant at 200 mm (8 in.). The increased width of the median profile resulted in increased barrier strength and, thus, required less steel reinforcement. As such, 10M bars, which were originally eliminated from the bridge rail configuration options due to a lack of adequate strength, were re-considered for use in the median barrier. Finally, the median barrier was required to have the same or greater strength as the tested bridge rail configuration, or a calculated design strength of 874 kN (196 kips) instead of the original design strength of 845 kN (190 kips).

The median barrier was optimized using the same process detailed in Section 4.1 for the bridge rail. Each configuration option was analyzed utilizing Yield Line analysis, and the maximum stirrup spacing to satisfy the design strength criteria was determined for each longitudinal rebar configuration and stirrup size combination. Finally, the amount of steel in each configuration was calculated per unit length, in kg/m, and these values were utilized to compare the relative costs of each design configuration. Results from the median barrier analysis are shown in Table 16 for both interior and end sections of the barrier.

Since the majority of an installation will be comprised of interior barrier sections, the selection of an optimal design focused on the interior section results. The median barrier analysis of interior sections resulted in a four-way tie for the lowest amount of steel, 22.7 kg/m (15.3 lb/ft). Looking at the end sections associated with these four designs, one configuration also had the lowest amount of steel for an end section. This configuration, highlighted in Table 16, was also the only of the four configurations to consist of 10 longitudinal bars instead of 12, so it would require less steel ties. Therefore, the median barrier configured with ten 10M longitudinal bars and 20M stirrups spaced at 400 mm (15¾ in.) and 300 mm (12 in.) for the interior and end sections, respectively, was selected as the optimal design. Details for the selected median barrier design are shown in Figures 49 and 50.

During the Yield Line analysis of the selected configuration, a critical length of 2.6 m (8.5 ft) was calculated for the end section. Thus, the end section reinforcement characterized by a reduced stirrup spacing should be utilized over a distance of at least 2.6 m (8.5 ft). Incorporating a stirrup spacing of 300 mm (11¾ in.) and 75 mm (3 in.) of concrete cover, the length of the median barrier end section was specified to be 2.785 m (9 ft – 2 in.), as shown in Figure 49.

To ensure proper performance, the median barrier should be anchored to a reinforced concrete foundation slab similar to the anchorage of the bridge rail to the deck. Figure 49 illustrates two anchorage options. Option 1 utilizes 15M dowel bars epoxied into the foundation slab, while Option 2 utilizes 15M U-bars cast into the foundation slab. The anchorage bars for either option were placed adjacent to each barrier stirrup. Additionally, both anchorage options required 200 mm (8 in.) of embedment, so a minimum thickness of 280 mm (11 in.) was recommended for the foundation slab. The foundation slab may be either an extension of or tied directly to the roadway slab in order to prevent rotation of the median barrier system. If the foundation slab is separate from any other roadway slabs, it should be at least 2 m (6.5 ft) wide and contain reinforcement comparable to the bridge deck to provide enough strength to support the median barrier system.

Table 16. Optimization Analysis Results for Median Barrier Configurations

Top Barrier Width (mm)	Longitudinal Steel		Transverse Steel	Interior Section			End Section		
	Size	No. of Bars	Size	Transverse Steel Spacing (mm)	Barrier Strength (kN)	Total Steel (kg/m)	Transverse Steel Spacing (mm)	Barrier Strength (kN)	Total Steel (kg/m)
200	10M	10	10M	100	1,160	27.7	50	1,679	47.6
200	10M	12	10M	150	897	22.7	100	877	29.3
200	15M	10	10M	150	1,040	28.9	100	914	35.6
200	15M	12	10M	200	914	28.8	100	932	38.7
200	20M	10	10M	200	986	33.5	100	956	43.4
200	20M	12	10M	250	918	36.2	100	979	48.1
200	10M	10	15M	250	975	23.7	200	876	27.7
200	10M	12	15M	300	897	22.7	200	879	29.3
200	15M	10	15M	350	939	27.0	200	916	35.6
200	15M	12	15M	400	914	28.8	200	934	38.7
200	20M	10	15M	450	917	32.4	200	958	43.4
200	20M	12	15M	500	918	36.2	200	981	48.1
200	10M	10	20M	400	930	22.7	300	875	27.7
200	10M	12	20M	450	897	22.7	300	878	29.3
200	15M	10	20M	600	874	25.6	300	916	35.6
200	15M	12	20M	600	915	28.8	300	933	38.7
200	20M	10	20M	700	896	32.1	300	957	43.4
200	20M	12	20M	750	918	36.2	300	980	48.1

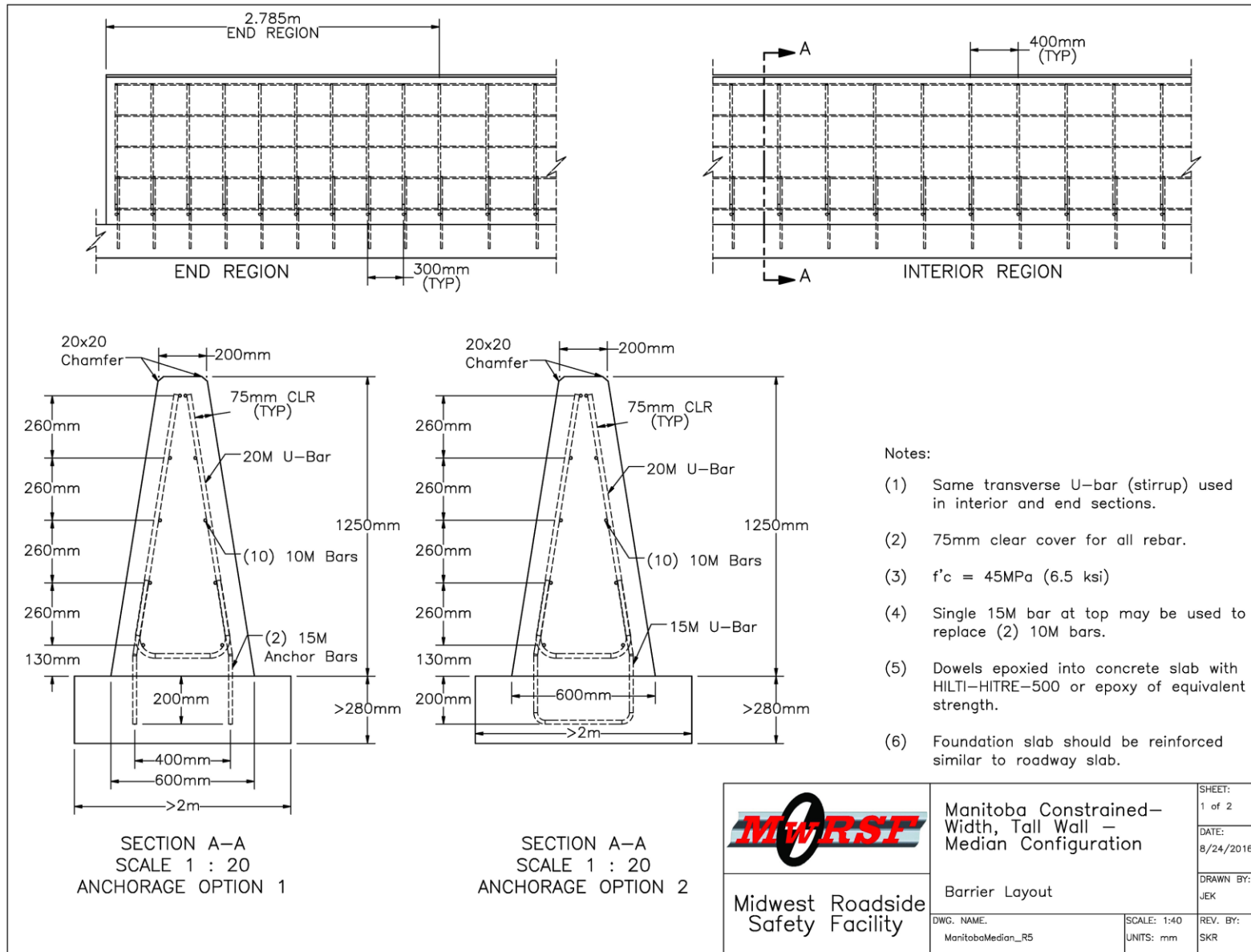


Figure 49. Manitoba Constrained-Width, Tall Wall, Median Barrier Details

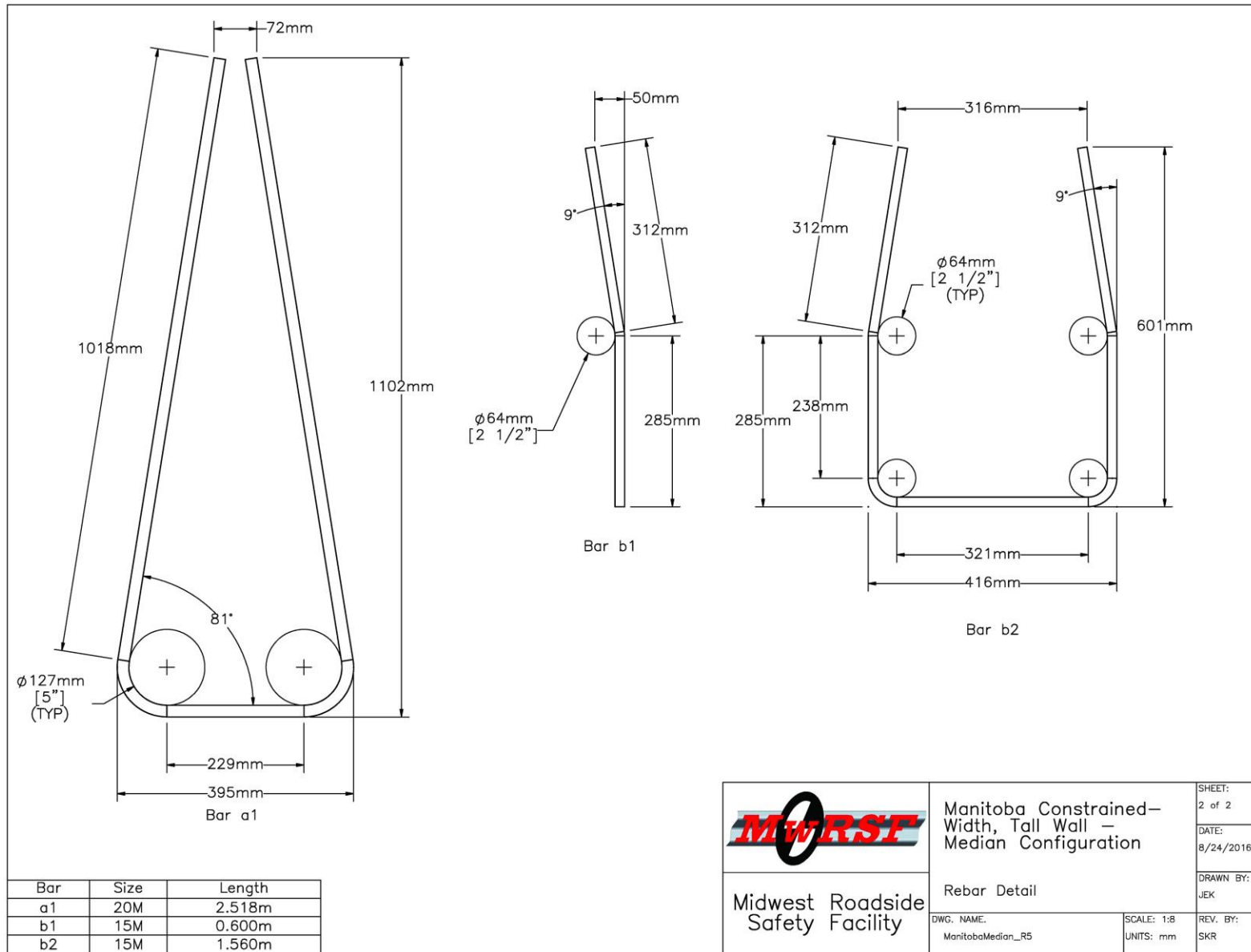


Figure 50. Median Barrier Reinforcement Details

10.2 Alternative Anchorage Options for Median Barrier

Real-world installation sites may exist where the median is too narrow for a median barrier foundation slab. In such situations, the foundation may be required to be as narrow as the 600-mm (23³/₄-in.) footprint of the median barrier itself. Thus, a narrow-width, anchorage footing was designed to support the Manitoba Constrained-Width, Tall Wall median barrier.

Previous studies have utilized the design methodology that barrier footings should have the torsional strength to support the full overturning strength of the barrier in which they support [17, 33]. The torsion design load was calculated by multiplying the barrier's overturning moment capacity by the critical length of the barrier section, M_c and L_{CR} from the Yield Line analysis, respectively. Since the impact load can be distributed both upstream and downstream from impacts located on interior sections of the barrier, the interior-section design load was divided by two. For the selected TL-5 median barrier, this process resulted in torsion design loads of 244 kN-m (180 kip-ft) and 456 kN-m (337 kip-ft) for barrier's interior and end sections, respectively.

Reinforced concrete footings were then designed utilizing the torsion reinforcement methodology from the *Building Code Requirements for Structural Concrete (ACI 318-11)* [34]. For an interior section, a 600-mm wide x 600-mm deep (23³/₄-in. x 23³/₄-in.) concrete footing incorporating 20M stirrups at 400-mm (15³/₄-in.) spacing and six 15M longitudinal bars was found to satisfy the required design strength. Due to the increased design load near end sections, the size of the end section footing had to be increased beyond the desired 600-mm (23³/₄-in.) width. The resulting end section footing was 900 mm wide x 600 mm deep (35¹/₂ in. x 23³/₄ in.) and incorporated 20M stirrups at 300-mm (12-in.) spacing and eight 20M longitudinal bars. Details for the footing designs are shown in Figures 51 and 52. The stirrup spacing for both footings matched the transverse steel spacing for the corresponding barrier sections, so they could be tied together utilizing either of the barrier anchorage options shown in Figure 49. The end section footing was designed for placement below the entire 2.785 m (9 ft – 2 in.) long barrier end section. The barrier is to be centered over the end footing.

Asphalt keyways are another anchorage method commonly used to support concrete median barrier systems. Asphalt keyways are typically 75 mm (3 in.) thick and are placed on both sides of the barrier system to restrict movement during an impact event. This type of anchorage has been utilized previously in successful crash testing of TL-5 barriers with widths similar to the median barrier developed herein [17-18]. Thus, an asphalt keyway system may be capable of anchoring the new Manitoba Constrained-Width, Tall Wall median barrier at interior sections.

When utilizing a 75-mm (3-in.) thick asphalt keyway, the total height of the concrete barrier should be increased to 1,325 mm (52¹/₄ in.) in order to maintain an effective height of 1,250 mm (49¹/₄ in.). Additionally, the height of the transverse steel U-bars was increased by 75 mm (3 in.), and the U-bars maintained a 75-mm (3-in.) clear cover throughout the barrier cross section. Details of the Manitoba Constrained-Width, Tall Wall median barrier anchored with an asphalt keyway are shown in Figure 53.

Asphalt keyways are only recommended for use to anchor interior sections of the new median barrier. Asphalt keyways can be placed over the entire system length, but anchorage requirements will increase for impacts adjacent to barrier discontinuities. Unfortunately, testing of concrete barriers in asphalt keyways has not been conducted on a barrier end section. Thus, the actual strength, durability, and effectiveness of an asphalt keyway remain unknown for barrier end sections. Therefore, the barrier end sections should be anchored to a foundation slab or footing, as shown in Figures 49 through 52.

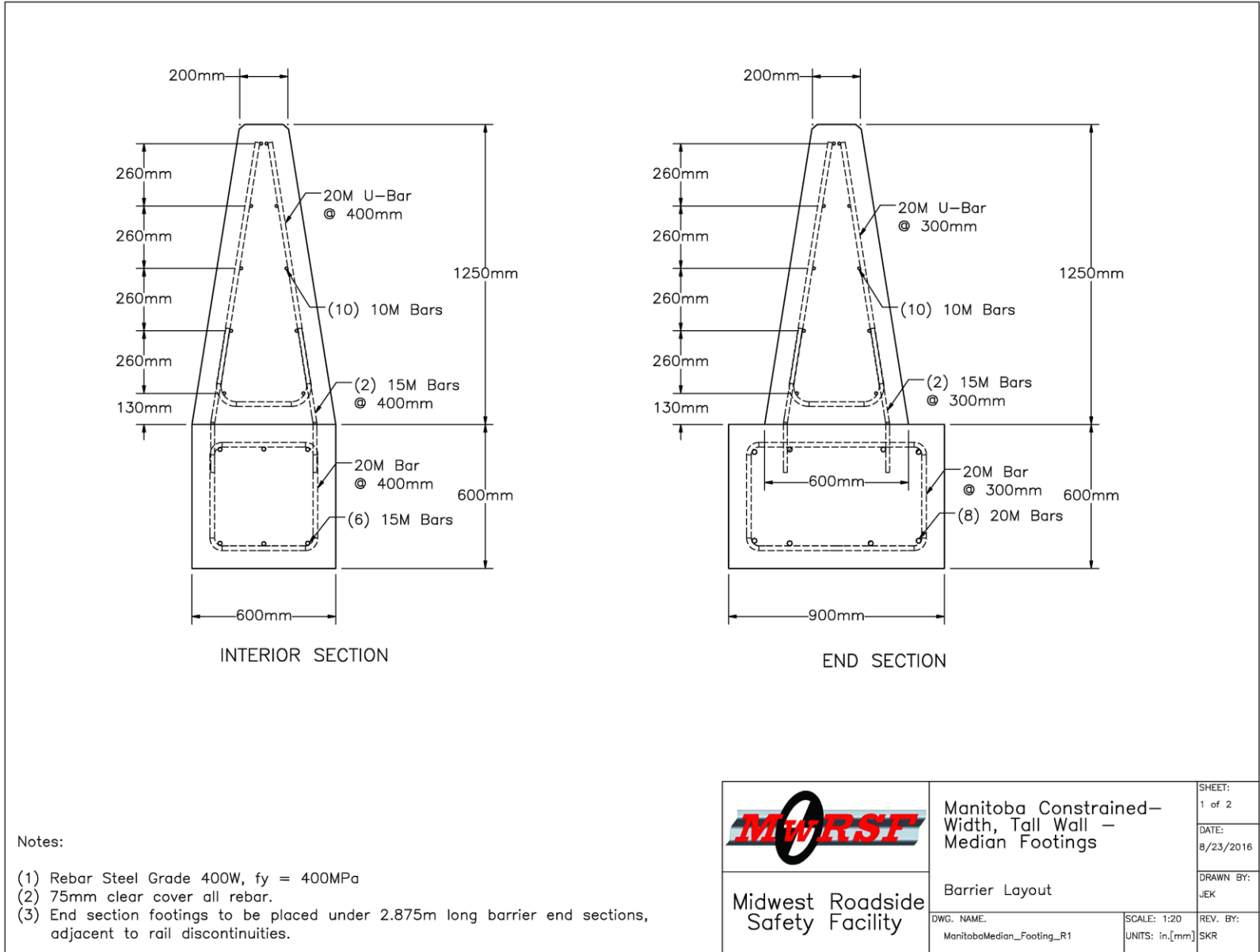


Figure 51. Footing Anchorage Details for Median Barrier

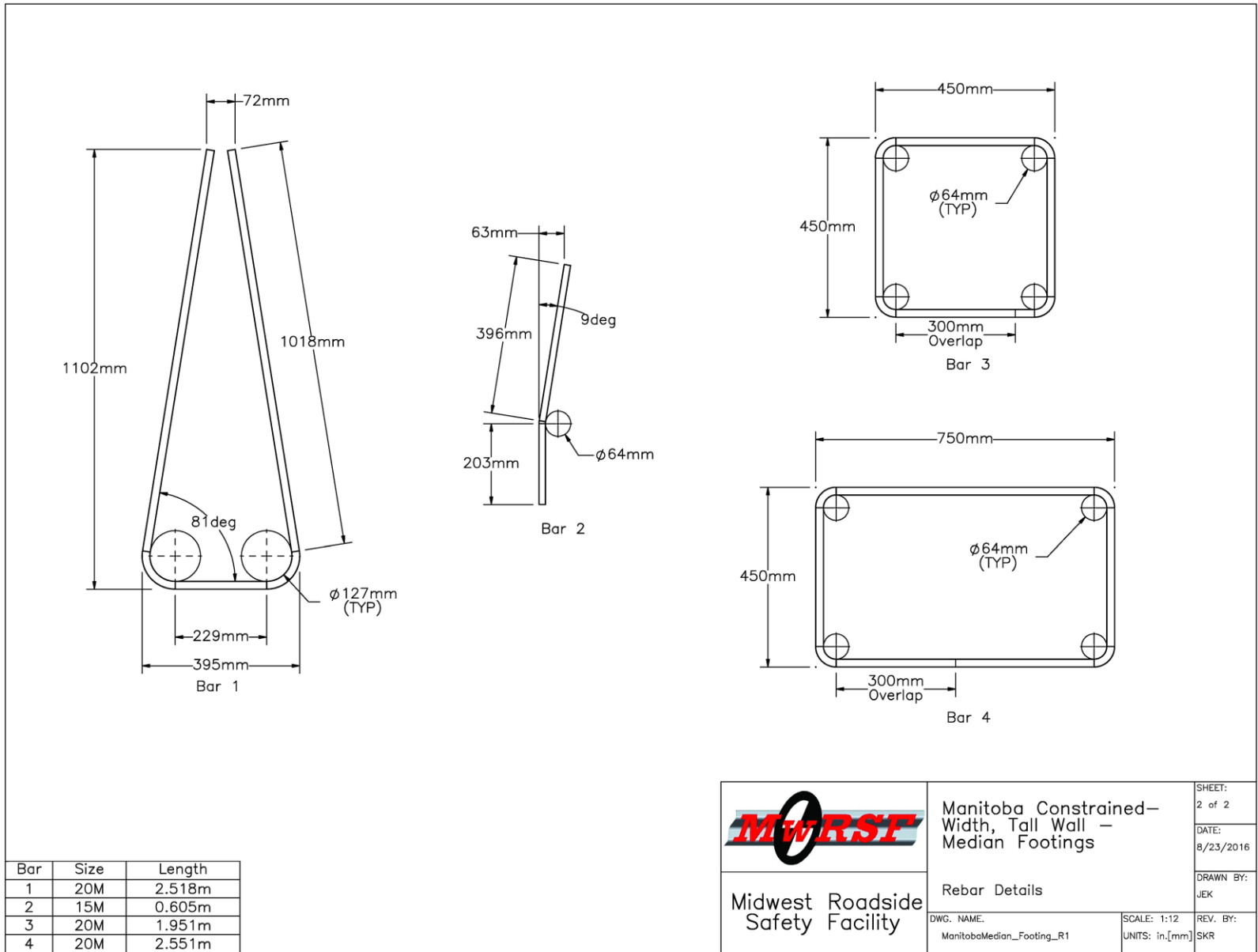


Figure 52. Footing Reinforcement Details for Median Barrier

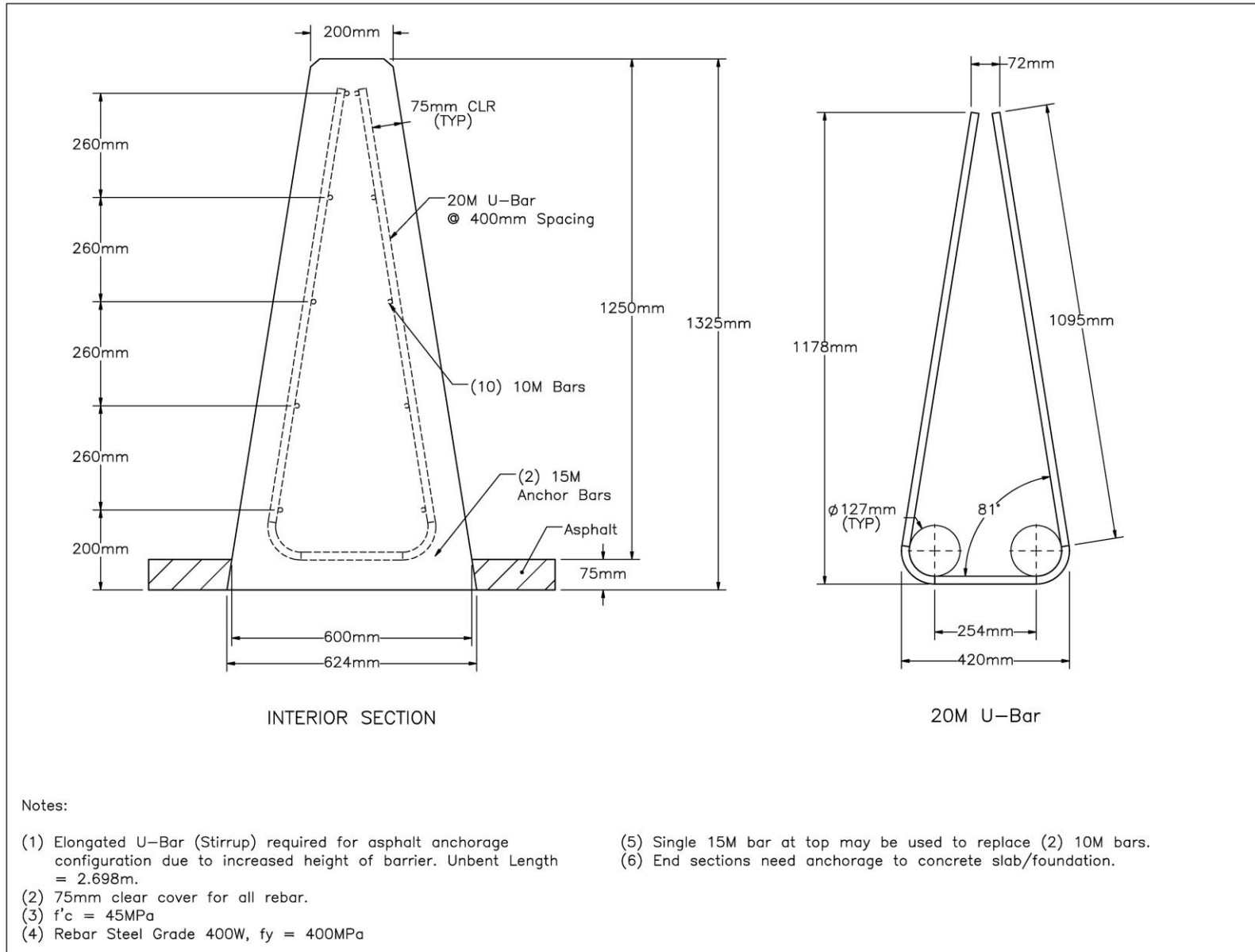


Figure 53. Asphalt Keyway Anchorage Details for Median Barrier Interior Sections

10.3 TL-4 Median Barrier Configuration

MI also desired to have a MASH TL-4 version of the Manitoba Constrained-Width, Tall Wall median barrier. The TL-4 version was desired to utilize the same base width and face slope as the TL-5 version. This would allow the same forms to be used during fabrication of either barrier version by simply blocking out the top of the form to the desired height. Additionally, a steel reinforcement configuration similar to the TL-5 median barrier was desired to make the transition between the two barriers relatively easy. Thus, eight 10M bars was selected for use as the longitudinal steel reinforcement for the TL-4 median barrier, eliminating the top two bars from the TL-5 median barrier configuration.

Since the TL-4 version of the barrier was not going to be crash tested, the barrier was conservatively designed in terms of height and strength. Previous crash testing has shown that the old TL-4 standard height of 813 mm (32 in.) will not satisfy the new MASH TL-4 standards, and the 10,000 kg (22,000 lb) single-unit truck, designated as the 10000S vehicle, will roll over the top of the barrier [35-36]. Computer simulations have suggested that vertical-faced barriers with heights as low as 876 mm (34.5 in.) may be tall enough to contain the 10000S vehicle [37]. However, there have not been any MASH TL-4 crash tests at this barrier height. One MASH TL-4 crash test was conducted on a 914-mm (36-in.) tall, single-slope (11 degrees from vertical), concrete barrier, and the barrier contained the vehicle and satisfied all MASH evaluation criteria [38]. Therefore, 914 mm (36 in.) was selected as the height for the TL-4 version of the median barrier.

With limited MASH TL-4 crash tests conducted to date, the design load for a MASH TL-4 barrier has not yet been determined. Various studies have suggested a design load ranging between 355 kN and 445 kN (80 kips and 100 kips) for a MASH TL-4 barrier [32, 37]. To be conservative, a design load of 423 kN (95 kips) was selected for the TL-4 median barrier developed herein.

Yield Line analysis was utilized to calculate the design strength for various barrier configurations. Although a full optimization analysis was not completed, multiple reinforcement configurations were analyzed to determine a barrier configuration that satisfied the strength criteria while limiting the amount of steel reinforcement. The selected interior barrier configuration utilized 10M U-bar stirrups spaced at 400 mm (15¾ in.) and had a design strength of 423 kN (95 kips), while the selected end section utilized 15M U-bars spaced at 300 mm (12 in.) and had a design strength of 431 kN (97 kips). As desired, both barrier sections utilized eight 10M longitudinal bars. The required length of the end section adjacent to barrier discontinuities was 1.59 m (5.25 ft). The TL-4 median barrier configurations are shown in Figure 54.

The stirrups in Figure 54 were shown as U-bars to match the stirrup designs for the bridge rail and TL-5 median barrier. However, the width of the TL-4 median barrier would allow the use of closed-loop stirrups. Although they require more steel, closed-loop stirrups would provide more stiffness and stability during construction, especially during slipforming operations. Thus, either U-bar or closed-loop stirrups may be utilized within the TL-4 median barrier. Additionally, due to the similarity between the TL-4 and TL-5 barriers, the TL-4 median

barrier may be anchored utilizing either foundation slab, footing, or asphalt keyway, as shown in Sections 10.1 and 10.2.

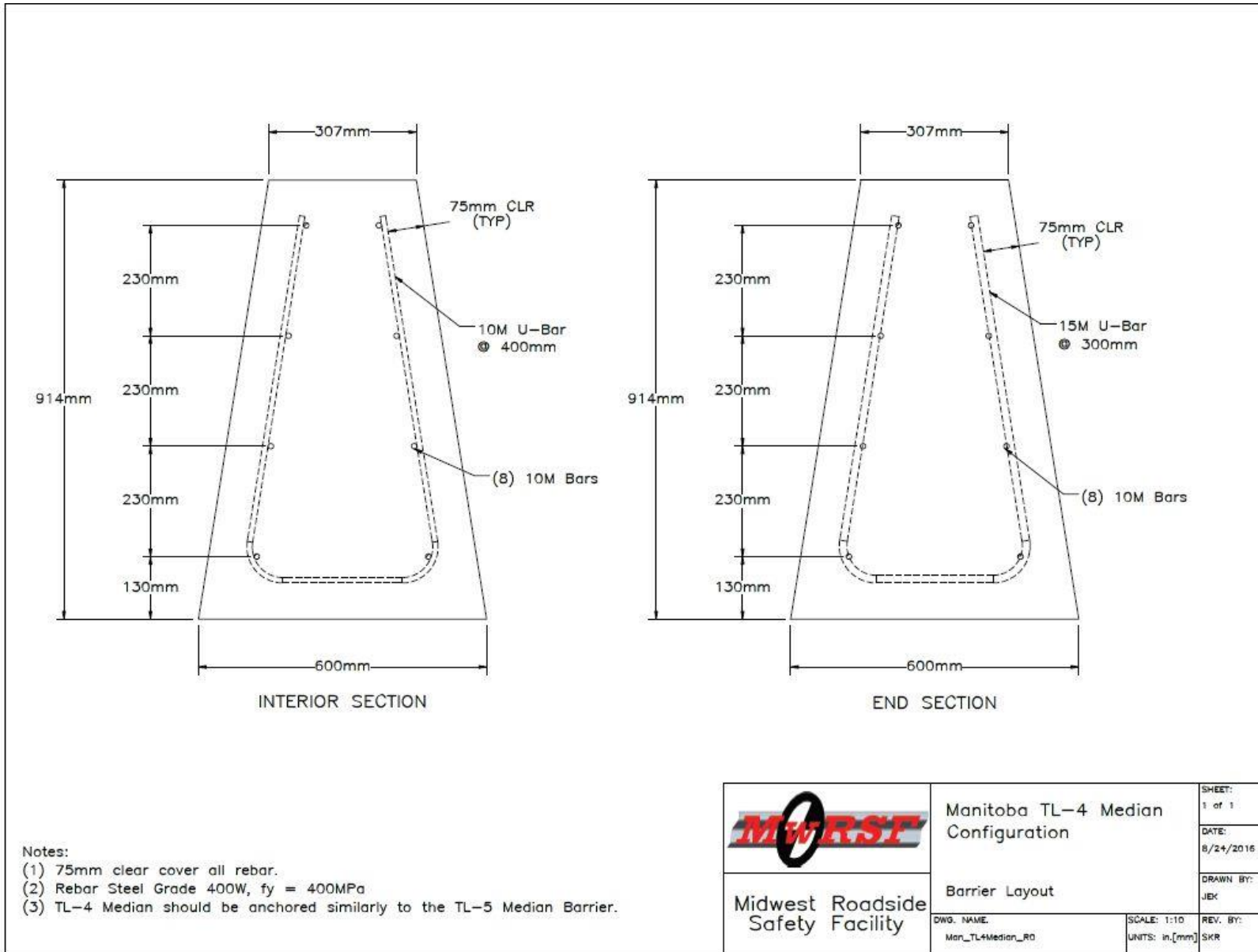


Figure 54. TL-4 Median Barrier Details

10.4 TL-5 Roadside Barrier Anchorage Options

A single-sided roadside version of the Manitoba Constrained-Width, Tall Wall was desired for barrier installations requiring TL-5 capabilities. Roadside applications can be treated with the crash-tested TL-5 bridge rail configuration, except that the bridge deck would be replaced with alternative anchorage options. Anchorage options similar to the TL-5 median barrier were developed for the roadside configuration. However, asphalt keyways require asphalt placement on both sides of the barrier, and asphalt placement behind a barrier (non-traffic side) would not be reasonable. Additionally, the narrower base width of the single-sided barrier configuration requires additional strength to prevent rotation/overturning. Thus, asphalt keyways are not recommended for anchoring the roadside version of the Manitoba Constrained-Width, Tall Wall barrier.

Anchoring of the roadside barrier to roadway slabs was designed with two options similar to the anchorage options of the median barrier to foundation slabs, as shown in Figures 55 and 56. Option 1 utilized 15M dowel bars, while Option 2 utilized a 15M U-bar. Both options require 200 mm (8 in.) of embedment and are spaced to match the U-bar stirrups of the barrier. The foundation slab should be an extension of the roadway slab, or tied directly to it, and contain steel reinforcement. The anchorage bars were different from the median anchorage bars only because the backside of the roadside barrier was vertical. The back side of the barrier should be offset at least 50 mm (2 in.) from the edge of the slab.

Footings were also designed to anchor the roadside barrier using the design methodology described in Section 10.2. The footing for interior barrier sections was 1,000 mm wide x 500 mm deep (39.4 in. x 19.7 in.) and utilized 20M stirrups spaced at 400 mm (15¾ in.) and eight 15M longitudinal bars. The end section footing was 1,000 mm wide x 700 mm deep (39.4 in. x 27.6 in.) and utilized 20M stirrups spaced at 400 mm (15¾ in.) and eight 20M longitudinal bars. For either section configuration, the barrier should be centered over the footing. Both footing details are shown in Figures 57 and 58. The footing stirrups were designed with spacing to match the U-bars in the barrier, so all of the transverse steel within the barrier system could be tied together. Finally, the end section footing should be used directly below any barrier end sections for a distance of at least 2.875 m (9.43 ft).

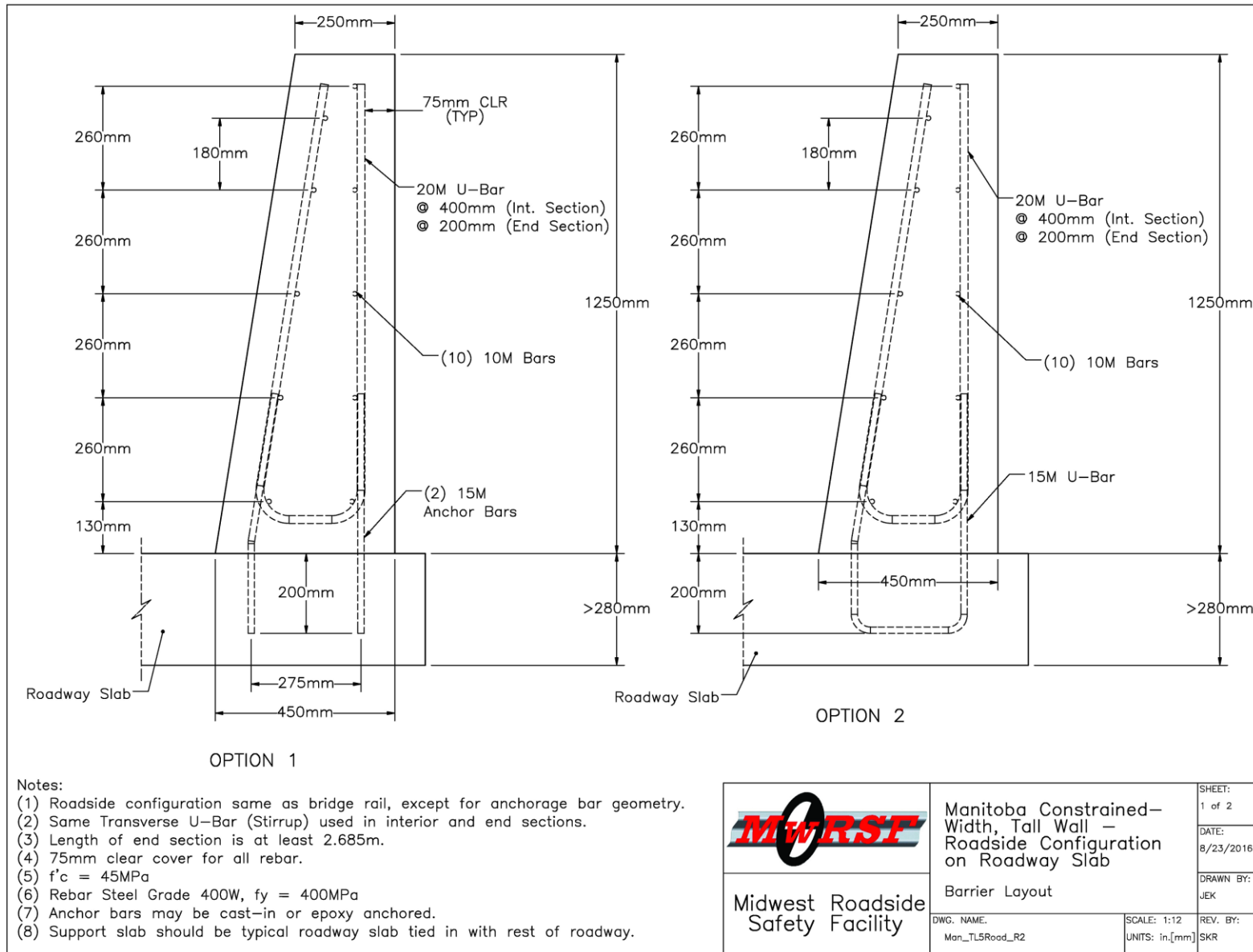


Figure 55. TL-5 Roadside Barrier Details

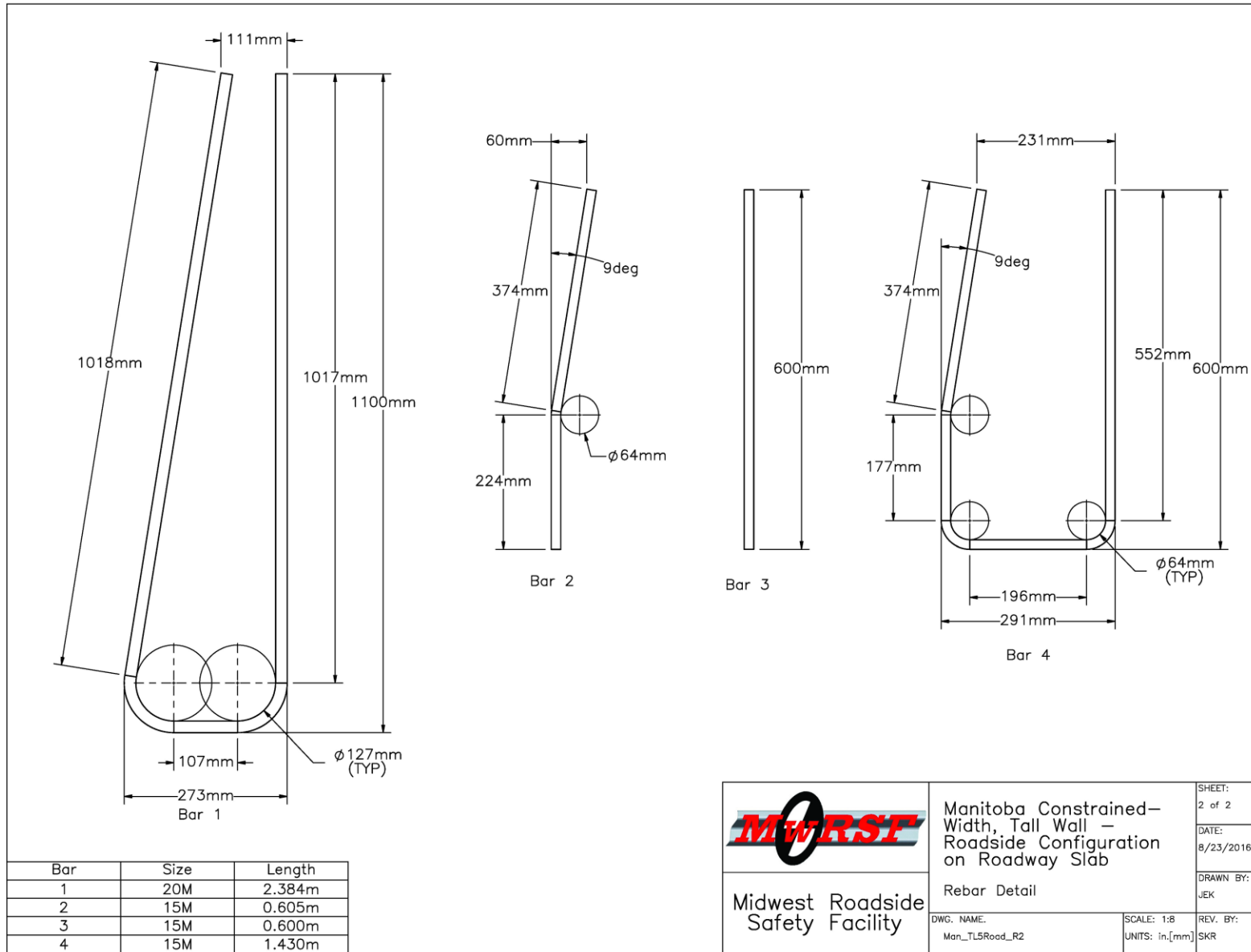


Figure 56. TL-5 Roadside Barrier Anchorage Bar Details

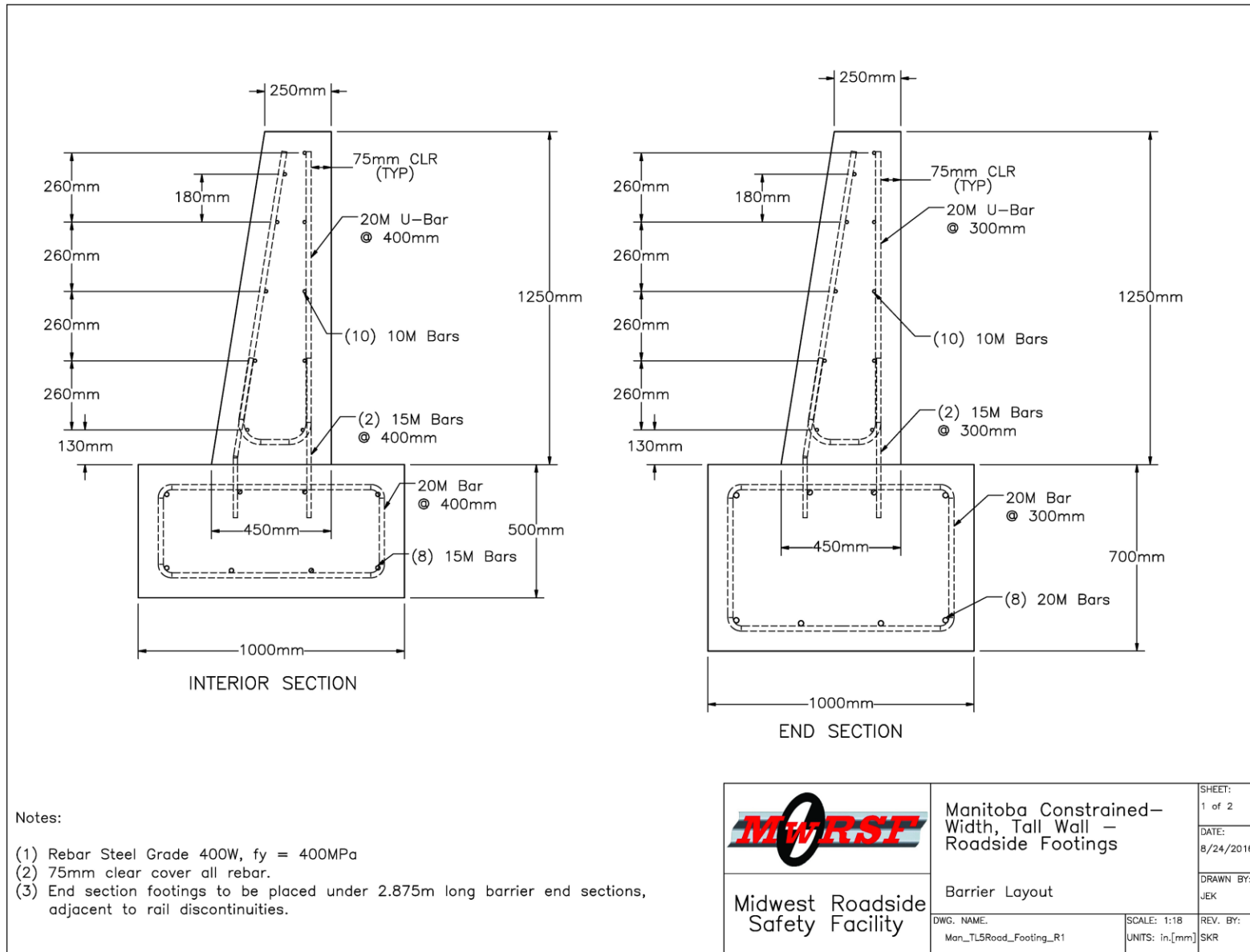


Figure 57. TL-5 Roadside Configuration Footing Details

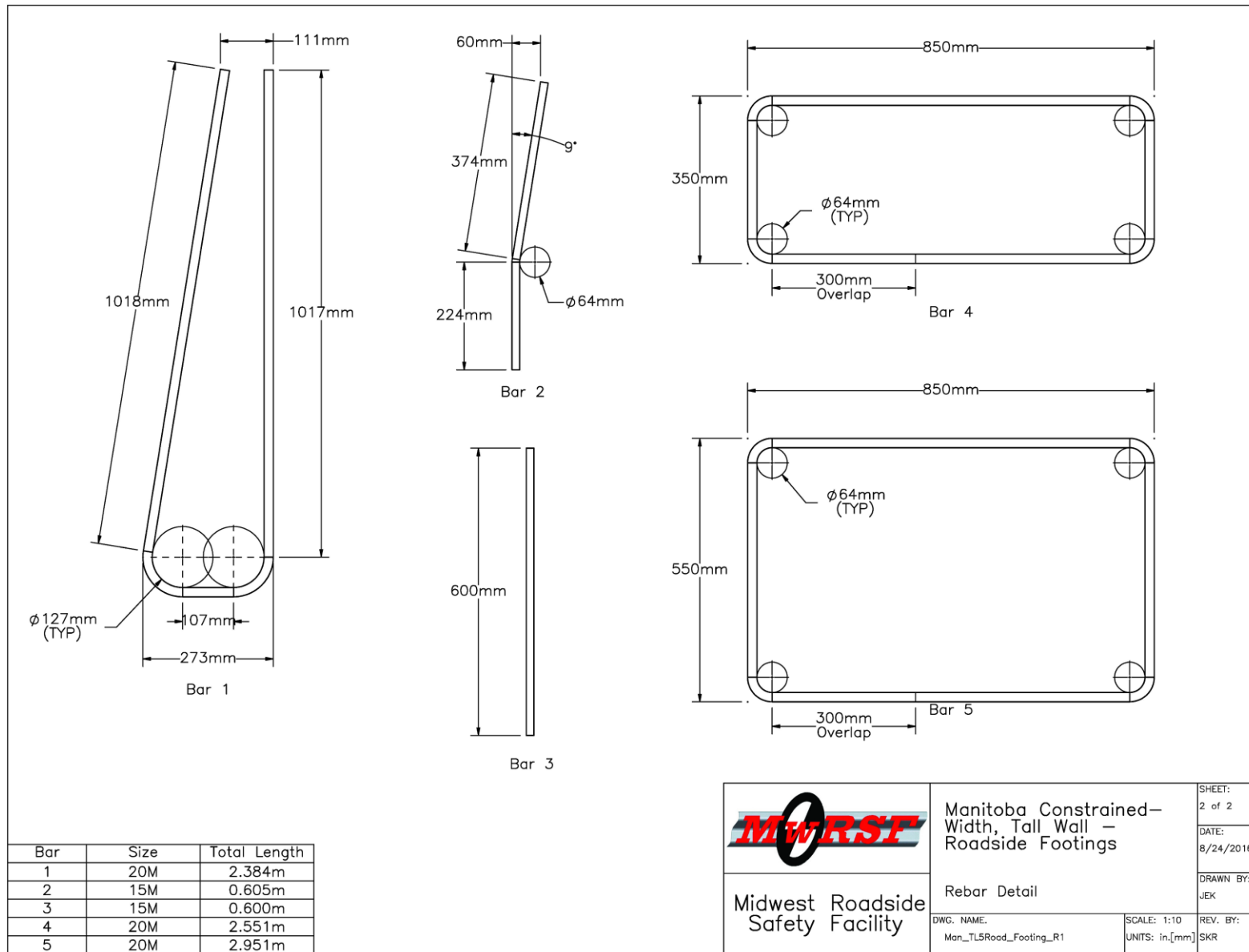


Figure 58. TL-5 Roadside Configuration Footing Reinforcement Details

11 TL-5 Barrier Transitions

Following the development of the Manitoba Constrained-Width, Tall Wall, transition details were required to connect the TL-5 median barrier to various other new and existing concrete barriers including: (1) TL-4 single-slope median barrier; (2) 815-mm (32-in.) Tall F-Shape median barrier; (3) dual, back-to-back TL-5 roadside barriers; and (4) dual, back-to-back F-shape roadside barriers. Additionally, a transition from TL-4 median barrier to a vertical parapet for guardrail and/or crash cushion attachment was desired. Finally, details were needed for the treatment of gaps within TL-5 median barrier spanning across existing overhead sign supports.

The transitions were all designed to maintain the barrier's redirective strength, minimize the potential for vehicle snag, and minimize the risk of vehicle instabilities during impact events. When analyzing the barrier strength, many of these transitions were assumed to transfer minimal load from one barrier configuration to another. MI commonly utilizes a set of smooth dowel bars, stacked vertically through the barriers' centerline, to aid shear load transfer across barrier joints. However, these steel bars will not transfer bending moment and result in discontinuities in the barrier. Thus, the barrier end sections developed for both the TL-5 and TL-4 configurations of the Manitoba Constrained-Width, Tall Wall were utilized to provide adequate strength adjacent to barrier discontinuities at transition points.

To prevent vehicle snag and instabilities, changes in barrier heights and/or lateral offsets were transitioned gradually. Barrier height changes have previously been designed and successfully crash tested with vertical slopes up to 5:1 [39]. Thus, all barrier height transitions should be transitioned at vertical slopes of 5:1 or flatter. The Roadside Design Guide [22] recommends utilizing lateral flare rates flatter than 20:1 for rigid barrier systems. However, these barrier system flare rates were thought to be extremely conservative when applied to barrier shape changes as many transition buttresses have successfully utilized much steeper lateral tapers. A recent computer simulation study on concrete barrier transitions indicated that lateral slopes up to 6:1 may be crashworthy according to MASH. However, the simulations indicated that both OIV values and occupant compartment deformations to passenger vehicles were approaching the MASH limits. Thus, the study recommended utilizing lateral slopes of 10:1 for rigid barrier shape changes [40]. Based on that research, all lateral offset changes between barrier configurations for this project were to be transitioned with lateral slopes of 10:1 or flatter. The following sections provide the design details for each of the noted transitions utilizing these geometric constraints.

11.1 TL-5 Median Barrier to TL-4 Median Barrier

As described in Section 10.3, the TL-4 single-slope median barrier was designed with the same base width and face slope as the TL-5 median barrier so that the same forms could be utilized for either barrier configuration. This also simplified the transition between the two systems as only a height change was necessary. Utilizing the 5:1 maximum vertical slope, the 335 mm (13¼ in.) difference in barrier heights required 1.675 m (5.50 ft) of longitudinal distance

for the transition. Details for the transition between the Manitoba Constrained-Width, Tall Wall median barrier and the TL-4 single slope barrier are shown in Figures 59 and 60.

A joint was placed between the transition segment and the TL-4 barrier, which incorporated three dowel bars placed down the centerline of the barrier. As such, end section reinforcement should be utilized for at least 1.585 m (5.20 ft) within the TL-4 barrier adjacent to the transition. The end section reinforcement for the TL-5 barrier was recommended to begin at the joint and continue for the recommended distance of 2.785 m (9.14 ft), which included the entire transition segment and a short distance of the adjacent TL-5 barrier. By utilizing the TL-5 end section reinforcement through the transition region, the beginning of the TL-5 barrier length of need is located at the beginning of the TL-5 barrier installation (for traffic traveling toward the TL-5 system). For traffic traveling toward the TL-4 barrier, the end of the TL-5 barrier length of need would be approximately 21.3 m (70 ft) upstream of the transition segment. This distance was based on the distance traveled by the vehicle trailer during test no. MAN-1 before returning to a level position and no longer leaning on the barrier to prevent rollover.

If desired, the longitudinal bars from the TL-4 barrier could be extended into the transition segment during construction, which would eliminate the need for the three dowel bars placed across the joint. Providing the proper lap splice length between the longitudinal bars of the TL-4 barrier and transition segment and casting the transition segment directly adjacent to the TL-4 barrier (no gaps) would eliminate the barrier discontinuity and the need for end section reinforcement in the TL-4 barrier. TL-5 end section reinforcement is still recommended in the transition segment adjacent portion of the TL-5 barrier to maximize the length of need distance of the TL-5 barrier. Although not shown in the drawings, the entire barrier system should be properly anchored utilizing a foundation slab, footing, or asphalt keyway, as discussed in Chapter 10.

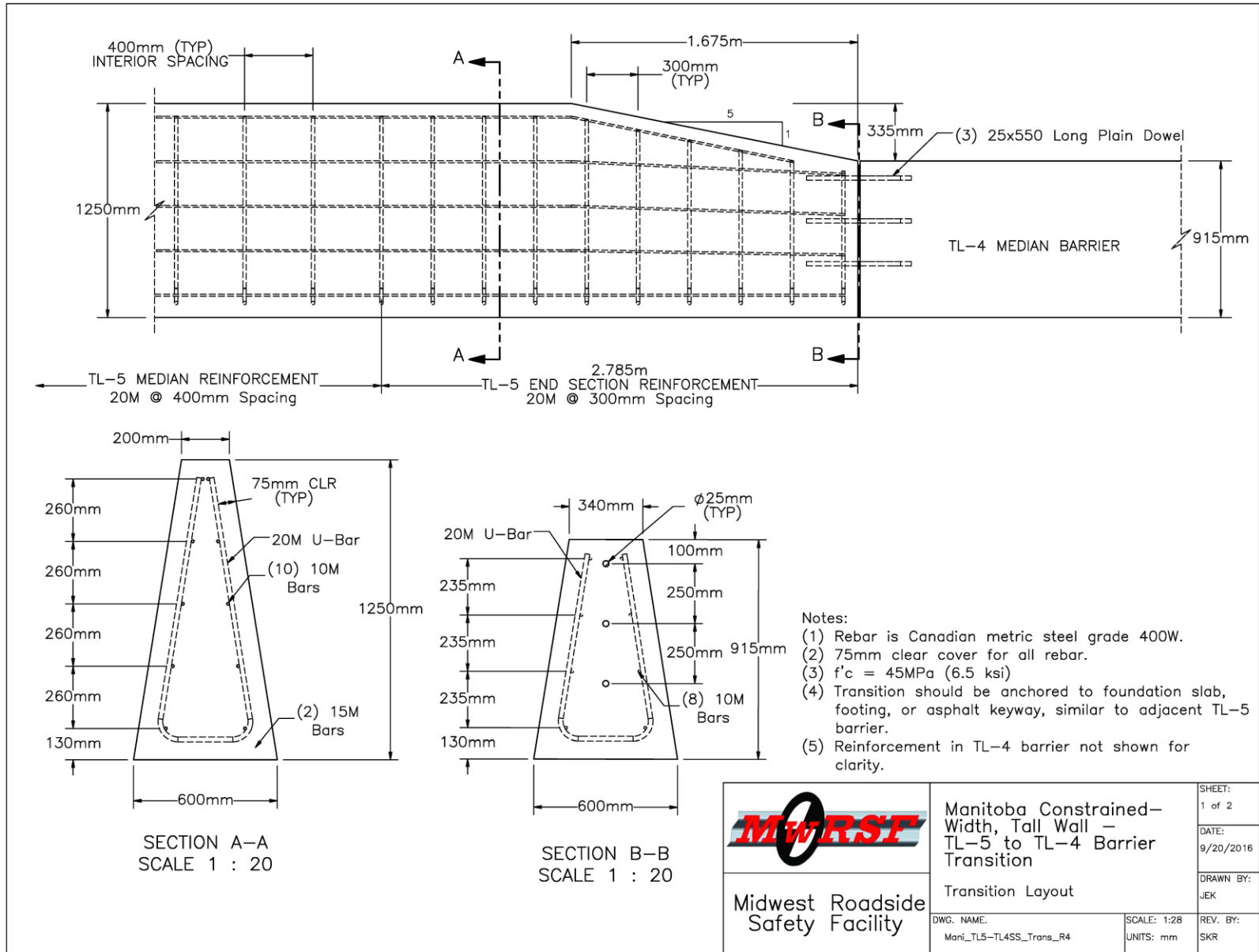


Figure 59. Transition Details, TL-5 Median Barrier to TL-4 Single Slope Barrier

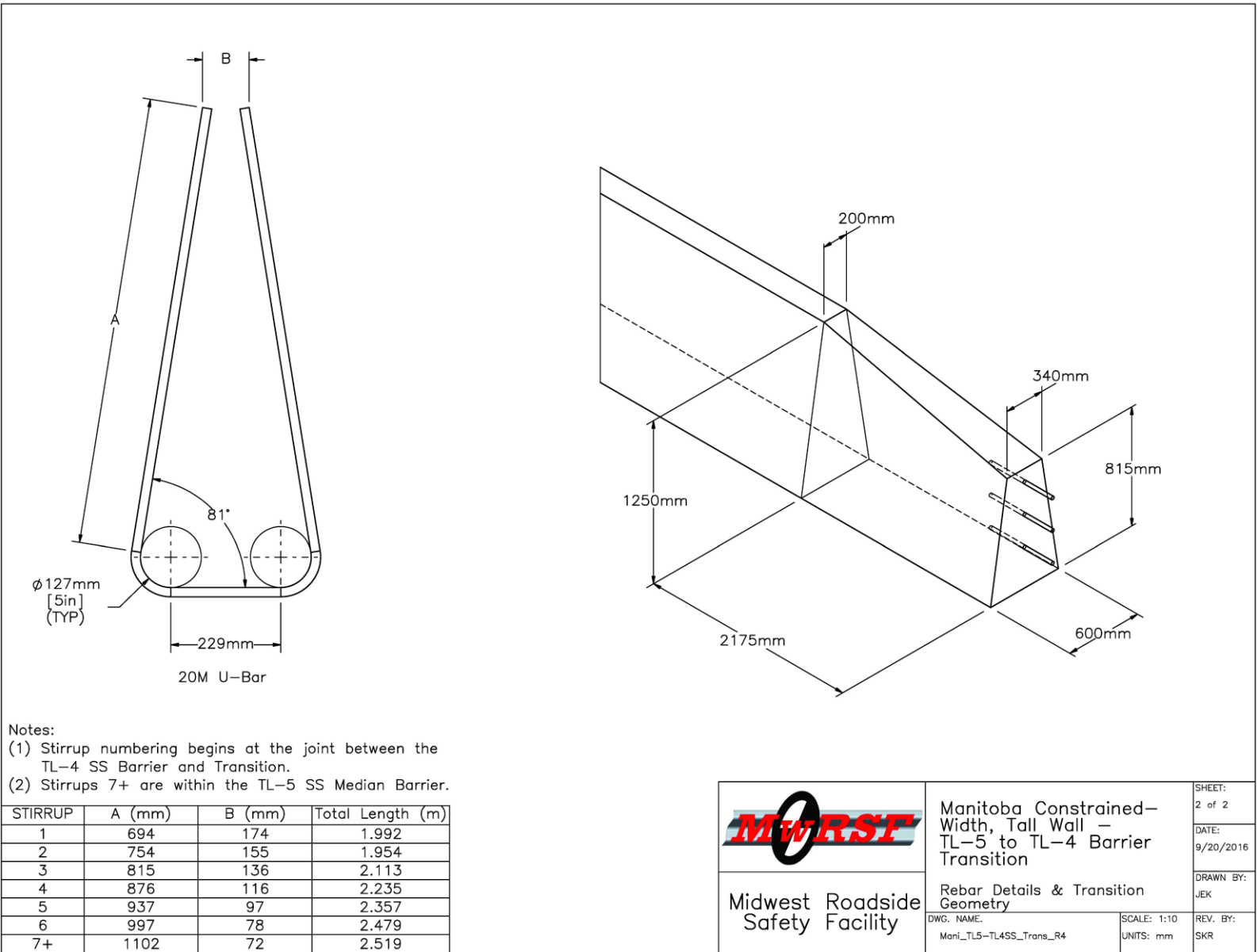


Figure 60. Transition Details, TL-5 Median Barrier to TL-4 Single Slope Barrier

11.2 TL-5 Median Barrier to 815-mm (32-in.) Tall F-Shape Barrier

Installation sites may exist where the Manitoba Constrained-Width, Tall Wall barrier will be placed adjacent to existing F-shape barriers. Thus, a transition was required to safely connect these two barrier types. MI's typical F-shape barrier was 815 mm (32 in.) tall, or 435 mm (17¼ in.) shorter than the TL-5 single slope barrier. Utilizing the 5:1 maximum vertical slope to transition between barrier heights, the transition required 2.175 m (7.14 ft) of longitudinal distance. The greatest change in lateral distance between the two barriers occurred at a height of 250 mm (10 in.) above the ground, or the slope transition point of the F-shape barrier. At this height, the F-shape barrier was 346 mm (13.6 in.) wide, while the TL-5 single slope was 520 mm (20.5 in.) wide, as shown in Figure 61. With a lateral offset distance of 87 mm (3.4 in.) on each side and a maximum lateral slope of 10:1, the changes to the barrier face geometry required a transition length of 870 mm (34.3 in.). Thus, the required transition length for the height change controlled the design, and the transition length was selected to be 2.175 m (7.14 ft). This transition length allows for a constant lateral taper of 25:1. Details for the transition between the Manitoba Constrained-Width, Tall Wall median barrier and F-shape median barrier are shown in Figures 62 and 63.

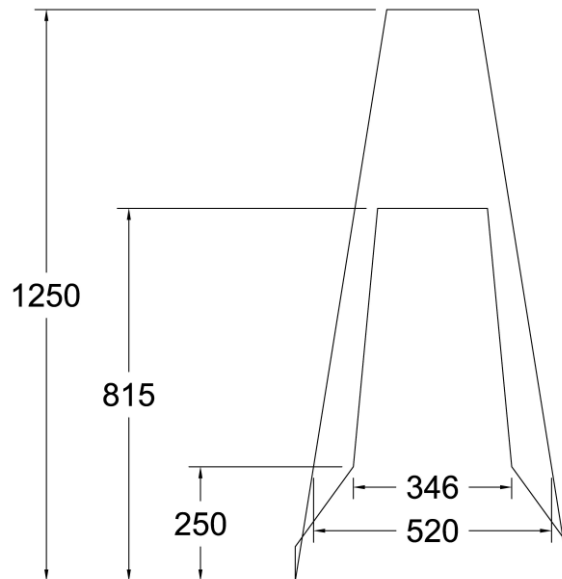


Figure 61. TL-5 Median Barrier and F-Shape Median Barrier Comparison

Similar to the transition to TL-4 single slope median barrier, a joint was placed between the transition segment and the F-shape barrier, which incorporated three dowel bars stacked vertically. End section reinforcement for the TL-5 barrier, which required a length of 2.785 m (9.14 ft), was recommended to be placed through the entire transition segment and a short distance of the adjacent TL-5 barrier. By utilizing the TL-5 end section reinforcement through the transition region, the beginning of the TL-5 barrier length of need is located at the beginning of the TL-5 barrier installation (for traffic traveling toward the TL-5 system). For traffic traveling toward the TL-4 barrier, the end of the TL-5 barrier length of need would be approximately 21.3 m (70 ft) upstream of the transition segment. Though not shown in the

drawings, the barrier transition should be properly anchored utilizing on of the anchorage options discussed in Chapter 10.

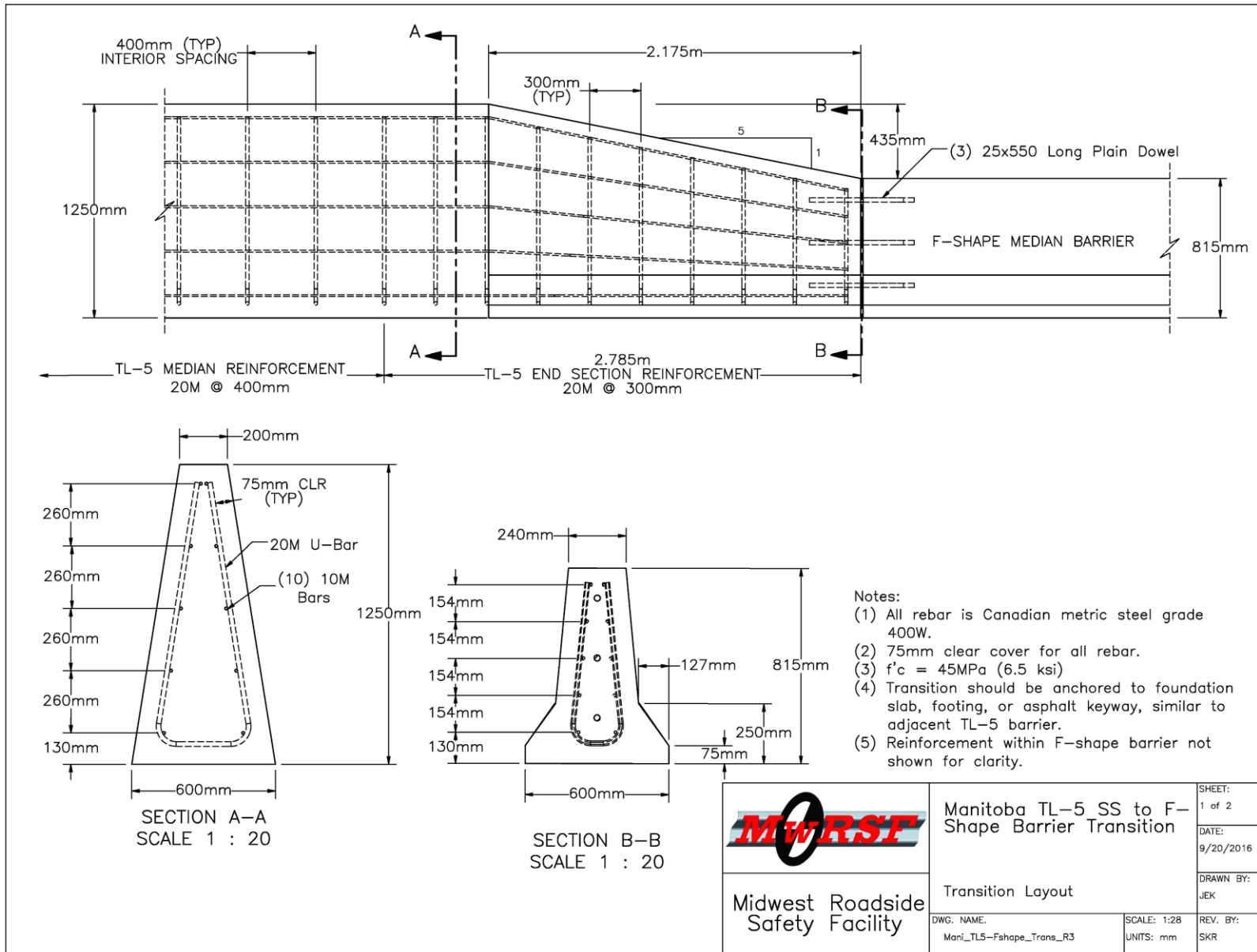


Figure 62. Transition Details, TL-5 Median Barrier to F-Shape Barrier

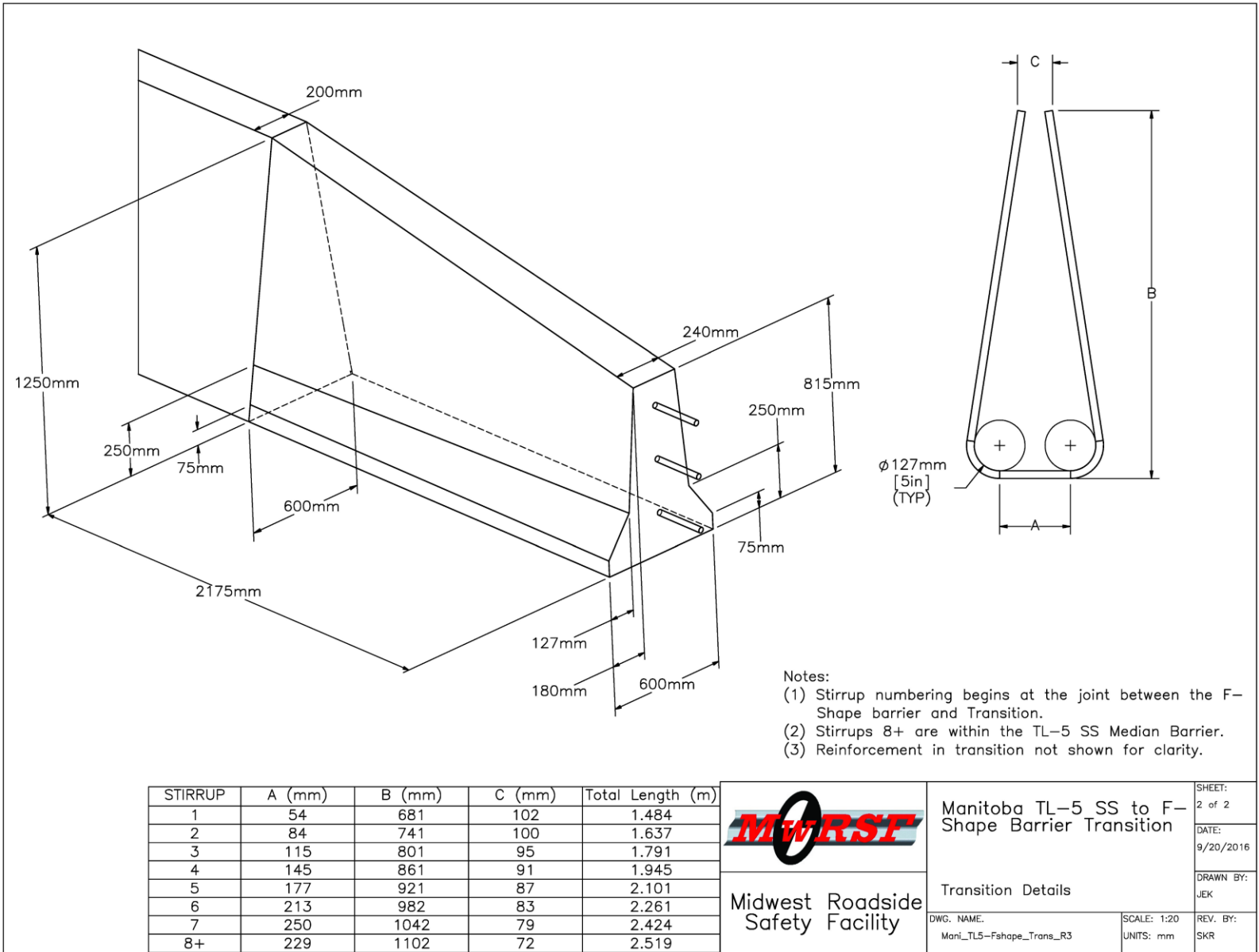


Figure 63. Transition Details, TL-5 Median Barrier to F-Shape Barrier

11.3 TL-5 Median Barrier to Dual TL-5 Roadside Barriers

Unique situations, such as bridge piers in the median and highway bridges with independent decks for each direction of traffic, may require the use of dual, back-to-back roadside barriers placed between opposing traffic. For these sites, a barrier transition was desired for use between the Manitoba Constrained-Width, Tall Wall median barrier and dual, back-to-back, roadside barriers.

For installations where the dual roadside barriers are single-sided configurations of the TL-5 Manitoba Constrained-Width, Tall Wall, the median barrier width is increased to match the combined width of the dual barriers. Thus, the transition segment utilized the maximum lateral slope of 10:1 to connect the median barrier to the dual roadside barriers. A gap width of 125 mm (5 in.) between the vertical backsides of the dual barriers was selected to allow enough room for the placement of formwork behind the barriers. Thus, the combined width at the base of the dual roadside barriers was 1,025 mm (40.4 in.). Utilizing the 10:1 maximum lateral slope and a median barrier base width of 600 mm (23¾ in.), the transition length was required to be 2.125 m (7.0 ft) long. Details for the transition between the Manitoba Constrained-Width, Tall Wall median barrier and dual TL-5 roadside barriers is shown in Figures 64 and 65.

Because the dual roadside barriers may be placed on bridge abutments and adjacent to expansion/contraction joints, an open joint was placed between the transition segment and the dual roadside barriers. The open joint was drawn with a nominal 50 mm (2 in.) width, but the actual gap width may vary. However, to prevent vehicle snag issues with passenger vehicles, the gap width should not exceed 100 mm (4 in.), which matches the joint gap width of typical portable concrete barrier systems. The barrier discontinuity required end section reinforcement in the individual roadside barriers as well as the TL-5 barrier and transition, as noted in Figure 64. The length of the TL-5 barrier end section, 2.785 m (9.14 ft), was greater than the length of the transition, so the reduced stirrup spacing of the TL-5 end section configuration encompassed the entire transition segment and a portion of the adjacent TL-5 median barrier. The use of end section reinforcement on both sides of the open joint ensured the entire system was MASH TL-5 crashworthy. Note, the stirrup widths varied throughout the transition segment, as shown in Figure 65. Additionally, the entire barrier system should be properly anchored utilizing a foundation slab, footing, or asphalt keyway, as discussed in Chapter 10.

The stirrups in Figure 64 were shown as U-bars to match the stirrup designs for the TL-5 median barrier. However, the extra width would allow the use of closed-loop stirrups as the transition section widens. Although they require more steel, closed-loop stirrups would provide more stiffness and stability during construction. Thus, either U-bar or closed-loop stirrups may be utilized within the transition segment.

Some installations may require a lateral offset between the dual barriers greater than the 125 mm (5 in.) detailed herein. Under these circumstances, the transition segment may be altered to accommodate the wider footprint. The 10:1 lateral slope, or flatter, must remain to prevent vehicle instability issues, so the transition segment would need to be extended longitudinally in order to widen the barrier. For large gap widths, utilizing a transition segment to span across the

entire width would be excessive. Thus, a better option may be to utilize the transition segment as detailed in Figures 64 and 65 and install the ends of the dual roadside barriers at a 10:1 flare, or flatter, until the desired gap distance is achieved, as shown in Figure 66.

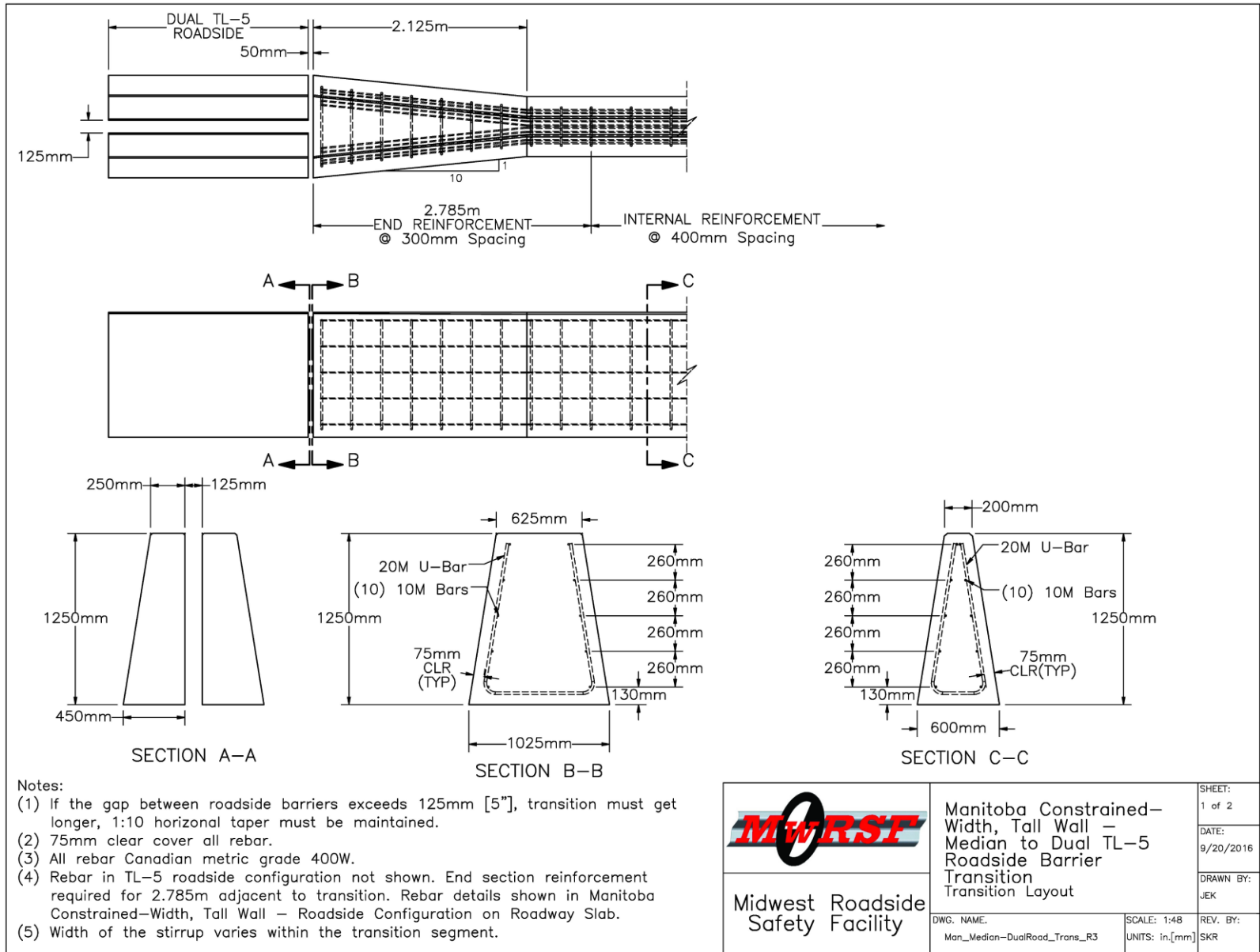
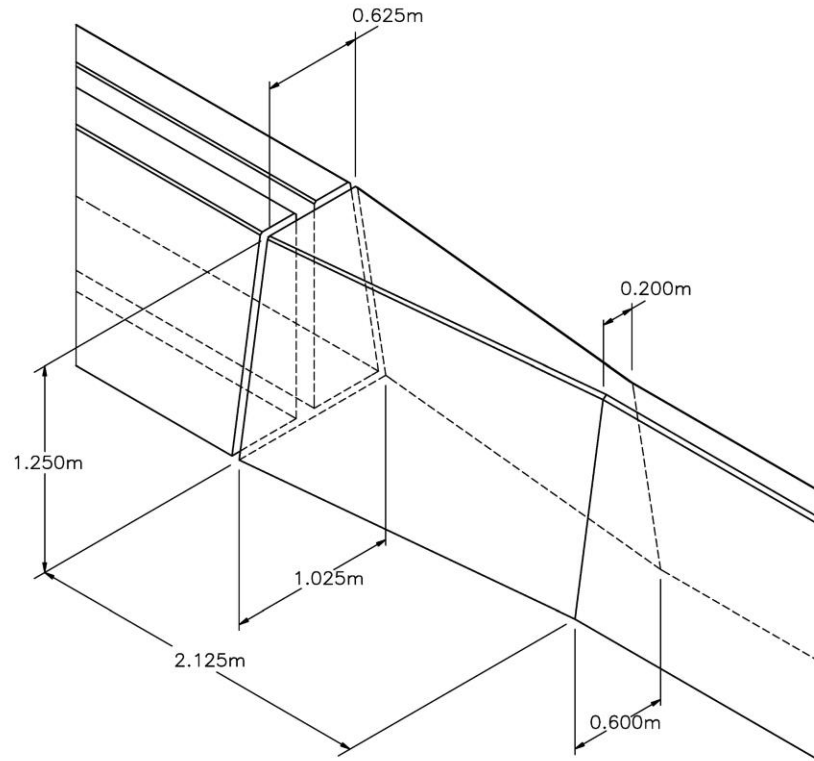


Figure 64. Transition Details, TL-5 Median Barrier to Dual TL-5 Roadside Barriers



Note:
 (1) Reinforcement not shown for clarity.


 Midwest Roadside Safety Facility	Manitoba Constrained- Width, Tall Wall - Median to Dual TL-5 Roadside Barrier Transition Transition Geometry		SHEET: 2 of 2
	DWG. NAME: Man_Median-DualRoad_Trans_R3		DATE: 9/20/2016
		SCALE: 1:30 UNITS: in,[mm]	DRAWN BY: JEK
			REV. BY: SKR

Figure 65. Transition Details, TL-5 Median Barrier to Dual TL-5 Roadside Barriers

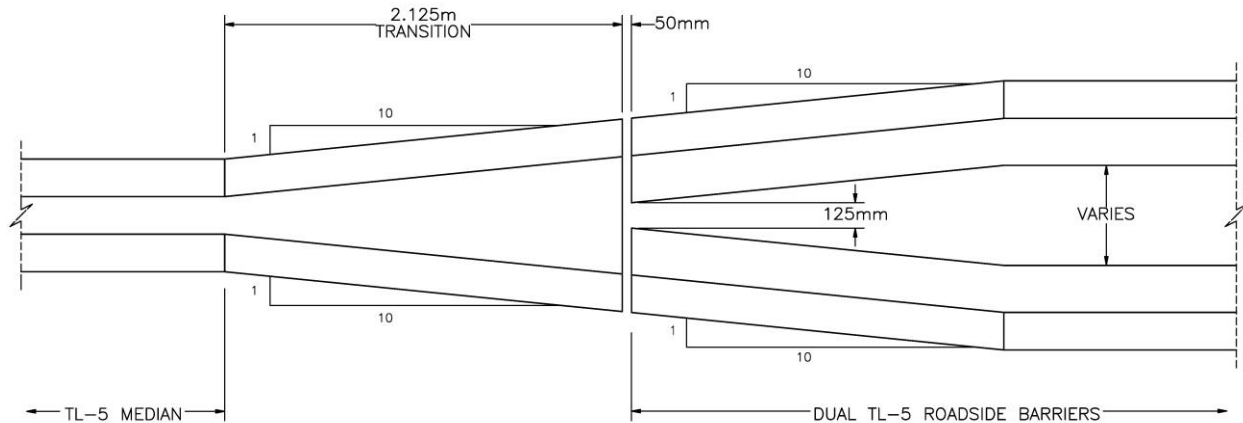


Figure 66. Flared Dual Roadside Barriers for Increased Gap Widths

11.4 TL-5 Median Barrier to Dual 815-mm (32-in.) F-Shape Roadside Barriers

Installations may also require a new TL-5 median barrier to be placed adjacent to existing dual, back-to-back, 815-mm (32-in.) tall F-shape barriers. Therefore, a barrier transition was required for use between the Manitoba Constrained-Width, Tall Wall median barrier and dual roadside F-shape barriers. Similar to the transition to dual TL-5 single-slope roadside barriers, a gap width of 125 mm (5 in.) was selected to provide enough room for the placement of formwork behind the dual barriers. This resulted in a combined base width of 965 mm (38 in.) for the dual F-shape barriers. Utilizing a 10:1 lateral slope and the TL-5 barrier’s base width of 600 mm (23¾ in.), the change in width required a minimum transition length of 1.825 m (5.99 ft). However, as described in Section 11.2, the height transition from the 1,250-mm (49¼-in.) tall TL-5 barrier to the 815-mm (32-in.) tall F-shape barrier required a transition length of 2.175 m (7.14 ft) to satisfy the 5:1 maximum vertical slope. Thus, the required transition length for the height change controlled the design, and the transition length was selected to be 2.175 m (7.14 ft). Details for the transition between the Manitoba Constrained-Width, Tall Wall median barrier and dual F-shape barriers are shown in Figures 67 and 68.

Because the dual F-shape barriers may be placed on bridge abutments and adjacent to expansion/contraction joints, an open joint was placed between the transition segment and the dual roadside barriers. The open joint was drawn with a nominal 50 mm (2 in.) width, but the actual gap width may vary. However, the gap width should not exceed 100 mm (4 in.) to prevent vehicle snag issues with passenger vehicles. The barrier discontinuity required end section reinforcement in the TL-5 barrier and transition, as noted in Figure 67. The length of the TL-5 barrier end section, 2.785 m (9.14 ft), was greater than the length of the transition, so the reduced stirrup spacing of the TL-5 end section configuration encompassed the entire transition segment and a portion of the adjacent TL-5 median barrier. By utilizing the TL-5 end section reinforcement through the transition region, the beginning of the TL-5 barrier length of need is located at the beginning of the TL-5 barrier installation (for traffic traveling toward the TL-5 system). For traffic traveling toward the TL-4 barrier, the end of the TL-5 barrier length of need would be approximately 21.3 m (70 ft) upstream of the transition segment. Note, stirrup widths

and heights varied throughout the length of the transition segment. Additionally, the barrier system should be properly anchored utilizing one of the anchorage options discussed in Chapter 10.

The stirrups in Figure 67 were shown as U-bars to match the stirrup designs for the TL-5 median barrier. However, as the transition section widens, the extra width would allow the use of closed-loop stirrups. Although they require more steel, closed-loop stirrups would provide more stiffness and stability during construction. Thus, either U-bar or closed-loop stirrups may be utilized within the transition segment.

Some installations will require a lateral offset between the dual barriers greater than the 125 mm (5 in.) detailed herein. For gaps widths up to 195 mm ($7\frac{5}{8}$ in.), the downstream width of the transition segment can be widened without changing the transition length as the lateral slope would remain below the 10:1 maximum. For lateral gaps larger than 195 mm ($7\frac{5}{8}$ in.), it is recommended to install new dual F-shape barrier segments adjacent to the transition segment at a 10:1 longitudinal flare until the desired gap distance is achieved. This option for large lateral gaps was previously discussed for the transition to dual TL-5 roadside barriers and sketched in Figure 66. The new flared F-shape barrier segments should be reinforced and tied into the existing F-shape barriers.

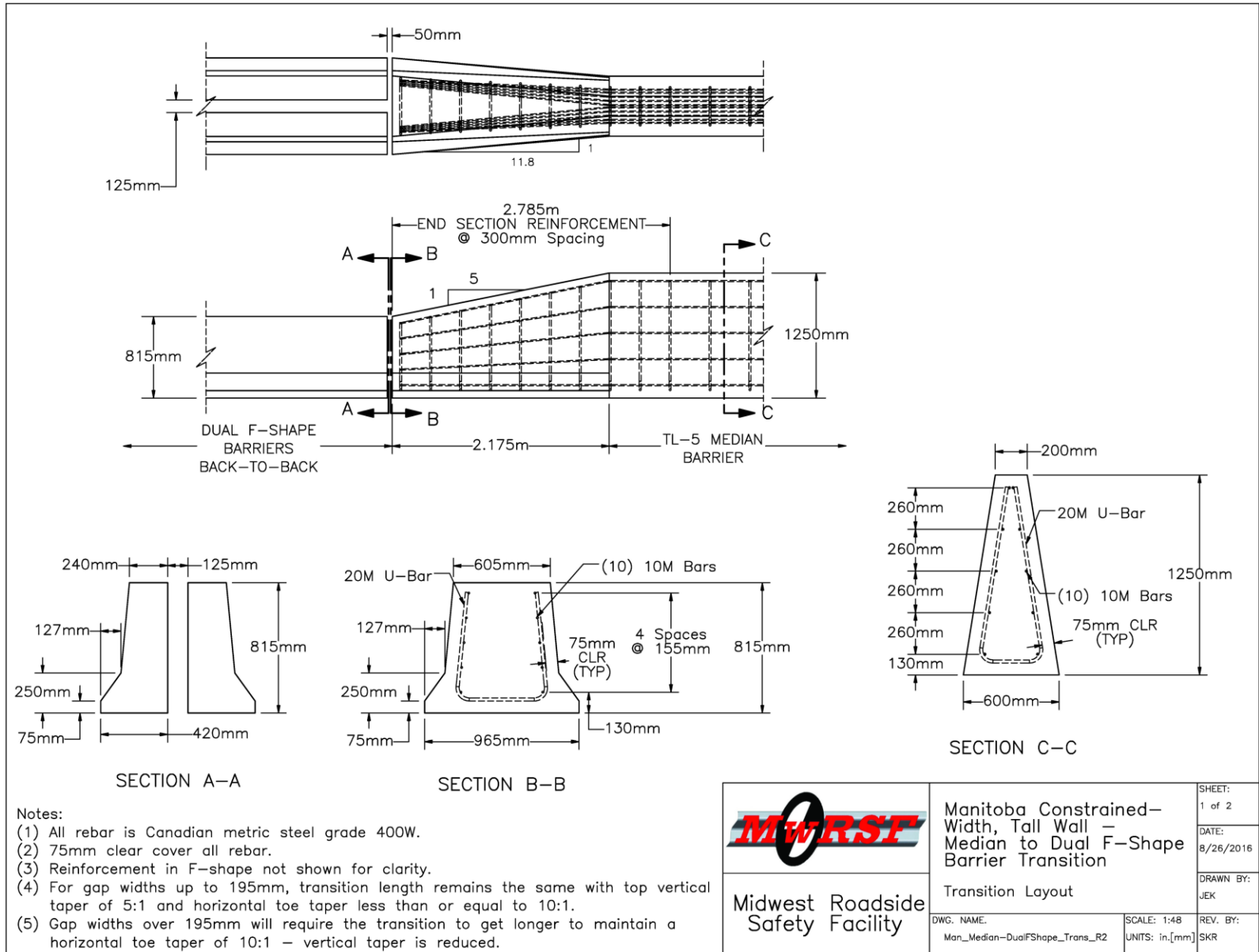
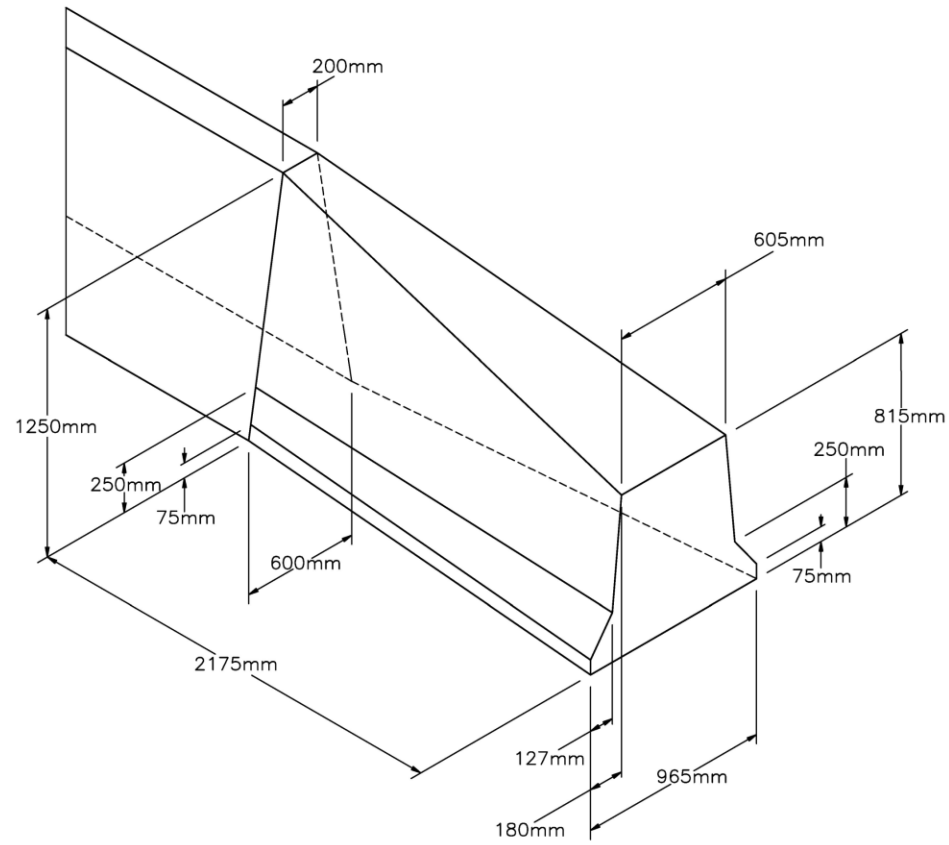


Figure 67. Transition Details, TL-5 Median Barrier to Dual F-Shape Roadside Barriers



Note:
 (1) Reinforcement not shown for clarity.



Midwest Roadside
 Safety Facility

Manitoba Constrained-
 Width, Tall Wall -
 Median to Dual F-Shape
 Barrier Transition

Transition Geometry

DWG. NAME:
 Man_Median-DualFShape_Trans_R2

SCALE: 1:25
 UNITS: in,[mm]

SHEET: 2 of 2
DATE: 8/26/2016
DRAWN BY: JEK
REV. BY: SKR

Figure 68. Transition Details, TL-5 Median Barrier to Dual F-Shape Roadside Barriers

11.5 TL-4 Median Barrier to Vertical Barrier

The termination points of concrete median barriers are often shielded from vehicle impacts by guardrails or crash cushions. These roadside barrier devices typically require vertical attachment surfaces in order to function properly. Thus, a transition was desired from the TL-4 single-slope barrier to a 600-mm (23¾-in.) wide vertical concrete parapet for the attachment of guardrails and crash cushions.

Most guardrails and crash cushions require a downstream barrier height of 815 mm (32 in.) in order to prevent vehicle snag on the blunt end of the concrete barrier above the top of the rail elements. Thus, the height of the TL-4 single-slope barrier was reduced from 915 mm (36 in.) to 815 mm (32 in.). This 100-mm (4-in.) height reduction requires a longitudinal transition distance of 0.50 m (1.64 ft) utilizing the maximum vertical slope of 5:1. However, the top of the barrier was widened from 307 mm (12.1 in.) to 600 mm (23¾ in.). Using a lateral slope of 10:1, this width transition required a longitudinal distance of 1.465 m (4.81 ft). Thus, the width transition controlled the design, and the transition length was selected to be 1.465 m (4.81 ft). Details for the transition from TL-4 single-slope median barrier to a vertical parapet are shown in Figures 69 and 70.

The vertical parapet was prescribed a length of 1.5 m (4.9 ft) to allow sufficient distance for the attachment of any necessary guardrails or crash cushion components. The end of the concrete parapet was reinforced with TL-4 end section reinforcement, which was previously calculated to require a length of 1.585 m (5.2 ft). Thus, the reduced stirrup spacing of the end section reinforcement covered the entire length of the vertical parapet and a short distance of the transition section. The rest of the transition segment and the TL-4 barrier were reinforced with the internal barrier reinforcement configuration. Due to the width of the vertical parapet, the stirrups were designed as closed loops within the outer 1.5 m (4.9 ft) of the barrier. If desired, closed-loop stirrups could also be utilized within the transition segment and the TL-4 median barrier, as discussed in Section 10.3. Note, the stirrups within the transition segment varied in shape, as shown in Figure 70. Although not shown in the drawings, the barrier transition should be properly anchored utilizing one of the foundation options discussed in Chapter 10.

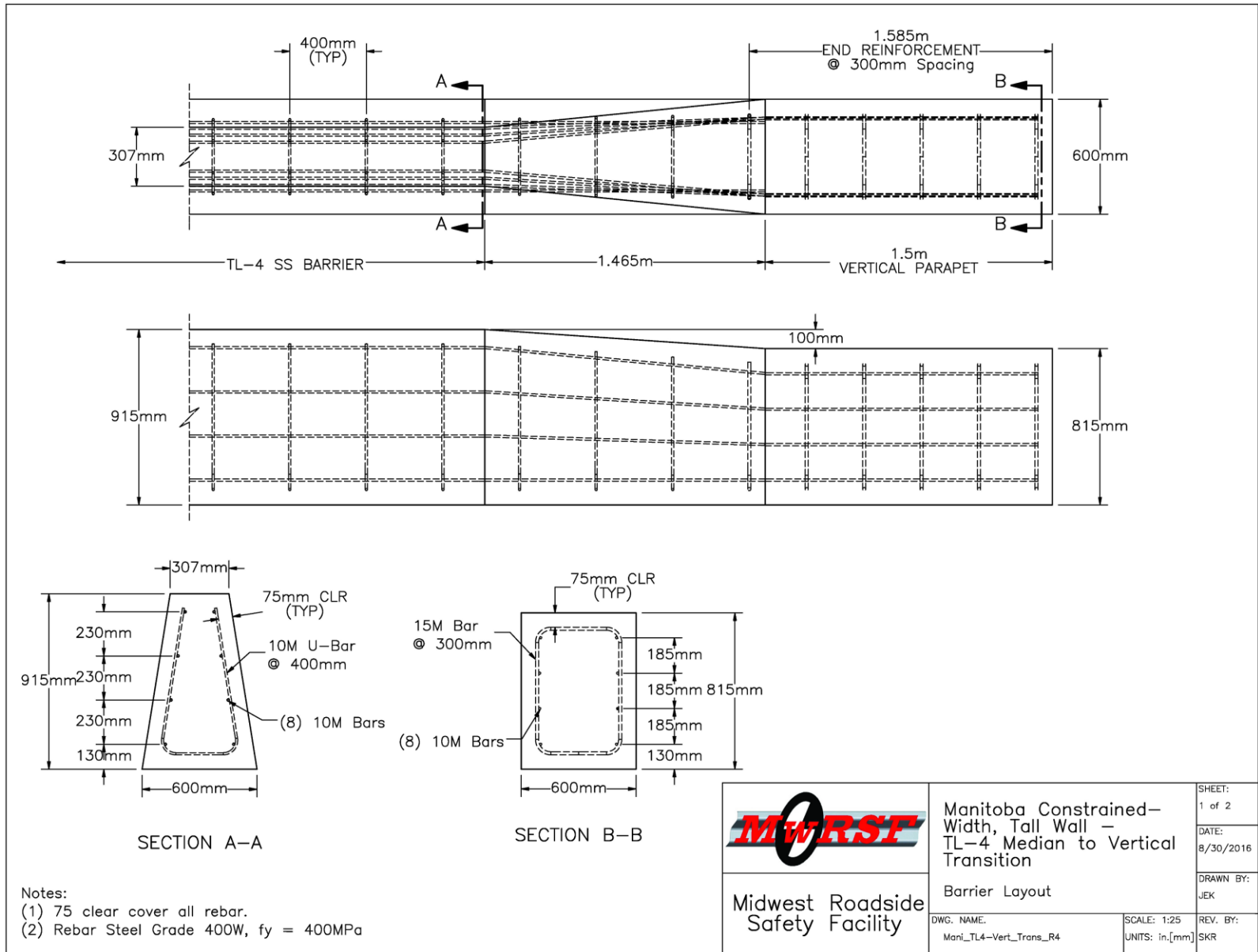


Figure 69. Transition Details, TL-4 Median Barrier to Vertical Parapet

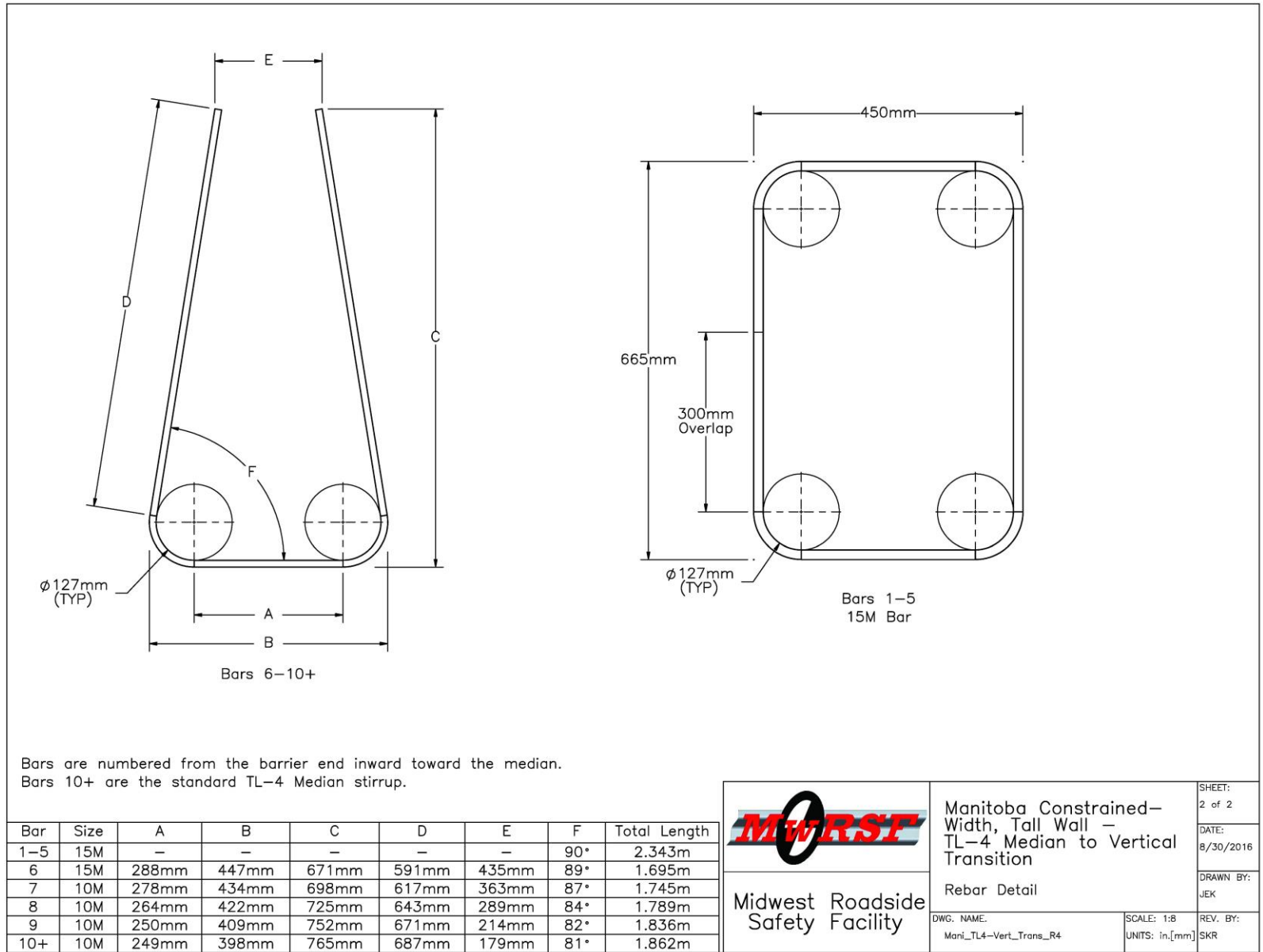


Figure 70. Transition Details, TL-4 Median Barrier to Vertical Parapet

11.6 Treatment for Gaps in TL-5 Median Barrier Spanning Sign Supports

MI currently has numerous overhead sign supports that occupy space in the middle of narrow medians on high-speed roadways. Due to cost constraints, it is unlikely that these sign supports will be removed when the median barrier surrounding these sign supports are replaced with the new Manitoba Constrained-Width, Tall Wall. Further, the narrow medians were restricted in width, so widening the median barrier to encompass the structure and shield it from vehicle impacts was not an option. Consequently, a gap must be formed in new median barrier installations to span across the sign support structure. Therefore, specialized barrier treatments were required for gaps within the Manitoba Constrained-Width, Tall Wall to shield vehicles from impacting overhead sign supports.

The size of the sign support structures varied by location, but a 3.0 m (9.8 ft) gap length would typically be required to span the structure. The existing sign supports and their support footings were not to be altered in any way, including the attachment of barrier hardware to the structure. Thus, barrier treatments needed to span across the gap and be anchored to the concrete median barrier segments. However, the treatment hardware was required to stay within the narrow median width of 600 mm (23¾ in.). The size of the support structure poles could be as large 250 mm (10 in.) in diameter, leaving only about 175 mm (7 in.) of width on each side of the sign supports in which to place barrier hardware. Due to these design restrictions, it was recognized that the treatment of these gaps would likely not satisfy MASH TL-5 safety standards and may not even satisfy MASH TL-3 criteria. Thus, the objective was to treat these unique hazards with hardware, which would provide the highest possible safety performance.

MI originally developed a concept of utilizing nested W-beam stacked above nested thrie beam to span the barrier gap, as shown in Figure 71. The median barrier was widened so the rail elements would encompass the support poles, but the barrier shape retained a single-slope geometry. Because the concrete barrier face was sloped backward, the cross-section width of the barrier with the additional rail elements remained inside the 600-mm (23¾-in.) median footprint. Standard terminal connectors were utilized to anchor the rail elements to the concrete barriers. Internal stiffeners were placed at multiple locations along the span length between the front and back rail elements. Thus, loading of rail elements on one side of the barrier treatment resulted in the loading of the corresponding rail elements on the back side at the same time. Finally, the bottom edges of the median barrier were tapered on the downstream end of the gap to reduce vehicle and tire snag on the ends of the concrete barrier (downstream side dependent on direction of traffic).

Analysis of this safety treatment concept began with the calculation of the redirective strength of the rails. Due to the height of the upper rail elements, the W-beam would only be subjected to significant loading from large trucks with cargo boxes that would lean onto the barrier. This barrier treatment was not expected to satisfy TL-4 or TL-5 loads, so the strength analysis of the barrier focused on the lower thrie beam rails. Standard 2.66-mm thick (12 ga.) thrie beam has a maximum plastic bending strength of 17.4 kN-m (153.5 kip-in.). Since the rails were nested and internal stiffeners connected the front and back rails, impacts into the thrie beams resulted in the loading of four thrie beam rails. With a gap length of 3.0 m (9.8 ft) and

loading at mid-span, the three beam rails had a capacity of 89 or 182 kN (20 or 41 kips), depending on the assumption of simple- or fixed-support reactions for the rail elements. The true constraint condition for the rail elements would be somewhere between simple and fixed, so the actual strength should fall between the provided values. Typical design loads for MASH TL-2 and TL-3 are 142 kN (32 kips) and 334 kN (75 kips), respectively. The strength of the dual-nested three beam rails was well below the TL-3 requirements, but providing strength equivalent to MASH TL-2 was a possibility. Additional strength due to tensile-membrane action was also considered, but rail slip between the connections at the terminal connector would require deflections into the sign supports prior to developing significant rail tension.

Design modifications were then made to the original treatment concept. First, the beam configuration was modified to stacked, nested three beam rails. Swapping out the top W-beam rails for three beam rails had many potential benefits. First, the increased strength of three beam rails reduced the risk of large trucks snagging on the sign supports. Additionally, the top three beams extended down to a height of 715 mm (28.1 in.). Thus, the top three beam rails would interact with passenger vehicles and provide additional strength capacity during redirection. The increased height of the three beam also resulted in the bottom three beams being shifted downward. The height to the bottom of the rail was reduced to 105 mm (4.1 in) above the ground, so the risk of tire snag on the barrier was reduced. Details for the recommended treatment of barrier gaps within TL-5 median barriers spanning sign support structures are shown in Figures 72 and 73.

The TL-5 single-slope concrete barriers were transitioned to vertical parapets prior to the sign support gaps. Utilizing a vertical barrier face allowed the guardrail elements to be installed vertically and would aid in vehicle stability. Vertical guardrails also simplified the design of the internal stiffeners by eliminating the sloped faces. Now the internal stiffeners may be rectangular steel tubes or even extended-width timber blockouts. Additionally, a vertical face would maximize the offset between the rail elements and the support structure, which would reduce the potential for vehicle snag.

The vertical parapet was given a width of 435 mm (17 in.) so that the addition of the dual 83-mm (3¼-in.) wide rails would result in a barrier width equal to the maximum allowable width of 600 mm (23¾ in.). The barrier shape transition from single-slope to vertical utilized a 10:1 taper and required a length of 1.175 m (3.85 ft). The lower edge of the downstream barrier segment (determined by direction of traffic) was tapered to reduce the risk of vehicle and tire snag. The taper was placed on the bottom 350 mm (13¾ in.) of the barrier, had a 75 mm (3 in.) lateral offset, and utilized a 4:1 slope. End section reinforcement should be placed over a length of 2.785 m (9.14 ft) on both sides of the gap, as shown in Figures 72 and 73. Finally, the concrete barrier segments should all be properly anchored utilizing a foundation slab or footing as discussed in Chapter 10.

The stirrups within the vertical parapet segments were shown as U-bars to match the stirrup designs for the TL-5 median barrier. However, the additional width at the top of the vertical parapet would allow the use of closed-loop stirrups. Although they require more steel, closed-loop stirrups would provide more stiffness and stability during construction. Thus, either

U-bar or closed-loop stirrups may be utilized within the vertical parapet segments of this specialized barrier treatment.

This treatment design is not intended to be TL-5 crashworthy. The treatment design should provide adequate safety performance for low-severity impacts, and may possibly provide enough strength to satisfy MASH TL-2 standards. However, barrier deflections and vehicle snag for this barrier system remain unknown. A complete evaluation of the treatment hardware would require full-scale crash testing according to MASH standards.

The performance of this gap treatment design is dependent upon the length of the barrier gap. Longer gaps will reduce the strength capacity of the system, while shorter gaps will increase the strength and performance. The system was drawn and analyzed assuming a 3.0-m (9.8-ft) gap length, but efforts should be made to cast the ends of the concrete parapets as close to the sign support structures as possible to maximize the performance of the system.

Finally, the use of 3.42-mm thick (10-ga.) thrie beam elements instead of the 2.66-mm thick (12 ga.) rails would increase the strength of the system by 28 percent. This change would not result in TL-3 design strength, but it would provide increased redirective capacity.

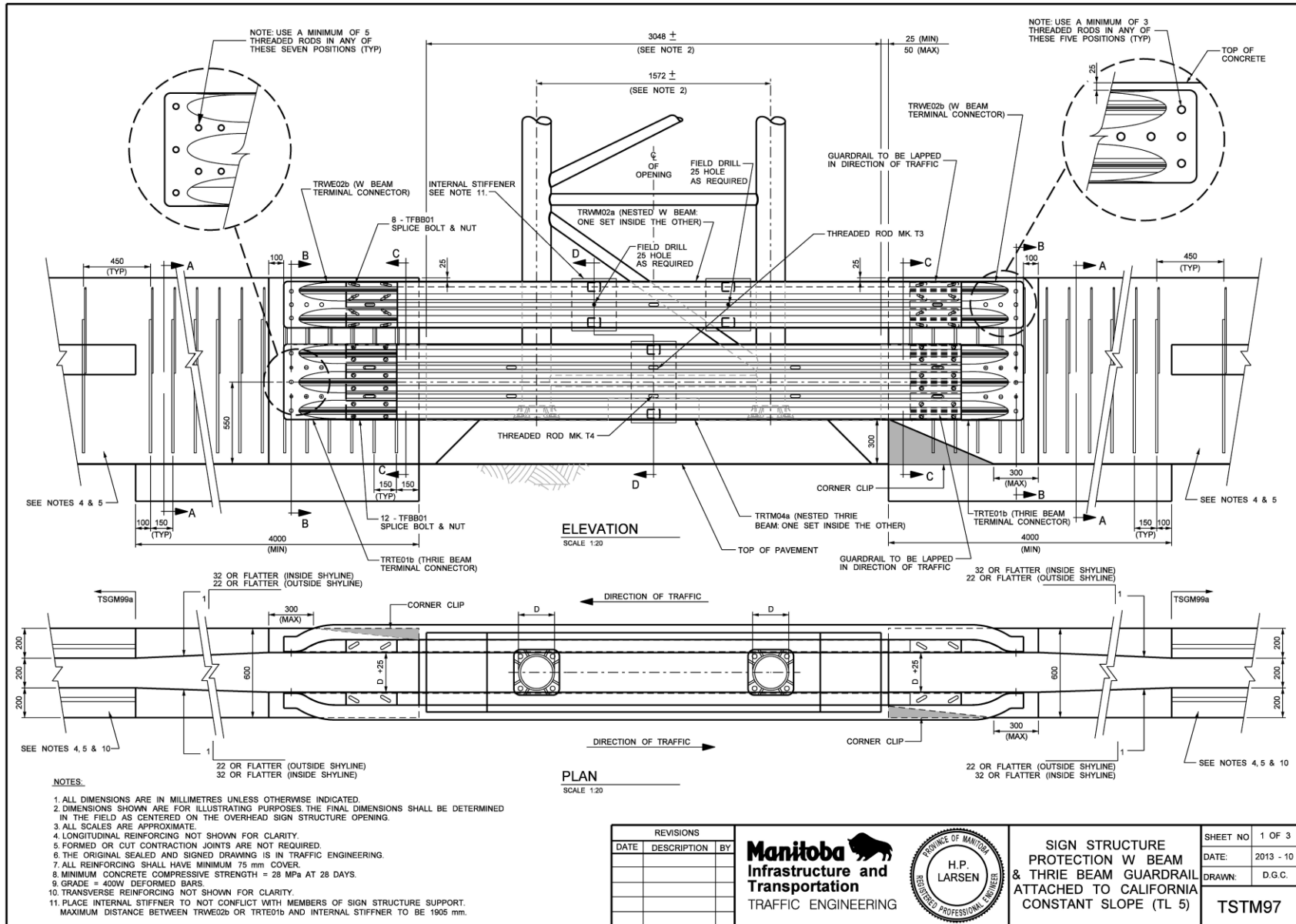


Figure 71. MI Treatment Concept for Barrier Gaps Spanning Sign Support Structures

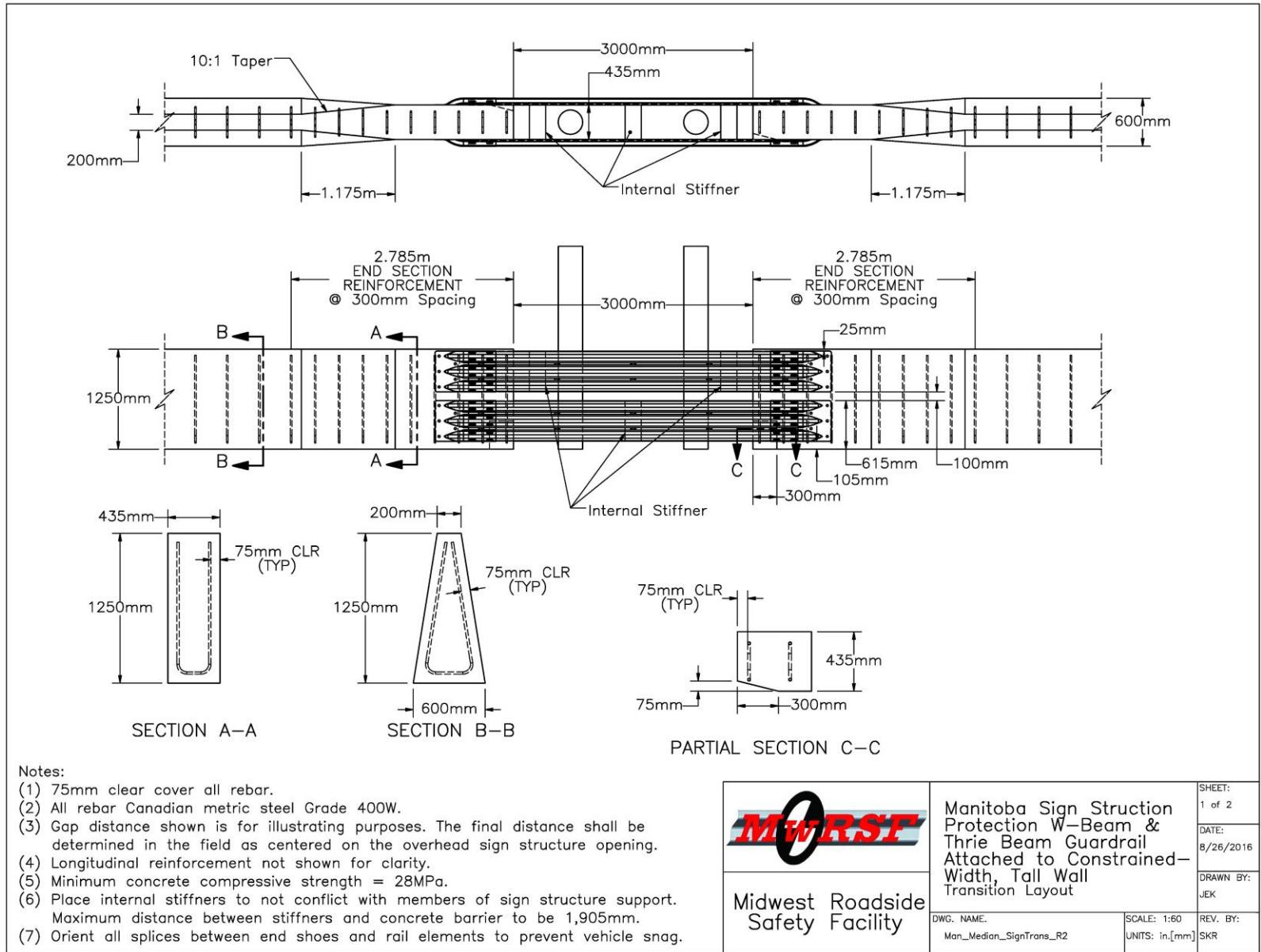


Figure 72. Treatment Details for TL-5 Barrier Gaps Spanning Large Sign Supports

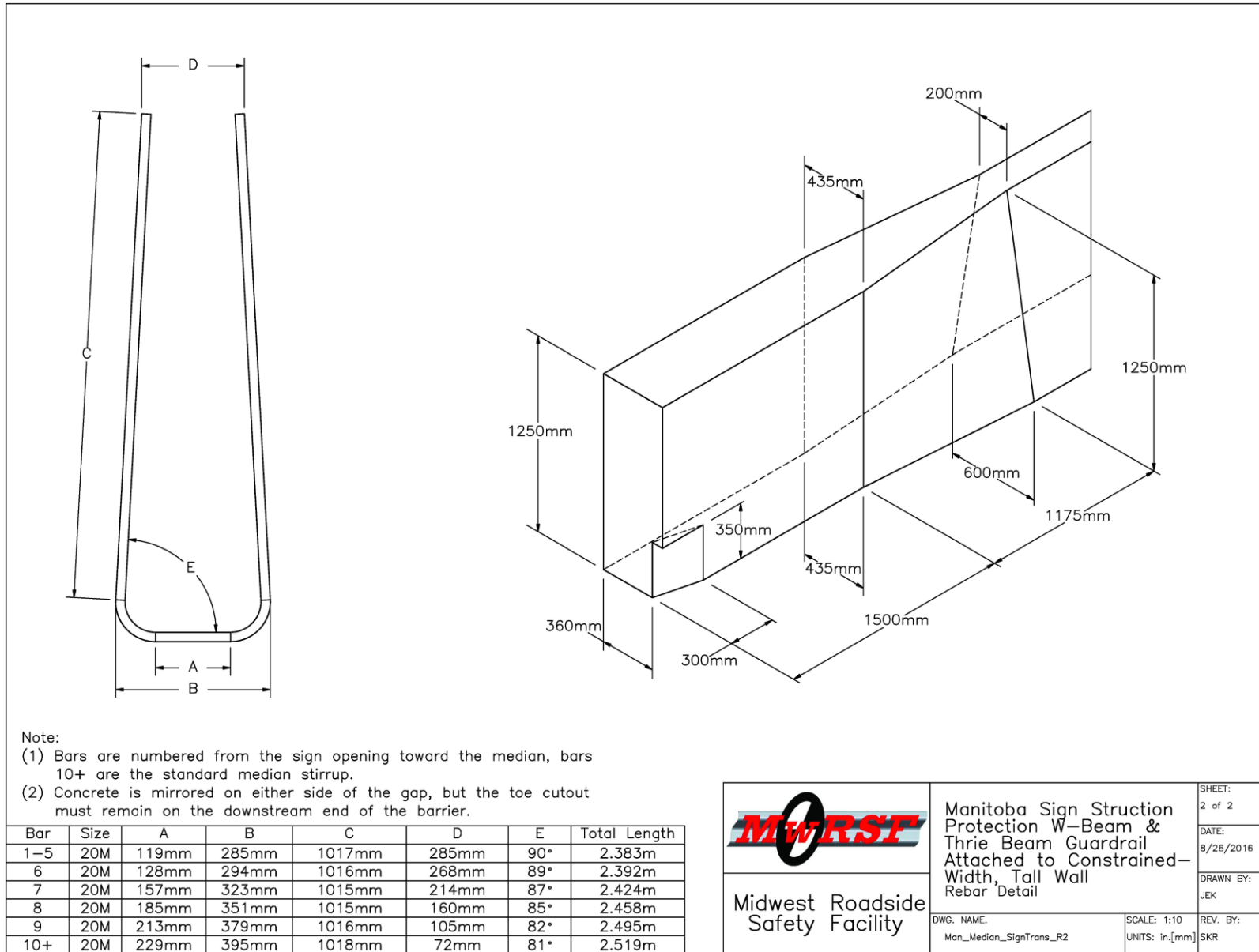


Figure 73. Treatment Details for TL-5 Barrier Gaps Spanning Large Sign Supports

12 SUMMARY, CONCLUSIONS, AND RECOMMENDATIONS

12.1 Summary and Conclusions

The objective of this study was to develop a 1,250-mm (49¼-in.) tall, single-slope concrete barrier system to satisfy MASH TL-5 safety standards. Barrier configurations of the Manitoba Constrained-Width, Tall Wall were developed for median, roadside, and bridge rail applications. The new barrier system maintained a narrow 600-mm (23¾-in.) footprint, while providing increased strength and vehicle stability during impact events as well as eliminating headlight glare from opposing traffic.

Because the single-sided bridge rail configuration had a reduced width and was supported by a cantilevered bridge deck, it was identified as the most critical configuration. Thus, the bridge rail was developed first and subjected to full-scale crash testing. Through a review of TL-5 barriers and crash tests, a barrier design load of 845 kN (190 kips) applied to the top of the barrier was selected. The bridge rail width and reinforcement configuration was optimized to resist the design load and minimize the amount of steel reinforcement in the barrier. Optimized interior and end section configurations were selected and recommended for evaluation through full-scale crash testing. The selected barrier configuration had a capacity of 872 kN (196 kips).

The test installation was 45.7 m (150 ft) long with a height of 1,250 mm (49¼ in.), a top width of 250 mm (10 in.), and a base width of 450 mm (17¾ in.). The upstream half of the bridge rail was installed on a 280-mm (11-in.) thick simulated bridge deck with an overhang distance of 1,300 mm (51¼ in.), while the downstream half was anchored to the concrete tarmac to provide runout length. At the mid-span of the simulated bridge deck, open gaps were placed in the bridge rail and deck measuring 168 mm (6⅝ in.) and 19 mm (¾ in.) respectively, to simulate an expansion-contraction joint. End section reinforcement was utilized in the bridge rail and deck on both sides of the open joint. A 13-mm (½-in.) thick steel cover plate was utilized to shield vehicles from snagging on the exposed ends of the bridge rail adjacent to the joint. The cover plate was bolted to the upstream side of the rail joint, and the front edge of the plate was chamfered to prevent vehicle snag.

One full-scale crash test was performed on the barrier according to MASH test designation no. 5-12. The impact point was selected to provide maximum loading to the bridge rail at the critical location, which was adjacent to the barrier joint. During test no. MAN-1, the tractor trailer initially impacted the barrier just upstream from the joint, as did the rear trailer tandem axles as a result of tail slap later in the impact event. The vehicle was contained and redirected with minimal damage to the barrier. Minor cracks were found in the barrier and the bridge deck, and a small area measuring less than 50 mm (2 in.) deep fractured away from the top of the bridge rail due to contact with the trailer's front-bottom corner. The bridge rail experienced no permanent deflections. A summary of the MASH safety performance evaluation results is shown in Table 17. The small car and pickup truck tests required by MASH TL-5 were not considered critical and, thus, not conducted due to prior successful small car and pickup truck impacts into similar rigid barriers. Thus, the barrier system was deemed crashworthy according to MASH TL-5 safety standards.

Onboard accelerometers were placed on the trailer near both sets of tandem axles in an effort to calculate the impact loads. An analysis of the accelerations recorded near the front tandem axles estimated the impact load to be between 1,027 kN and 1,183 kN (231 kips and 266 kips). Previous studies have concluded that the maximum impact load from 36000V vehicles likely occurred during the impact of the rear tandem axles. Analysis of the high-speed video from test no. MAN-1 revealed that the maximum barrier dynamic deflections occurred as a result of the rear tandem axles impacting the bridge rail. This result indicated that the rear tandem axles potentially applied a higher load to the barrier than the front tandem axles. Unfortunately, the accelerometer at the rear tandem axles experienced technical difficulties and did not record the event. Thus, the actual maximum impact loads were unknown. Regardless of the true maximum impact load, it was clear that the barrier experienced an impact load that was significantly higher than the design load of 872 kN (196 kips). The barrier suffered only minor damage, which indicated that the barrier had additional reserve capacity. Thus, the Yield Line analysis method of calculating concrete barrier strength provided a conservative estimate of the barrier capacity. The simplification of the impact load to a distributed load acting only at a singular height was thought to contribute, in part, to the low barrier strengths estimated by the Yield Line analysis.

After the successful crash testing of the Manitoba Constrained-Width, Tall Wall bridge rail, median and roadside configurations were also developed. The TL-5 median barrier utilized a 600-mm (23³/₄-in.) wide base and the same single-slope face geometry as the bridge rail. Barrier configurations were developed for both the interior and end sections of the TL-5 median barrier. The steel reinforcement for each section was optimized to provide the same structural capacity as the bridge rail as well as minimize the amount of steel rebar. A TL-4 version of the median barrier was also developed with the same width and slope as the median barrier so that the same forms could be utilized to install either barrier configuration. Anchorage options were then provided to support the median barrier with a reinforced concrete foundation slab, independent footing, or asphalt keyway. Details were also provided for a TL-5 roadside barrier, which was identical to the bridge rail, anchored with either a foundation slab or independent footing.

Transitions systems were developed for connecting the TL-5 Manitoba Constrained-Width, Tall Wall median barrier to: (1) a TL-4 single-slope median barrier; (2) an 815-mm (32-in.) tall F-shape median barrier; (3) dual TL-5 roadside barriers; and (4) dual 815-mm (32-in.) tall F-shape roadside barriers. A transition was also developed between the TL-4 median barrier and a vertical concrete parapet for connection to guardrail or crash cushions. All of these transitions were developed utilizing a maximum lateral taper of 10:1 and a maximum vertical taper of 5:1 to prevent vehicle instabilities during impact events. Finally, details were provided for the treatment of gaps within the TL-5 median barrier due to obstructions by overhead sign support structures.

Table 17. Summary of Safety Performance Evaluation Results

Evaluation Factors	Evaluation Criteria	Test No. MAN-1
Structural Adequacy	A. Test article should contain and redirect the vehicle or bring the vehicle to a controlled stop; the vehicle should not penetrate, underride, or override the installation although controlled lateral deflection of the test article is acceptable.	S
Occupant Risk	D. Detached elements, fragments or other debris from the test article should not penetrate or show potential for penetrating the occupant compartment, or present an undue hazard to other traffic, pedestrians, or personnel in a work zone. Deformations of, or intrusions into, the occupant compartment should not exceed limits set forth in Section 5.3 and Appendix E of MASH.	S
	G. It is preferable, although not essential, that the vehicle remain upright during and after collision.	S
MASH Test Designation Number		5-12
Pass/Fail		Pass

S – Satisfactory U – Unsatisfactory NA - Not Applicable

12.2 Installation Recommendations

As described in Section 4.3, the calculated strength of the selected bridge rail end section was greater than that provided by the interior section. Since the full-scale crash test was targeted to impact a barrier end section adjacent to the rail joint, the test installation end section reinforcement was modified to reduce the strength of the end section to 872 kN (196 kips), which was equivalent to the strength of the interior section. Thus, the spacing of the transverse steel stirrups in the end section was increased from the selected 200 mm (8 in.) to 230 mm (9 in.) for testing purposes only. The spacing of the transverse steel reinforcement in the deck were increased to match the barrier spacing. Test no. MAN-1 illustrated the barrier's ability to satisfy MASH TL-5 requirements with this increased reinforcement spacing. However, it may be easier to utilize the original steel configuration during construction as the end section spacings were exactly half of the interior section spacings. These recommended reinforcement configurations for the TL-5 bridge rail are shown in Figure 74.

Although the TL-5 median barrier developed herein was never full-scale crash tested, it was designed to have a greater strength than the crash-tested bridge rail. Additionally, the median barrier utilized the same barrier height and face geometry. Therefore, it should be considered a MASH TL-5 crashworthy system. Similarly, the TL-4 median barrier has a similar height and geometry as other successfully-tested MASH TL-4 barriers. Since it was designed with a higher strength than these barriers, it should also be considered crashworthy to MASH TL-4. Finally, the TL-5 roadside configuration developed herein was nearly identical to the crash-tested bridge rail. The anchorage of the roadside barrier to a reinforced concrete foundation slab or footing should provide adequate strength when compared to the thin, cantilevered bridge deck. Thus, the TL-5 roadside barrier should also be considered crashworthy to MASH TL-5.

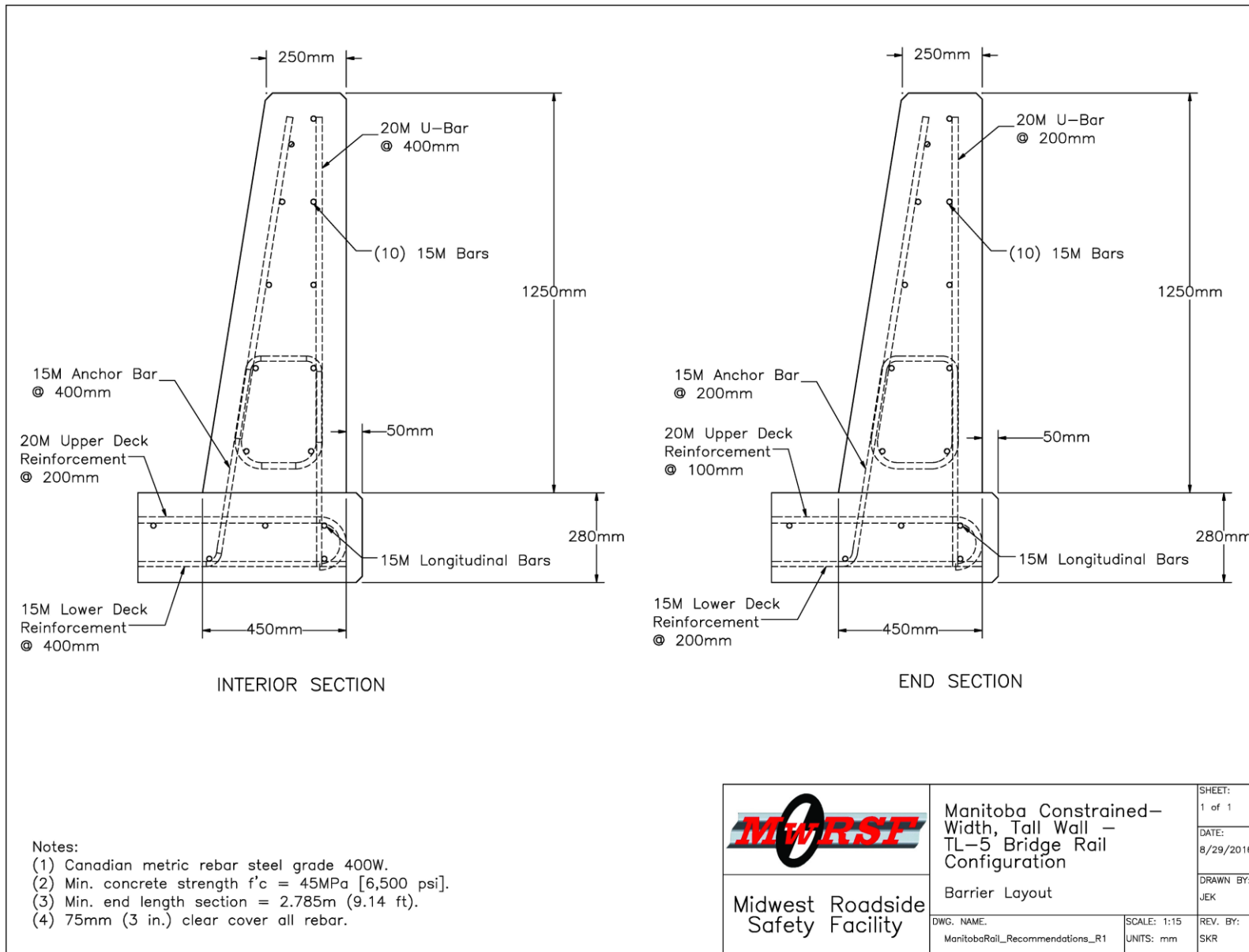


Figure 74. Recommended Reinforcement Configurations for the TL-5 Bridge Rail

MI commonly utilizes a Lineator Delineation System by 3M on its concrete barriers and desire to create longitudinal recesses in the concrete barriers for the placement of roadway delineators, as shown in Figure 75. These recesses were not implemented into the test article due to ease of construction. The small reduction in barrier cross section from the 20-mm ($\frac{3}{4}$ -in.) indentation should not affect barrier strength. Additionally, the recesses extend longitudinally along the barrier, so vehicle snag should not occur. Therefore, the inclusion of these recesses is not thought to negatively affect the performance of the Manitoba Constrained-Width, Tall Wall barrier.

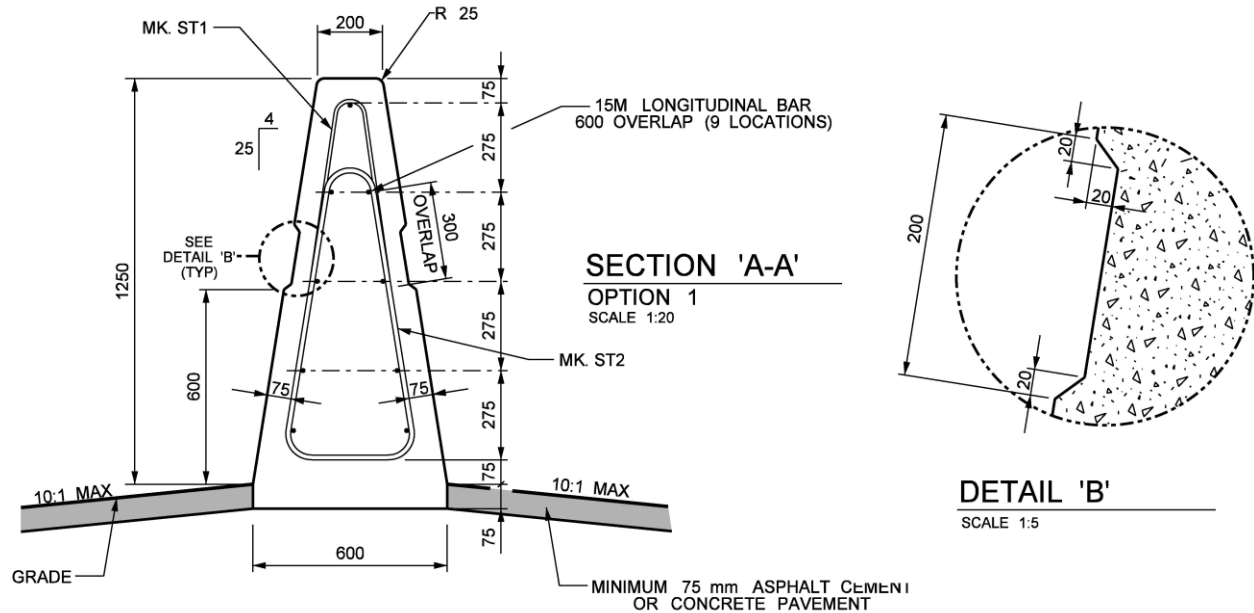
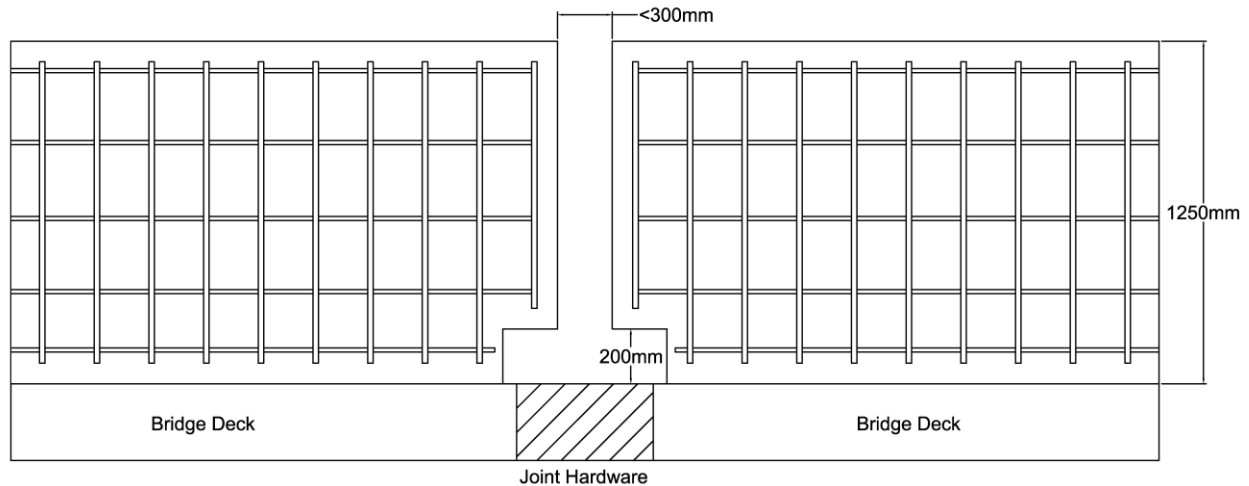


Figure 75. Longitudinal Recess for Roadway Delineators

The 168-mm ($6\frac{5}{8}$ -in.) gap placed in the bridge rail was selected to represent a typical joint opening and to align the transverse reinforcement spacings of the barrier and deck segments without having an odd spacing or extra bar. Joint openings larger than that utilized in test no. MAN-1 are likely to occur in real-world installations. Basic bending calculations indicate the cover plate should be sufficient to shield gap lengths up to 300 mm (12 in.) without it negatively affecting system performance. However, the only sure way to evaluate the maximum gap length is through full-scale crash testing. If gaps larger than 300 mm (12 in.) are necessary due to an inability to cast barrier segments directly to expansion joint hardware in the deck, it is recommended to cast cantilevered extension sections of the barrier over the expansion joint hardware to reduce the gap length. The cantilevered extensions of the barrier should have the same geometry as the adjacent barrier, only the bottom 200 mm (8 in.) of the barrier should be removed. The length of the cantilevered extensions should be held to a minimum while reducing the maximum gap length to less than 300 mm (12 in.), as shown in Figure 76. Barrier reinforcement should be continued into the cantilevered extensions to ensure proper strength. If necessary, the length the steel cover plate should be increased such that it covers at least 100 mm (4 in.) of the full barrier cross section on both sides of the joint.



- (1) Deck reinforcement and barrier anchor bars not shown for clarity
- (2) Steel cover plate and end caps not shown for clarity
- (3) Cantilevered barrier length need only be long enough to reduce gap below 300 mm

Figure 76. Cantilevered Barrier Extensions over Large Expansion Joints

The upstream edge on the front of the steel cover plate was chamfered to prevent vehicle snag during impacts. If the design is utilized in an installation where reverse directions are possible, then both sides on the front of the cover plate should be chamfered. If it is utilized in a median barrier, then both the front and back of the steel cover plate need to be chamfered. All chamfers should be 6 mm x 6 mm (1/4 in. x 1/4 in.).

The working width of the Manitoba Constrained-Width, Tall Wall barrier was found to be 949 mm (37.4 in.), as measured from high-speed video during test no. MAN-1. Working width is defined as the distance between the front of the barrier to the furthest lateral extent of the vehicle (or barrier component), while the zone of intrusion represents the area above and behind the barrier that a vehicle component may occupy during redirection. Since the top of the Manitoba Constrained-Width, Tall Wall is offset 200 mm (8 in.) from the front toe, the zone of intrusion for the barrier measures 749 mm (29.5 in.) laterally from the top-front corner of the barrier and extends upward the full height of a tractor trailer vehicle, or approximately 4.1 m (13.5 ft).

13 REFERENCES

1. *Manual for Assessing Safety Hardware (MASH)*, American Association of State Highway and Transportation Officials (AASHTO), Washington, D.C., 2009.
2. Beason, W.L., Ross, H.E., Perera, H.S., Campise, W.L., and Bullard, D.L., Development of a Single-Slope Concrete Median Barrier, Report 9429CDK-1, Texas State Department of Highways and Public Transportation, Texas Transportation Institute, College Station, TX, June 1989.
3. Beason, W.L., Ross, H.E., Perera, H.S., and Marek, M., *Single-Slope Concrete Median Barrier*, Transportation Research Record No. 1302, Transportation Research Board, National Research Council, Washington, D.C., 1991.
4. Jewell, J.R., *Vehicle Crash Tests of a Slip-Formed, Single Slope, Concrete Median Barrier with Integral Concrete Glare Screen*, California Department of Transportation, Division of New Technology, Materials and Research, 1997.
5. *Glare Screen Guidelines*, National Cooperative Highway Research Program (NCHRP), Synthesis of Highway Practice 66, Transportation Research Board, Washington D.C., 1979.
6. Ross, H.E., Sicking, D.L., Zimmer, R.A., and Michie, J.D., *Recommended Procedures for the Safety Performance Evaluation of Highway Features*, National Cooperative Research Program (NCHRP) Report 350, Transportation Research Board, Washington, D.C., 1993.
7. *Guide Specifications for Bridge Railings*, American Association of State Highway and Transportation Officials (AASHTO), Washington, DC, 1989.
8. Hirsch, T.J., and Arnold, A., *Bridge Rail to Restrain and Redirect 80,000-lb Trucks*, Research Report 230-4F, Research Study No. 2-5-78-230, FHWA/TX-81+230-4F, Performed for the Transportation Planning Division of the Texas State Dept. of Highways & Public Transportation, Performed by the Texas Transportation Institute, Texas A&M University System, College Station, Texas, November 1981.
9. Hirsch, T.J., Fairbanks, Wm.L., Buth, C.E., *Concrete Safety Shape with Metal Rail on Top to Redirect 80,000-lb Trucks*, Research Report 416-1F, Research Study No. 2-5-83-416, FHWA/TX-83/+416-1F, Performed for the Transportation Planning Division of the Texas State Dept. of Highways & Public Transportation, Performed by the Texas Transportation Institute, Texas A&M University System, College Station, Texas, December 1984.
10. Buth, C.E., Hirsch, T.J., and Menges, W.L., *Testing of New Bridge Rail and Transition Designs - Volume I: Technical Report*, FHWA-RD-93-058, Final Report on Contract No. DTFH61-86-C-00071, Performed for the Office of Safety and Traffic Operations R&D, Federal Highway Administration, Performed by the Texas Transportation Institute, Texas A&M University System, College Station, Texas, June 1997.

11. Alberson, D.C., Zimmer, R.A., and Menges, W.L., *NCHRP Report 350 Compliance Test 5-12 of the 1.07-m Vertical Wall Bridge Railing*, Contract No. DTFH61-95-C-000136, FHWA-RD-96-199, Performed for the Office of Safety and Traffic Operations R&D, Federal Highway Administration, Performed by the Texas Transportation Institute, Texas A&M University System, College Station, Texas, January 1997.
12. Polivka, K.A., Faller, R.K., Rohde, J.R., Sicking, D.L., and Holloway, J.C., *Development, Testing, and Evaluation of NDOR's TL-5 Aesthetic Open Concrete Bridge Rail*, Final Report to the Nebraska Department of Roads, Transportation Research Report No. TRP-03-148-05, Midwest Roadside Safety Facility, University of Nebraska-Lincoln, December 1, 2005.
13. Mastova, M. and Ray, M.H., *Evaluation of Crash Tests of the MDS-4 & MDS-5 Barriers According to Report 350*, Performed by German Federal Highway Research Institute (BASt), July 23, 2008.
14. Nicol, D.A., Letter from Federal Highway Administration, U.S. Department of Transportation to Malcolm H. Ray, P.E., Ph.D., Reference No. HSSD/B-165.
15. Buth, C.E. and Menges, W.L., *MASH Test 5-12 of the Schöck ComBAR Parapet*, Test Report No. 401761-SBG1, Contract No. P2010353, Performed for Competence Center ComBAR, Schöck Bauteile GmbH, Baden-Baden, Germany, Performed by the Texas Transportation Institute Proving Ground, Texas A&M University System, College Station, Texas, March 2011.
16. Buth, C.E. and Menges, W.L., *MASH Test 5-12 on the Ryerson/Pultrall Parapet*, Test Report No. 510605-RYU1, Contract No. P2012015, Performed for the Civil Engineering Department, Ryerson University, Toronto, Ontario, Canada, Performed by the Texas Transportation Institute Proving Ground, Texas A&M University System, College Station, Texas, February 2012.
17. Rosenbaugh, S.K., Sicking, D.L., and Faller, R.K., *Development of a TL-5 Vertical Faced Concrete Median Barrier Incorporating Head Ejection Criteria*, Research Report No. TRP-03-194-07, Midwest Roadside Safety Facility, University of Nebraska-Lincoln, Lincoln, NE, December 10, 2007.
18. Buth, C.E., Campise, W.L., Griffen III, L.I., Love, M.L., and Sicking, D.L., *Performance Limits of Longitudinal Barrier Systems*, Report to the Federal Highway Administration, Report No. FHWA-RD-86/153, Texas Transportation Institute, May 1986.
19. Mak, K.K. and Campise, W.L., *Test and Evaluation of Ontario "Tall Wall" Barrier with an 80,000-Pound Tractor-Trailer*, Project No. RF71620, Performed for the Ontario Ministry of Transportation, Performed by the Texas Transportation Institute, Texas A&M University System, College Station, Texas, September 1990.
20. *AASHTO LRFD Bridge Design Specifications - Customary U.S. Units - 2012*, American Association of State Highway and Transportation Officials (AASHTO), Washington, D.C., 2012.

21. Beason, W.L., Hirsch, T.J., and Campise, W.L., *Measurement of Heavy Vehicle Impact Forces and Inertia Properties*, Contract No. DTFH61-85-00101, Performed for the Office of Research, Federal Highway Administration, U.S. Department of Transportation, Performed by the Texas Transportation Institute, Texas A&M University, College Station, Texas, January 1989.
22. *Roadside Design Guide*, 4th Edition 2011, American Association of State and Highway Transportation Officials (AASHTO), Washington D.C., 2011.
23. Williams, W.F., Bligh, R.P., and Menges, W.L., *MASH Test 4-11 of the TxDOT Single Slope Bridge Rail (Type SSTR) on Pan-Formed Bridge Deck*, Final Report to the Texas Department of Transportation, Report No. FHWA/TX-11/9-1002-3, Texas Transportation Institute, Texas A&M University, College Station, Texas, March 2011.
24. Schmidt, J.D., Faller, R.K., Lechtenberg, K.A., Sicking, D.L., and Reid, J.D., *Development and Testing of a New Vertical-Faced Temporary Concrete Barrier for use on Composite Panel Bridge Decks*, Final Report to the Kansas Department of Transportation, MwRSF Research Report No. TRP-03-220-09, Midwest Roadside Safety Facility, University of Nebraska-Lincoln, Lincoln, Nebraska, October 13, 2009.
25. Polivka, K.A., Faller, R.K., Sicking, D.L., Rohde, J.R., Bielenberg, R.W., Reid, J.D., and Coon, B.A., *Performance Evaluation of the Permanent New Jersey Safety Shape Barrier – Update to NCHRP 350 Test No. 4-10 (2214NJ-1)*, Final Report to the National Cooperative Highway Research Program, MwRSF Research Report No. TRP-03-177-06, Midwest Roadside Safety Facility, University of Nebraska-Lincoln, Lincoln, Nebraska, October 13, 2006.
26. Bligh, R.P., Arrington, D.R., Sheikh, N.M., Silvestri, C., and Menges, W.L., *Development of a MASH TL-4 Median Barrier Gate*, Final Report to the Texas Department of Transportation, Report No. FHWA/TX-11/9-1002-2, Texas A&M University, College Station, Texas, Texas Transportation Institute, June 2011.
27. Bullard, D.L., Bligh, R.P., Menges, W.L., and Haug, R.R., *Volume I: Evaluation of Existing Roadside Safety Hardware Using Updated Criteria – Technical Report*, National Cooperative Highway Research Program Web Only Document 157, Transportation Research Board, Washington, D.C., 2010.
28. Hinch, J., Yang, T.L., and Owings, R., *Guidance Systems for Vehicle Testing*, ENSCO, Inc., Springfield, Virginia, 1986.
29. Society of Automotive Engineers (SAE), *Instrumentation for Impact Test – Part 1 – Electronic Instrumentation*, SAE J211/1 MAR95, New York City, NY, July, 2007.
30. *Vehicle Damage Scale for Traffic Investigators*, Second Edition, Technical Bulletin No. 1, Traffic Accident Data (TAD) Project, National Safety Council, Chicago, Illinois, 1971.

31. *Collision Deformation Classification – Recommended Practice J224 March 1980*, Handbook Volume 4, Society of Automotive Engineers (SAE), Warrendale, Pennsylvania, 1985.
32. *Design Guidelines for Test Level 3 (TL-3) through Test Level 5 (TL-5) of Roadside Barrier Systems Placed on MSE Retaining Walls*, Combined Quarterly Progress Report August 2012 – December 2012, NCHRP Project 22-20(2), TTI Project No. 478130, December 2012.
33. Rosenbaugh, S.K., Faller, R.K., Hascall, J.A., Allison, E.A., Bielenberg, R.W., Rohde, J.R., Sicking, D.L., Polivka, K.A., Reid, J.D., *Development of a Stand-Alone Concrete Bridge Pier Protection System*, Research Report No. TRP-03-190-08, Midwest Roadside Safety Facility, University of Nebraska-Lincoln, Lincoln, Nebraska, April 18, 2018.
34. *Building Code Requirements for Structural Concrete (ACI 318-11) and Commentary (ACI 318R-11): An ACI Standard*, Reported by ACI Committee 318, American Concrete Institute, Farmington Hills, MI, 2011.
35. Polivka, K.A., Faller, R.K., Sicking, D.L., Rohde, J.R., Bielenberg, R.W., Reid, J.D., and Coon, B.A., *Performance Evaluation of the Permanent New Jersey Safety Shape Barrier – Update to NCHRP 350 Test No. 4-12 (2214NJ-2)*, Final Report to the National Cooperative Highway Research Program, MwRSF Research Report No. TRP-03-178-06, Midwest Roadside Safety Facility, University of Nebraska-Lincoln, Lincoln, Nebraska, October 13, 2006.
36. Bullard, D.L., Bligh, R.P., and Menges, W.L., *MASH08 TL-4 Testing and Evaluation of the New Jersey Safety Shape Bridge Rail*, Preliminary Test Report to the National Cooperative Highway Research Program, Test Report No. RF 476460-1b, Texas Transportation Institute, Texas A&M University, College Station, Texas, November 2008.
37. Rosenbaugh, S.K., Faller, R.K., Bielenberg, R.W., Sicking, D.L., Reid, J.D., and Tadros, M.K., *Phase I Development of an Aesthetic, Precast Concrete Bridge Rail*, Research Report No. TRP-03-239-12, Midwest Roadside Safety Facility, University of Nebraska-Lincoln, Lincoln, Nebraska, February 13, 2012.
38. Sheikh, N.M., Bligh, R.P., and Menges, W.L., *Determination of Minimum Height and Lateral Design Load for MASH Test Level 4 Bridge Rails*, Cooperative Research Program Test Report No. 9-1002-5, Texas Transportation Institute, Texas A&M University, College Station, Texas, October 2011.
39. Wiebelhaus, M.J., Terpsma, R.J., Lechtenberg, K.A., Reid, J.D., Faller, R.K., Bielenberg, R.W., Rhode, J.R., and Sicking, D.L., *Development of a Temporary Concrete Barrier to Permanent Concrete Median Barrier Approach Transition*, Research Report No. TRP-03-208-10, Midwest Roadside Safety Facility, University of Nebraska-Lincoln, Lincoln, Nebraska, July 15, 2010.
40. Schmidt, T.L., *Development of a Transition Between an Energy-Absorbing Concrete Barrier and a Rigid Concrete Buttress*, Thesis Prepared in Fulfilment Requirements for the

Degree of Master of Science, University of Nebraska-Lincoln, Lincoln, Nebraska, July, 2016.

14 APPENDICES

Appendix A. Material Specifications

Table A-1. Test No. MAN-1, Bill of Materials

Item No.	QTY.	Description	Material Spec	Reference
a1	1	Bridge Rail Concrete 1 - 4.96 m ³ [378.93 ft ³]	f'c = 45 MPa [6.5 ksi]	Cylinder Testing Matrix
a2	1	Bridge Rail Concrete 2 - 17.97 m ³ [528.66 ft ³]	f'c = 45 MPa [6.5 ksi]	Cylinder Testing Matrix
a3	2	Bridge Deck Concrete - 10.73 m ³ [378.93 ft ³]	f'c = 45 MPa [6.5 ksi]	Cylinder Testing Matrix
a4	1	Grade Beam Concrete - 8.23 m ³ [290.64 ft ³]	f'c = 45 MPa [6.5 ksi]	Cylinder Testing Matrix
b1	136	M20 Bar - 3.332 m [131 1/4"] Long, Deck	Steel Grade 400W	Heat # - 52069671/02
b2	38	M15 Bar - 11.320 m [445 3/4"] Long, Deck	Steel Grade 400W	Heat # - 61099893/02
b3	70	M15 Bar - 2.740 m [107 7/8"] Long, Deck	Steel Grade 400W	Heat # - 61105170/06
b4	10	M15 Bar - 11.196 m [440 3/4"] Long, Rail A	Steel Grade 400W	Heat # - 61099893/02
b5	10	M15 Bar - 34.056 m [1340 3/4"] Long, Rail B	Steel Grade 400W	Heat # - 61099893/02
b6	6	#4 Bar - 22.735 m [895 1/8"], Grade Beam	ASTM A615 Gr. 60	Heat # - 58021938/02
b7	57	M15 Bar - 1.438 m [56 5/8"] Long, Rail B	Steel Grade 400W	Heat # - 61105170/06
b8	68	#5 Bar - 2.166 m [85 1/4"], Grade Beam	ASTM A615 Gr. 60	Heat # - 55040423/02
b9	68	M15 Bar - 1.897 m [74 5/8"] Long, ,Deck ,	Steel Grade 400W	Heat # - 61105170/06
b10	125	M20 Bar - 2.384 m [93 7/8"] Long, Rail	Steel Grade 400W	Heat # - 52069671/02
b11	68	#6 Bar - 1.143 m [45"] Long, Bridge Deck	ASTM A615 Gr. 60	Heat # - 58022155/03
b12	68	#5 Bar - 0.678 m [26 3/4"] Long, Deck	ASTM A615 Gr. 60	Heat # - 55040423/02
b13	136	#5 Bar - 0.950 m [37 3/8", Grade Beam	ASTM A615 Gr. 60	Heat # - 55040423/02
c1	1	800x264x13 [31 1/2"x10 3/8"x1/2"] Plate	ASTM A572	Heat # - B5J664
c2	1	1238x800x13 [48 3/4"x31 1/2"x1/2"] Plate	ASTM A572	Heat # - T2012
c3	1	1255x800x13 [49 7/16"x31 1/2"x1/2"] Plate	ASTM A572	Heat # - T2012
c4	1	386x76x6 [15 3/16"x3"x1/4"] Plate	ASTM A572	Heat # - A600686
c5	1	1230x294x6 [48 3/8"x11 5/8"x1/4"] Plate	ASTM A572	Heat # - T2251
c6	2	1230x430x6 [48 3/8"x16 7/8"x1/4"] Plate	ASTM A572	Heat # - T2251
c7	1	1246x294x6 [49"x11 5/8"x1/4"] Plate	ASTM A572	Heat # - T2251
c8	1	1230x444x6 [48 3/8"x17 1/2"x1/4"] Plate	ASTM A572	Heat # - T2251
c9	1	1246x444x6 [49"x17 1/2"x1/4"] Plate	ASTM A572	Heat # - T2251
d1	8	3/4" [19] Dia. 2-1/2" [64] Long Flat Head Countersunk Bolt	Grade A307 or Higher (A449 Preferred)	Heat # - 3S060
d2	8	3/4" [19] Dia. Hex Nut	A563	NA
d3	32	5/8" [16] Dia. x 4" [102] Long Stud	Steel Any Grade	Heat # - 20368220
e1	1	Chemical Epoxy Adhesive	Bond Strength = 10 MPa [1,450 psi]	Powers 100+ Gold

Table A-2. Concrete Compressive Strength Data

	Pour Date	14 Day Compressive Strength (psi)		28 Day Compressive Strength (psi)		Compressive Strength 2 Days After Test Day (psi)	
		Truck #1	Truck #2	Truck #1	Truck #2	Truck #1	Truck#2
Grade Beam	11/3/2015	5,660	5,770	7,090	6,450	M: 8,300	N: 8,260
Deck A (US)	1/14/2016	5,630	6,110	6,280	6,140	K: 7,720	L: 7,380
Deck B (DS)	1/26/2016	n/a	n/a	6,360	6,890	I: 8,510	J: 8,650
Bridgerail #1	2/11/2016	5,890	5,970	6,730	7,020	G: 8,210	H: 7,080
Bridgerail #2	2/17/2016	5,640	5,390	6,360	6,250	E: 6,760	F: 7,500
Bridgerail #3	2/26/2016	5,730	5,900	6,610	6,880	C: 7,140	D: 7,290
Bridgerail #4	3/4/2016	5,230	5,440	5,960	6,290	A: 5,980	B: 5,240
		Average 28 Day Compressive Strength		6,522 psi			
				45.0 MPa			

Manitoba Countersunk Bolts
R#16-0195 SMT

YFS

FANG SHENG SCREW CO., LTD.

FANG SHENG TESTING LABORATORY

NO. 17, BEN GONG 2nd ROAD, BEN CHOU INDUSTRIAL PARK, KANGSHAN 820, KAOHSIUNG, TAIWAN, ROC TEL:886-7-0230300 FAX:886-7-0230392 E-mail:bsales@mail.yfs.com.tw

CERTIFICATE OF INSPECTION

PURCHASER :BRIGHTON-BEST INTERNATIONAL INC.
ADDRESS :5855 OBISPO AVE. LONG BEACH, CA 90805, USA

DESCRIPTION :SOCKET FLAT HEAD CAP SCREW(THERMAL BLACK OXIDE)
INSP. DATE :05/07/2014 ISSUED DATE:09/03/2014
ORDER NO. :U18847 LOT NO. :14105WSA6
INVOICE NO. :B101-1408291 CERT. NO. :10976037
MATERIAL TYPE:SCM435 MANU. DATE :04/22/2014
SAMPLE SIZE :REFER TO ASME B18.18.2M-87 SIZE :3/4NC*2-1/2
HEAT NO. :35060 (1020276) LOT SIZE : 30000
MANUFACTURER :FANG SHENG SCREW CO., LTD. PART NO. :211376

DIMENSIONAL INSPECTIONS		SPEC.:ASME B18.3-03			
CHARACTERISTICS	SPECIFIED	ACTUAL RESULT	ACCE.	REJE.	
VISUAL APPEARANCE	ASTM F788-13 ,F835-12	PASSED	32	0	
THREAD	3A ASME B1.1(JNR)	PASSED	8	0	
MAJOR DIA.	18.73-19.05	18.88-18.94	8	0	
HEX. SOCKET WIDTH	12.700-12.827(1/2)	PASSED	8	0	
HEAD DIA.	34.42-36.52	34.81-34.96	8	0	
HEAD HEIGHT					
KEY ENGAGEMENT	5.60 MIN.	6.22-6.35	8	0	
BODY DIA.					
THREAD LENGTH					
TOTAL LENGTH	62.00-63.50	62.32-62.39	8	0	
HEAD MARKING	YFS	YFS	8	0	

MECHANICAL PROPERTIES		SPEC.:ASTM F835-12			
CHARACTERISTICS	TEST METHOD	SPECIFIED	ACTUAL RESULT	ACCE.	REJE.
HARDNESS	ASTM F606-11	37-44 HRC	40-41	4	0
TENSILE STRENGTH	ASTM F606-11	933 MIN.	1296-1307	4	0
DECARB./ CARB.	ASTM F2328-05	CLASS 3	PASSED	1	0

CHEMICAL COMPOSITION % (THE DATA TRANSCRIBE FROM MILL TEST REPORT)

C	Si	Mn	P	S	Cu	Ni	Cr	Mo	Al	B	V
0.360	0.22	0.72	0.012	0.008	0.01	0.01	1.02	0.17	0.059	0.0000	0.00

INSP. RESULT:SAMPLES TESTED CONFORM TO ALL OF THE SPECIFICATION AS ABOVE.

LAB. CHIEF/CERT. SIGNATORY:  (NAN-KU LIN) PAGE: 1 OF 1

REMARKS:
 *DIMENSION-mm, TENSILE-MPa
 *THE REPORT MUST NOT BE REPRODUCED EXCEPT IN FULL AND RELATE ONLY TO THE ITEM TESTED.
 *THE REPORT IS ISSUED ACCORDING TO EN10204 3.1.
 *THE QMS IS APPROVED TO ISO/TS16949, NO:44111066627, VALID TO JUN.29.15
 *TEMPERING TEMPERATURE CONFORM TO THE REQUIREMENT OF ASTM F835.

Figure A-1. Countersunk Bolts, Item d1

Fasteners and Weld Studs



Tru-Fit Products • Tru-Weld

460 Lake Road • Medina, Ohio • 44256 • U.S.A.
Phone: (330) 725-7741 • Fax: (330) 725-0161 • Toll Free: (800) 321-5588

Since 1928

TSA MANUFACTURING INC
14901 CHANDLER ROAD
OMAHA, NE 68138

C.A. 3,000 PCS.
5/8 X 4-3/16 B/W
P/N CA1006711
(Formerly P/N 1111-10-067)

P.O. NO.:36566 SHIPMENT NO.:196304 CERT. DATE: 08/21/2015
----- CERTIFICATION -----

THIS IS TO CERTIFY THAT THIS PRODUCT HAS BEEN MANUFACTURED TO CONFORM TO:
AASHTO, AWS D1.1/D1.5-10, ISO13918, BS EN10204 3.1 SPECIFICATIONS, OF MATERIAL
CONFORMING TO ASTM-A108-13/A29 LOW CARBON STEEL
HAVING THE FOLLOWING CHEMICAL COMPOSITION AND PHYSICAL PROPERTIES:

HEAT NO. 20368220
GRADE C1015
CHEMICAL COMPOSITION
CARBON .170 %
MANGANESE .540 %
PHOSPHOROUS .008 %
SULFUR .001 %
NICKEL .000 %
CHROMIUM .000 %
CEV % .303 %

Lot 17808
Manitoba 5/8" Weld Studs
R#16-0232 H#20368220 L#17808
December 2015 SMT

MECHANICAL PROPERTIES
REFERENCE TW15-225
ULTIMATE 72543 PSI
500 N/mm2
YIELD (0.2% OFFSET) 54593 PSI
376 N/mm2
REDUCTION OF AREA 65.5
ELONGATION 35.9

BEND TEST PASSED
FAILURE LOCATION SHANK

MECHANICAL PROPERTIES ABOVE ARE DERIVED FROM FINISHED PRODUCT.
TFP CORP. CERTIFIES THAT THIS IS A COPY OF THE ORIGINAL MECHANICAL
CERTIFICATION ON FILE, THAT THIS PRODUCT IS MELTED AND MANUFACTURED
IN THE U.S.A., AND IS FREE FROM MERCURY CONTAMINATION.

BY: *Fred Heppner*
Fred Heppner
Q.A. MANAGER
TRU-WELD DIVISION
TFP CORP

Figure A-2. 5/8-in. Diameter, 4-in. Long Stud, Item d3



CA-ML-WHITBY
 HOPKINS STREET SOUTH
 WHITBY, ON L1N 5T1
 Canada

CERTIFIED MATERIAL TEST REPORT

CUSTOMER SHIP TO COWIN STEEL 1137 PACIFIC AVE WINNIPEG, MB R3E 1G7 Canada		CUSTOMER BILL TO COWIN STEEL 1137 PACIFIC AVE WINNIPEG, MB R3E 1G7 Canada		GRADE 400W	SHAPE / SIZE Rebar / 20MM			
SALES ORDER 2231209/000030		CUSTOMER MATERIAL N°		LENGTH 18M 00CM	WEIGHT 52,490 LB	HEAT / BATCH 52069671/02		
CUSTOMER PURCHASE ORDER NUMBER 101615			BILL OF LADING 1302-0000030252	DATE 05/20/2015	SPECIFICATION / DATE or REVISION CSA G30.18-09			
CHEMICAL COMPOSITION								
C %	Mn %	P %	S %	Si %	Cu %	Ni %	Cr %	CEq _{A706} %
0.26	1.05	0.010	0.037	0.19	0.28	0.09	0.10	0.45
MECHANICAL PROPERTIES								
YS MPa		UTS MPa		Elong. %	Bend Test			
446		603		16.90	OK			
446		606		17.50	OK			
COMMENTS / NOTES								

145

The above figures are certified chemical and physical test records as contained in the permanent records of company. We certify that these data are correct and in compliance with specified requirements. This material, including the billets, was melted and manufactured in Canada. CMTR complies with EN 10204 3.1.

Bhaskar Yalamanchili BHASKAR YALAMANCHILI
 QUALITY DIRECTOR

Leonardo Nunes LEONARDO NUNES
 QUALITY ASSURANCE MGR.

Figure A-3. Description of component 20M Rebar, Item b1, b10

SYS

PAGE 1 OF 1



MATERIAL CERTIFICATION
Central Steel & Wire Company

P.O. Box 5100 - Chicago, IL 60680-5100
1-773-471-3800 1-800-621-8510
(FAX 1-773-471-3962)

DATE: 11/20/15

CSW SO: 582019

CUSTOMER PO: 42513

CSW PO: 039247	DESCRIPTION: 1/2" X 48" X 120" HR EX-TEN 50 OR ASTM A 572 GR 50	SPECIFICATION(S): ASTM A572-15 GR 50 ASTM A709-13A GR 50 ASME SA572-10ED(-11A) GR 50
COIL ID: PYN867		
IAC: 19644		
HEAT: T2012	MILL COIL: 5133525	MILL SOURCE: NLMK INDIANA

CHEMICAL ANALYSIS (%)

C	MN	P	S	SI	NI	CR	MO	CU	AL	V	CB	CA	TI	B	N	
.06	.81	.010	.007	.02	.078	.074	.025	.144	.042	.003	.023	.002	.001	.000	.011	

MECHANICAL PROPERTIES

TESTID	LOC	YIELD (2%)	UM	TENSILE	UM	% ELONG	% R of A	DIR	HARDNESS	Bend
PYN867	F	66.3	KSI	75.3	KSI	30.0 (2")		T		
	M	65.3		73.8		27.0				

COMMENTS

This Document certifies that the product represented was sampled in accordance with ASTM A 6 or A 20, tested for mechanical properties at an A2LA accredited laboratory per ASTM A 370 instructions and conforms to the material specification(s) listed. The heat analysis is traceable to the original heat reported and processed. Strand cast product represents a minimum hot rolled reduction ratio of 3:1. This product was not weld repaired, is free of mercury contamination at the time of shipment and complies with environmental requirements of QS9000.

ANY MODIFICATION, CHANGES OR ADDITIONS TO THIS DOCUMENT ARE PROHIBITED AND WILL VOID CENTRAL STEEL AND WIRE'S LIABILITY AND WARRANTY.

Ryan Rathbun

RYAN RATHBUN - MANAGER
METALLURGY & TEST REPORTS

Central Steel & Wire Company

Figure A-4. Steel Cover Plate, Items c2 and c3

SYS

PAGE 1 OF 1



MATERIAL CERTIFICATION
Central Steel & Wire Company

P.O. Box 5100 - Chicago, IL 60680-5100
1-773-471-3800 1-800-621-8510
(FAX 1-773-471-3962)

DATE: 11/20/15

CSW SO: 582019

CUSTOMER PO: 42513

CSW PO: 039254	DESCRIPTION: 1/4" X 48" X 120" HR EX-TEN 50 OR ASTM A 572 GR 50	SPECIFICATION(S): ASTM A572-15 GR 50 ASTM A709-13A GR 50 ASME SA572-10ED(-11A) GR 50
COIL ID: KZY834		
IAC: 17958		
HEAT: T2251	MILL COIL: 5134545	MILL SOURCE: NLMK INDIANA

CHEMICAL ANALYSIS (%)

C	MN	P	S	SI	NI	CR	MO	CU	AL	V	CB	CA	TI	B	N
.06	.65	.008	.007	.01	.056	.061	.016	.126	.031	.003	.021	.002	.001	.000	.006

MECHANICAL PROPERTIES

TESTID	LOC	YIELD (2%)	UM	TENSILE	UM	% ELONG	% R of A	DIR	HARDNESS	Bend
KZY834	F	62.7	KSI	71.3	KSI	31.0 (2")		T		
	M	61.6		70.9		30.0				

COMMENTS

This Document certifies that the product represented was sampled in accordance with ASTM A 6 or A 20, tested for mechanical properties at an A2LA accredited laboratory per ASTM A 370 instructions and conforms to the material specification(s) listed. The heat analysis is traceable to the original heat reported and processed. Strand cast product represents a minimum hot rolled reduction ratio of 3:1. This product was not weld repaired, is free of mercury contamination at the time of shipment and complies with environmental requirements of QS9000.

ANY MODIFICATION, CHANGES OR ADDITIONS TO THIS DOCUMENT ARE PROHIBITED AND WILL VOID CENTRAL STEEL AND WIRE'S LIABILITY AND WARRANTY.

Ryan Rathbun

RYAN RATHBUN - MANAGER
METALLURGY & TEST REPORTS

Central Steel & Wire Company

Figure A-5. Steel End Caps, Items c5, c6, c7, c8, c9

STEEL AND PIPE SUPPLY

SPS Coil Processing Tulsa
5275 Bird Creek Ave.
Port of Catoosa, OK 74015

METALLURGICAL TEST REPORT

PAGE 1 of 1
DATE 11/18/2015
TIME 13:17:34
USER H.ZAVALA

S
O
L
D

66031-1127

S
H
I
P

13716
Kansas City Warehouse
401 New Century Parkway
NEW CENTURY KS

Order	Material No.	Description	Quantity	Weight	Customer Part	Customer PO	Ship Date
40252045-0040	721696120A2	1/2 96 X 120 A572GR50 MILL PLATE	3	4,900.800			11/18/2015

Chemical Analysis

Heat No.	Vendor	DOMESTIC										Melted and Manufactured in the USA			
Batch	SSAB - MONTPELIER WORKS	Mill SSAB - MONTPELIER WORKS										Produced from Coil			
Carbon	Manganese	Phosphorus	Sulphur	Silicon	Nickel	Chromium	Molybdenum	Boron	Copper	Aluminum	Titanium	Vanadium	Columbium	Nitrogen	Tin
0.0500	1.1200	0.0100	0.0050	0.0200	0.1300	0.1100	0.0400	0.0000	0.2900	0.0300	0.0000	0.0530	0.0030	0.0000	0.0000

Mechanical/ Physical Properties

Mill Coil No.	Tensile	Yield	Elong	Rckwl	Grain	Charpy	Charpy Dr	Charpy Sz	Temperature	Olsen
B5J6640625	74300.000	60800.000	34.50			215	Longitudinal	7.5	-20 F	
	77700.000	66200.000	31.50			10	Longitudinal	7.5	-20 F	
						35	Longitudinal	7.5	-20 F	

THE CHEMICAL, PHYSICAL, OR MECHANICAL TESTS REPORTED ABOVE ACCURATELY REFLECT INFORMATION AS CONTAINED IN THE RECORDS OF THE CORPORATION.

148

Figure A-6. Steel Cover Plate, Item c1

STEEL AND PIPE SUPPLY

SPS Coil Processing Tulsa
5275 Bird Creek Ave.
Port of Catoosa, OK 74015

METALLURGICAL TEST REPORT

PAGE 1 of 1
DATE 02/22/2016
TIME 10:39:07
USER WILLIAMR

R#16-428 March 2016 SMT

The Steel Cap was redone after troubles fitting it to the Concrete This is the new "c4" piece

S
O
L
D
T
O

66031-1127

S
H
I
P
T
O

13716
Kansas City Warehouse
401 New Century Parkway
NEW CENTURY KS

Order	Material No.	Description	Quantity	Weight	Customer Part	Customer PO	Ship Date
40256663-0010	70872120TM	1/4 72 X 120 A36 TEMPERPASS STPMLPL	7	4,288.200			02/22/2016

Chemical Analysis

Heat No.	Vendor	DOMESTIC										Milled				Melted and Manufactured in the USA	
A600686	STEEL DYNAMICS COLUMBUS	7 EA 4,288.200 LB										STEEL DYNAMICS COLUMBUS				Produced from Coil	
Carbon	Manganese	Phosphorus	Sulphur	Silicon	Nickel	Chromium	Molybdenum	Boron	Copper	Aluminum	Titanium	Vanadium	Columbium	Nitrogen	Tin		
0.2000	0.8200	0.0150	0.0020	0.0300	0.0200	0.0400	0.0100	0.0001	0.0600	0.0320	0.0010	0.0040	0.0010	0.0067	0.0040		

Mechanical/ Physical Properties

Mill Coil No.	Tensile	Yield	Elong	Rckwl	Grain	Charpy	Charpy Dr	Charpy Sz	Temperature	Olsen
16B582241	76000.000	53200.000	29.50			0	NA			
	74100.000	50400.000	26.20			0	NA			

Chemical Analysis

Heat No.	Vendor	DOMESTIC										Milled				Melted and Manufactured in the USA	
A600686	STEEL DYNAMICS COLUMBUS	16 EA 9,801.600 LB										STEEL DYNAMICS COLUMBUS				Produced from Coil	
Carbon	Manganese	Phosphorus	Sulphur	Silicon	Nickel	Chromium	Molybdenum	Boron	Copper	Aluminum	Titanium	Vanadium	Columbium	Nitrogen	Tin		
0.2000	0.8200	0.0150	0.0020	0.0300	0.0200	0.0400	0.0100	0.0001	0.0600	0.0320	0.0010	0.0040	0.0010	0.0067	0.0040		

Mechanical/ Physical Properties

Mill Coil No.	Tensile	Yield	Elong	Rckwl	Grain	Charpy	Charpy Dr	Charpy Sz	Temperature	Olsen
16B582241	76000.000	53200.000	29.50			0	NA			
	74100.000	50400.000	26.20			0	NA			

THE CHEMICAL, PHYSICAL, OR MECHANICAL TESTS REPORTED ABOVE ACCURATELY REFLECT INFORMATION AS CONTAINED IN THE RECORDS OF THE CORPORATION.
The material is in compliance with EN 10204 Section 4.1 Inspection Certificate Type 3.1

149

September 26, 2016
MWRSEF Report No. TRP-03-356-16

Figure A-7. Steel Cover Plate, Item c4



GERDAU

US-ML-SAYREVILLE
NORTH CROSSMAN ROAD
SAYREVILLE, NJ 08872
USA

CERTIFIED MATERIAL TEST REPORT

CUSTOMER SHIP TO COWIN STEEL 1137 PACIFIC AVE WINNIPEG, MB R3E 1G7 Canada		CUSTOMER BILL TO COWIN STEEL 1137 PACIFIC AVE WINNIPEG, MB R3E 1G7 Canada		GRADE 400W	SHAPE / SIZE Rebar / 15MM
SALES ORDER 2616991/000040		CUSTOMER MATERIAL N°		LENGTH 18M 00CM	WEIGHT 21,309 LB
CUSTOMER PURCHASE ORDER NUMBER 101666		BILL OF LADING 1331-0000038389	DATE 09/25/2015	SPECIFICATION / DATE or REVISION CSA G30.18-09	
				HEAT / BATCH 61105170/06	

CHEMICAL COMPOSITION											
C %	Mn %	P %	S %	Si %	Cu %	Ni %	Cr %	Mo %	Sn %	V %	CEq %
0.27	1.02	0.010	0.031	0.17	0.38	0.18	0.05	0.034	0.021	0.027	0.45

MECHANICAL PROPERTIES							
YS PSI	YS MPa	UTS PSI	UTS MPa	G/L mm	Elong. %		
61935	427	87000	600	200.0	17.00		
62000	427	86710	598	200.0	15.00		

MECHANICAL PROPERTIES	
Bend Test	
OK	
OK	

GEOMETRIC CHARACTERISTICS			
%Light	Def Hgt Inch	Def Gap Inch	Def Space Inch
5.20	0.033	0.139	0.417
5.50	0.033	0.139	0.417

COMMENTS / NOTES

The above figures are certified chemical and physical test records as contained in the permanent records of company. We certify that these data are correct and in compliance with specified requirements. This material, including the billets, was melted and manufactured in the USA. CMTR complies with EN 10204 3.1.

Bhaskar BHASKAR YALAMANCHILI
QUALITY DIRECTOR

Joseph Homic JOSEPH HOMIC
QUALITY ASSURANCE MGR.

150

Figure A-8. 15M Rebar, Items b3, b7, b9



US-ML-SAYREVILLE
 NORTH CROSSMAN ROAD
 SAYREVILLE, NJ 08872
 USA

CERTIFIED MATERIAL TEST REPORT

CUSTOMER SHIP TO COWIN STEEL 1137 PACIFIC AVE WINNIPEG, MB R3E 1G7 Canada		CUSTOMER BILL TO COWIN STEEL 1137 PACIFIC AVE WINNIPEG, MB R3E 1G7 Canada		GRADE 400W	SHAPE / SIZE Rebar / 15MM
SALES ORDER 1185692/000010		CUSTOMER MATERIAL N°		LENGTH 06M 00CM	WEIGHT 96,709 LB
CUSTOMER PURCHASE ORDER NUMBER 101512		BILL OF LADING 1331-0000023526		DATE 09/04/2014	
SPECIFICATION / DATE or REVISION 1-CSA G30.18-09					
HEAT / BATCH 61099893/02					

C	Mn	P	S	Si	Cu	Ni	Cr	Mo	Sn	V	CE _{eq} A706
%	%	%	%	%	%	%	%	%	%	%	%
0.26	1.02	0.018	0.031	0.21	0.31	0.18	0.12	0.055	0.017	0.026	0.46

MECHANICAL PROPERTIES		YS	UTS	UTS	G/L	Elong.
PSI	MPa	PSI	MPa	mm	%	
66097	456	90097	621	200.0	15.00	
66774	460	91387	630	200.0	16.00	

MECHANICAL PROPERTIES	
Bend Test	
OK	
OK	

GEOMETRIC CHARACTERISTICS			
%Light	Def Hgt	Def Gap	Def Space
%	Inch	Inch	Inch
5.20	0.034	0.098	0.414
5.50	0.034	0.098	0.414

COMMENTS / NOTES
 R#16-0190 October 2015 SMT
 Manitoba Metric Rebar

The above figures are certified chemical and physical test records as contained in the permanent records of company. We certify that these data are correct and in compliance with specified requirements. This material, including the billets, was melted and manufactured in the USA. CMTR complies with EN 10204 3.1.

Bhaskar

BHASKAR YALAMANCHILI
 QUALITY DIRECTOR

Joseph T Homic

JOSEPH T HOMIC
 QUALITY ASSURANCE MGR.

151

Figure A-9. 15M Rebar, Items b2, b4, b5



GERDAU

US-ML-MIDLOTHIAN
300 WARD ROAD
MIDLOTHIAN, TX 76065
USA

CERTIFIED MATERIAL TEST REPORT

PD# 112922

Page 1/1

CUSTOMER SHIP TO REGAL METALS INTERNATIONAL INC 207 SENTRY DR MANSFIELD, TX 76063-3609 USA		CUSTOMER BILL TO REGAL METALS INTERNATIONAL INC 207 SENTRY DR MANSFIELD, TX 76063-3609 USA		GRADE 60 (420)	SHAPE / SIZE Rebar / #4 (13MM)		
SALES ORDER 2199645/000010		CUSTOMER MATERIAL N°		LENGTH 20'00"	WEIGHT 48,136 LB	HEAT / BATCH 58021938/02	
CUSTOMER PURCHASE ORDER NUMBER 347749		BILL OF LADING 1327-0000157942		DATE 06/02/2015		SPECIFICATION / DATE or REVISION ASTM A615/A615M-14	

C	Mn	P	S	Si	Cu	Ni	Cr	Mo	Sp	V	Nb	Al
%	%	%	%	%	%	%	%	%	%	%	%	%
0.42	0.86	0.010	0.032	0.23	0.29	0.15	0.18	0.054	0.007	0.018	0.000	0.002

CHEMICAL COMPOSITION CE _{eq} A706 %	0.60
----------------------------------------------------	------

MECHANICAL PROPERTIES YS PSI	YS MPa	UTS PSI	UTS MPa	G/L inch	G/L mm
73096	504	107760	743	8.000	200.0

MECHANICAL PROPERTIES Elong. %	Bend Test
15.20	OK

COMMENTS / NOTES

The above figures are certified chemical and physical test records as contained in the permanent records of company. We certify that these data are correct and in compliance with specified requirements. This material, including the billets, was melted and manufactured in the USA. CMTR complies with EN 10204 3.1.

Bhaskar

BHASKAR YALAMANCHILI
QUALITY DIRECTOR

Tom Harrington

TOM HARRINGTON
QUALITY ASSURANCE MGR.

152

Figure A-10. Grade Beam #4 Rebar, Item b6



US-ML-KNOXVILLE
1919 TENNESSEE AVENUE N. W.
KNOXVILLE, TN 37921
USA

CERTIFIED MATERIAL TEST REPORT

CUSTOMER SHIP TO NEBCO INC STEEL DIVISION HAVELOCK, NE 68529 USA		CUSTOMER BILL TO CONCRETE INDUSTRIES INC LINCOLN, NE 68529-0529 USA		GRADE 60 (420) TMX	SHAPE / SIZE Rebar / #5 (16MM)	
SALES ORDER 2568179/000010		CUSTOMER MATERIAL N°		LENGTH 60'00"	WEIGHT 119,904 LB	HEAT / BATCH 55040423/02
CUSTOMER PURCHASE ORDER NUMBER 114168			BILL OF LADING 1326-0000037900	DATE 08/01/2015		
SPECIFICATION / DATE or REVISION ASTM A615/A615M-14						

CHEMICAL COMPOSITION											
C %	Mn %	P %	S %	Si %	Cu %	Ni %	Cr %	Mo %	Sn %	V %	CEq ^A 706 %
0.30	0.60	0.010	0.020	0.19	0.30	0.10	0.07	0.033	0.011	0.000	0.45

MECHANICAL PROPERTIES						
YS PSI	YS MPa	UTS PSI	UTS MPa	G/L inch	G/L mm	
84200	581	100180	691	8.000	200.0	

MECHANICAL PROPERTIES	
Elong. %	Bend Test
15.00	OK

GEOMETRIC CHARACTERISTICS			
%Light	Def Rgt Inch	Def Gap Inch	Def Space Inch
4.22	0.044	0.138	0.400

COMMENTS / NOTES

The above figures are certified chemical and physical test records as contained in the permanent records of company. We certify that these data are correct and in compliance with specified requirements. This material, including the billets, was melted and manufactured in the USA. CMTR complies with EN 10204 3.1.

Bhaskar
BHASKAR YALAMANCHILI
QUALITY DIRECTOR

Lisa K Churnetski
LISA CHURNETSKI
QUALITY ASSURANCE MGR.

153

Figure A-11. Grade Beam #5 Rebar, Items b8, b12, b13



US-ML-MIDLOTHIAN
300 WARD ROAD
MIDLOTHIAN, TX 76065
USA

CERTIFIED MATERIAL TEST REPORT

Page 1/1

CUSTOMER SHIP TO NEBCO INC STEEL DIVISION HAVELOCK,NE 68529 USA		CUSTOMER BILL TO CONCRETE INDUSTRIES INC LINCOLN,NE 68529-0529 USA		GRADE 60 (420)	SHAPE / SIZE Rebar / #6 (19MM)							
SALES ORDER 2289519/000010		CUSTOMER MATERIAL N°		LENGTH 60'00"	WEIGHT 183,128 LB	HEAT / BATCH 58022155/03						
SPECIFICATION / DATE or REVISION ASTM A615/A615M-14				CUSTOMER PURCHASE ORDER NUMBER 112909		BILL OF LADING 1327-0000158009	DATE 06/03/2015					
CHEMICAL COMPOSITION												
C %	Mn %	P %	S %	Si %	Cu %	Ni %	Cr %	Mo %	Sn %	V %	Nb %	Al %
0.45	0.85	0.020	0.043	0.23	0.33	0.10	0.19	0.022	0.007	0.025	0.000	0.003
CHEMICAL COMPOSITION CEq _{max} A706 %												
0.61												
MECHANICAL PROPERTIES												
YS PSI		YS MPa		UTS PSI		UTS MPa		G/L Inch		G/L mm		
76273		526		109561		755		8.000		200.0		
MECHANICAL PROPERTIES												
Elong. %		Bend Test										
13.40		OK										
COMMENTS / NOTES												

The above figures are certified chemical and physical test records as contained in the permanent records of company. We certify that these data are correct and in compliance with specified requirements. This material, including the billets, was melted and manufactured in the USA. CMTR complies with EN 10204 3.1.

Bhaskar
BHASKAR YALAMANCHILI
QUALITY DIRECTOR

Tom Harrington
TOM HARRINGTON
QUALITY ASSURANCE MGR.

154

Figure A-12. Grade Beam #6 Rebar, Item b11

Appendix B. Vehicle Center of Gravity Determination

Test: MAN-1

Date 4/13/2016

Vehicle: International 9200

Vehicle CG Determination

VEHICLE	Equipment	Weight (lb)	Vert CG (in.)	Vert M (lb-in.)	
	Unbalasted Vehicle (Curb)	29720	NA	NA	
+	Guidance Hub	46	18.875	868.25	
+	Tow Pin Plate	10	12.5	125	
+	Pnumatic Tank (Nitrogen)	27	53.5	1444.5	
+	Strobe/Brake Battery	5	51	255	
+	Brake receivers/wires	7.5	107.25	804.375	
+	Brake Actuator Frame	7	58.5	409.5	
+	Cab DAS & Mounting Plate	7	49.375	345.625	
+	DTS Unit	17	52.5	892.5	
+	Front Trailer DAS & Mount	42	55	2310	
+	Rear Trailer DAS & Mount	38	32.75	1244.5	
	Rear Truck DAS & Mount	5	38	190	
-	Interior	-39	65	-2535	
-	Washer fluid	-17	55	-935	
-	Fuel	-162	24	-3888	
+	Pnumatic Tank 2 (Nitrogen)	28	58.25	1631	
+	Brake Actuator Frame 2	7	56	392	
+	2nd Strobe/ Brake Battery	5	51	255	
BALLAST	+	From Ballast page	48740	71.42557	3481282.5
		Ballast Hardware	912	48.625	44346
		Straps and Foam	715	71.42557	51069.28575

Note: (+) is added equipment to vehicle, (-) is removed equipment from vehicle

Ballast Weight (lb): 50367 3576697.786
 Ballast Vertical C.G. Location: 71.01272
 Estimated Total Weight (lb): 80120.5

Center of Gravity	36000V MASH Targets	Test Inertial	Difference
Test Inertial Weight (lb.)	79,300 ± 1100	80076	776.0
Longitudinal CG (in.)	NA	379.2724	
Lateral CG (in.)	NA	0.555195	
Ballast Vertical CG (in.)	73 ± 2	71.01	-1.98728

Note: Long. CG is measured from front axle of the test vehicle

Note: Lateral CG measured from centerline - positive to vehicle right (passenger) side

	Curb Weight (lbs.)			Test Inertial Weight (lbs.)		
	Left	Right	Total Axle	Left	Right	Total Axle
Tractor Front Axle	4588	4642	9230	4916	4858	9774
Tractor Tandem Front	2742	2886	5628	8264	8808	17072
Tractor Tandem Rear	2778	2898	5676	7806	9188	16994
Trailer Front Axle	2022	2444	4466	9024	8988	18012
Trailer Rear Axle	2448	2272	4720	9450	8774	18224
	Total Curb Weight		29720	Total Test Inertial Weight		80076

Figure B-1. Vehicle Mass Distribution, Test No. MAN-1

Test: 0 Date 1/0/1900 Vehicle: 0 0

Vehicle CG Determination

VEHICLE	Equipment	Long CG (in.)	Lat CG (in.)	Long M (lb-in.)	Lat M (lb-in.)
	Unbalasted Vehicle (Curb)	274.2946	0.729828	8152037	21690.5
+	Guidance Hub	0	-50	0	-2300
+	Tow Pin Plate	0	0	0	0
+	Pnumatic Tank (Nitrogen)	47	12	1269	324
+	Strobe/Brake Battery	40	12	200	60
+	Brake receivers/wires	73	0	547.5	0
+	Brake Actuator Frame	30	-18	210	-126
+	Cab DAS & Mounting Plate	53	0	371	0
+	DTS Unit	52	-7.5	884	-127.5
+	Front Trailer DAS & Mount	152.75	0	6415.5	0
-	Rear Trailer DAS & Mount	690	0	26220	0
-	Rear Truck DAS & Mount	118	0	590	0
-	Interior	45	13.5	-1755	-526.5
-	Washer fluid	11	34	-187	-578
-	Fuel	58	34	-9396	-5508
-	Pnumatic Tank 2 (Nitrogen)	47	19	1316	532
-	Brake Actuator Frame 2	30	22	210	154
-	2nd Strobe/ Brake Battery	71	12	355	60
BALLAST	From Ballast page	458.519	0.049341	22348217	2404.875
	Ballast Hardware	458.519	0.049341	418169.3	44.99889208
	Straps and Foam	458.519	0.049341	327841.1	35.27873666

Note: (+) is added equipment to vehicle, (-) is removed equipment from vehicle

	31273514	16139.65263
Ballast Horizontal C.G. Location	458.519	0.04934089
Estimated Horizontal C.G. Location:	390.331	0.201442235

Vehicle Weights			
	Gross Static Weight (lbs.)		
	Left	Right	Total Axle
Tractor Front	4916	4858	9774
Tandam Front	8264	8808	17072
Tandem Rear	7806	9188	16994
Trailer Front	9024	8988	18012
Trailer Rear	9450	8774	18224
Total Gross Static Weight			80076

Calibrated Scales Used		
Manufacturer	Serial #	Capacity
Intercomp	25702540	10000 lbs.
Intercomp	25702541	10000 lbs.
Intercomp	25702546	10000 lbs.
Intercomp	25702547	10000 lbs.
Intercomp	25702548	10000 lbs.
Intercomp	25702549	10000 lbs.
Pennsylvania	95-228908	5000 lbs.
Pennsylvania	95-228909	5000 lbs.

Figure B-2. Vehicle Mass Distribution, Test No. MAN-1

Appendix C. Vehicle Deformation Records

VEHICLE PRE/POST CRUSH
FLOORPAN - SET 1

TEST: MAN-1
VEHICLE: International 9200

POINT	X (in.)	Y (in.)	Z (in.)	X' (in.)	Y' (in.)	Z' (in.)	ΔX (in.)	ΔY (in.)	ΔZ (in.)
1	17.935	4.740	4.441	17.589	5.675	4.323	-0.346	0.935	-0.118
2	18.167	10.801	4.123	17.514	11.566	3.238	-0.654	0.764	-0.885
3	18.271	15.654	3.770	17.384	16.326	2.339	-0.887	0.672	-1.430
4	18.356	20.503	3.449	17.218	21.103	1.395	-1.137	0.600	-2.054
5	15.584	4.718	1.045	15.398	5.190	0.815	-0.186	0.472	-0.230
6	15.933	10.506	0.647	15.478	10.743	-0.219	-0.456	0.237	-0.865
7	16.120	15.123	0.302	15.400	15.324	-1.076	-0.720	0.201	-1.378
8	16.056	19.559	-0.061	15.011	19.644	-1.867	-1.045	0.085	-1.805
9	13.165	4.855	0.939	12.978	5.063	0.746	-0.187	0.208	-0.193
10	13.501	10.318	0.338	13.033	10.387	-0.413	-0.468	0.069	-0.750
11	13.656	14.812	0.143	12.935	14.895	-1.120	-0.721	0.083	-1.262
12	13.707	19.271	-0.081	12.734	19.196	-1.667	-0.973	-0.075	-1.587
13	10.269	4.986	0.770	10.047	5.042	0.750	-0.222	0.056	-0.020
14	10.585	10.185	0.364	10.197	10.264	-0.175	-0.387	0.079	-0.538
15	10.815	14.606	0.184	10.192	14.525	-0.931	-0.623	-0.081	-1.115
16	10.871	19.350	-0.097	9.867	19.299	-1.482	-1.004	-0.051	-1.385
17	7.381	5.159	0.733	7.294	5.022	0.785	-0.087	-0.137	0.052
18	8.043	10.184	0.309	N/A	N/A	N/A	N/A	N/A	N/A
19	8.469	14.455	0.200	7.896	14.303	-0.715	-0.573	-0.152	-0.915
20	8.504	19.050	-0.125	7.629	18.714	-1.300	-0.875	-0.336	-1.175
21	4.221	5.263	0.505	4.055	5.062	0.458	-0.167	-0.201	-0.047
22	4.709	10.210	0.276	4.361	9.912	0.335	-0.347	-0.298	0.059
23	5.034	14.427	0.179	4.393	14.082	-0.402	-0.641	-0.345	-0.581
24	5.259	18.837	-0.132	4.396	18.451	-1.085	-0.863	-0.386	-0.953
25	0.408	5.119	0.778	0.280	4.556	0.621	-0.129	-0.563	-0.157
26	0.291	9.730	0.202	N/A	N/A	N/A	N/A	N/A	N/A
27	0.370	15.476	-0.066	-0.318	14.953	-0.286	-0.688	-0.522	-0.220
28	0.645	19.313	-0.240	-0.317	18.765	-0.752	-0.962	-0.548	-0.512

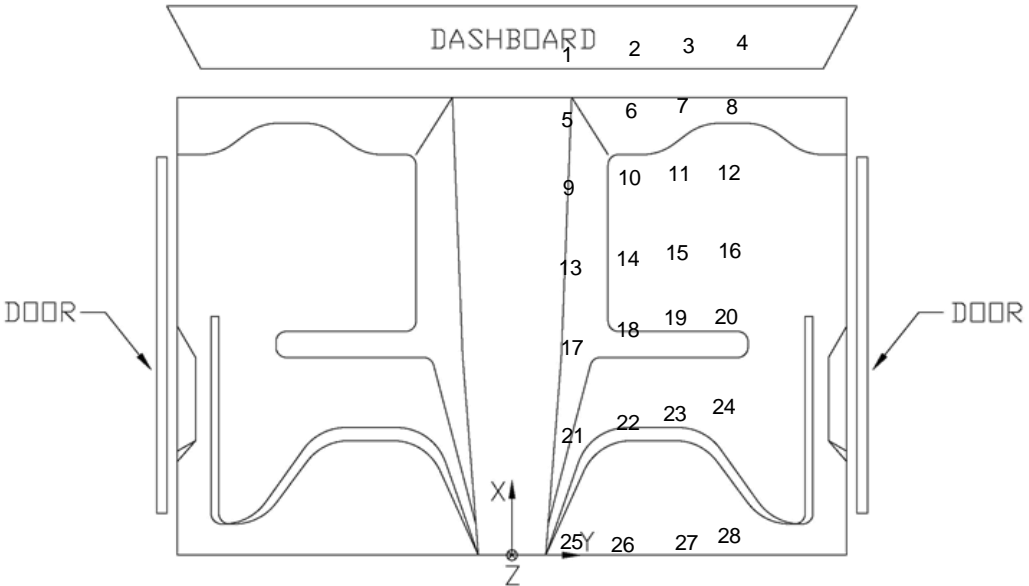


Figure C-1. Floor Pan Deformation Data – Set 1, Test No. MAN-1

VEHICLE PRE/POST CRUSH
FLOORPAN - SET 2

TEST: MAN-1
VEHICLE: International 9200

POINT	X (in.)	Y (in.)	Z (in.)	X' (in.)	Y' (in.)	Z' (in.)	ΔX (in.)	ΔY (in.)	ΔZ (in.)
1	36.226	9.175	4.296	35.236	8.506	3.938	-0.990	-0.669	-0.359
2	36.436	15.159	4.329	35.356	14.474	3.500	-1.080	-0.686	-0.829
3	36.518	20.040	4.269	35.392	19.365	3.135	-1.126	-0.676	-1.133
4	36.598	25.012	4.274	35.377	24.207	2.697	-1.221	-0.805	-1.577
5	33.753	9.348	0.943	33.023	8.372	0.459	-0.730	-0.976	-0.485
6	34.135	15.131	0.864	33.227	14.213	0.007	-0.908	-0.918	-0.857
7	34.307	19.733	0.820	33.335	18.762	-0.366	-0.972	-0.971	-1.186
8	34.277	24.150	0.748	33.220	23.139	-0.710	-1.057	-1.010	-1.458
9	31.357	9.463	0.850	30.556	8.474	0.452	-0.801	-0.989	-0.398
10	31.704	14.983	0.605	30.850	13.932	-0.152	-0.855	-1.052	-0.757
11	31.859	19.476	0.709	30.828	18.465	-0.401	-1.031	-1.011	-1.109
12	31.803	23.877	0.783	30.707	22.870	-0.499	-1.096	-1.006	-1.282
13	28.417	9.621	0.746	27.588	8.573	0.488	-0.829	-1.047	-0.259
14	28.828	14.842	0.696	27.903	13.756	0.108	-0.925	-1.086	-0.588
15	28.962	19.228	0.820	28.099	18.152	-0.176	-0.863	-1.075	-0.996
16	28.996	23.975	0.830	28.036	22.847	-0.287	-0.960	-1.128	-1.116
17	25.675	9.722	0.805	24.902	8.587	0.568	-0.773	-1.135	-0.237
18	26.291	14.727	0.700	N/A	N/A	N/A	N/A	N/A	N/A
19	26.633	19.049	0.865	25.771	18.005	0.032	-0.862	-1.044	-0.832
20	26.742	23.662	0.832	25.621	22.457	-0.138	-1.122	-1.205	-0.970
21	22.358	9.882	0.667	21.690	8.705	0.290	-0.668	-1.177	-0.376
22	22.939	14.870	0.744	22.160	13.663	0.645	-0.779	-1.207	-0.099
23	23.246	19.016	0.902	22.315	17.876	0.344	-0.931	-1.140	-0.558
24	23.472	23.480	0.855	22.460	22.311	0.137	-1.013	-1.169	-0.717
25	18.566	9.728	1.038	17.814	8.332	0.590	-0.751	-1.396	-0.448
26	18.979	13.661	0.746	N/A	N/A	N/A	N/A	N/A	N/A
27	18.594	20.068	0.823	17.582	18.884	0.568	-1.011	-1.184	-0.255
28	18.473	24.389	0.880	17.716	22.622	0.518	-0.757	-1.767	-0.362

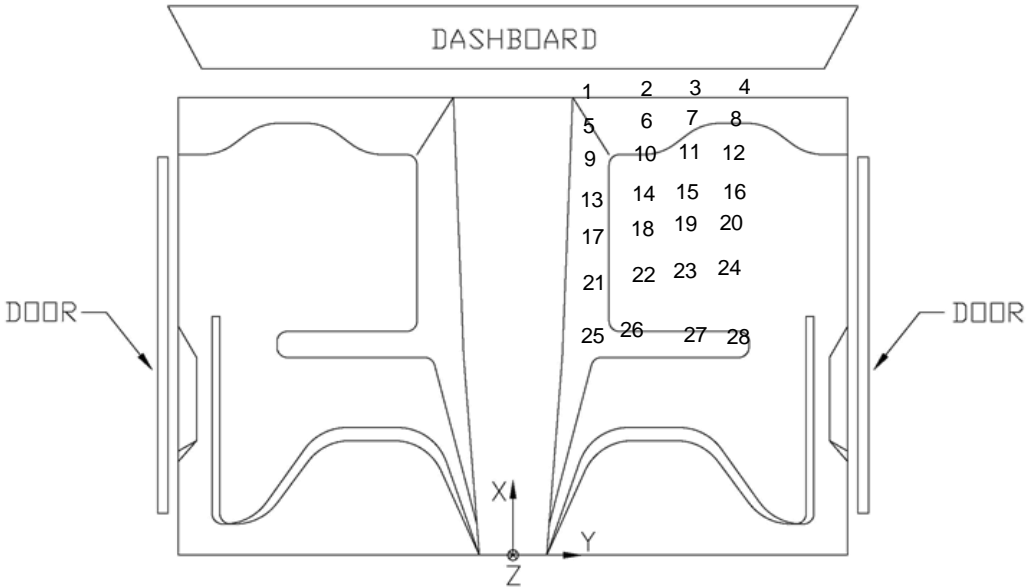


Figure C-2. Floor Pan Deformation Data – Set 2, Test No. MAN-1

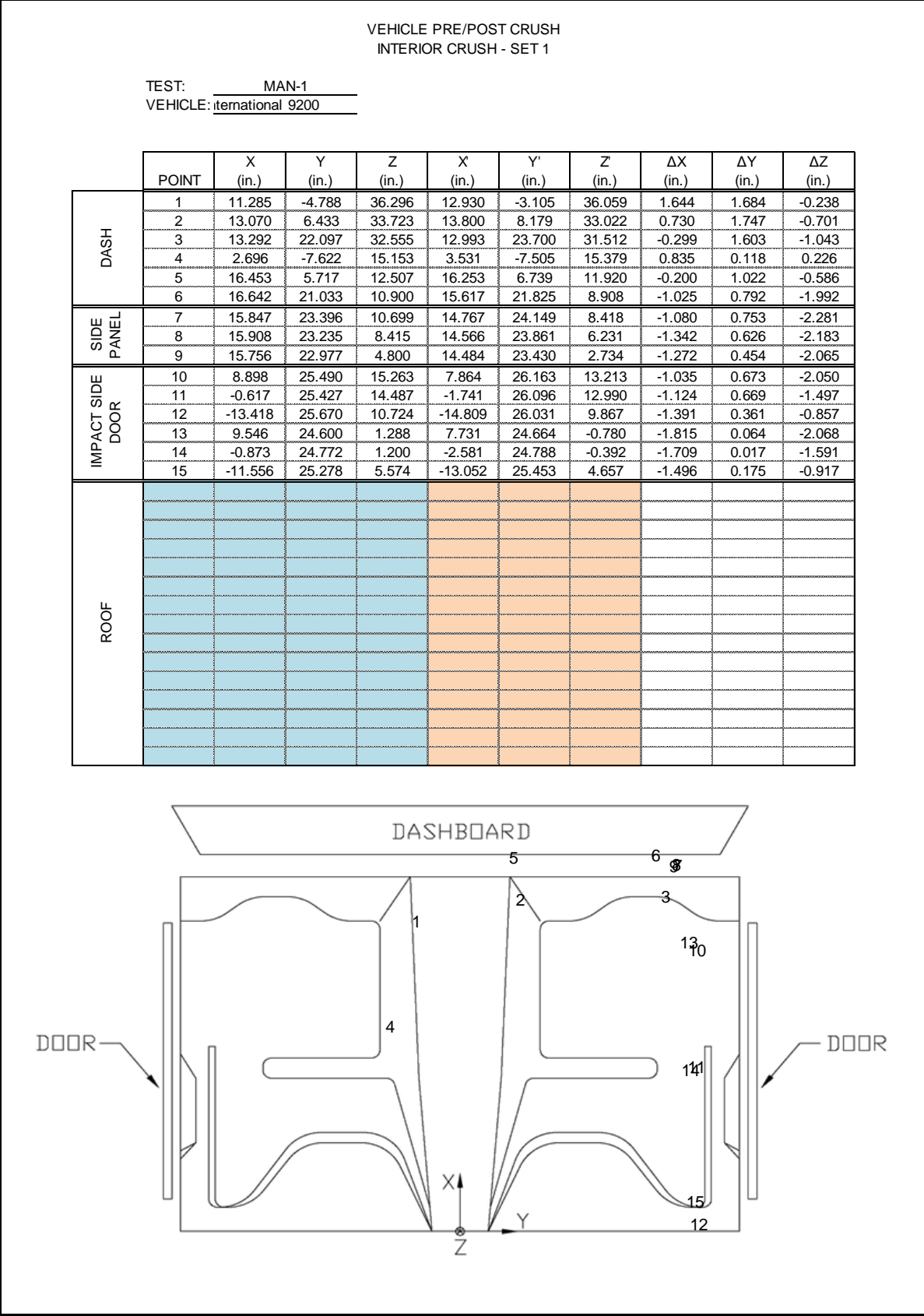


Figure C-3. Occupant Compartment Deformation Data – Set 1, Test No. MAN-1

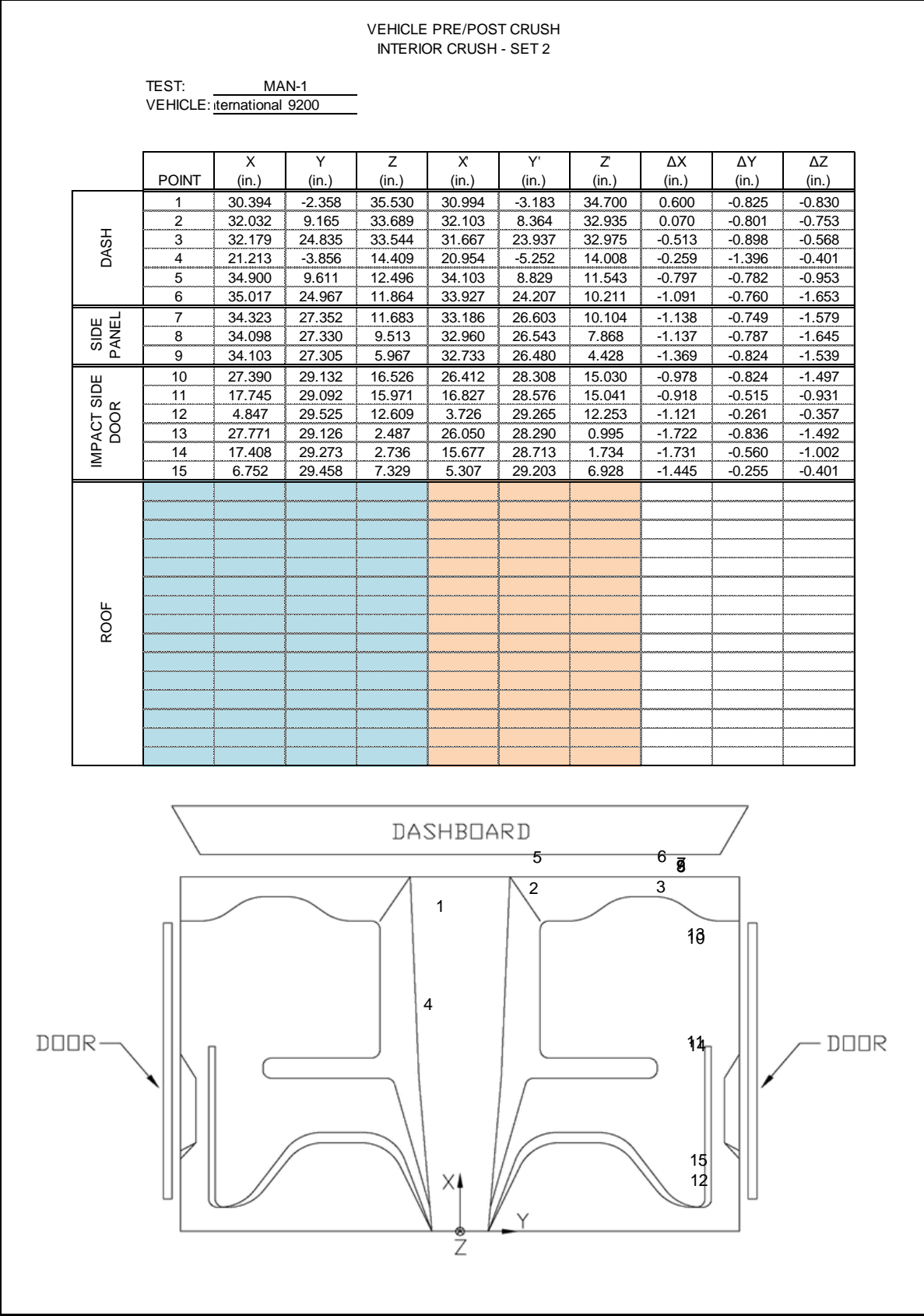


Figure C-4. Occupant Compartment Deformation Data – Set 2, Test No. MAN-1

Appendix D. Accelerometer and Rate Transducer Data Plots, Test No. MAN-1

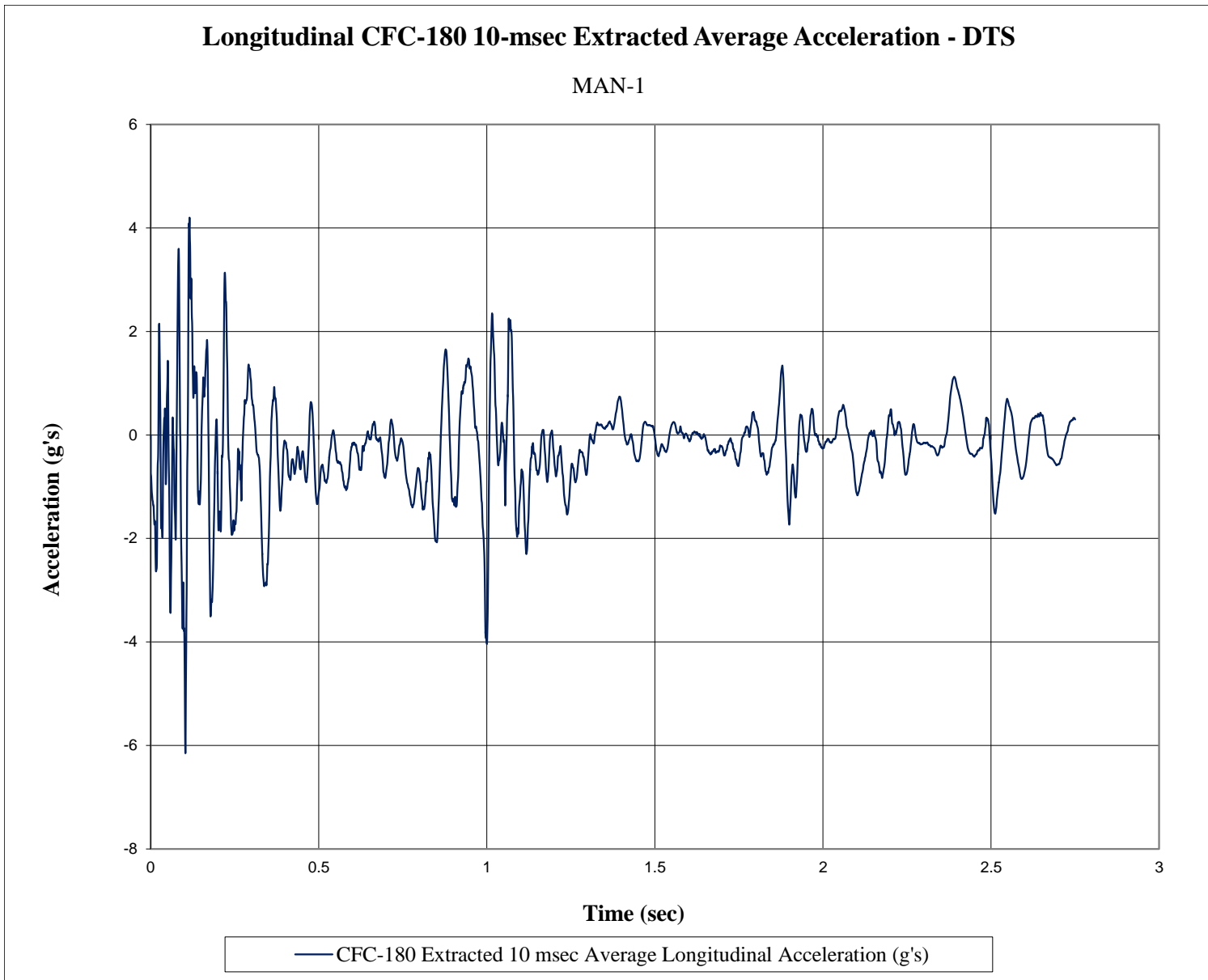


Figure D-1. 10-ms Average Longitudinal Deceleration (DTS - Cab), Test No. MAN-1

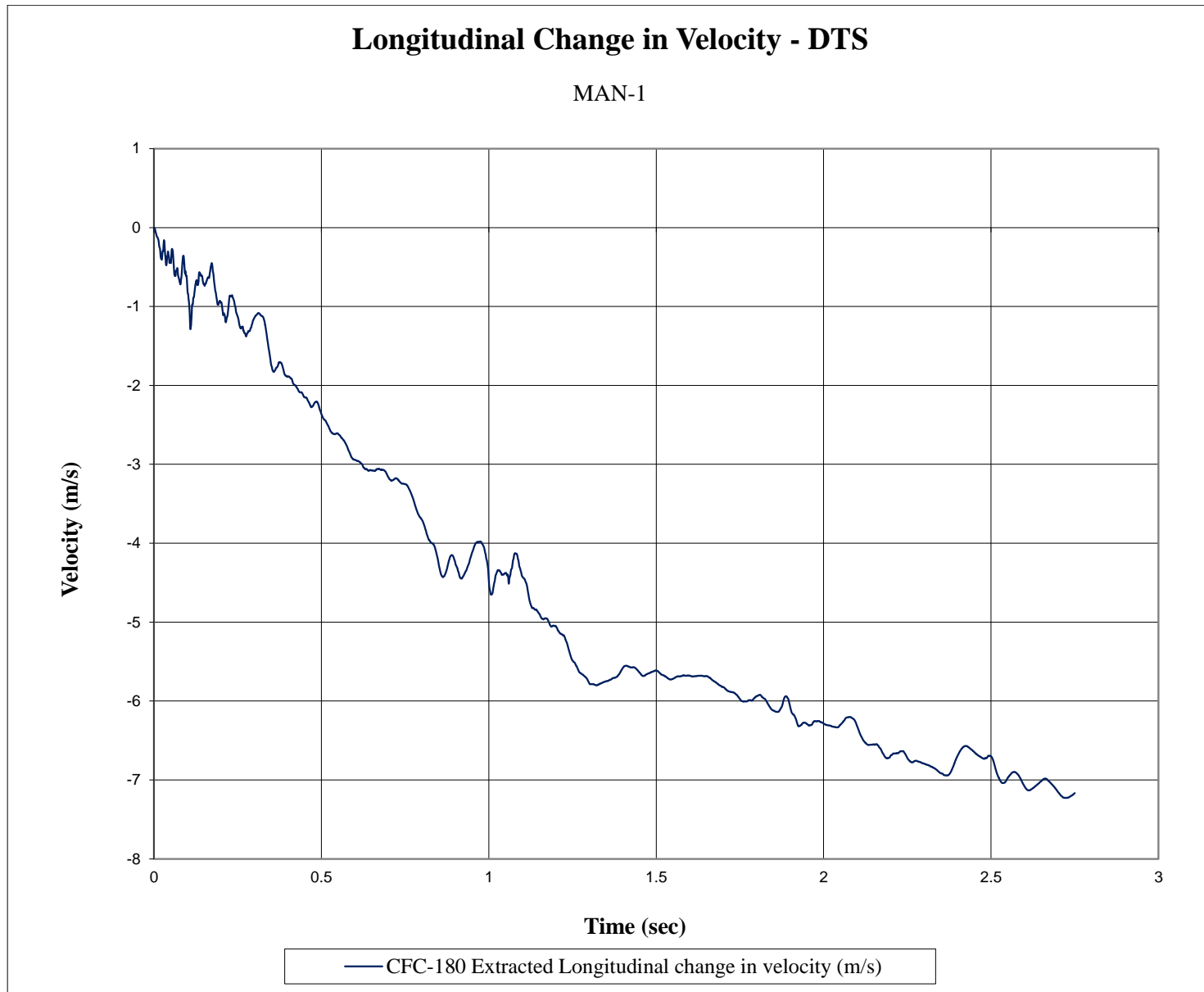


Figure D-2. Longitudinal Change in Velocity (DTS - Cab), Test No. MAN-1

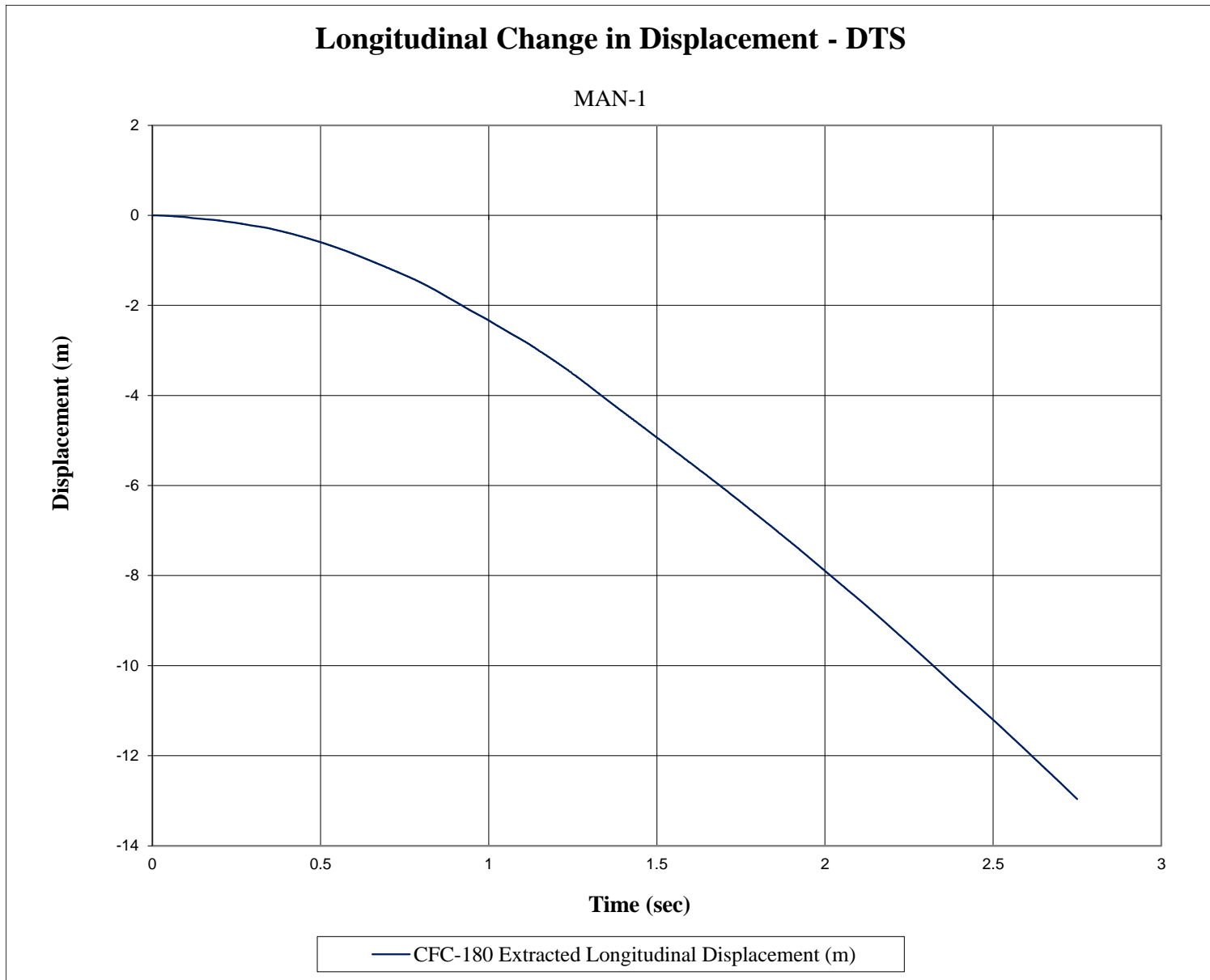


Figure D-3. Longitudinal Occupant Displacement (DTS - Cab), Test No. MAN-1

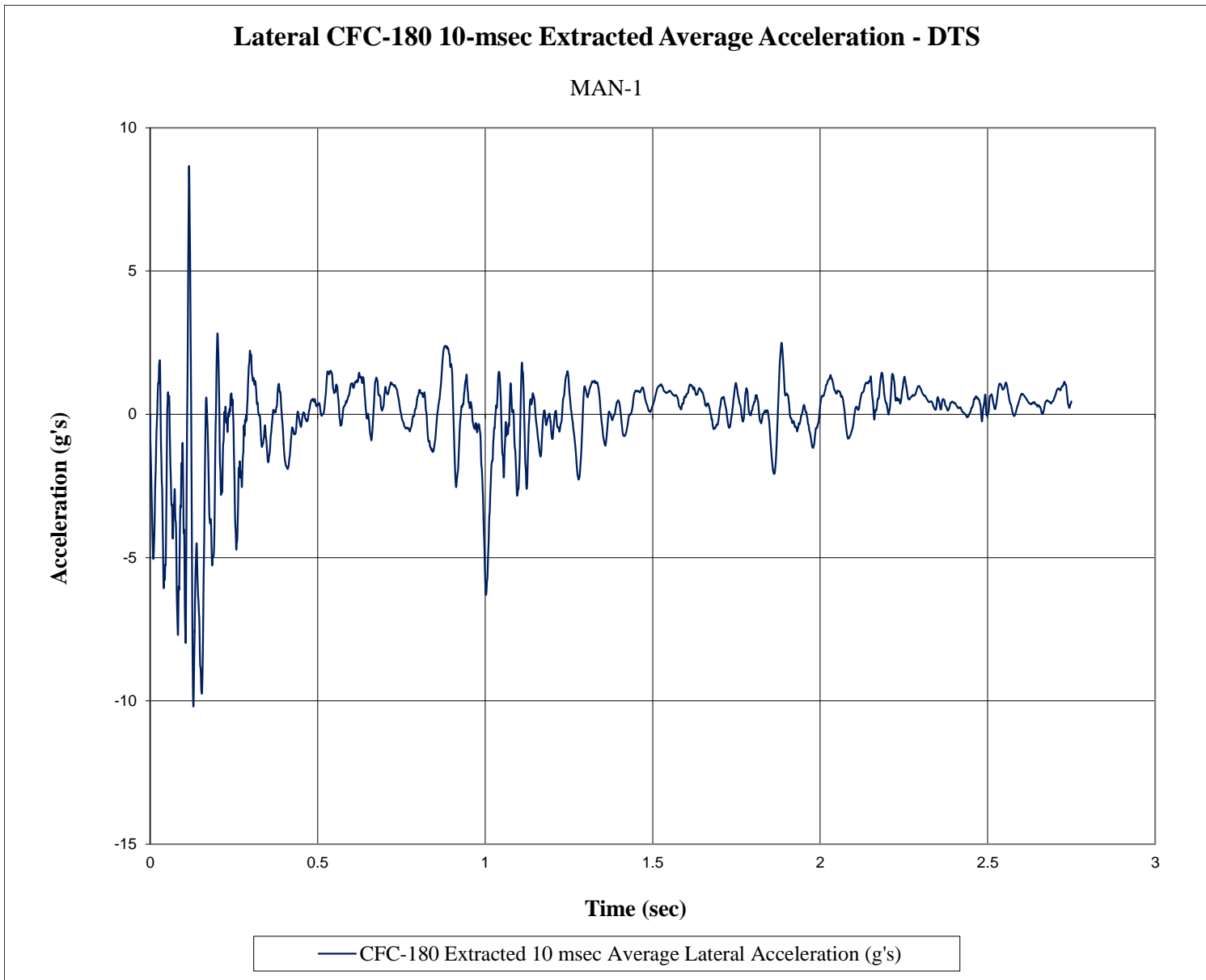


Figure D-4. 10-ms Average Lateral Deceleration (DTS - Cab), Test No. MAN-1

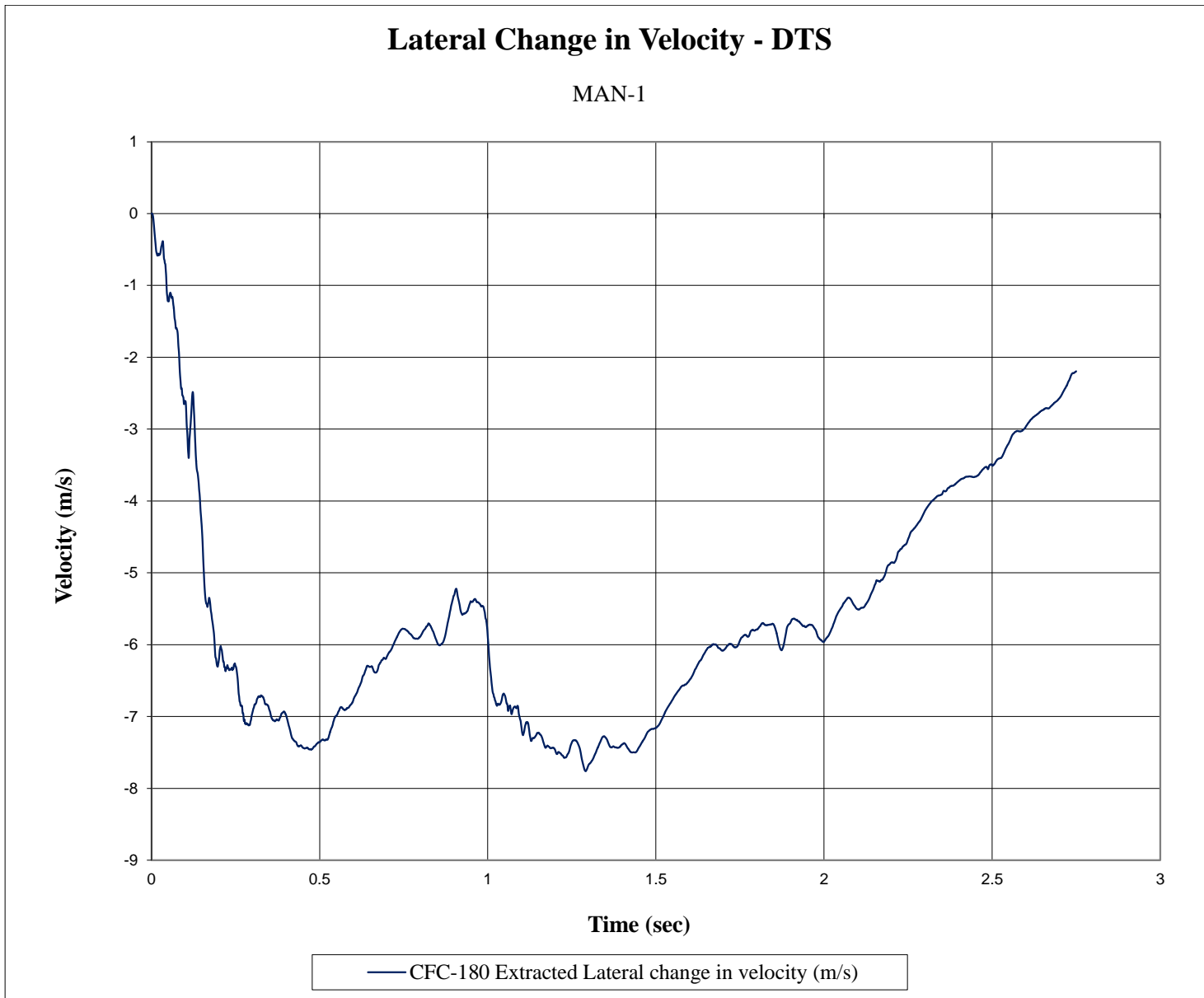


Figure D-5. Lateral Change in Velocity (DTS - Cab), Test No. MAN-1

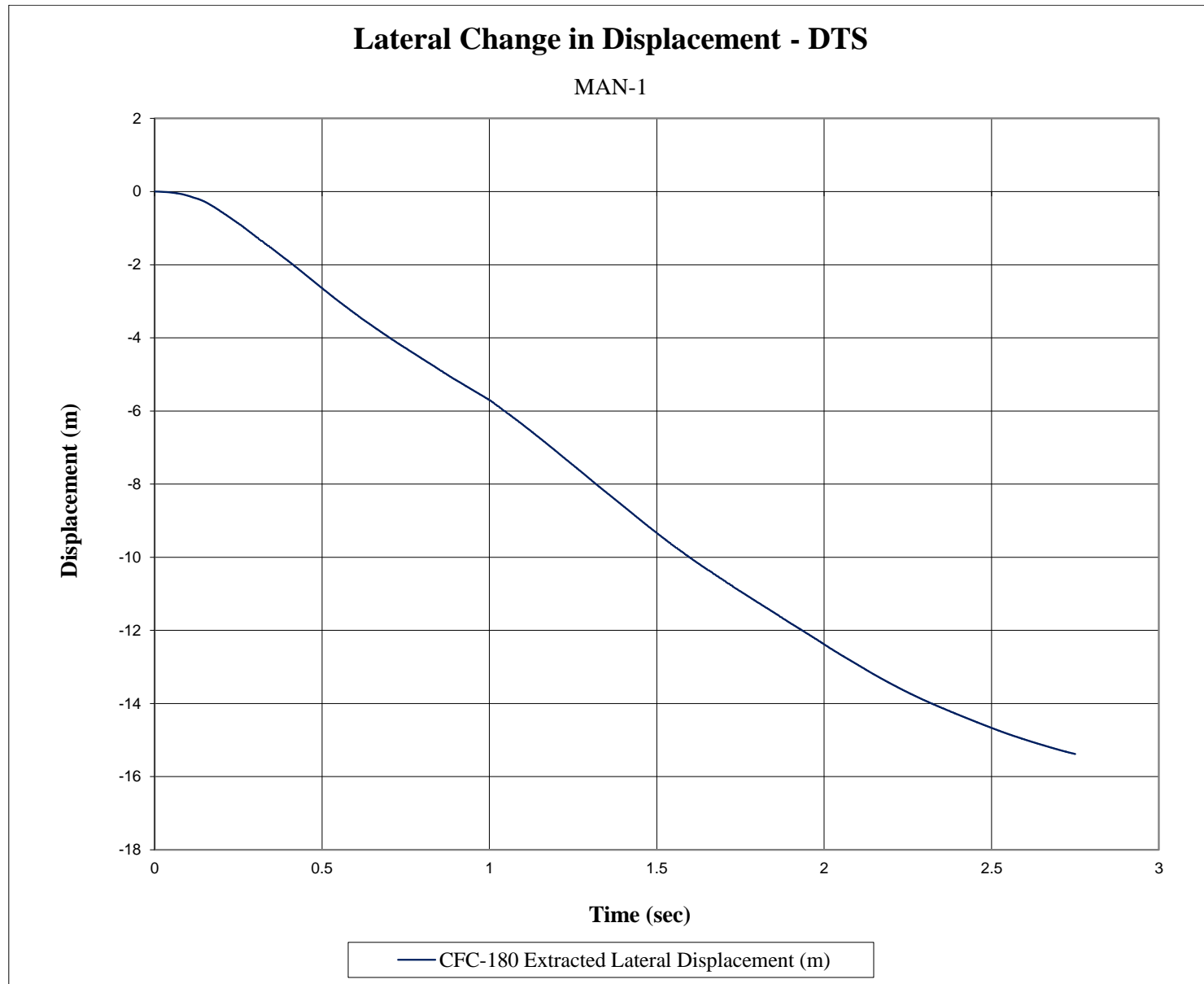


Figure D-6. Lateral Occupant Displacement (DTS - Cab), Test No. MAN-1

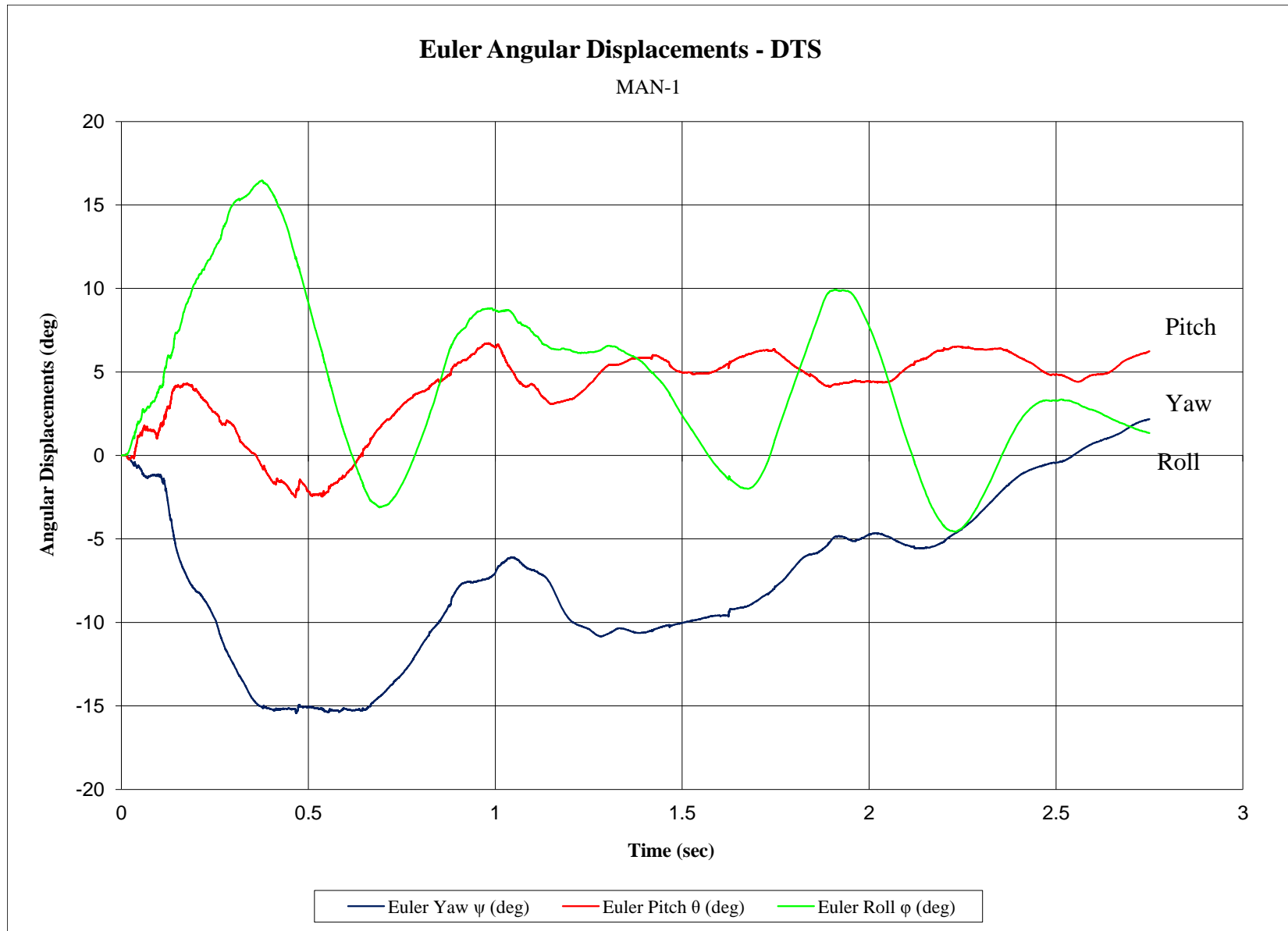


Figure D-7. Vehicle Angular Displacements (DTS - Cab), Test No. MAN-1

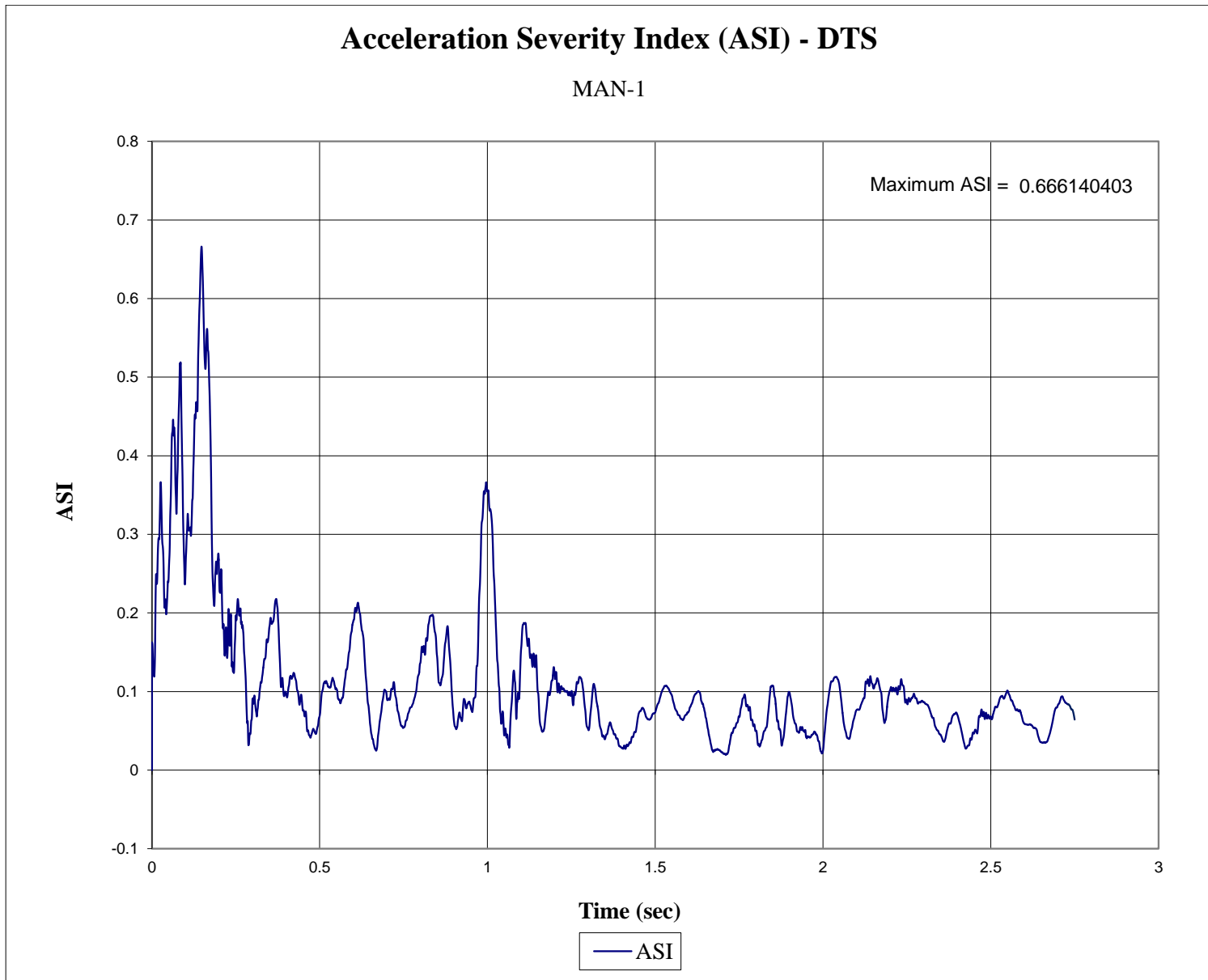


Figure D-8. Acceleration Severity Index (DTS - Cab), Test No. MAN-1

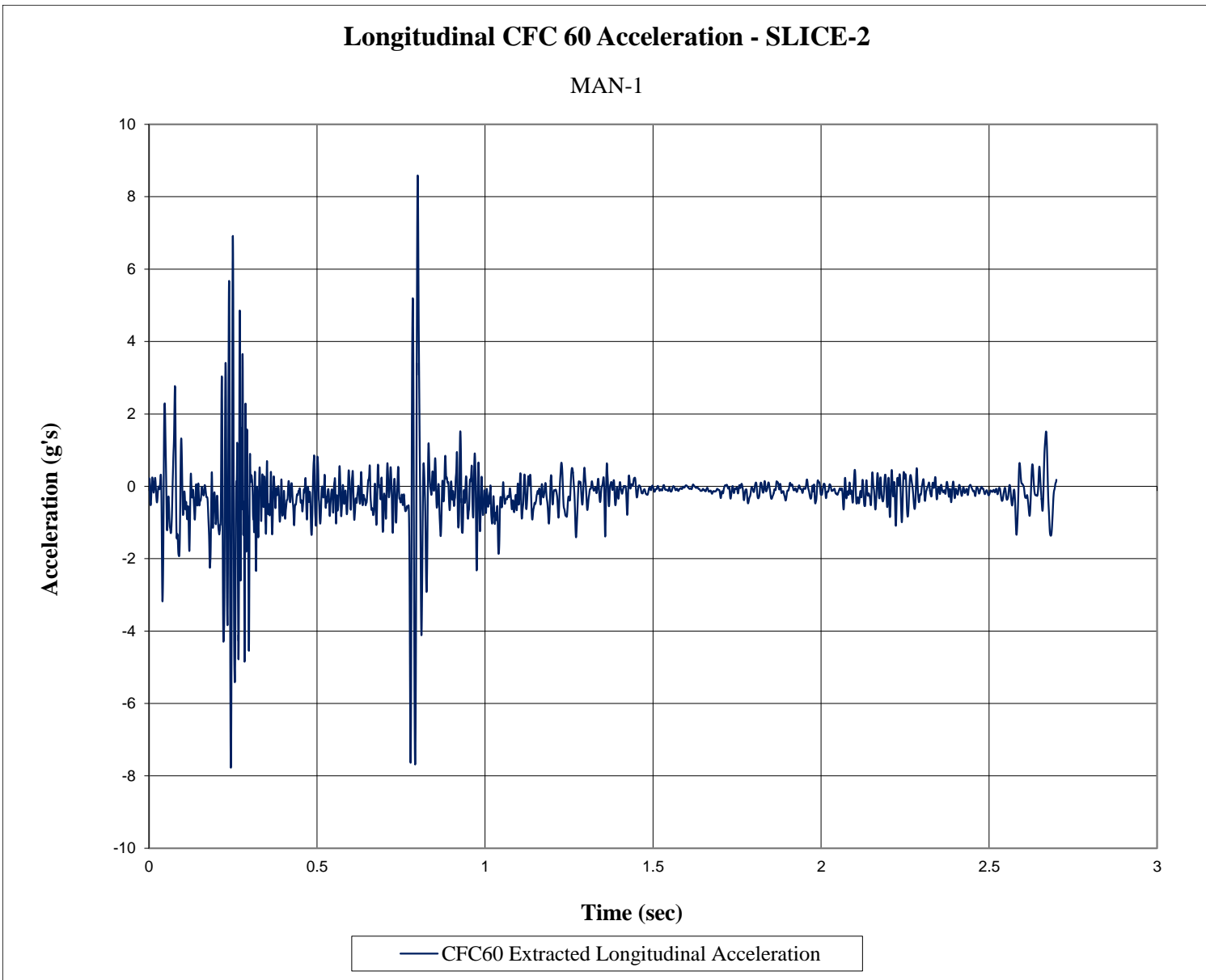


Figure D-9. CFC 60 Longitudinal Deceleration (SLICE-2 - Trailer), Test No. MAN-1

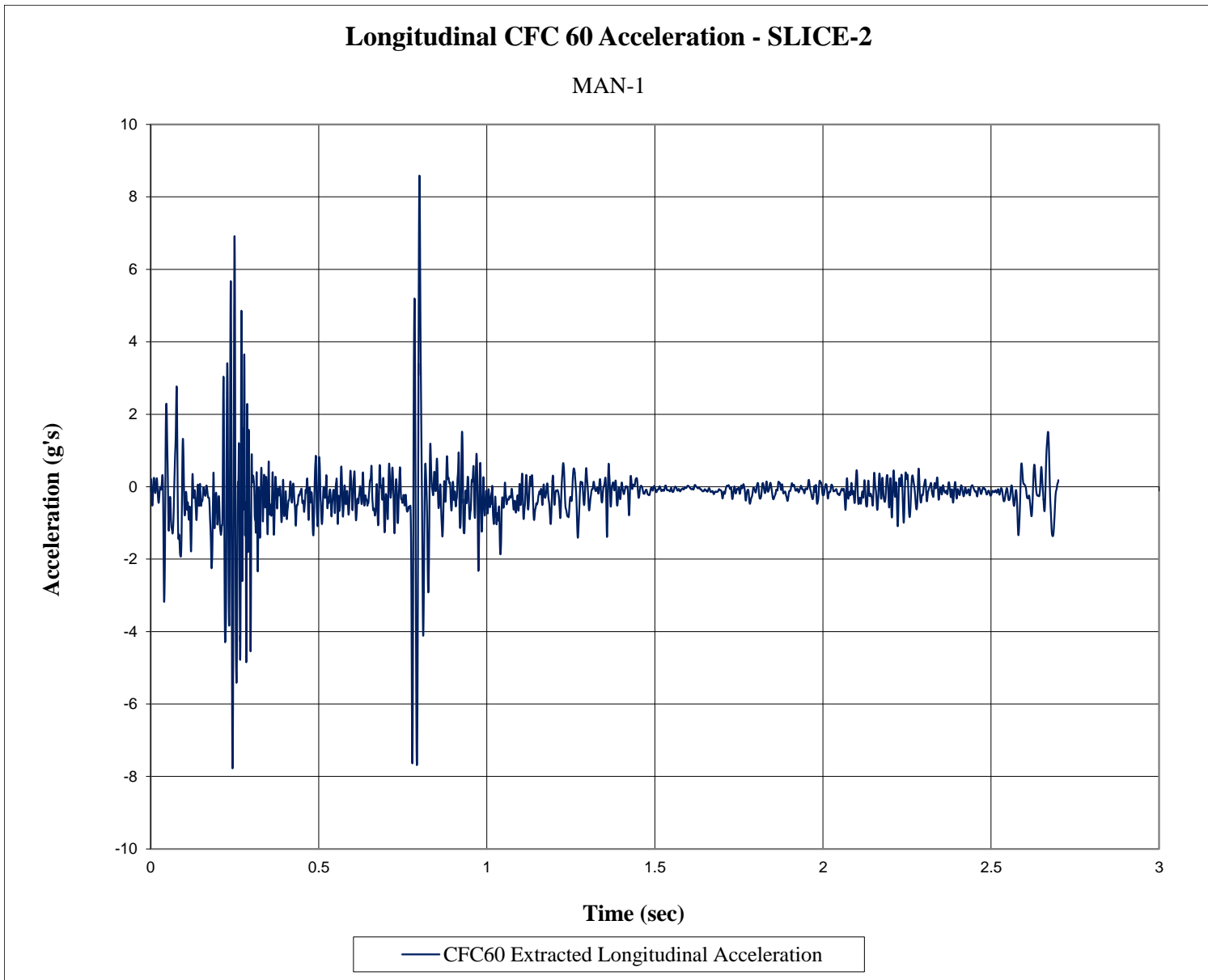


Figure D-10. CFC 60 50-ms Average Longitudinal Deceleration (SLICE-2 - Trailer), Test No. MAN-1

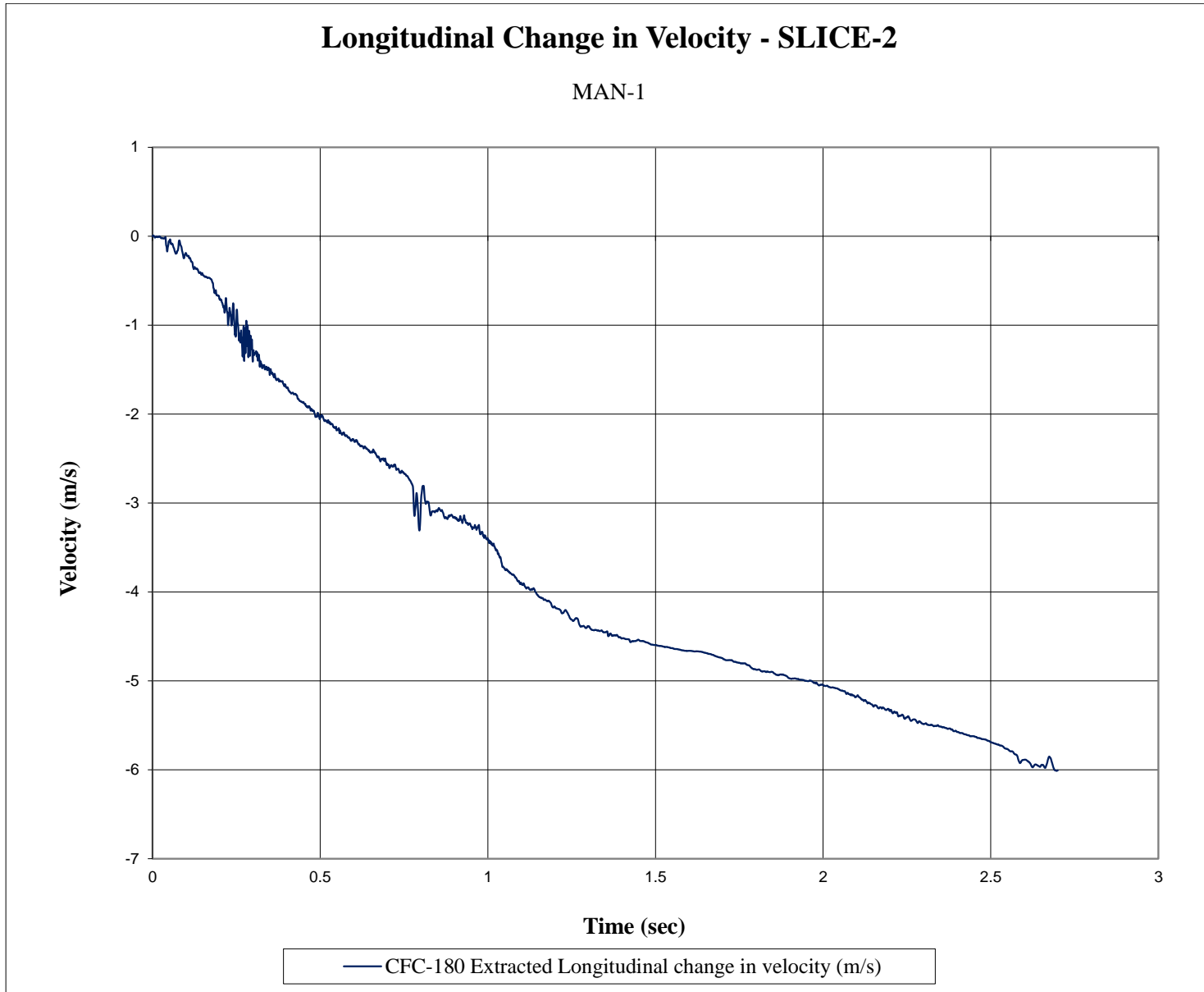


Figure D-11. Longitudinal Change in Velocity (SLICE-2 - Trailer), Test No. MAN-1

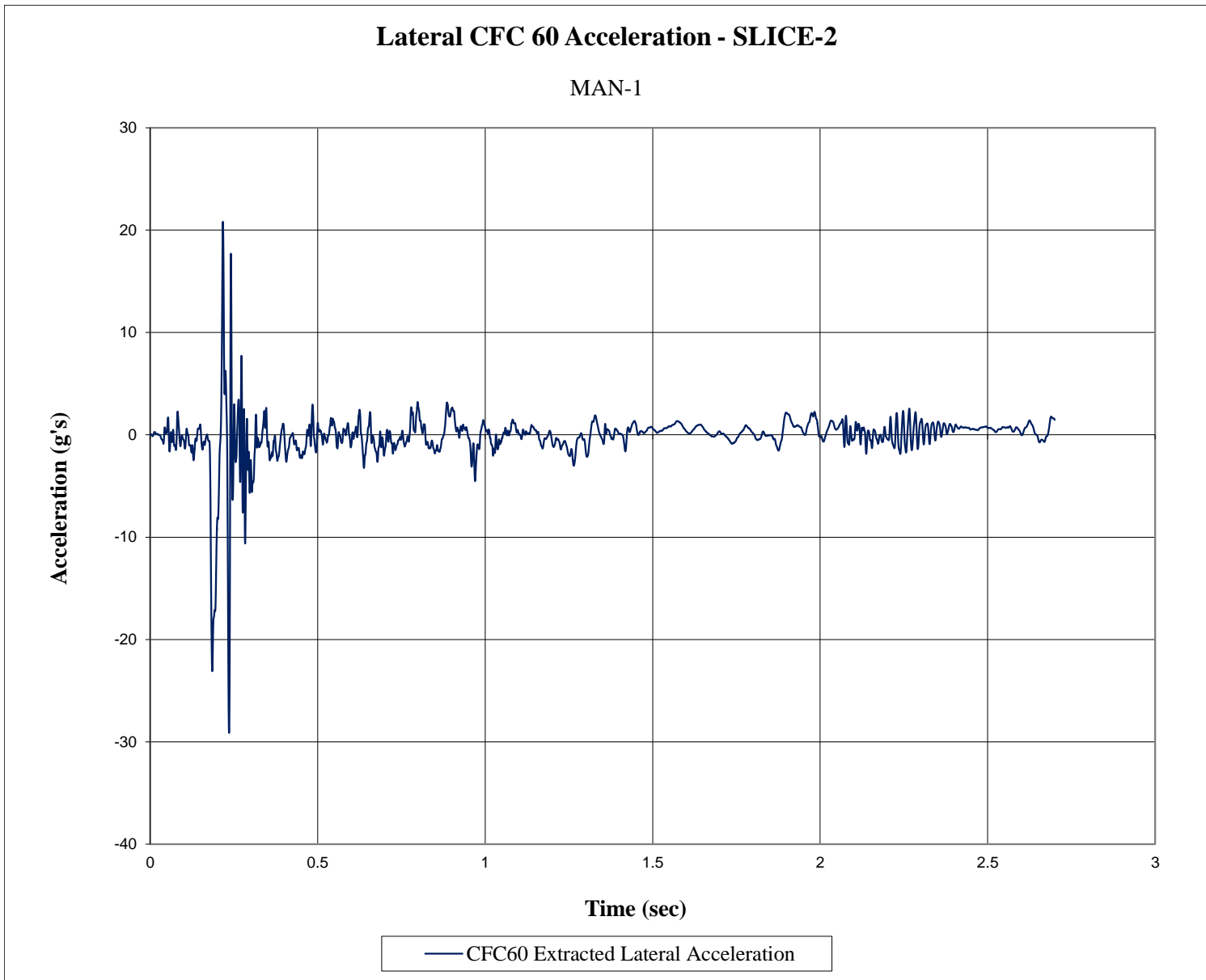


Figure D-12. CFC60 Lateral Deceleration (SLICE-2 - Trailer), Test No. MAN-1

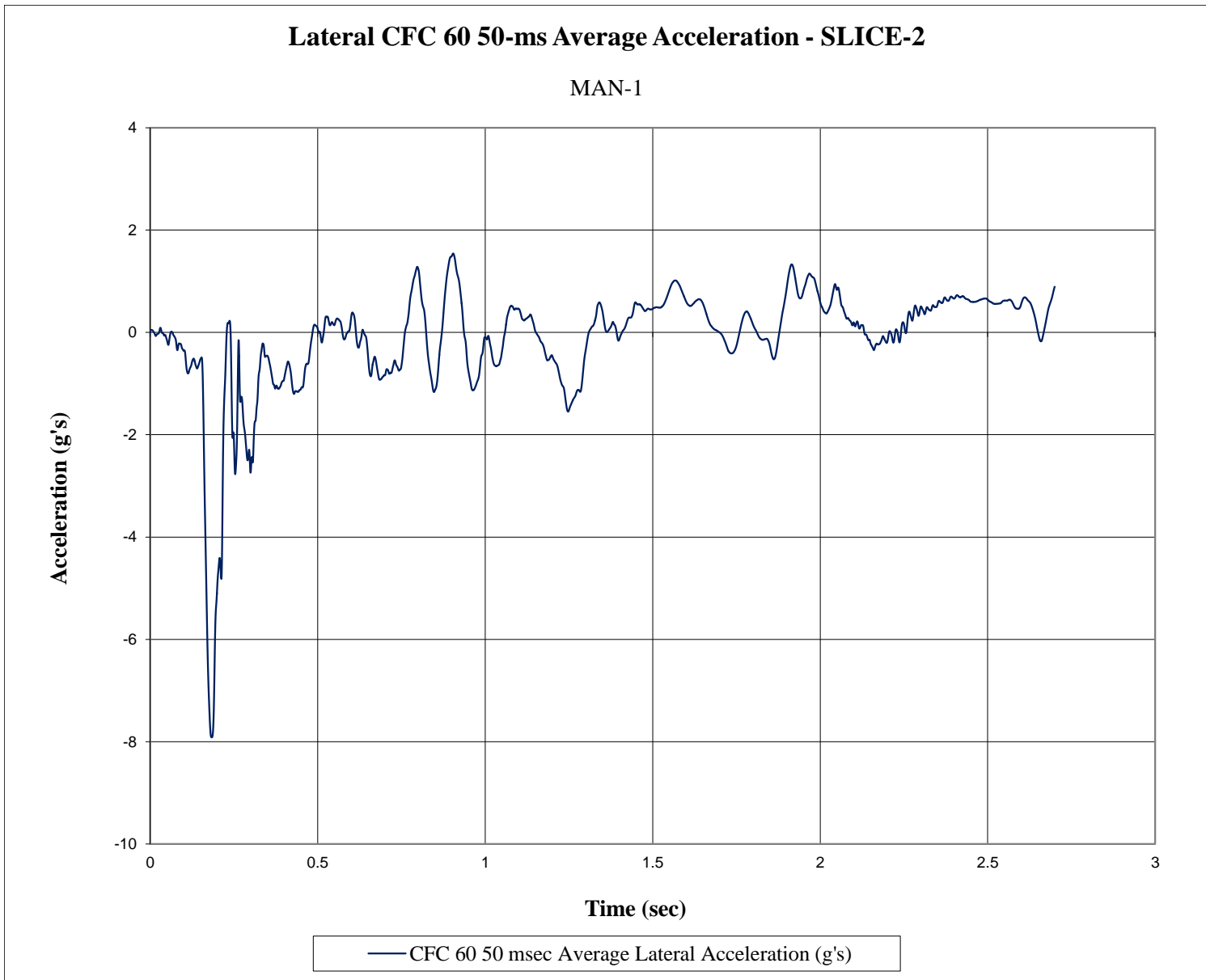


Figure D-13. CFC60 50-ms Average Lateral Deceleration (SLICE-2 - Trailer), Test No. MAN-1

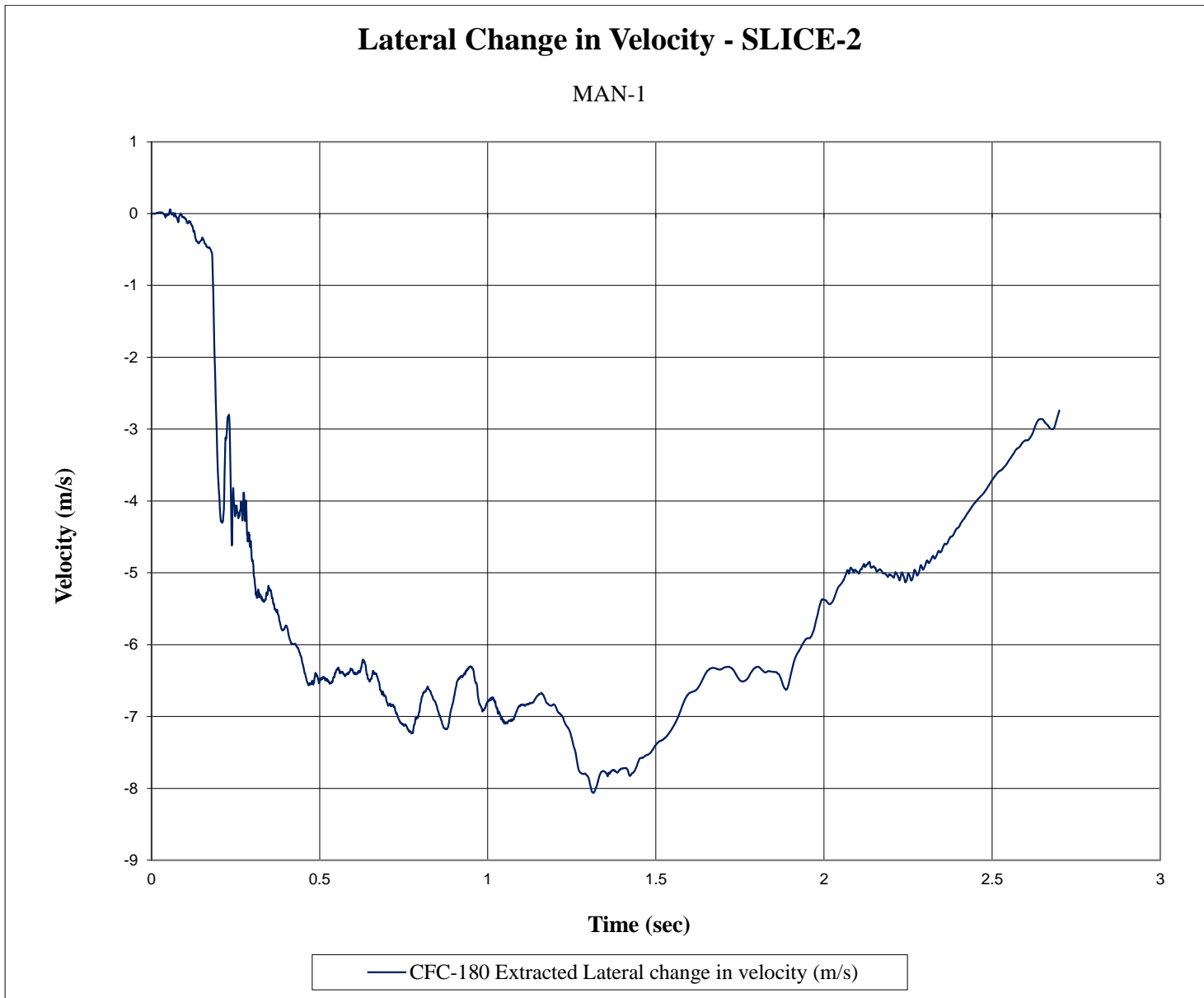


Figure D-14. Lateral Change in Velocity (SLICE-2 - Trailer), Test No. MAN-1

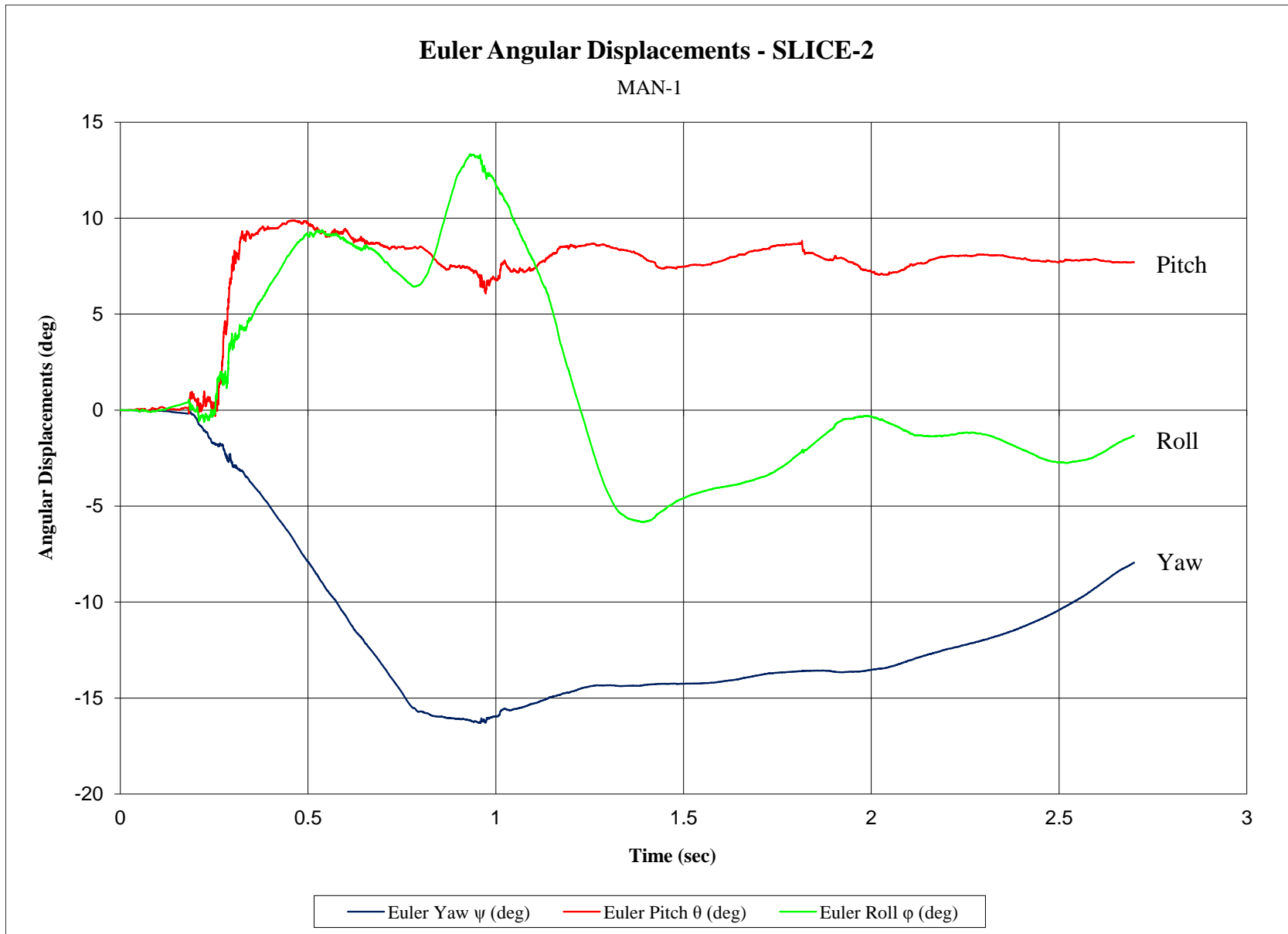


Figure D-15. Vehicle Angular Displacements (SLICE-2 - Trailer), Test No. MAN-1

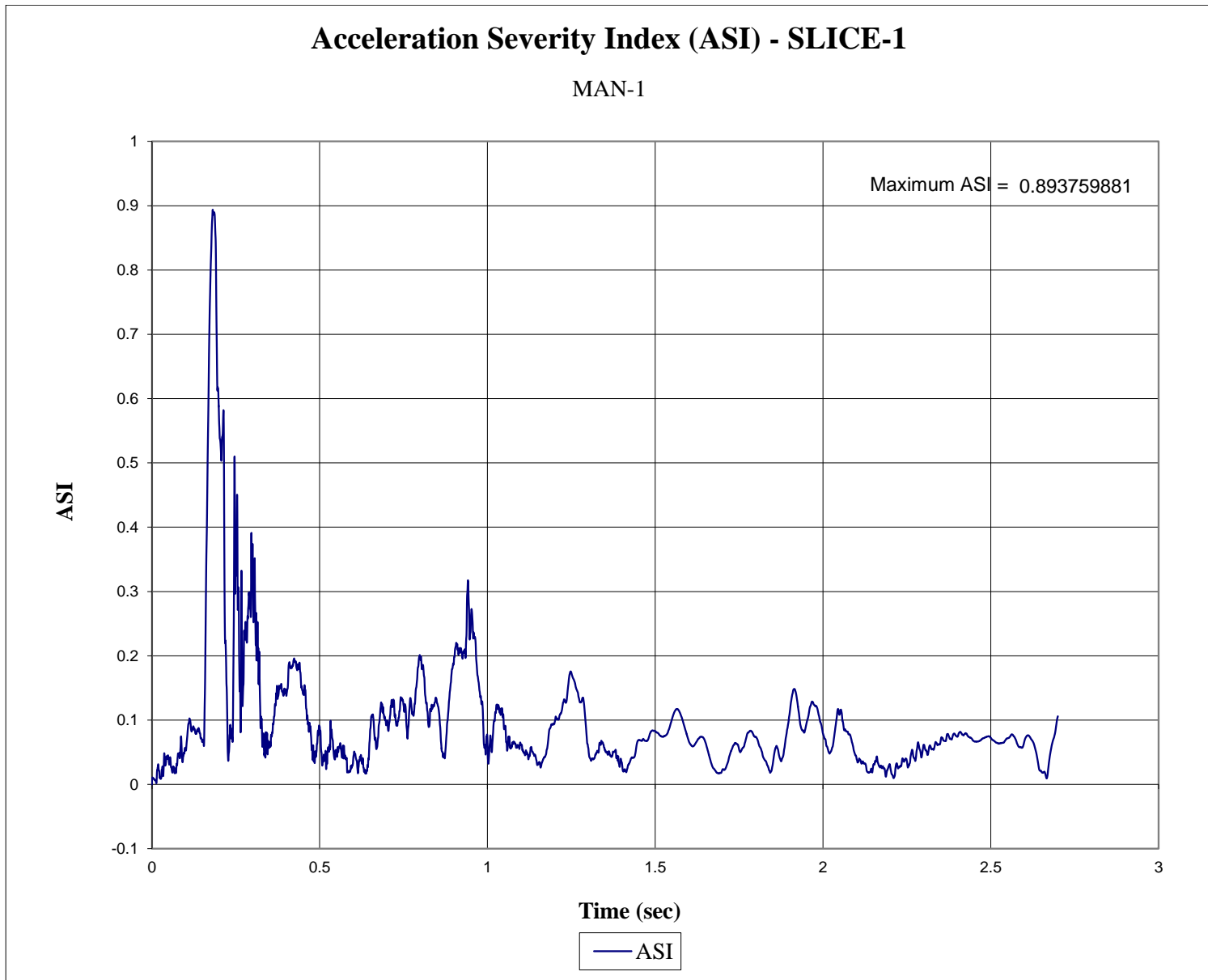


Figure D-16. Acceleration Severity Index (SLICE-2), Test No. MAN-1

END OF DOCUMENT